Puri, Sanyogitta (2007) Novel functionalized polymers for nanoparticle formulations with anti cancer drugs. PhD thesis, University of Nottingham.

NOVEL FUNCTIONALIZED

POLYMERS FOR

NANOPARTICLE

FORMULATIONS WITH ANTI

CANCER DRUGS

Sanyogitta Puri, B.Pharm.

Thesis submitted to the University of Nottingham for the the degree of Doctor of Philosophy

May 2007

If you can keep your calm when all around you is in chaos,
you haven't properly understood the severity of the
situation

-

Anon

ACKNOWLEDGEMENTS

Table of Contents

V

List of Figures

List of Tables

List of Abbreviations

CYT-ARA   Cytosine Arabinofuranoside

DSC   Differential Scanning Calorimetry

DXMP   Dexamethasone Phosphate

DXM   Dexamethasone

ETO   Etoposide

ETO-P   Etoposide Phosphate

FT-IR   Fourier Transformed Infrared Spectroscopy

HPLC   High Performance Liquid Chromatography

IPD   Interfacial Deposition Method

mPEG   methoxy Poly Ethylene Glycol

MPS   Mononuclear Phagocyte system

NP(s)   Nanoparticle(s)

PCL   Polycaprolactone

PCS   Photon Correlator Spectroscopy

PEG   Poly Ethylene Glycol

PGA   Poly glycerol adipate

PLA   Poly Lactic Acid

PLGA   Poly Lactide-co-glycolic acid

PTx   Paclitaxel

RES   Reticulo endothelial system

TEM   Transmission Electron Microscope

UV   Ultraviolet spectroscopy

ABSTRACT

The chemistry and structure of Poly (glycerol adipate) facilitate its substitution with various pendant functional groups leading to modifications of the physicochemical properties of the polymer. Modified backbones then can be selected based upon the properties of the compound to be incorporated. Thus, this could be explored as a drug delivery system without many of the limitations of commercially available polymers. The aim of this study was investigate whether various polymers and drugs interact in a specific manner and whether the nature of these interactions influence the physicochemical characteristics of the particles and their drug loading and release profile.

By investigating drugs belonging to various classes and with different properties it has been possible to correlate properties associated with drugs and pendant functional groups of the polymer which are ultimately responsible for the drug loading and release characteristics. For some drug polymer formulations, good loading and controlled release rates have been achieved. Compared to various conventional polymer systems reported for nanoparticle formulations, poly (glycerol adipate) polymers have also demonstrated the ability to control rate of release of highly water soluble drugs, even from the most hydrophilic polymer backbone in its unsubstituted form.

From the various drug loading and release profiles it has been demonstrated that, unlike reported literature, particle size is not the primary factor influencing drug release over the relatively small range of particle sizes seen in this study. Neither is the water solubility of either the drug or the polymer alone responsible for the rapid and uncontrolled release profile from nanoparticles.

Thus, Drug polymer interactions are more likely to influence drug loading and release and unlike common reports in the literature, hydrophilicity, molecular weight or concentration of polymer / drug are less likely to affect these parameters in isolation.

CHAPTER 1. INTRODUCTION

1.1. A Brief Overview of Nanoparticle Delivery Systems

Biodegradable polymers have been studied extensively over the past few decades to fabricate various novel drug delivery systems such as nanoparticles, microparticles, microspheres, liposomes etc. Considerable research is being directed towards developing biodegradable polymeric nanoparticles for drug delivery and tissue engineering, in view of their applications in providing controlled release of drugs, effectiveness in stabilising labile drug molecules such as proteins, peptides, or DNA from degradation and site specific drug targeting.

The late 1960's and early 1970's saw the advent of polymer nanoparticles based on acrylamide micelle polymerisation [1]. Since then, along with different polymerisation methods, use of preformed polymers have also been developed and studied [1-3]. The majority of studies on nanoparticles reported to date have dealt with NPs of poly (D,L lactide), poly (lactic acid) PLA, poly (D,L glycolide) [PLG], poly (lactide-co-glycolide) [PLGA] and poly- cyanoacrylate [PCA] [3].

1.2. Review of Nanoparticle Delivery Systems

Nanoparticles are solid, colloidal particles consisting of macromolecular substances that vary in size from 10 nm to 1000 nm [1]. The drug of interest is dissolved, entrapped, adsorbed, attached or encapsulated into the nanoparticle

matrix. Depending on the method of preparation, nanoparticles, nanospheres or nanocapsules can be obtained with different properties and release characteristics for the encapsulated therapeutic agent [2-4]. Nanocapsules are vesicular systems in which the drug is confined to a cavity surrounded by a polymer membrane, whereas nanospheres are matrix systems in which the drug is physically and uniformly dispersed (See Fig. 1.1)
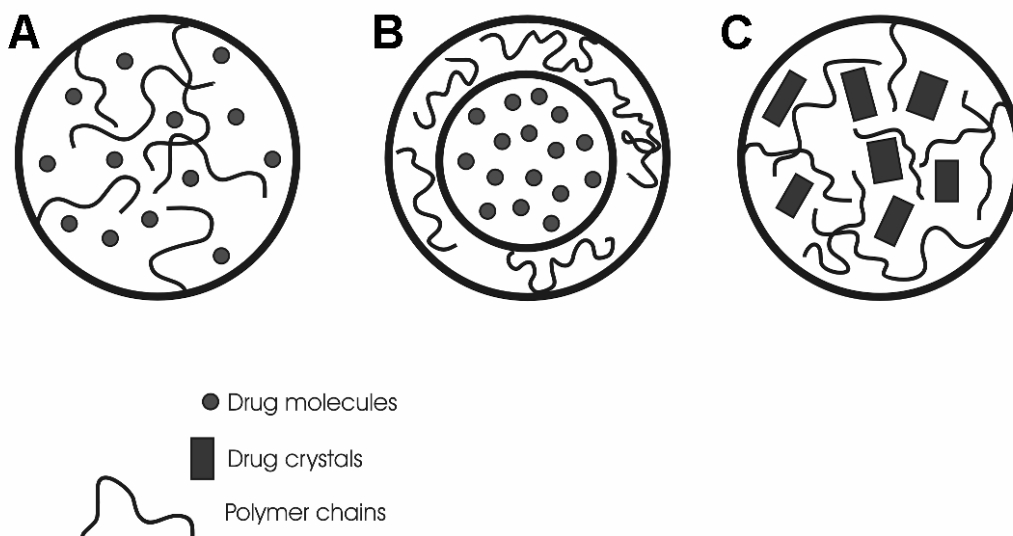
Fig. 1.1. Schematics of exemplary types of drug nanoparticles. A. Matrix type nanosphere, drug molecules are evenly dispersed in the polymer matrix. B. Core shell nanocapsule, drug molecule is presented in a core covered with a polymer shell. C. Matrix type nanosphere where drug crystals are embedded in a polymer matrix [5]

1.2.1. Applications and advantages as drug carrier vehicle

Polymeric nanoparticles made from natural and synthetic polymers have received the majority of attention due to higher stability and the opportunity for further surface nanoengineering [6, 7]. They can be tailor-made to achieve both controlled drug release and disease specific localization by tuning the polymer characteristics and surface chemistry [8-11]. It has been established that

nanocarriers can become concentrated preferentially in the tumour mass, inflammatory sites, and at infectious sites by virtue of the enhanced permeability and retention (EPR) effect of the vasculature. Once accumulated at the target site, hydrophobic biodegradable polymeric nanoparticles can act as a local drug depot depending upon the make-up of the carrier, thus providing a source for a continuous supply of encapsulated therapeutic compound at the disease site, such as, a solid tumour. These systems in general can be used to provide targeted (cellular/tissue) delivery of drugs, to improve oral bioavailability, to sustain drug/gene effect in the target tissue, to solubilize drugs for intravascular delivery, and to improve the stability of therapeutic agents against enzymatic degradation (nucleases and proteases), especially of protein, peptide, and nucleic acids drugs [12]. Thus, the advantages of using nanoparticles for drug delivery result from two main basic properties viz. small size and use of biodegradable materials. Nanoparticles, because of their small size, can extravasate through the sites of inflammation and cancer cells or penetrate into smaller capillaries, cross the fenestration present in the epithelial lining (e.g., liver), and are generally taken up efficiently by the cells which allow efficient drug accumulation at the target sites [8, 9, 13]. Many studies have demonstrated that nanoparticles of sub-micron size have a number of advantages over microparticles as a drug delivery system [14]. Nanoparticles have a further advantage over larger microparticles as they are better suited for intravenous (i.v.) delivery. The smallest capillaries in the body are 5–6 μm in diameter. The size of particles being distributed into the bloodstream must be significantly smaller than 5 μm, without forming aggregates to ensure that the particles do not form an embolism. In some cell lines, only submicron nanoparticles can be taken up but not large size microparticles.

Generally nanoparticles have relatively higher intracellular uptake compared to microparticles and are available to a much wider range of biological targets due to their small size and relative mobility. Desai *et al*. found that 100 nm nanoparticles had a 2.5 fold greater uptake than 1 µm microparticles, and 6 fold greater uptake than 10 µm microparticles in a Caco-2 cell line [13]. In a similar study, the nanoparticles penetrated throughout the submucosal layers in a rat in situ intestinal loop model, while microparticles were predominantly localized in the epithelial lining [15]. Secondly, the use of biodegradable materials for nanoparticle preparation allows sustained drug release within the target site over a period of days or even weeks. Biodegradable nanoparticles formulated from poly $_{DL}$-lactide co-glycolide (PLGA) and polylactide (PLA) have been developed for intracellular sustained drug delivery, especially for drugs with an intracellular target [9, 16, 17]. Rapid escape of PCL nanoparticles from the endo-lysosomal compartment to the cytoplasmic compartment has been demonstrated [16, 18]. Thus, nanoparticles could be an effective drug delivery mechanism for drugs whose targets are cytoplasmic. Greater and sustained antiproliferative activity was observed in vascular smooth muscle cells which were treated with dexamethasone-loaded nanoparticles compared to that seen with drug in solution [19]. Nanoparticles were effective in sustaining intracellular dexamethasone levels, thus allowing a more efficient interaction with the glucocorticoid receptors which are cytoplasmic.

1.2.2. Targeted drug delivery

The development of nanoparticulate delivery systems for targeted drug delivery has been reviewed recently by Moghimi *et al.* [10]. Targeted delivery can be achieved by either active or passive targeting. Active targeting of a therapeutic

agent is achieved by conjugating the therapeutic agent or the carrier system to a tissue or cell-specific ligand [20]. Passive targeting is achieved by incorporating the therapeutic agent into a macromolecule or nanoparticle that passively reaches the target organ. Drugs encapsulated in nanoparticles or drugs coupled to macromolecules such as high molecular weight polymers passively target the tumour tissue through the enhanced permeation and retention (EPR) effect. The alternative approach involves the infusion of a nanoparticle suspension to the accessible target organ or tissue using infusion catheters. Localized delivery of nanoparticles in restenosis may be a useful strategy as it may provide a sustained drug effect in the target artery [21, 22].

Solid Lipid Nanoparticles and liposomes are also useful for the delivery of pharmaceutical agents after binding to target cellular epitopes by a mechanism called 'contact facilitated drug delivery'. Binding and close apposition to the targeted cell membrane permits enhanced lipid–lipid exchange with the lipid monolayer of the nanoparticle, which accelerates convective flux of lipophilic drugs (e.g. paclitaxel) dissolved in the outer lipid membrane of the nanoparticles into the targeted cells [23]. Such nanosystems can serve as drug depots exhibiting prolonged release kinetics and long persistence at the site.

Another characteristic function of nanoparticles is their ability to deliver drugs across several biological barriers to the target site [24, 25]. The brain delivery of a wide variety of drugs, such as antineoplastics and anti-HIV drugs is markedly hindered because they have great difficulty in crossing the Blood–Brain Barrier (BBB) .The application of nanoparticles to brain delivery is a promising way of overcoming this barrier. It has been reported that nanoparticles can cross the

Nanoparticle	Size (nm)	Carried therapeutic agent	Examples of potential targeted therapeutic application	Advantage
Polymeric biodegradable nanoparticles	10-1,000	Plasmid DNA, proteins, peptides, low molecular weight compounds	Brain tumor therapy [Olivier et al., [1999]]; Kreuter et al., [2003]], bone healing [Labhasetwar et al., [1999]], vaccine adjuvant [Raghuvanshi et al., [2001]], coating gut suture [Cohen et al., [2000]], restenosis [Guzman et al., [1996]; Panyam et al., [2002], inflamed colonic mucosa [Lamprecht et al., [2001]], diabetes therapy [Al Khouri et al., [1986]]; Watnasirichailkul et al., [2000]]	Sustain localized drug therapeutic agent for weeks
Silica nanoparticles	<100	Proteins, DNA, anticancer therapeutic agents, high molecular weight compounds	Photodynamic therapy [Roy et al., [2003b]], liver therapy [Roy et al., [2003a]; Dey, [2005]], diabetes therapy [Cherian et al., [2000]]	Can be easily prepared, water-soluble, and stable in biological environment
Metallic nanoparticles	<50	Anticancer therapeutic agents, proteins, DNA	Cancer therapy [Wang et al., [2004]; Priyabrata et al., [2005]]	Extremely small size with vast surface area to carry large dose
Polymeric micelles	<100	DNA, anticancer therapeutic agents, proteins	Solid tumors therapy [Yokoyama et al., [1990]; Kataoka et al., [2001]; Rapoport et al., [2003]], antifungal treatment [Yu et al., [1998]]	Have hydrophobic core, and so they are suitable carriers for water-insoluble drug
Liposomes	50-100	Proteins, DNA, anticancer therapeutic agents	Tumors therapy [Goren et al., [1996]; Versluis et al., [1998]; Lasic et al., [1999]], HIV therapy [Slepushkin et al., [1996]], vaccine delivery [Rao and Alving, [2000]]	Effective in reducing system toxicity and can stay longer in targeted tissue
Dendrimers	<10	DNA, anticancer therapeutic agents, antibacterial therapeutic agents, antiviral therapeutic agents, high molecular weight compounds	Tumors therapy [Kobayashi et al., [2001]; Quintana et al., [2002]; Latallo et al., [2005]], bacterial infection treatment [Chen and Cooper, [2002]; Boas and Heegaard, [2004]], HIV therapy [Witvrouw et al., [2000]; Rojo and Delgado, [2004]]	Can be modified to carry hydrophobic or hydrophilic drug

Table 1.1 Summary of applications of various colloidal carriers as targeted drug delivery system [118].

blood-brain barrier following the opening of tight junctions by hyperosmotic mannitol, which may provide sustained delivery of therapeutic agents for difficult-to-treat diseases like brain tumours [26]. Tween 80 coated nanoparticles have also been shown to cross the blood-brain barrier [27]. A range of different types of nanoparticles and their applications are outlined in Table 1.1.

1.2.3. Polymers used in nanoparticle formulations

Common classes of polymers used to encapsulate drugs in colloidal systems include polyamides, poly(amino acids), polyesters, polyorthoesters and polyanhydrides [14, 28].

1.2.3.1. Polyesters

Recently, biodegradable polyesters such as poly (lactic acid), poly (glycolic acid) and the copolymers of lactic and glycolic acid, i.e., poly (lactide-co-glycolide). (PLGA) have been used extensively for biomedical applications. Being biodegradable they have the advantage of not requiring surgery for removal after they have served their purposes. They protect the entrapped drug against degradation and control its site specific delivery. They are synthesised through ring opening polymerisation of cyclic lactones. These copolymers (with varying lactide: glycolide ratios) are amorphous and easily dissolve in organic solvents such as dichloromethane and ethyl acetate. The degradation rate in water is a function of the molecular weight and the lactide:glycolide ratio [29]. Higher glycolide content and lower molecular weight increase the degradation rate. As they are all strongly hydrophobic they are more efficient for encapsulation of hydrophobic drugs than hydrophilic drugs. A burst release is another

7

characteristic observed with nanoparticles made from PLGA. The drug release from PLGA microparticles often has a tri-phasic pattern in vitro [30] as well as in vivo. A fast initial release phase (burst) followed by a second slow release phase lasting days or weeks and a third rapid release phase is seen in particular with peptide and protein drugs. The burst release is undesirable in most of the sustained-drug delivery applications, since the dosage of the potent drug encapsulated is required to be released over a long period of time. Even a small percentage of the drug immediately released would increase its local concentration to an extent near or above that at which the drug becomes toxic in vivo. The defence mechanism of the body would respond to this increased toxicity level by forming additional layers of tissues on the polymer surface, thereby disrupting the entire release profile and mechanism. Any drug released during the burst stage may be metabolized and excreted without being effectively utilized as it may not reach its target tissue [31]. Except for vaccines, a tri-phasic drug release is generally not desirable for most drug therapies. Insufficient drug may be delivered to maintain the desired pharmacological effect in the slow release phase and toxicity problems may occur during the rapid initial and third release phases because of too high drug levels.

The fast initial release (burst) is commonly attributed to drug localised on the surface of particles [32, 33] or to easily accessible drug, for example, in the case of highly porous microparticles [34]. Thereafter, a diffusion-controlled slower release phase follows. Finally, when the molecular weight of PLGA approaches a certain lower threshold, the weight of the microparticles decreases rapidly and an erosion-controlled rapid release phase occurs [35]. Recently, the formation of a nonporous film around the microparticles after incubation in the release medium

has been reported [34]. The decreased surface porosity of the microparticles led to reduced drug permeability and resulted in the slow release phase without burst release.

1.2.3.2. Poly (Ethylene glycol) based Block Co Polymers

The nature of the surface of the nanoparticles largely influences their biodistribution following in vivo adminstration. Hydrophobic nanoparticles are rapidly cleared from the systemic circulation by the MPS, ending in the liver or in the spleen. The hydrophobic nature of most biodegradable particles could limit the applicability of these carriers in many drug delivery applications. In order to overcome concerns of clearance by the MPS, surface modification techniques have been utilised. These modification techniques ultimately produce a particle that is not recognized by the MPS by rendering the surface of the particle hydrophilic.

Several types of surface modified nanoparticles have been described in recent literature. The most common moiety used for surface modification is poly (ethylene glycol) (PEG). PEG is a hydrophilic, non-ionic polymer that has been shown to exhibit excellent biocompatibility. PEG molecules can be added to the particles via covalent bonding or by surface adsorption. The presence of a PEG-brush on the surface of nanoparticles besides increasing residence time in the systemic circulation can also reduce protein and enzyme adsorption on the surface and thus can retard particle degradation. The degree of protein adsorption can be minimized by altering the density and molecular weight of PEG on the surface [36]. The stability of PLA particles has been shown to increase in simulated gastric fluid (SGF) with the addition of PEG on the particle surface.

After 4 hours in Simulated Gastric Fluid, 9% of the PLA nanoparticles converted to lactate versus 3% conversion for PEG-PLA particles [37]. PEG is also believed to facilitate transport through the Payer's patches of the Gut-associated lymphoreticular tissue [38]. Usually PEG block co polymers show quite different properties compared to the constituent polymers lactic acid and glycolic acid. PLGA – PEG block co polymers are hence used as biomaterials with their own unique properties and classified as triblock, star block, branched or graft block co polymers as illustrated in Fig. 1.2 [27, 39-41].
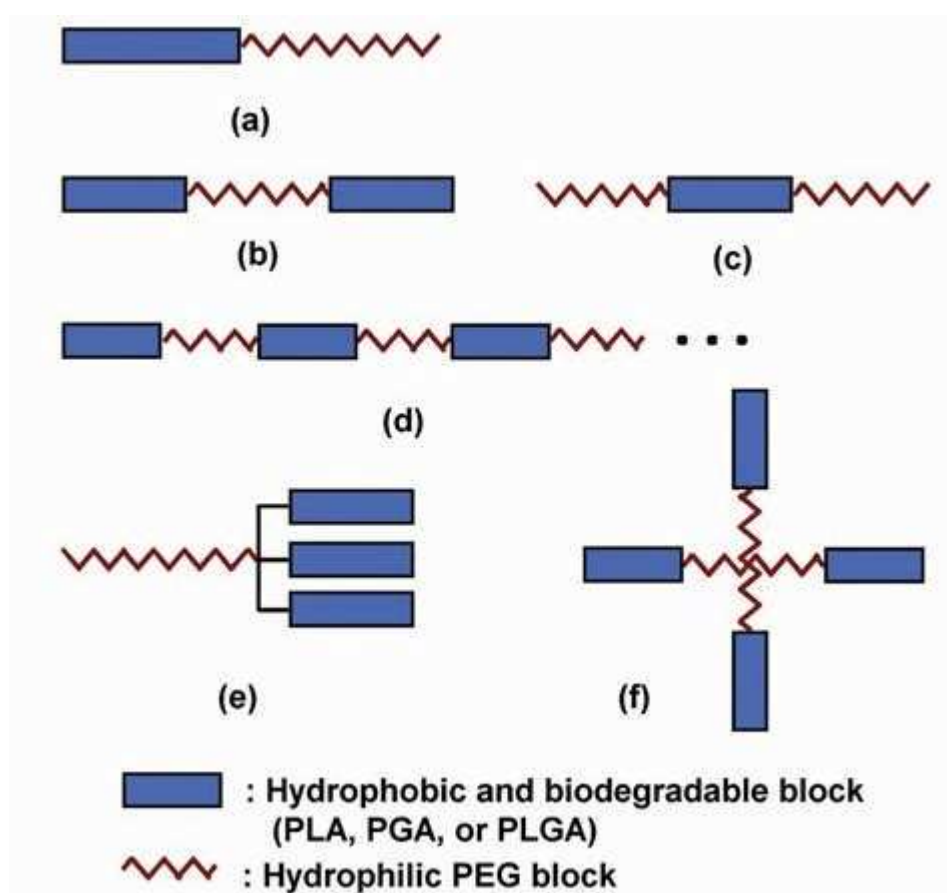
Fig. 1.2. Schematic representation of (a) diblock, (b) and (c)triblock, (d)multiblock, (e) multiblock branched or comb, (f) star shaped. (Adapted from [42])

10

PLGA degradation shows autocatalysis wherein bulk degradation occurs with a decrease in pH resulting from the release of lactic acid and glycolic acid monomers. The resulting carboxyl groups, oligomeric PLGA etc can increase degradation of the PLGA formulation. Block co polymers with PEG have also gained attention as an alternative for overcoming these side effects. Another main drawback of these polymers is their non specific interaction with cells and plasma proteins, leading to accumulation in non target cells causing limitations in practical drug formulations. Hence, surface modified nanoparticles have been developed to control their interactions. PEG coated (sterically stabilised) nanoparticles can avoid sequestration by the Mononucleur Phagocyte system (MPS) and hence show increased circulation time in the body. However, these coated nanoparticles lack functional groups for ligand coupling. Some successful attempts have been reported for PEG systems where a terminal functional group has been added to PEG [43]. Polysaccharide coatings have also been studied since they are alternative hydrophilic molecules. Some polysaccharides facilitate mucoadhesion or function as recognition factors allowing recognition. For example PEG Dextran [30] or Dextran PLA [44].

Biodegradable and biocompatible polymers such as poly (lactide) (PLA) [45], poly (ε-caprolactone) (PCL) [46], poly (β-benzyl L-aspartate) (PLBA) [47], and poly (γ-benzyl L-glutamate) (PLBG) [48] have been commonly used for the core material of micelles while PEO and PEG are used as hydrophilic blocks. Studies on polymeric micelles comprised of PEO as hydrophilic block and PCL, PLA, PLBA, PLBG as hydrophobic block have been carried out by many groups. Amphiphilic block copolymers have the ability to produce nanoparticles by self assembling in an aqueous environment [49-51]. The hydrophobic blocks of the

copolymer form the core of the micelle, while the hydrophilic blocks form the corona or outer shell. The solubility of the hydrophobic drug in the aqueous media is greatly increased by the use of micelles. Thus, incorporating a drug in the micelle is an effective method of preparing an efficient drug delivery system.

1.2.3.3. Polycaprolactones (PCL)

Poly(ε-caprolactone) (PCL) obtained by ring opening polymerisation of ε-caprolactone was first reported by Pitt *et al*. [52] for the controlled release of steroids and narcotic antagonists as well as to deliver opthalmic agents. PCL, aliphatic polyester has been intensively investigated as a biomedical material. It demonstrates a low melting point (57°C) and a low glass-transition temperature (-62°C). Under physiological conditions, PCL can be degraded by micro-organisms as well as by hydrolysis [3]. Under certain circumstances, it is possible to enzymatically degrade crosslinked PCL (termed enzymatic surface erosion). Low molecular-weight fragments of PCL are also reportedly absorbed by macrophages intracellularly [18]. The rate of biodegradation for PCL is slower than other biodegradable materials thus making it suitable for design of long term implantable systems. For example, Capronor, a US FDA approved contraceptive device. Another interesting property of PCL is its propensity to form compatible blends with a wide variety of polymers.

Molpeceres *et al.* studied cyclosporine encapsulation within Polycaprolactone nanoparticles and reported 95% encapsulation efficiency within the particles. They also showed that this formulation offered a good alternative to existing cyclosporine formulations as far as drug monitoring is concerned [53]. Lemarchand *et al* have reported synthesis of amphiphilic copolymer based on Dextran grafted with PCL chains which significantly reduced protein absorption

[54]. Recently, Merle and coworkers reported encapsulation of vancomycin in biodegradable PCL microparticles for bone implantation [55].

1.2.3.4. Poly (alkylcyanoacrylates)

Poly (alkylcyanoacrylate)s have been used as tissue adhesives in surgery since these are well tolerated in vivo [56, 57]. Unlike PLA and PGA, here only the side chains are biodegradable and not the backbone. Their delayed degradation characteristics thus do not generate an acidic environment during drug release. This has prompted intense research for their use in many nanoparticle formulations. Couvreur [56] reported the production of NPs by mechanically polymerizing the dispersed methyl or ethyl cyanoacrylate in aqueous acidic medium without irradiation or an initiator in the presence of polysorbate-20 as a surfactant. Layre *et al*. studied busulfan entrapment by nanoprecipitation into five different types of poly (alkyl cyanoacrylate) polymers. The polymers leading to the highest busulfan loading efficiencies were poly(isobutyl cyanoacrylate) (PIBCA) and poly (ethyl cyanoacrylate) nanoparticles displaying busulfan loading ratios equal to 5.9% (w/w) together with nanoparticle yields of 71% (w/w). The in vitro release studies under sink conditions, in water, or in rat plasma showed a fast release in the first 10 min followed by a slower one over 6 h [58]. Vauthier *et al* demonstrated the potential of poly (alkylcyanoacrylate) (PACA) NPs to overcome multidrug resistance problems at cellular level and in relation to drug biodistribution [7]. Resistant cells treated with doxorubicin-loaded poly (alkyl cyanoacrylate) nanoparticles showed a much higher sensitivity to the drug, relative to the free drug when compared with NPs using other biodegradable polymers [59]. The mechanism proposed to explain the ability of doxorubicin-loaded PACA nanoparticles to overcome the resistance to

doxorubicin in resistant cancer cells was based on the adhesion of the nanoparticles to the cell surface, followed by the simultaneous release of the drug and nanoparticle degradation product (poly cyanoacrylic acid) that combine as an ion-pair able to cross the cell membrane without being recognized by the P-glycoprotein [60]. To date, only the poly (alkyl cyanoacrylate) nanoparticles have been identified as to be fulfilling these requirements to overcome the resistance caused by the P- glycoprotein complex. Lipid nanocapsules prepared using poly (alkyl cyanoacrylates) were between 25 to 100 nm in size and showed fast initial release of 60 to 75% in the first 48 hours. However the major limitations associated with use of this polymer are the particle size, high cell uptake and toxicity [57]

1.2.3.5. Poly (ortho-esters) (POE)

Poly (orthoesters) is another important group of hydrophobic polymer with drug delivery applications and are synthesised by the addition of polyols to diketene acetals. POEs possess acid sensitive orthoester linkages that undergo rapid hydrolysis at physiological pH and an even faster rate in an acidic pH. Therefore, incorporation of a small amount of acidic excipients may help to control the hydrolysis rate. On the other hand, incorporation of basic excipients stabilises the bulk of the matrix but facilitates erosion at the surface. Wan *et al* have studied poly (phosphoester) ionomers as tissue engineering scaffolds [61]. The polymers conjugated with N- hydroxysuccimide were hydrolyzed in a biphasic mode, with a fast initial phase occurring in the first few hours, followed by a slower phase in the next few days. These ionomers represent a novel class of biomaterials with readily controllable physical and chemical attributes for tissue engineering.

1.2.3.6. Polyanhydrides (PA)

Polyanhydrides are hydrophobic and contain water sensitive linkages that may undergo hydrolytic bond cleavage to generate water-soluble degradation products. Surface erosion takes place due to water sensitive linkages. The majority of Polyanhydrides studied are based on sebacic acid (SA), p-(carboxyphenoxy) propane (CPP) and p-(carboxyphenoxy) hexane (CPH) [62]. The Sebacic acid component of biodegradable PAs is utilised as a surface eroding drug delivery device. A wide variety of drug and proteins have been incorporated into PAs and their modified forms e.g. poly (anhydride-esters), poly (anhydride-imides) etc. and their potential release characteristics have been evaluated [63].

1.2.3.7. Polyamides

Polyamides form another important class of polymers particularly as drug delivery matrices. Polyamides with a structural resemblance to polypeptides are used as matrices for the transport of drugs.

Examples include different types of poly (amino acids) [64, 65] such as poly (L-glutamic acid), poly (aspartic acid) are derived from the corresponding natural amino acids. Nakanishi and co-workers have developed a polymeric micelle carrier system consisting of PEG-conjugated doxorubicin: poly (aspartic acid) for the transport of doxorubicin. This carrier system has a highly hydrophobic inner core, and therefore, it can also entrap a useful amount of doxorubicin in addition to the conjugated doxorubicin. It circulated in the blood for a long-time and evaded RES uptake due to the hydrophilic polyethylene glycol outer layer. It was effectively accumulated in the tumour tissue by the EPR effect. The entrapped

Doxorubicin was released from the inner core by diffusion and expressed stronger activity than free Doxorubicin against all the tumour lines tested [66].

Li and co-workers have synthesised a novel biodegradable poly (ester amide) derived from 3-morpholine and ε-caprolactone. Increase in morpholine content enhanced water absorption of the polymers In vitro degradation data and release profiles of 5-fluorouracil showed that both the degradation rate and drug release rate increased with an enhanced morpholine content in the polymers [67].

1.2.4. Approaches towards functionalization of polyesters

Extensive studies are been directed towards functionalising polyesters in order to enhance the range of drugs / molecules that can be incorporated to a significant extent within the polymeric particles and also to provide a controlled release profile. Copolymerization of monomers and blending of polyesters have also been investigated to control physicochemical properties and biodegradation rate. Most polyesters do not have functional groups that could enhance their potential applications. Such applications are greatly broadened when functional pendant groups are incorporated into the polymer backbone. Introduction of functional groups that can be easily substituted or conjugated with the compound of interest is a challenge. A number of synthetic approaches have been used to introduce functional groups, and following are some examples of reported conjugations.

 Feijen investigated synthesis of poly (ester amide) with pendant carboxyl or amine groups polymerised with ($_{D,L}$) Lactic acid or caprolactone [68]. Barerra *et al* synthesised poly (lactic acid-co-lysine) with pendant amino groups. However, only 2 mol% lysine units were incorporated into the polymer backbone and it failed to produce a polymer that could be introduced as a successful delivery system [16]. Zhao *et al* have reported synthesis of a series of multiblock co

polymers PLGA-(L- Asp-alt-diol) x – PLGA with different contents of functional pendant amino groups. Its fabrication into drug encapsulated delivery system however has not yet been reported [69].

Synthetic pathways to introduce functional groups into degradable polyesters may follow two general strategies. One is pre-functionalization, in which functional monomers are prepared prior to polymerization. The other is post-functionalization, where functional groups are introduced after polymerization. Thus, a general synthetic

route would involve (1) preparation of protected functional monomers, (2) polymerization of the monomers, and (3) deprotection

Yao *et al*. prepared poly [(L-lactic acid)-*co*-(citric acid)] by direct polycondensation of L-lactic acid and citric acid to introduce both carboxyl and hydroxyl groups [70].

Some authors recently demonstrated direct coupling of unprotected functional groups to the polymer backbone under mild reaction conditions. For example, the selective coupling between ketone-bearing aliphatic polyesters and aminooxy-terminated functional groups [71].

Most of the polyesters developed had low molecular weight, which could be attributed to the poor reactivity of the functional monomers during polymerization or degradation of the backbone during deprotection of functional groups [71]. The synthesis of most functional polyesters requires a complex multistep synthesis of protected functional monomers before polymerization. Molecular weights of the resulting polymers are usually not high enough for use, likely because bulky protecting groups decrease monomer reactivity. Copolymerization of functional monomers with the parent or other monomers

has thus been studied. However, due to the large differences in monomer reactivity, incorporation of functional monomers into the polymer chain has not been easy to control, and the polymers obtained generally have low molecular weight, large polydispersity, and poor physical properties. Furthermore, the protecting groups must be subsequently removed prior to further chemical manipulation, which often causes degradation of the polymer backbone.

Lipases have been used for preparation of polyesters by polycondensation reactions, with the advantage that the enzyme catalyzed reaction proceeds without the need for protection of the pendant functional groups.

This background formed the rationale for the synthesis of a novel polyester poly (glycerol adipate) with the aim of achieving better drug incorporation and controlled release of a wide range of drugs. Kallinteri *et al* reported the synthesis of Poly Glycerol adipate using divinyl adipate and glycerol based on the method by Kline, The specificity of lipase to acylate only the primary hydroxyl groups was exploited thus leading to synthesis of polyesters with free secondary hydroxyl groups that were available for further substitution and modifications. The polymer yield and configuration was controlled [72]. Jerome *et al*. developed ε-CL derivatives via a Baeyer–Villiger oxidation of cyclohexanedione derivatives, γ-ethylene ketal and triethylsilyloxy-ε-CLs [73]. Deacetalization of γ-ethylene ketal followed by reduction of the resulting ketone produced a hydroxyl group. Incorporated triethylsilyloxy groups when hydrolysed further resulted in hydroxyl group formation. Gimenez and others reported carboxyl-bearing PCL by extracting α-hydrogen with lithium *N*, *N*-diisopropylamide followed by the addition of carbon dioxide [74]. A 4-hydroxy-L-proline, was

also employed as a monomer unit having a pendant amine, and polymerized by polycondensation after protection of the amine group [75].

Ketal-ε-CL synthesised by Jerome and coworkers seems to be very promising, due to its comparable ring opening reactivity to ε-CL and ability to produce high-molecular-weight polyesters. Its potential to produce a successful drug delivery system is currently under investigation.

Taniguchi *et al.* employed ketone-bearing PCL as the functionalized backbone to which PEO side chains were conjugated. They found that PCL- PEO copolymers with PEO contents above 30 wt% completely inhibit cell adhesion, and become water

soluble when the PEO content was over 50 wt%. In addition, free hydroxyl end groups of the PEO side chains allow further chemical manipulations. As an example, the cell-signalling peptide RGD was conjugated to PEO side chains, and the resulting RGD-bearing copolymer showed NR6 WT fibroblast adhesion through receptor-ligand recognition. Use of free hydroxyl groups for drug conjugation has not yet been investigated [76].

1.2.5. Recent advances in PLGA chemistry for colloidal drug delivery

Jiang *et al* synthesised a new class of polyanhydrides of alternate poly (ester-anhydrides) containing a para-hydroxy benzoic acid moiety. This has the potential to be used as a polymeric prodrug for malaria and hepatitis B. Little work has been reported on modifying the hydrophobic segments of homopolymers like PLA or PCL [77]. Haixiong *et al* developed amphiphilic block copolymers with PEG as middle block and PCl/PLA copolymers as other blocks. They studied the effect of changes in caprolactone / lactic acid ratio in the hydrophobic blocks on size, encapsulation efficiency and release of

nimodipine. The PCL block favours chain flexibility and lowered bulk modulus while the PLA block increases the rate of biodegradation thus resulting in particles with good permeability and favourable biodegradability [12] .

The self assembling characteristics of elastin like proteinaceous polymers was explored by Vanrell *et al.* in their study with poly (L-valine-L-proline-L-alanine-L-valine-L-glycine) (VPAVG), forming stable microparticles that could be used as vehicles for controlled release formulations. Mucoadhesive polymers have been studied for targeting to the mucus covering the intestinal epithelium [6]. Prego *et al* encapsulated calcitonin within chitosan nanocapsules [78]. Amphiphilic diblock co polymer micelles are reported to be effective for hydrophobic drugs, either by covalent coupling to the block co polymer or by physical incorporation within the hydrophobic cores [79]. Polymer drug conjugation is gathering attention to improve physicochemical and biopharmaceutical properties of drugs like Paclitaxel (PTx), Adriamycin etc. Poly (aspartic acid)-PEG evaluated as a carrier showed high drug loading and long circulation time for adriamycin [80, 81]. Methoxy (PEG) PLA, PLGA or PCL copolymers, poly glutamate, albumin etc have been conjugated with PTx as carriers [82-84]. Major limitations however are obtaining drug derivatives and functional polymers with suitable chemical functional groups, physicochemical, biopharmaceutical properties and the multistep reactions necessary to obtain conjugates [84].

Novel biodegradable polyesters, consisting of short poly (lactone) chains grafted onto poly (vinyl alcohol) (PVA) or charge-modified sulfobutyl-PVA biodegradable. (SB-PVA) were prepared by bulk melt polymerization of lactide and glycolide in the presence of core polyols. The modified backbones were

obtained by reacting the activated PVA with the sulfobutyl groups. These polymers undergo spontaneous self-assembly to produce NPs, which form stable complexes with a number of proteins such as human serum albumin and cytocrome C. [85].

1.2.6. Methods of preparation

1.2.6.1. Emulsification Solvent Evaporation

The most common method used for the preparation of solid, polymeric nanoparticles is the emulsification–solvent evaporation technique. The preparation of particles by the classical method follows the general protocol of dissolving the polymer in a water immiscible, volatile organic solvent which is then emulsified with an aqueous phase to stabilise the system. The organic solvent is then evaporated inducing the formation of polymer particles from the organic phase droplets. The solvent evaporation method was described by Niwa *et al* and has since been widely used to prepare particles from a range of polymeric materials, particularly PLA and PLGA [86]. This technique has been successful for encapsulating hydrophobic drugs. However, results for incorporation of hydrophilic bioactive agents have been poor. A modification of this procedure has led to the protocol favoured for encapsulating hydrophilic compounds and proteins viz., the double or multiple emulsion technique. First, a hydrophilic drug and a stabilizer are dissolved in water. The primary emulsion is prepared by dispersing the aqueous phase into an organic solvent containing a dissolved polymer. This is then reemulsified in an outer aqueous phase also containing stabilizer [6, 45, 87-89]. From here, the procedure for obtaining the nanoparticles is similar to the single emulsion technique for solvent removal. The main problem with trying to encapsulate a hydrophilic molecule like a protein or

peptide-drug is the rapid diffusion of the molecule into the outer aqueous phase during the emulsification.

Several parameters can influence the properties of the particles produced, these parameters include:

- nature of polymer

- polymer molecular weight

- nature of organic phase

- polymer concentration in the organic phase

- volume ratio of organic: aqueous phase

- nature of surfactant

- surfactant concentration and molecular weight

- stirring speed.

The main drawback of this method, besides the problem of preparing particles which are sub 200 nm in diameter is the need for the removal of excipients post production. Any residual organic solvents will have toxicological implications. In addition the excess surfactant used is difficult to remove. Another limitation is that surfactant must be present for preparation of nanoparticles in order to stabilize the system. Particles therefore cannot be produced naked and then post adsorbed with a surfactant. polyvinyl alcohol (PVA) is most frequently used as a stabilizing emulsifier to fabricate nanoparticles. However, PVA has some problems in that it remains at the surface of the nanoparticles and is difficult to remove subsequently. It is known that PVA existing on the surface of nanoparticles changes biodegradability, biodistribution, particle cellular uptake, and drug-release behaviour [90].

1.2.6.2. Interfacial Polymer Deposition (IPD) Method

The IDP method was first described by Fessi *et al* [91]. The technique involves addition of polymer, dissolved in a water miscible solvent (usually acetone) into an aqueous non solvent under stirring. The non-solvent is usually an aqueous surfactant or drug solution without surfactant. The rapid diffusion of solvent into the aqueous phase causes a decrease in the interfacial tension between the two phases which, together with the increased interfacial surface area created by the turbulence, results in the formation of small droplets of organic solvent without the need for high shear mechanical stirring. The solvent then diffuses further into the aqueous phase and water concurrently diffuses into the solvent droplets, resulting in the formation of polymer particles from the droplets. Particles are stabilised by a layer of polymer deposited at the interface. Thus, polymer properties may alter the physicochemical properties at the interface as explained in the Marangoni effect [92].

 Decreased miscibility of organic solvents with water is associated with an increase in their resultant interfacial tension and thus increases the size of the particles. The higher the viscosity of the organic phase, the greater the surface tension and hence the size of the particles. An increase in molecular weight of polymers is associated with a decrease in the number of end carboxyl groups and hence lowers the zeta potential of the resulting particles. Additives present in the formulation may also significantly affect this surface charge. Carla *et al* studied PLA nanocapsules in the presence and absence of lecithin. PLA with high molecular weight (109 and 251 kDa) yielded poorly stable nanocapsules larger in size and susceptible to aggregation. In the presence of lecithin, polymer charges

were masked and zeta potential was determined by amount of lecithin present on the outer surface either mixed with or surrounding the polymer film [93].

The presence of surfactant in the system acts as a stabilizer to prevent coalescence of the droplets. However Fessi *et al* reported that particles could be prepared using his method, in presence of water alone as the aqueous phase. Paclitaxel and mPEG-PLGA nanoparticles prepared without surfactant exhibited a smaller size and higher encapsulation efficiency. Surfactants like PVA were important to form nanoparticles in a technique like emulsification as here they prevent coalescence of newly formed droplets. However, Pluronic F-68 like surfactants may be added to improve steric stability of particles produced by the IPD method but are not primarily responsible for formation of particles [94].

A distinct advantage of the IPD method is that there are no residual solvents left in the system, which is important from a toxicological point of view. Another advantage, from the viewpoint of using particles as a drug carrier, is that the particles produced are in the nanometer size range. Fessi *et al* prepared particles below 200 nm, and PLGA particles have been prepared which are sub 100 nm. In addition, the samples exhibit low polydispersity and the preparation of particles in the absence of surfactant allows the effect of post adsorption of surfactants. In particular, the in vivo behaviour of the coated and uncoated particles can be compared in order to determine the role of coating surfactant in preventing particle recognition by the Mononuclear Phagocytic System (MPS).

1.2.6.3. Spray Drying

In the classical spray drying technique the polymer and drug are dissolved in an organic solvent and sprayed through a fine nozzle. Solid, spherical particles form on the immediate evaporation of the solvent. High temperatures are generally

employed in this process, which can create problems, particularly in the encapsulation of peptides, and proteins that are easily denatured. Spray drying produces particles that are in the micrometer size range and hence will not be considered further here.

1.2.6.4. Salting Out

Bindschaedler and co workers patented this technique in 1988 [95]. The technique involves the preparation of particles by an emulsification technique but avoids the use of chlorinated solvents. In brief, a saturated salt solution containing a stabilizing agent such as PVA is added under stirring to an acetone solution of the polymer. An o/w emulsion forms as the salt prevents the water and acetone mixing. Sufficient water is then added to allow the acetone to diffuse into the external aqueous phase and induce particle formation. Allemann *et al* used this technique to prepare Savoxepine nanoparticles. From the perspective of drug encapsulation, this method is most appropriate for water insoluble compounds, although the loading of water-soluble compounds can be improved by techniques such as altering the pH of the aqueous phase [96]. Salts permeate biological systems and are crucial for life. However, salts also affect the stability of proteins. It has been reported since many years that neutral salts perturb various protein structures in ways that go well beyond simple, nonspecific charge effects [97].

1.2.6.5. Supercritical fluid expansion method

Recently the field of supercritical fluids has been investigated as an approach to the preparation of sub micron sized particles [94].

The rapid expansion of supercritical solutions consists in saturating a supercritical fluid with the substrate(s), then depressurizing this solution through a heated nozzle into a low pressure chamber in order to cause an extremely rapid nucleation of the substrate(s) in form of very small particles or fibres, or films when the jet is directed against a surface that are collected from the gaseous stream. The major merits of these processes include: production of organic-solvent free particles, mild operating temperatures for processing biological materials, and easier micro-encapsulation of drugs for controlled release of the therapeutic agents [98]. Unfortunately, none of these techniques can produce small protein particles in the sub-micron range less than 300 nm having a very narrow size distribution. Fine particles of model compounds cholesterol acetate (CA), griseofulvin (GF), and megestrol acetate (MA) were produced by extraction of the internal phase of oil-in-water emulsions using supercritical carbon dioxide [99].

1.2.6.6. Complex Coacervation

Complex coacervation is a phase separation process that spontaneously occurs when two oppositely charged polyelectrolytes are mixed in an aqueous solution. Compared to other methods, this process can be performed entirely in an aqueous solution and at low temperature and thus has a better chance to preserve activity of the encapsulated substances. The colloidal particles produced are in the nanometer or micrometer scale depending on the substrates or the processing parameters used for example; pH, ionic strength and polyelectrolyte concentrations [100-102]. The major drawback of this technique is that complex coacervates have low drug loading efficiency and poor stability. Therefore, crosslinking of the complex by chemical reagents such as toxic glutaraldehyde is

necessary. Jiang B *et al* have reported a modified method called 'co-precipitation' where they chose positively charged and water-soluble Dextran as a coating layer [103]. The process included precipitation of negatively charged Ibuprofen in a supersaturated solution and deposition of Dextran onto the precipitated Ibuprofen particles through electrostatic interaction.

1.2.7. Drug Release Mechanisms

Nanoparticles exhibit their special drug delivery effects in most cases by direct interaction with their environment, i.e., their biological environment. Drug release may occur by-

- Desorption of surface bound drug

- Diffusion through the nanoparticle matrix

In the case of Nanocapsules, diffusion through the polymer wall

- Nanoparticle matrix erosion

- A combined erosion diffusion process.

Biodegradable materials are intended to degrade within the body after the release of the active agent has been completed. This eliminates the need for removal of the material after drug release.

Extensive research has been dedicated towards the hydrolytic degradation characteristics of PLA homo- and copolymers in recent years [104]. Internal autocatalysis is a characteristic phenomenon which results in a concentration difference in carboxyl end groups between the surface and the centre. PLA samples that were thicker degraded more rapidly inside than at the surface [105]. The enzymatic degradation of PLA has also been extensively investigated during the past two decades, and among numerous selected enzymes, proteinase K, pronase, and bromelain have an acceleration effect on the degradation of PLA

[106]. Further studies have reported that proteinase K degraded l-lactyl units preferentially while d-lactyl ones are biostable [104].

Surface biodegradable polymers include polycarbonates, polyanhydrides, and polyorthoesters. Their matrices were highly hydrophobic, and unstable chemical bonds exist in the polymer main chains [107]. Degradation studies on pure polymer implants have shown that solid-state morphology and the polymer composition (homo- or *co*-polymers of lactic or glycolic acid), tacticity ($_D$ - or $_L$ isomers, racemic mixtures of $_D$, $_L$) can influence polymer degradation [105]. Polymer properties such as molecular weight, crystallinity and glass transition temperature also control the degradation rate of the polymers. Studies have shown that the choice of dissolution conditions under which the degradation process is studied can also influence the degradation process [108].

Most biodegradable polyesters are designed to degrade as a result of hydrolysis of the polymer chains into biologically acceptable, and progressively smaller, compounds. For example, polylactides, polyglycolides, and their copolymers eventually break down to lactic acid and glycolic acid, enters the Kreb's cycle, and is further broken down into carbon dioxide and water and excreted through normal processes. Kenley *et al* extensively studied quantitative correlations between PLGA physical / chemical properties and degradation rates. For PLGA 50:50 they concluded that polymer erosion proceeds via internal, not surface hydrolysis. Dissolution, polymer erosion and molecular weight degradation at 37°C, pH 4.5, to 7.4 in vitro accurately model the processes in vivo, and PLGA degradation adheres to pseudo-first-order kinetics governed by the rate of macromolecular ester bond cleavage. Also, PLGA erosion initially does not parallel macromolecular bond heterolysis. Therefore directly relating polymer

erosion to parameters (e.g. lactide: glycolide ratio) that control the bond cleavage kinetics is potentially misleading [109]. Secondly, the (presumably acidic) microenvironment interior to hydrolyzing PLGAs could potentially accelerate the degradation of drugs or other materials dispersed throughout the PLGA matrix material.

Polyamides: Although polyamides contain the same amide linkage that is found in polypeptides, their rate of biodegradation is much lower than the polyaminoacids. It is so slow that often they are reported to be nondegradable. The higher crystallinity of polyamides due to strong interchain interactions (as compared with the more flexible polyesters with analogous structures), is responsible for lower rates of biodegradation. Copolymers with both amide and ester groups are generally found to be readily degraded [110]. The rate of degradation increases with increasing ester content.

Polyurethanes: Polyurethanes can be considered to have the structural characteristics of both polyesters and polyamides. Although polyureas might be viewed as poly (diamides), their susceptibility to biodegradation can be expected to be similar to that of polyesters and polyamides, with differences in rates. In general the biodegradability of polyurethanes was shown to be dependent on whether the prepolymer is a polyester or a polyether [111]. The polyether-based polyurethanes are resistant to biodegradation whereas the polyester polyurethanes are readily attacked. It has been observed that the degradation rate increases with increasing polyester segment length. It has also observed that polyurethanes derived from aliphatic diisocyanates are degraded faster than those derived from aromatic diisocyanates [112].

Aliphatic polyanhydrides degrade within a few days while aromatic polyanhydrides can degrade slowly over a period of several years. An increase in the aliphatic chain length between the acid groups not only increases their molecular weight but also notably improves their hydrolytic stability [113].

Poly (alkyl acrylates) and polycyanoacrylates generally resist biodegradation. However, they are often referred to as 'biodegradable' referring to the loss of the alkyl chain. Poly (methyl-2-cyanoacrylate) is the most degradable among the alkyl esters; degradability decreases as alkyl size increases [114].

Thus, depending upon the polymer chemistry, degradation may take place through bulk hydrolysis, in which the polymer degrades in a fairly uniform manner throughout the matrix (see Fig. 1.3 a) or in case of polyanhydrides and polyorthoesters, through surface degradation, in which rate of release is proportional to surface area of the particles (see Fig. 1.3 b).
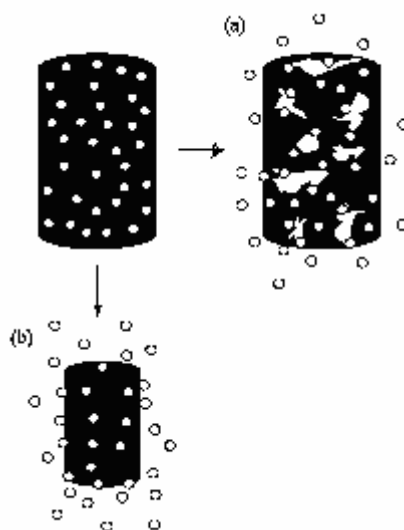
Fig. 1.3. Drug delivery from (a) bulk-eroding and (b) surface-eroding biodegradable systems.

The type of polymer and design of the system (composition and geometry) controls different physicochemical processes involved in the rate of drug release.

Thus, the erosion of the polymer may play an important role. In surface eroding systems, polymer degradation is much faster than the water imbibition into the polymer bulk. Thus, degradation occurs predominantly within the outermost polymer layers. Consequently, erosion affects only the surface and not the inner parts of the system (heterogeneous process). In contrast, bulk eroding polymers degrade more slowly and the imbibition of water into the system is much faster than the degradation of the polymer. Hence, these polymers are rapidly wetted and polymer chain cleavage occurs throughout the system. Consequently, erosion is not restricted to the polymer surface only (homogeneous process). As a basic rule, polymers containing very reactive functional groups tend to degrade fast and tend to be surface eroding, whereas polymers with less reactive functional groups tend to be bulk eroding. PLGA-based microparticles can generally be regarded as bulk eroding dosage forms [115].

The release mechanism, the diffusion coefficient, and the biodegradation rate are the main factors governing the drug release rate. The release rate of drugs is also strongly influenced by the biological environment. This environmental influence is far more important in larger dosage forms; nanoparticles may be coated by plasma proteins, which can establish a significant additional diffusion barrier and lead to a retardation of release [116]. Nanoparticles also interact with biological or artificial membranes, in this case leading to an enhanced delivery of drugs through these membranes in comparison to a simple solution. As a consequence it has been frequently observed that in vitro drug release may have very little in common with the delivery and release situation in vivo. Nevertheless, for characterization purposes and for quality control reasons, the determination of the in vitro release of drug from nanoparticles is important.

The characterization of the in vitro drug release from a colloidal carrier is technically difficult to achieve. This can be attributed to the inability of effective and rapid separation of the particles from the dissolved or released drug in the surrounding solution owing to the small size of the particles [109].

1.2.7.1. Methods of determination of drug release

The following methods for the determination of the in vitro release have been used:

1. Side by side diffusion cells with artificial or biological membranes

2. Dialysis bag diffusion technique

3. Reverse dialysis sac technique

4. Ultracentrifugation

5. Ultra filtration (Centrifugal) technique

The dialysis technique is a very popular method to study the release of drugs from colloidal suspensions. The limits of this technique have been discussed by Washington [117], who reported that the colloidal dispersions were not diluted inside the bag. The release rate of the drug and its appearance in the dissolution medium is governed by the partition coefficient of the drug between the polymeric phase and the aqueous environment in the dialysis bag and by the diffusion of the drug across the membrane as well. This technique thus allows the comparison of different formulations.

1.2.7.2. Factors affecting Drug Release

- *Water permeability and solubility (hydrophilicity/hydrophobicity)*
- *Chemical composition*
- *Mechanism of hydrolysis (non catalytic,autocatalytic,enzymatic)*
- *Additives (acidic,basic,monomers,solvents,drugs)*

- *Morphology (crystalline, amorphous)*
- *Device dimensions (size, shape, surface to volume ratio)*
- *Porosity*
- *Glass transition temperature (glassy, rubbery)*
- *Molecular weight and molecular weight distribution*
- *Physio-chemical factors (ion exchange, ionic strength, pH)*
- *Sterilization*
- *Site of implantation*

Table 1.2. Factors affecting hydrolytic degradation behaviour of polyesters [118].

Besides polymer erosion, a number of interrelated factors govern rate of release from particles (Table 1.2). Mainly the physicochemical properties associated with particles such as size, shape, porosity, morphology etc. These, in turn are influenced by a variety of factors, for example; method of preparation, formulation parameters to name a few.

1.2.7.2.1. Particle size

As reported by Washington [117], for particles only a few hundred nanometres in diameter the release can be very rapid with a very high rate of release due to the large surface area of the particles. Larger particles have a smaller initial burst and longer sustained release than smaller particles [119]. Increased size and zeta potential of particles may enhance uptake of particles by the Reticulo - Endothelial System (RES) while decrease in size and increase zeta potential may lead to increased stability of the particles. Size also affects fate of the particles after administration. Smaller particles accumulate in tumour sites due to facilitated extravasation and greater endocytosis also occurs. Size less than 200 nm greatly reduces filtering and uptake by the spleen. In their study with chitosan nanocapsules encapsulating calcitonin (CT) Prego *et al* found that size of the capsules depends upon chain length of chitosan, it decreased with increase

in molecular weight of chitosan. They found similar zeta potential values irrespective of chitosan molecular weight, but an increase in the initial amount of oil phase decreased the surface charge. Oligomers showed no release for 6 hours while 20% calcitonin was released rapidly with the medium molecular weight chitosan. Lack of fast release from oligomers may again be due to reduced amount of chitosan on the coating and less interference with calcitonin binding [78].

1.2.7.2.2. Nature of drug/ additives

Besides particle size, many other parameters have been shown to affect the drug release profiles. The nature of the drug or other additives is obviously very influential and log P, pKa and molecular weight are some of the important parameters. Additives through their acidic or basic nature as well as loading level in the case of therapeutic agents may markedly affect the degradation rate of microspheres. Maulding *et al* have reported on the acceleration of microsphere degradation rates by incorporation of a tertiary amino compound, thioridazine. They suggested that the nucleophilic nitrogen of the thioridazine base participated in the degradation of ester bonds as little effect was seen when the amino group of thioridazine was protonated and the salt (pamoate) was incorporated in the microspheres [120].

Basic compounds can catalyze ester linkage scission and thus accelerate polymer degradation. On the other hand, appropriate amounts of basic compounds can neutralize carboxyl end groups and thus decrease the rate of degradation. In a study by Li on degradation of PLA in the presence of caffeine it was found that in the early stages basic catalysis occurs by caffeine as only a few carboxyl

groups were present and the molecular weight of the matrix was high. As degradation proceeded, new carboxyl end groups were formed, caffeine was provided with more chances for interaction with carboxyl end groups and thus neutralization of the newly formed carboxyl groups became the main factor responsible for decreasing the rate of degradation [121]. This potential effect by the acidic / basic nature of the therapeutic agent incorporated in the microspheres must be considered in the design of the delivery system.

The degree of drug loading is often correlated with the release profile, especially since the drug may be crystallized in the carrier matrix at high loadings. For example, PLA nanoparticles containing 16.7% savoxepine released 90% of their drug load in 24 h as opposed to particles containing 7.1% savoxepine which released their content over 3 weeks [122].

Some studies have investigated inclusion of various additives that enhanced drug incorporation and eventually controlled drug release. Encapsulation efficiency of propafenone HCl in PEG-g-PLA polymer prepared without triethyleneamine (TEA) was 10%. It increased to 43% with the use of TEA probably due to the scavenging action of TEA on Propafenone HCl. This set free the pure hydrophobic base and enhanced its interaction with the hydrophobic PLA core of the polymer [123]. Okada *et al* have also shown that increased interactions between carboxyl groups of PLA and amino groups of basic drugs like leuprorelin acetate enhances their encapsulation efficiency and reduces rate of release [124]. The rate of release is also influenced by the method of drug loading. Fresta *et al* reported 60 to 70% initial burst for particles incorporating drug by adsorption. Thus, a method of incorporating drug into the matrix provides more sustained release profile [125].

For chemically conjugated drug, release occurred over a period of 25 days compared to unconjugated drug where all drug release takes place within 5 days [126]. Also, release of conjugated drug will be influenced by the chemistry of attachment to the polymer.

1.2.7.2.3. Polymer properties and drug loading

The parameters of the polymer can be selected to influence the release profile. With PLGA for example, the molecular weight, crystallinity and lactide: glycolide ratio can be chosen to alter drug release. Duan *et al* synthesised monomethoxypolyethylene glycol-PLGA monomethoxypolyethylene glycol (mPEG-PLGA-mPEG) nanoparticles using mitoxantrone as a model drug [127]. PLGA co polymers with varying molar ratios of lactic acid to glycolic acid and different molecular weights and contents of mPEGs were synthesised and evaluated. They found that the amount of mitoxantrone released increased as mPEG contents increased and the molar ratio of lactic acid decreased. Increase in drug loading led to a slower release rate than from lower drug loading. Increased drug loading was observed with increased lactate ratio. Thus, increased lactic acid led to an increase in hydrohobicity that enhanced drug loading and decreased rate of drug release. Also, lower the molecular weight of the polymer faster is the degradation and drug release rate. Higher molecular weight polymers have a lower number of carboxyl groups and hence decreased solubility. Higher water solubility of the polymer contributes to lower surface tension and decreased size which may be responsible for an increase in the rate of release [128]. To minimise this effect in the pre nanoparticle formation stage several researchers have explored the possibility of modifying the backbone in order to decrease burst effect. Hata *et al* patented a sustained release preparation wherein

they substituted a 2(N- benzylcarbonyl) - aminoethanol group to the terminal carboxyl end of PLGA and reported improved rate of incorporation of a bioactive substance containing acidic groups. They also observed that this modification suppresses drug leakage early after administration, and exhibits constantly suppressed release for an extended period of time [129]. Oh *et al* conjugated the hydrophobic fluorenylmethoxycarbonyl (FMoc) protected amino acid tryptophan (Boc-try) to the hydroxyl end of PLGA. They hypothesised that when conjugated PLGA chains are randomly hydrolysed water soluble fractions are leeched out and drug bound to terminal ends of cleaved PLGA will be released concomitantly. Further in vitro and in vivo studies are reported to be in progress [130].

After water imbibition into PLGA-based microparticles, drug dissolution and the cleavage of the hydrolytically unstable ester bonds occurs. Simultaneously, the drug diffuses out of the device due to concentration gradients. Drug diffusion can occur: (i) predominantly through the polymer matrix; (ii) predominantly through water-filled pores; or (iii) through both, the macromolecular network and water-filled cavities in parallel and/or in sequence [131]. Several researchers have tried to explore the mechanisms of burst and prevent it by several methods such as surface coating of the polymer [19, 132, 133], changing the surfactant [130], changing the molecular weight of the polymer [88] etc.

1.2.7.2.4. Porosity

Altering the porosity of the particles also affects the drug diffusion and polymer degradation rate. Lemaire suggested that if a drug molecule is present within a network of micropores it will have to diffuse towards the closest pore to be released outside. Movement of the drug within the porous media is highly

restricted due to limited space available and is influenced by diffusivity of drug, porosity and tortuosity of matrix [134]. Rapid release of savoxepine and estradiol from P$_{(DL)}$LA nanoparticles prepared using the salting out method and release of dexamethasone from PEO-P$_{(DL)}$LA nanoparticles have been explained by presence of pores in the particles [135-137]. The presence of pores and a high water uptake of PEO-PLGA nanoparticles led to high permeability of drug in the polymer matrix. The release was rapid and was complete within 5 hours for the untreated nanoparticles [136].

1.2.7.2.5. Method of preparation

The method of preparation also plays an important role in drug release. NP preparation by o/w emulsion is a complex process in which organic solvent generates pores in the structure on evaporation which may then lead to a change in the microstructure of NPs and affect their release kinetics. In addition, the products generated by polymer degradation can significantly alter the microenvironment conditions, e.g., the H$^+$ concentration within the system. Lactic and glycolic acid resulting from the degradation of PLGA polymers can lead to significantly decreased pH values in the core matrix [137]. As the degradation of PLGA is catalyzed by protons, this decrease in pH can lead to autocatalytic effects and thus, to accelerated polymer degradation [138]. Furthermore, degradation products of polymer can crystallise within the core leading to modified porosities which can enhance their diffusion [139]. Depending on their solubility and the respective microenvironmental conditions, these degradation products subsequently dissolve more or less rapidly and diffuse out of the device. At a critical time-point, the polymeric structure of the

system becomes unstable and leads to the breakdown of the macromolecular network.

The nature of organic solvent used is also influential in rate of release. For example, solubility of dichloromethane (DCM) in water is low. After formation of a primary emulsion DCM gradually diffuses out of the nascent particles, dissolves in the water and disperses. Slow evaporation leads to good spherical particles with a porous microstructure. Acetone, due to its high miscibility dissolves faster in the aqueous phase and hence irregular shaped particles are formed. When used in combination to form the organic phase, dispersion of the water soluble solvent would result in a decreased surface tension and size [140]. Increase in water insoluble solvent would lead to further size reduction without pores. This would also lead to an increased drug loading and decreased rate of release. Finally, it should be highlighted that the nature of release medium is extremely important. As yet, there is no defined in vitro dissolution test for colloidal particles intended for potential administration and as a result, many types of release medium have been used.

1.2.7.2.6. Physical state of drug and polymer

Physical state of the drug inside the nanoparticles plays a key role in the drug diffusion from nanoparticles. An amorphous form of the drug may lead to an increase in the rate of dissolution of the drug. Amorphous materials do not have any long range order such as crystal lattice as crystalline materials do. They have a higher internal energy, a larger free volume, and greater molecular mobility in comparison to the crystalline state. These properties are responsible for greater solubility and hence fast release. Small drug molecules can also easily crystallise and consequently both crystalline and amorphous state are possible.

The physical state of polymer is also instrumental in influencing drug release rate. Amorphous or crystalline drug may be present in either amorphous or crystalline polymer. The DSC technique can provide qualitative and quantitative information about the physicochemical status of the drug in the particles, which may be involved in either an endothermic or exothermic process [141]. The related thermal transitions include melting, recrystallization, decomposition, out-gassing, or a change in heat capacity. DSC is useful to monitor different samples of the same material to assess their similarities or differences or the effects of additives on the thermal properties of a material. Using DSC analysis of drug, polymer materials and the resulting nanoparticles, the nature of the drug inside the polymer matrix can be assessed, which may be present in a solid solution, metastable molecular dispersion or in a crystalline form and may display relevant properties during in vitro release. There is no detectable melting endotherm if the drug is present in a molecular dispersion or a solid solution state in the polymeric microspheres loaded with sufficient drug. When the glass transition temperature (Tg) of polymer is higher than ambient temperature, the polymer is in a glassy state and the material is brittle and hard. Below the Tg polymer is in a rubbery state and hence promotes mobility and release of drugs. Drugs or additives if well dissolved in the particles may act as a plasticizer and reduce the Tg of nanoparticles. On the other hand, a crystalline form may act as reinforcing filler and cause an increase in Tg. [142, 143].

1.2.8. Drug Loading

A successful NP system may be one which has a high loading capacity to reduce the quantity of the carrier required for administration. Drug loading into NPs is achieved by two methods: one, by incorporating the drug at the time of NP

production or secondly, by adsorbing the drug after the formation of NPs by incubating them in the drug solution. A larger amount of drug can be entrapped by the incorporation method than by adsorption. Couvreur *et al* reported the adsorption of two antineoplastic drugs viz, dactinomycin and methotrexate onto (poly methylcyanoacrylate) and poly (ethylcyanoacrylate) nanoparticles [112]. The capacity of adsorption is thus related to the hydrophobicity of the polymer and the specific area of the NPs. In the case of entrapment methods, an increase in concentration of the monomer increases the loading efficiency of drug, but a reverse trend is observed with an increase in the initial drug concentration in solution [144].

In addition to adsorption and incorporation, an alternative method of drug loading was proposed by Yoo and co workers [126]. In this method, the drug was chemically conjugated to the NPs. The conjugated doxorubicin–PLGA and doxorubicin-loaded PLGA NPs were prepared by the spontaneous emulsion–solvent diffusion method. An encapsulation efficiency of 96.6% and drug loading of 3.5% of doxorubicin–PLGA conjugate were achieved. For the unconjugated doxorubicin, these values were 6.7% and 0.3% (w/w) respectively.

In a study of encapsulation of calcitonin within Chitosan oligomer, encapsulation efficiency within the nanocapsules was higher (60%) than when prepared using medium molecular weight chitosan polymer (44%). This was attributed to a lower amount of chitosan oligomers forming a coat on the preformed nanoemulsion compared to medium MW chitosan, thus competition to associate with the nanoemulsion surface was less and more peptide got incorporated [78]. Watanabe *et al* studied the entrapment of various charged and uncharged molecules within chitosan nanospheres. Chitosan is polycationic in

nature. Texas red, DNA (negatively charged), Ovalbumin (amphoteric), Trypsin (positively charged) were successfully incorporated within the nanospheres. However, there was no entrapment of FITC-dextran (non ionic) [128]. Thus, electrostatic interaction plays a pivotal role for use of this polymer as a carrier system and hydrophobic interaction only rarely contributes to entrapment into these nanoparticles. They also found that the encapsulation efficiency influenced the size and zeta potential to a small extent as the negatively charged compounds were incorporated to a greater extent and formed particles slightly larger in size. Zeta potential varied depending on the charge of the incorporated compound.

1.2.8.1. Factors affecting encapsulation efficiency

The extent of drug entrapment in the polymeric core by physical means is dependent on several factors, including the molecular volume of the solubilizate, its interfacial tension against water, length of the core and shell-forming blocks in the copolymer, and solubilizate concentration [145]. The partition coefficient of the hydrophobic molecule between the micellar core and surrounding aqueous medium describes the extent of drug entrapment in polymeric micelles. The greatest degree of solubilization occurs when high compatibility exists between the micellar core and the solubilizate, assessed by the Flory–Huggins interaction parameter (Xsp).

In the case of PLGA / PLA nanoparticles with a suitable size for intravenous administration, major obstacles to clinical use include the complicated process of preparation and the low encapsulation efficiency of bioactive molecules. The efficiency of encapsulating bioactive molecules into PLGA / PLA microparticles / nanoparticles largely depends on the physical properties of the molecules. Chemical modifications of bioactive molecules such as esterification increase

their encapsulation efficiency, but may decrease their bioactivity. Drug-loading of ketoprofen-containing biodegradable and biocompatible poly ($_{DL}$-lactic-co-glycolic acid) (PLGA) microspheres, prepared by the solvent evaporation method, were investigated by Gabor *et al* [146]. For both drug-free and drug-loaded microspheres; smaller microspheres with a narrower size distribution were obtained when the stirring rate or the volume of the organic phase was increased. Incorporation of ketoprofen was found to increase with increasing volume of the organic phase and decreasing pH of the aqueous phase, but was independent of the acidity and the inherent viscosity of the PLGA used. Formulations involving solvated β-estradiol (especially using ethyl acetate) showed maximum encapsulation of hormone within PLGA microparticles when compared with formulations without ethyl acetate. Also, the organic phase used was a mixture of dichloromethane/methanol, as the methanol quickly partitioned to the aqueous phase [147]. The ratio of dichloromethane / methanol played an important role in the encapsulation of the drug. The β-estradiol is considerably more soluble in the co-solvent system than just methanol. Thus, relatively large quantities of drug could be dissolved in the co-solvent that otherwise would not dissolve in methanol alone. Encapsulation of solid β-estradiol was also enhanced by making the dispersed phase more viscous. Reducing the volume of the organic solvent used (DCM) would serve to increase the viscosity of the dispersed phase as well as decrease the microparticle hardening time. Both factors result in enhancing the encapsulation of the solid drug [147]. Molecular weight and concentration of polymer used can also affect the encapsulation efficiency of drugs. The molecular weight of the polymer has contradictory effects on nanoparticle size and encapsulation efficiency. Smaller size

nanoparticles can be prepared with lower molecular weight polymer, but, at the expense of reduced encapsulation efficiency. On the other hand increase in polymer concentration increases encapsulation efficiency and size of nanoparticles [88, 148].

Thus, we can see from the literature review that over the last 20 years, increasing attention has been paid to synthetic aliphatic polyesters derived from lactones, lactides, and glycolide for applications in medicine and surgery. Nevertheless the shortage of polyester chains bearing functional pendent groups is a severe limitation to further progress in the field. Indeed, the availability of functional pendant groups is highly desirable for enhancing drug incorporation and lowering burst release especially for water soluble drugs along with the fine tuning of properties in view of, e.g., attachment of drugs, improvement of biocompatibility, and promotion of bioadhesion. However, chemistry involved in the synthesis of the functional monomer is most often complex and / or tedious, whereas the subsequent polymerization is generally out of control [133].

We have investigated poly (glycerol adipate) polymers synthesised by a lipase catalysed reaction to provide a polymer backbone with pendant hydroxyl groups. It is the presence of these free pendant hydroxyl groups on the backbone that allows for substitution of different functional groups and thus modifies the properties of the backbone. NPs were prepared using a combination of various substituted polymers. The drugs used were mainly anticancer drugs and belonging to different classes; water soluble Dexamethasone phosphate, Cytosine arabinofuranoside, Etoposide phosphate and water insoluble Etoposide and

Paclitaxel. Results presented in this study are of the polymer backbone in its unsubstituted form along with a library of substituted polymers namely acyl substituted and aromatic amino acid substituted polymers. These were evaluated for drug incorporation and release. Thus, besides investigating the potential of this polymer for use as a promising drug carrier system this study also helps to obtain a deeper understanding of the physicochemical phenomena involved during nanoparticle formation.

CHAPTER 2. EXPERIMENTAL METHODS

2.1. Synthesis of polymer backbone and acylated polymers

The Poly (glycerol- adipate) polymer backbone and backbone substituted with acyl groups with chain lengths from C_2 to C_{10} and in varying (20, 40 and 100%) was provided by Dr. S.Higgins, Dr.G.Hutcheon, Liverpool John Moores University, UK as a part of BBSRC grant no. E 19350.

The Polymer backbone is a polyester of glycerol and adipic acid linked together by esterification (Fig. 2.1). The polymers have pendant hydroxyl groups which were then further substituted by fatty acyl / amino acid groups. The polymer is a readily hydrolysable polymer, synthesis of which is enzyme catalysed. The enzyme used is Novozyme435, which is a *lipase* derived from *Candida Antartica*.
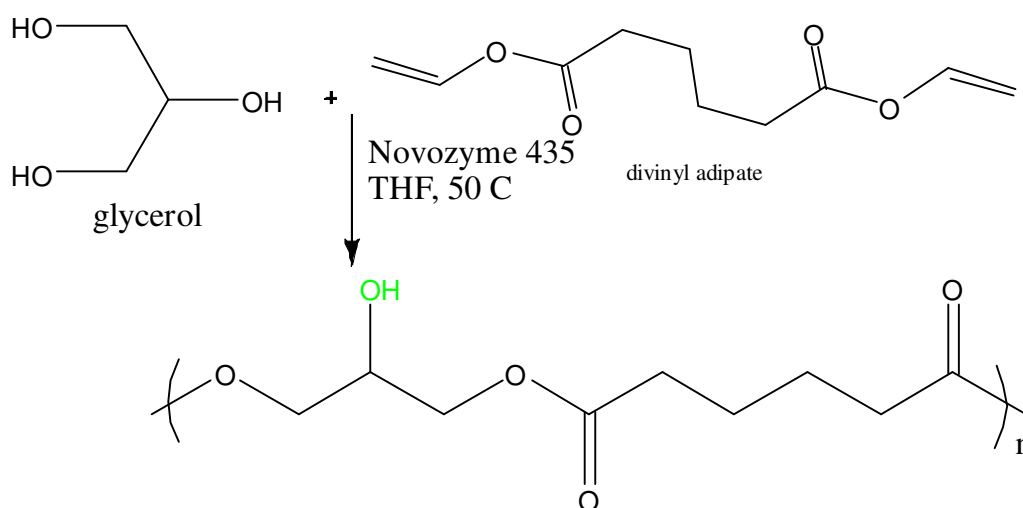
Fig. 2.1. Structure of Poly (glycerol adipate) backbone.

Synthesis of the polymer is a single step reaction and takes place as shown above. Details of reaction mechanism and polymer synthesis reaction conditions are described in detail by Kallinetri *et al* [72].

2.2. (B) Acylation of backbone polyester

The polymer backbone was substituted with acyl groups by a reaction between the pendant hydroxyl groups and various linear aliphatic acid chlorides. The chain lengths of the acyl groups varied from 2 to 10 carbon atoms depending upon the parent carboxylic acid. They were then coupled to the backbone using Pyridine as a catalyst and acid scavenger [72].

2.3. Synthesis of amino acid substituted polymers

2.3.1. Synthesis of 5% tryptophan substituted polymer

The number of reactive hydroxyl sites per gram of polymer with average molecular weight 12 kDa was calculated to be 5 mmoles. Hence polymer backbone (200 mg corresponding to 1 mmole) was dissolved in 5 ml DMF and added to a dry pre weighed round bottomed flask. To this was added 1.5 mmole equivalent EDAC (14.38 mg) and N-Acetyl tryptophan (0.05 mmole = 12.32 mg) under positive pressure followed by addition of 2 ml DMF making the total reaction volume to 7 ml. The reaction mixture was then stirred with gentle magnetic stirring at 4°C for an hour following which 2.5mg of dimethypropyl aminopyridine (DMAP) was added as a catalyst. The mixture was again placed in a cold room at 4°C overnight. Product was obtained by removal of DMF using a rotary evaporator. Excess unreacted tryptophan was removed with a simple washing of 25 ml each of water and methanol. The polymer was then freeze

dried for 2 days till a constant weight was recorded. The resulting product was characterised using NMR and FTIR. Polymer solution (10 mg/ml in acetonitrile) approximately 10 to 12 ml was then passed through a calibrated sephadex LH-20 column for purification and the fractions corresponding to the void volume were collected. Eluent was mixture of ACN/MeOH (75:25).

 Yield of the reaction mixture was 90-92 %.

Similarly polymers with 10, 20, 40 and 60% substitution were prepared using 24.68 mg, 49.26 mg, 100 mg and 147.76 mg N- acetyl tryptophan respectively.

2.3.2. Synthesis of 5% tyrosine substituted polymer

Polymer backbone was substituted with N- acetyl tyrosine in a method similar to that for tryptophan substitution using 11.16 mg tyrosine corresponding to 5% substitution.

2.3.3. Synthesis of 40% C8 + 5% tryptophan substituted polymer

The number of reactive hydroxyl sites per gram of 40% C_8 acylated polymer with an average molecular weight 12 kDa was calculated to be 3 mmoles. Hence 330 mg of 40% acylated polymer (equivalent to 1 mmole) was allowed to react with 12.32 mg N- acetyl tryptophan as described in section 2.2.1.

2.4. Preparation of Nanoparticles

2.4.1. Interfacial deposition method

 (A) Polymer backbone and acylated polymers**:** Nanoparticle dispersions were prepared using the interfacial deposition method of Fessi *et al*.,[91] Briefly, 20 mg of polymer was dissolved in acetone (2 ml) and this solution was added drop

wise into 5 ml of aqueous solution with or without drug. The dispersions were left overnight in a fume hood to allow acetone to evaporate. All particles were made in the absence of surfactants. The particles were filtered through a 1.0 μm filter (Whattman, cellulose nitrate membrane filters) to remove flocculated particles and polymers, when it was necessary. This method was used for water soluble drugs (DXMP, CYT-ARA, ETO-P) in a concentration of 4 mg/ml.

(B) Tryptophan / Tyrosine substituted polymers: 1 ml of polymer solution (10mg/ml) in acetone was added drop wise to 5 ml aqueous solution of 10mM HEPES with/ without drug. The solution was left under gentle magnetic stirring overnight.

2.4.2. Simultaneous Emulsification solvent evaporation method

1 ml Polymer backbone and acylated polymers (10mg/ml) in DCM along with 5 ml polysorbate 80 (1%) was sonicated at 30 W for 30 seconds. Solution was left under gentle magnetic stirring overnight. The emulsification method was only used for the DXMP particles for method comparison purposes.

2.4.3. Interfacial deposition method with reconstituted matrix

This method involves a slight modification of the interfacial deposition method and was used only for the hydrophobic drugs Etoposide and Paclitaxel. Powdered drug (2 mg) was dissolved in the polymer solution (10 mg/ml) in acetone. The organic solvent was allowed to evaporate and the dried mixture was reconstituted in 1 ml of acetone which was then added drop wise to 5 ml water / HEPES solution depending upon the polymer used followed by gentle magnetic stirring overnight.

2.5. Separation of unincorporated drug from drug loaded particles

(A) Particles prepared using backbone and acylated polymers (3-4 ml) were passed through a glass Gel chromatography column (C2.5/40, Pharmacia, bed volume 147 ml) packed with Sepharose CL-4B gel. Fractions, 2 ml per tube, were collected by a fraction collector. Water was used as the eluent. Particles eluted in the earlier fractions were collected and concentrated to 6 ml total volume using vivaspin concentrators in a CENTAUR 2 centrifuge and centrifuged at 3000 rpm for 15 minutes.

(B) For particles prepared using amino acid substituted polymers samples were passed through a column packed with Sephadex G-25 gel. A peristaltic pump was used to maintain the flow of eluent at 1 ml/min, through the column. Fractions, 2 ml per tube, were collected by a fraction collector. HEPES (10nM, pH 7.35) was used as the eluent. Particles eluted in the earlier fractions were collected and concentrated to 6 ml total volume using vivaspin concentrators and centrifuged at 3000 rpm for 15 mins.

2.6. Physicochemical characterization

2.6.1. Particle size

The particle size was determined by dynamic light scattering, using a Malvern system 4700 instrument, with vertically polarised light supplied by an argon-ion laser (Cyonics) operated at 40 mW. All experiments were performed at a temperature of 25.0 ± 0.1^0C at a measuring angle of 90^0 to the incident beam. The analysis mode was CONTIN and 30 readings were taken for each sample.

<u>Principle of working:</u> The PCS method consists in determining the velocity distribution of particle movement by measuring dynamic fluctuations of intensity

of scattered light. The disperse particles or macromolecules suspended in a liquid medium undergo Brownian motion which causes fluctuations of the local concentration of the particles, resulting in local inhomogeneities of the refractive index. This in turn results in fluctuations of intensity of the scattered light. The line width of the light scattered spectrum Γ(defined as the half-width at half-maximum) is proportional to the diffusion coefficient of the particles D (Eq.1):

$$\Gamma = Dk^2 \qquad \text{Equation 1}$$

where,

$$k = (4\pi n/\pi)\sin(\Theta/2)$$

n is the refractive index of the medium, λ the laser wavelength, and Θ the scattering angle. With the assumption that the particles are spherical and non-interacting, the mean radius is obtained from the Stokes-Einstein equation:

$$R = k_B T/6\pi\eta D,$$

where k_B is the Boltzmann constant, T the temperature, and ή the shear viscosity of the solvent.

Information about the light-scattering spectrum can be obtained from the autocorrelation function G (τ) of the light-scattering intensity. For the simplest case of spherical monodisperse non-interacting particles in a dust-free fluid, the characteristic decay time of the correlation function is inversely proportional to the linewidth of the spectrum. Therefore, the diffusion coefficient and either particle size or viscosity can be found by fitting the measured correlation function to a single exponential function.

This method is also referred to as dynamic light scattering and quasi-elastic light scattering. It is applicable to particles suspended in a liquid, which are in a state of random movement due to Brownian motion (i.e. particles generally of 2 -3 µm diameter and smaller). The speed of the movement is inversely proportional to particle size (the smaller the particles are, the faster they move, or diffuse), and the speed can be detected by analyzing the time dependency of the light intensity fluctuations scattered from the particles when they are illuminated with a laser beam.

2.6.2. Surface charge measurement

The ζ-potential of the nanoparticles was determined by laser doppler anemometry using a Malvern Zetasizer also called Doppler Electrophoretic Light Scatter Analyzer. The instrument is a laser-based multiple angle particle electrophoresis analyzer. Using Doppler frequency shifts in the dynamic light scattering from particles, the instrument measures the electrophoretic mobility (or zeta potential) distribution together with the hydrodynamic size of particles (size range 10 to 30 µm) in liquid suspensions by photon correlation spectroscopy

 Measurements were performed at 25 ± 0.1^0 C, on samples appropriately diluted with the medium described each time. Five measurements of the ζ -potential for each sample were made.

2.6.3. Transmission Electron Microscopy

Morphology of the particles was examined using TEM. A sample of particle suspension was diluted with 3% w/v phosphotungstic acid adjusted to pH 7.5

with potassium hydroxide corresponding to a 1:1 ratio before examination. One drop of sample was placed for 1 minute on a copper grid coated with a formvar carbon film. The excess of sample was wicked away with the aid of filter paper. The sample was then ready for analysis by TEM.

2.7. Differential Scanning Calorimetry

The thermal behaviour of the particles was analyzed using a DSC2920 TAINS instrument. Approximately 10 mg of nanoparticle suspension was accurately weighed into a 40-µL hermetic aluminium pan and sealed. A temperature range of 0° C to 200° C was scanned using a heating rate of 10° C /min. Indium was used as the standard reference material to calibrate the temperature and energy scale of the apparatus.

2.8. Nuclear Magnetic Spectroscopy (NMR)

Polymer samples (2 mg) were dissolved in 0.86 ml deuterated acetone, while pure amino acids (2 mg) were dissolved in 1 ml deuterated methanol and subjected to NMR analysis. The NMR spectra were recorded on a Bruker 400 MHz spectrometer. The data was processed using the Omnispin software

2.9. Fourier Transformed Infrared Spectroscopy (FTIR)

Fourier transform infrared (FT-IR) spectra were obtained on a Nicolet AVATAR 360 FT-IR spectrometer. Samples of pure drug or nanoparticles (with or without drug) were prepared in KBr disks (2 mg sample in 200 mg KBr). The scanning range was 450–4000 cm^{-1} and the resolution was 1 cm^{-1}. Sample analysis were carried out by the E2 OMNIC software for analysis

2.10. Determination of drug loading

<u>Indirect Estimation</u>: Encapsulation of DXMP was first determined using an indirect method. From the calibrated Sepharose column, fractions corresponding to free drug were collected together and concentrated. The total amount of free or unincorporated drug was determined using UV spectroscopy at 240 nm and a calibration curve for DXMP. The amount of drug incorporated in the particles was determined after subtracting unincorporated drug amount from total known amount of drug added.

<u>Direct estimation</u>: Nanoparticle suspension was freeze dried and from the lyophilised material drug was extracted by addition of Acetone / MeOH (1:2) for hydrophobic drugs and acetone / Phosphate buffer saline (0.01%) for hydrophilic drugs, followed by evaporation of acetone and centrifugation in a MSE microcentrifuge at 13500 rpm for 5 mins. The supernatant was analysed depending on the drug used by UV or HPLC.

The drug loading (%) was calculated using the following formula:

$$\text{Drug loading (\%)} = \frac{\text{Amount of drug in nanoparticles (mg)}}{\text{Polymer mass (mg)}} \times 100$$

2.11. Drug release studies

Nanoparticle suspension (2ml) was placed in a dialysis membrane (Spectra Pore MWCO 1000) and immersed in 4 ml water or 10mM tween in HEPES for 30 days at 37 °C in an agitating water bath.

Sampling was carried out at predetermined time points, 1 ml of aliquot taken for analysis (UV/ HPLC); remaining media was replaced with fresh distilled water at each time point

CHAPTER 3. INCORPORATION AND RELEASE OF DEXAMETHASONE PHOSPHATE AND CYTOSINE ARABINOSIDE FROM POLY GLYCEROL ADIPATE NANOPARTICLES.

3.1. Introduction

Glucocorticoids can be highly effective in treating joint inflammation, but their systemic application is limited because of a high incidence of serious adverse effects, especially related to long term treatment. Dexamethasone has been used to reduce brain tumour-associated vascular permeability and cerebral oedema, reduce intracranial pressure, improve accompanying symptoms, and provide palliation of patients with malignant gliomas by prolonging useful neurologic function and life span [149]. PLGA-nanosteroid for intra-articular preparation has been reported but the encapsulation rate of steroids is low and their size is not suitable for intravenous administration. Ishihara patented the preparation of PLGA and PLA nanoparticles with water soluble steroids where they reported the encapsulation of steroid salts to be between 0.5 and 2% w/w Also the release rate has been reported to be associated with a high burst release for most steroid salts [150]

Cytosine arabinoside has been reported to be widely used in chemotherapy for sporadic primary central nervous system lymphoma. Depofoam™ is one of the currently marketed products containing Cytarabine. It is a liposomal intrathecal

formulation, where cytarabine is formulated inside small particles of a synthetic lipid material called DepoFoam. This dosage form slowly releases the drug and provides a sustained action.

In this study we present size, zeta potential, drug loading and release studies using the water soluble drugs Dexamethasone phosphate (DXMP), an anti inflammatory agent, and Cytosine arabinoside (CYT-ARA), an anti cancer drug, in functionalised poly (glycerol adipate) nanoparticles. The presence of free pendant hydroxyl groups on the backbone introduces synthetic flexibility in the backbone as they are available for substitution with different functional groups and different chemistries. Dexamethasone phosphate was chosen as a model anti inflammatory, low toxicity drug for initial studies in order to establish the potential of poly (glycerol adipate) polymers for drug incorporation within nanoparticles. Since we aim to introduce these polymers for nanoparticle formulations in cancer therapy, CYT-ARA was chosen as an example of a water soluble anti cancer drug. From literature it has been proved that steroid hormones interact with fatty acyl groups of cholesterol and sphingomyelins [151]. We hypothesised that on addition of acyl groups to the backbone a similar interaction could occur between the steroidal nucleus of DXMP and polymer backbone acyl groups. The steroidal nucleus is believed to be oriented parallel to the phospholipid groups of the bilayer membrane and stacked between them. Hence, we introduced within the backbone, acyl groups of varying chain lengths from C_2 to C_{10} and in varying degrees of acylation from 20% to 100% substituted polymer. The lack of a steroidal nucleus in the structure of CYT-ARA provided an excellent example for comparison with the steroid containing DXMP.

Particles were prepared using two different methods reported in the literature for nanoparticle formulations namely: The Interfacial deposition [91] and the simultaneous emulsification methods [86]. Extensive studies were carried out using DXMP in order to identify the optimum chain length of acyl group, method of preparation and MW of backbone polymer based on physicochemical properties of particles and drug incorporation. The polymer was also assessed for cytotoxicity and was found to be non toxic to HepG62 cell lines. From the in vivo biodistribution studies of radiolabelled samples intavenously, around 15% of the particles were found in the blood after 3 hours which is better than the PLGA particles [72].

In this study, results with DXMP were compared with results obtained using another water soluble drug CYT-ARA under similar formulation conditions and polymer specifications. The nanoparticles manufactured using various recipes and under various conditions were characterized by Photon correlation spectroscopy (PCS) for size and size distribution, Transmission electron microscopy (TEM) for morphological properties, and zeta-potential for surface charge. The drug encapsulation efficiency and the drug release kinetics under in vitro conditions were measured by high performance liquid chromatography (HPLC). Also, during the study we compared the drug loading and encapsulation efficiencies determined using an indirect method and a direct method of analysis.

Aims of the Chapter:

- To determine the optimum chain length of the acyl groups for maximum loading of DXMP.

- To evaluate the methods of nanoparticle preparation and select the method for best drug incorporation.

- To study the influence of polymer functionalisation and degree of acylation on DXMP and CYT-ARA incorporation.

- To compare the drug loading and release profile of DXMP and CYT-ARA within various polymers.

3.2. MATERIALS AND METHODS

3.2.1. Materials

Polymer backbone and acylated polymers were synthesised as described in Chapter 2.
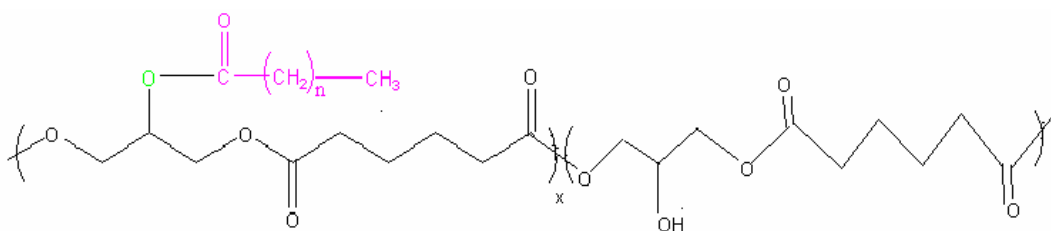
n = 2 to 10

x/ x + y = 20%, 40% and 100% substituted.

Fig. 3.1. Structure of poly glycerol adipate backbone substituted with acyl groups.

Dexamethasone Phosphate and Cytosine Arabinoside were purchased from Sigma Aldrich (UK). Sepharose 4B-CL gel was purchased from Pharmacia UK. All organic solvents were of HPLC grade. Water used in the experiments was ELGA water (18 kΩ resistivity).
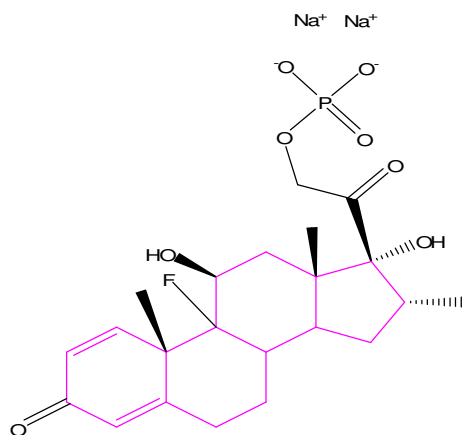
Chemical name: fluoro-11(beta), 17-dihydroxy-16(alpha)-methyl-21-

(phosphonooxy)pregna-1, 4- diene-3, 20-dione disodium salt.

Molecular Formula: $C_{22} H_{28} FNa_2 O_8 P$

Molecular Weight: 516.41

Fig. 3.2. Molecular structure and identity of DXMP
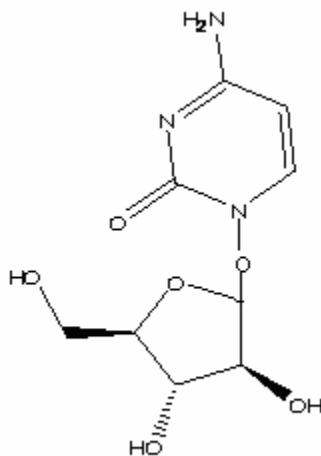
Chemical name   : 4-Amino-1-β –D- arabinofuranosyl- 2 (1H pyrimidinone)

 Molecular formula : $C_9H_{13}N_3O_5$

 Molecular weight: 243.22

Fig. 3.3. Molecular structure and identity of CYT-ARA.

3.3. Methods

3.3.1. Preparation of nanoparticles

Nanoparticles were prepared using methods described in 2.4.1 and 2.4.2 in Chapter 2.

3.3.2. Separation of free drug from nanoparticles

 The nanoparticle suspension was passed through a Sepharose 4B-CL column (32 cm x 2.5 cm) using water as eluent at a flow rate of 1 ml /min. Particles eluted in the earlier fractions were collected, concentrated using vivaspin ultrafiltration tubes in a CENTAUR 2 centrifuge and subjected to characterisation.

3.3.3. Measurement of Particle size and Zeta Potential

Measurement of particle size was carried out using PCS (Malvern Instruments Ltd., Malvern,UK). The analysis mode was CONTIN. The nanoparticle suspension (200 μL) was diluted with ultrapure water in a cylindrical glass cell to give 500-600 kcps. The particle size was expressed as the mean particle hydrodynamic diameter +/- standard deviation of 30 readings. Measurements of surface charge were performed using a Malvern Zetasizer IV (Malvern Instruments Ltd., UK) at 25° C. Results are expressed as the mean ± standard deviation of 6 readings.

3.3.4. Transmission Electron Microscopy (TEM)

 Morphology of the particles was examined using TEM (Jeol Jem 1010 electron microscope, Japan). A sample of particle suspension was diluted with a solution of phosphotungstic acid (3% w/v, pH 4.7) and observed under TEM.

3.3.5. Determination of entrapment efficiencies

Drug loading for DXMP nanoparticles was determined using both indirect and direct estimation methods described in Chapter 2.

Direct method: Particles loaded with either DXMP or CYT-ARA were lyophilized. To the freeze dried product acetone and Phosphate buffered saline 0.01M (1:2) were added, the mixture was centrifuged in a MSE Microcentaur centrifuge at 13500 rpm for 10 min and the supernatant was analysed. For CYT-ARA the supernatant was analysed using UV spectroscopy at 271 nm and the concentration of the solution was assessed from a calibration line based on the Beer Lamberts law [152]. For DXMP the supernatant was analysed by HPLC.

3.3.6. HPLC method for DXMP determination

High-performance liquid chromatography (HPLC) analyses were performed with a Gilson Model 600 pump equipped with a Gilson photodiode array detector (set at the wavelength of 240 nm), a 20 μl loop injection autosampler and Empower software. For analysis, a reversed phase Lichrosphere 100 RP-18 (25 cm × 4.6 mm; 5μ) endcapped column in conjunction with a precolumn C_{18} insert was eluted with Phosphate buffer (0.1 M) pH 3.5: Methanol : Acetonitrile 50:36:14 in isocratic mode. The flow rate of 1 ml/min was maintained and the column eluent was monitored continuously at 240 nm. Quantitation of the compounds was carried out by measuring the peak areas in relation to those of standards chromatographed under the same conditions. DXMP was eluted with a retention time of 5.02 minutes and monitored at 240 nm [153].

3.3.7. In vitro Drug release studies

Nanoparticle samples (2ml) enclosed in dialysis bags (Spectra Pore, MWCO 12000) were placed in 4 ml water at 37°C under mild agitation in a water bath. At pre-determined time intervals, 1 ml samples were withdrawn from the release medium and analysed with UV-Vis spectroscopy for CYT-ARA and by HPLC for DXMP using the conditions as described in section 3.3.6. After sampling the entire medium was removed and replaced with same amount of fresh media.

3.4. RESULTS

3.4.1. Particle size and zeta potential

In order to study the influence of degree of acylation on particle formation, size and zeta potential of various drug loaded and empty polymers were examined. The effect of the nature of drug and its correlation with degree of substitution on particle sizes and zeta potential were also studied.

Table 3.1 shows the sizes and zeta potential of particles prepared using various series of polymers and different drugs. Empty particles were particles formed without the drug. Among the polymer backbone series with different molecular weights no specific trend could be observed for the empty particles. Backbone with MW 6 kDa formed the largest particles. The sizes of the empty particles were larger than those containing drugs. No distinct correlation could be observed between the particle sizes and the degree of acylation in the absence of drugs. Particles formed with the polymer backbone were the smallest and those formed with the 40% acylated polymer were the largest.

Between the two different formulations, the sizes of DXMP and CYT-ARA particles in the backbones of 2 kDa and 6 kDa were almost the same. The only significant effect was observed in the 12 kDa backbone where CYT-ARA

particles were larger than the DXMP particles. For the acylated polymers, DXMP loaded particles were smaller in size than the CYT-ARA loaded particles.

POLYMER TYPE	EMPTY PARTICLES		(+) CYT-ARA		(+) DXMP	
	SIZE nm (SD) [polydispersity]	ξ-POTENTIAL mV (SD)	SIZE nm (SD) [polydispersity]	ξ-POTENTIAL mV (SD)	SIZE nm (SD)[polydispersity]	ξ-POTENTIAL mV (SD)
Polymer backbone	169.6(2.2)[0.57]	-20.2(0.4)	159.2(1.8)[0.041]	-27.3 (1.0)	150.6(1.3)[0.206]	-32.1(0.6)
20%C8-12	211.1 (6.8) [0.30]	-30.1(0.1)	217.5(5.9)[0.07]	-30.8 (0.45)	124.3(1.037)[0.41]	- 36.9(6.01)
40%C8-12	267.5 (3.09) [0.33]	-29.75(3.7)	200.8(0.63)[0.28]	-28.6 (1.5)	147.3(9.68)[0.35]	-34.4 (0.5)
100%C8-12	201.3 (0.57) [0.23]	-27.3(0.3)	196.35(2.5)[0.1]	-28.9 (0.62)	152.5(1)[0.25]	-29.4(2.2)
PB-6kDa	221.7(2.7)[0.41]	-25.8(4.5)	128.2(0.9)[0.073]	-29.2 (0.5)	132.9(3.1)[0.05]	-33.7(2)
PB-2kDa	172.9(1.1)0.72]	-28.7(0.2)	129.3(1.1)[0.103]	-31.4 (0.8)	127.3(3)[0.14]	-33(0.5)

Table 3.1 Particle size and Zeta potential of particles prepared from various polymers by the Interfacial deposition method. Polymer type is designated by % of acylation (20, 40, 100%), acyl group chain length (C8) and molecular weight (2, 6, 12 kDa). Results are mean of 3 readings, SD standard deviation, PB polymer backbone.

Amongst the acylated series, an increase in polymer acylation increased the particle size for DXMP while it decreased for CYT-ARA. However, acylated DXMP loaded particles were still smaller than the unloaded particles made from the same polymers.

Sizes of the DXMP particles prepared by the emulsification method were between 200 and 250 nm. (Data not shown). No significant trend could be observed between degree of acylation and particle size. However, empty particles were larger in size than drug loaded particles.

Zeta potential for all empty and CYT-ARA particles was around -30 mV while it was between -30 and -37 mV for the DXMP particles. For the empty polymer backbone particles zeta potential became less negative as the MW increased and was within an overall range from -20 mV to -28 mV. Acylation and DXMP incorporation slightly increased negative zeta potential values. CYT-ARA incorporation into the 12 kDa polymer backbone also increased the negative zeta potential of the particles to a small extent.

3.4.2. TEM Images
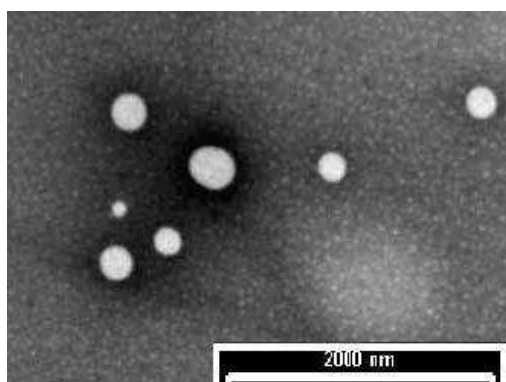
Fig. 3.4. TEM Image of CYT-ARA nanoparticle in 40% acylated PGA, MW 12kDa.
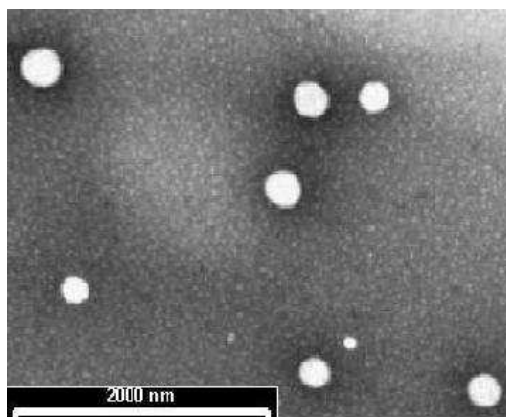
Fig. 3.5.TEM Image of DXMP nanoparticle in 40% acylated PGA, MW 12kDa

From Figs. 3.4 and 3.5, particles appeared to be spherical with smooth rounded surfaces. DXMP and CYT-ARA particles appeared similar in size in the 40% acylated polymer and also had similar polydispersities. The drug loaded particles had a higher polydispersity compared to empty particles (Table 3.1).

3.4.3. Drug Incorporation

A number of studies have reported drug incorporation using an indirect method of estimation based on determination of free drug after encapsulation compared to total amount of drug used [154]. Initial studies carried out in the group focussed on this method of determination of described in Chapter 2 for drug loading and encapsulation efficiency [72]. Based on the results obtained by this method we saw substantial amount of loading within the particles (Fig. 3.6). However, during the course of this study, the method for direct estimation of drug loading in particles was developed and compared with results for similar polymers using the previous method.

DXMP Incorporation in various polymers (Indirect estimation)
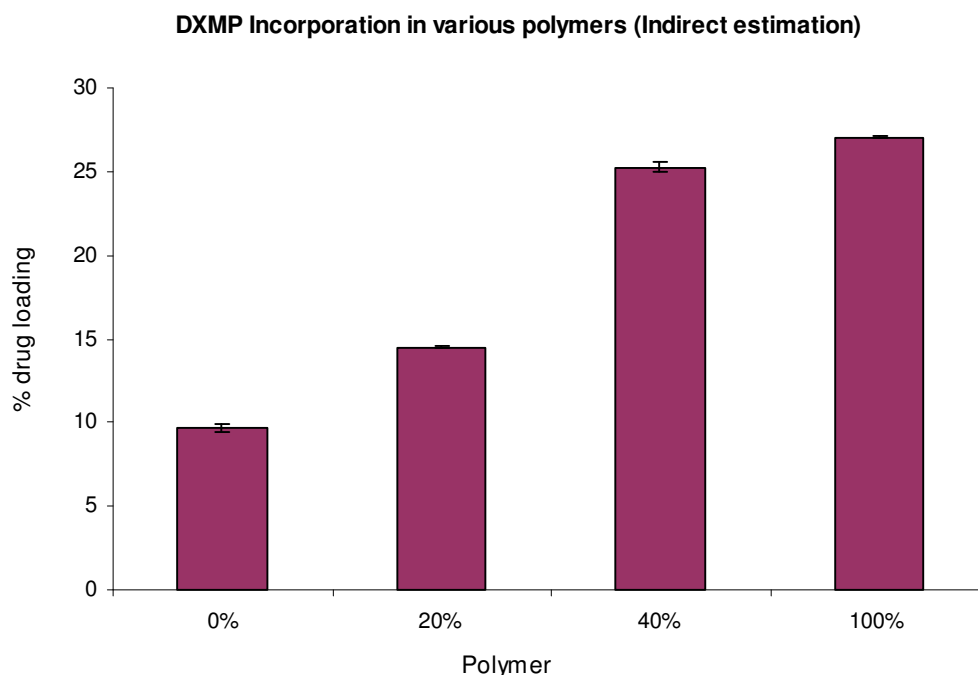
Fig. 3.6. Influence degree of polymer acylation on Dexamethasone phosphate analysed using indirect method of estimation

Based on the results obtained from indirect estimation, increase in acylation led to an increase in drug loading within the particles. Around 30% drug loading was observed in the 100% C_8 acylated polymers and 9% loading was observed in the polymer backbone.

3.4.3.1. Validation of DXMP determination

In the new method, the amount of drug loaded directly within the particles was determined after extraction from the nanoparticles followed by its analysis by HPLC. Results obtained for validation of the direct method and HPLC analysis of the drug loaded nanoparticles are presented below.
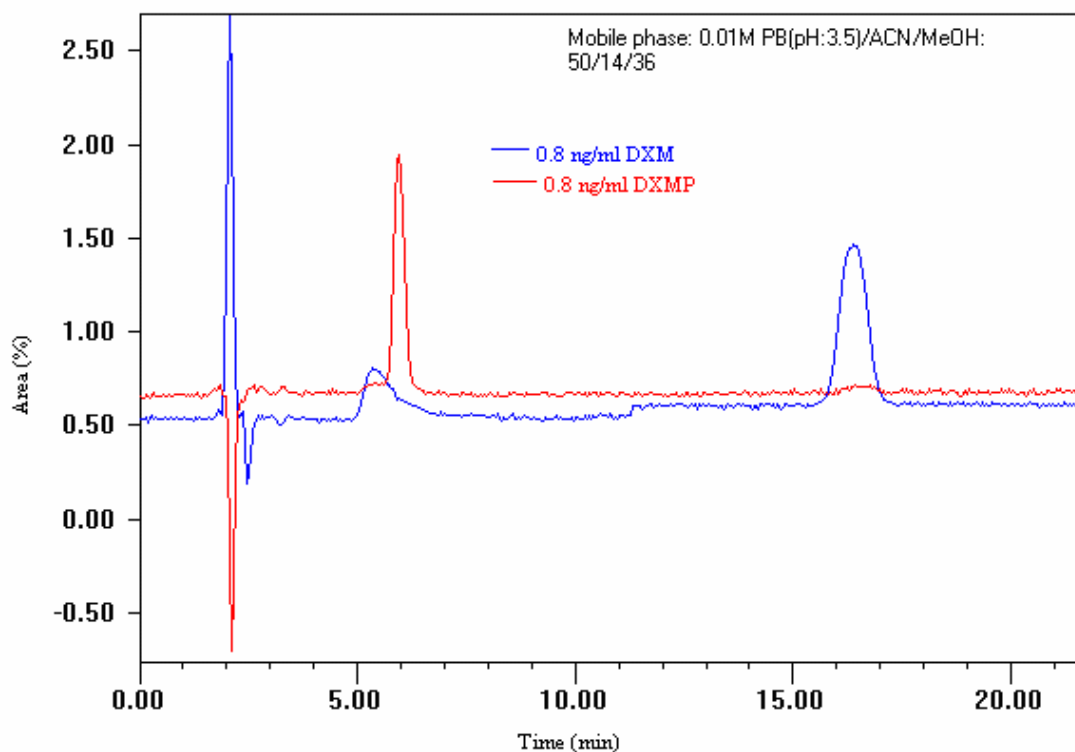
Fig. 3.7. Determination of retention time for standard solutions of DXMP and DXM using conditions as described in 3.3.6

3.4.3.2. (B) Calibration curve

Due to its highly unstable nature, some DXMP is degraded to DXM as evident from the HPLC curve for the standard solution of DXMP (Fig. 3.7). Hence, in order to account for the total amount of DXMP present in the samples it is essential to quantify the amount of DXMP present in the form of DXM. In order to estimate the amount of DXMP and DXM present in the samples calibration curves was prepared with known amounts of DXMP and DXM and analysed by HPLC (Figs. 3.8 and 3.9).

69

Standard curve for DXM-P in water

$$y = 43015x + 601.11$$
$$R^2 = 0.9981$$
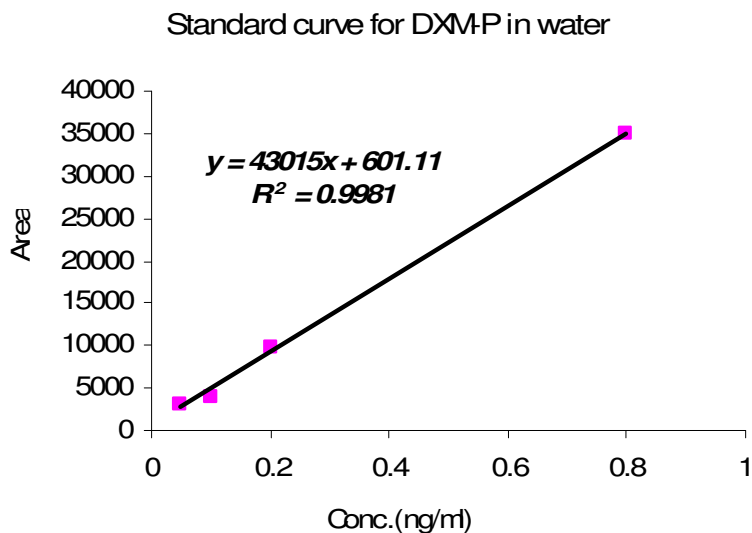
Fig. 3.8. Calibration curve for DXMP in water.

.

Sample (DXMP)	Area	Conc.(ng/ml) (*100 dilution factor)	µg/tot.fr.vol[†] (2ml)	Total (µg) (DXMP+DXM)	Efficiency (%)	Avg. efficiency (SD)
Control-1	21659	47.54	95.07	95.5233	95.5233	
Control-2	20370	44.71	89.41	89.6191	89.6191	**91.2%**
Control-3	19998	43.83	87.75	88.3658	88.3658	**(3.82)**

[†] total free volume

Table 3.2. Extraction efficiency for control samples of DXMP (100µg) using conditions as described in 3.3.6
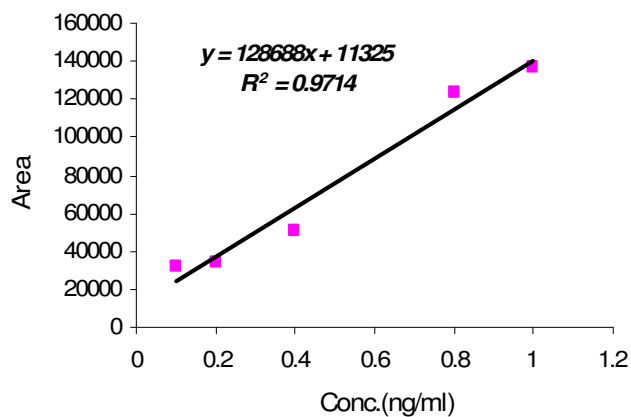
Fig. 3.9. Calibration curve for DXM in MeOH

Sample (DXM)	Area	Conc.(ng/ml)	µg/tot.fr.vol.[†] (2ml)
Control-1	23321	0.125	0.22
Control-2	30280	0.228	0.46
Control-3	35125	0.3	0.63

[†] total free volume

Table 3.3. Extraction efficiency for control samples of DXM using conditions as described in 3.3.6

.

The above method illustrates analysis of both DXM and DXMP from the samples treated as described for extraction in section 3.3.6.
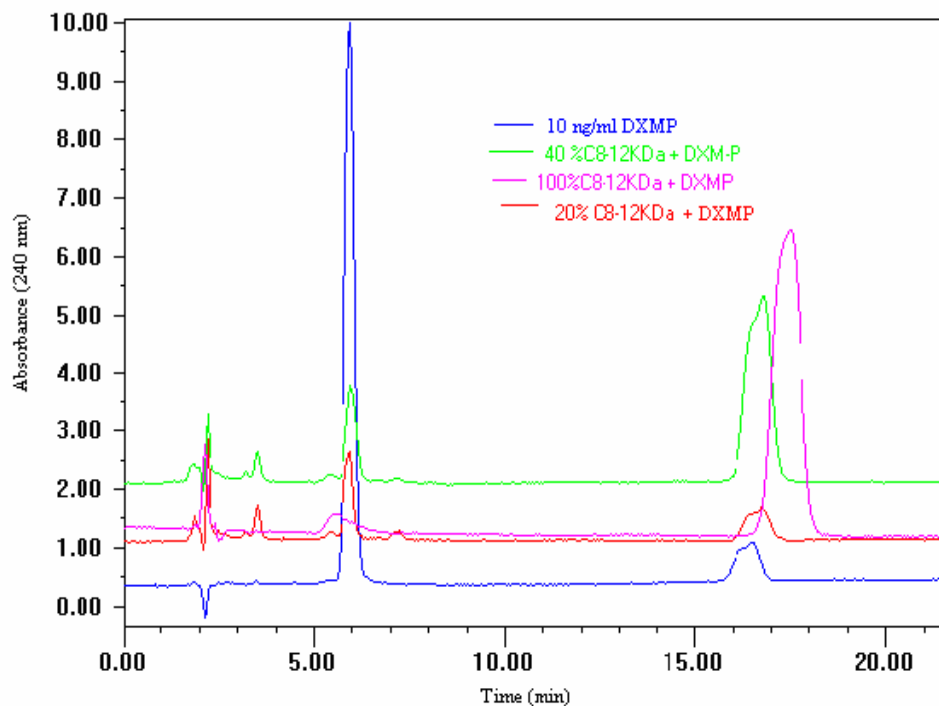
Fig. 3.10. HPLC analysis of DXMP loaded samples within the 20, 40 and 100% acylated polymers along with a standard DXMP solution (10ng/ml)

As can be seen from the standard chromatogram (Fig. 3.7) standard samples of DXMP are contaminated with some amount of DXM. This is due to the inherent instability of the phosphate group in DXMP. Retention time for DXMP and DXM was 5.02 minutes and 15.5 minutes respectively using mobile phase ACN/ Phosphate buffer (pH 3.5)/ MeOH: 14/50/36. As a control, 100 μg pure drug was added to a suspension of empty nanoparticles. Its recovery was determined in order to assess the efficiency of the analytical procedure (Table 3.2, Table 3.3). The calibration curves for DXMP in water (Fig. 3.8) and DXM in MeOH (Fig. 3.9) were used to calculate the amount of DXMP and DXM in the samples. The amount of DXM present was taken into consideration while calculating total amount of DXMP in the samples. Fig. 3.10 shows the analysis of drug loading of some samples compared with the standard solutions.

The average efficiency of the extraction procedure was 91% for DXMP (Table 3.2) and the results obtained for drug loading were divided by 0.9 to obtain the final amount of DXMP loaded in the samples.

3.4.3.3. Validation of CYT-ARA determination

CYT-ARA was analysed spectroscopically. Standard solutions of known concentrations of CYT-ARA in water were analysed at 271 nm on a UV-Vis spectrophotometer and a calibration curve was prepared (Fig. 3.11). Samples were extracted using the method described in Chapter 2. Control samples containing a known amount of CYT-ARA (200 μg) were added to the empty nanoparticles (4 ml) and analysed to determine the efficiency of the method.

Standard curve of CYT-ARA in d.H2O

$y = 0.0298x + 0.0012$
$R^2 = 0.9702$
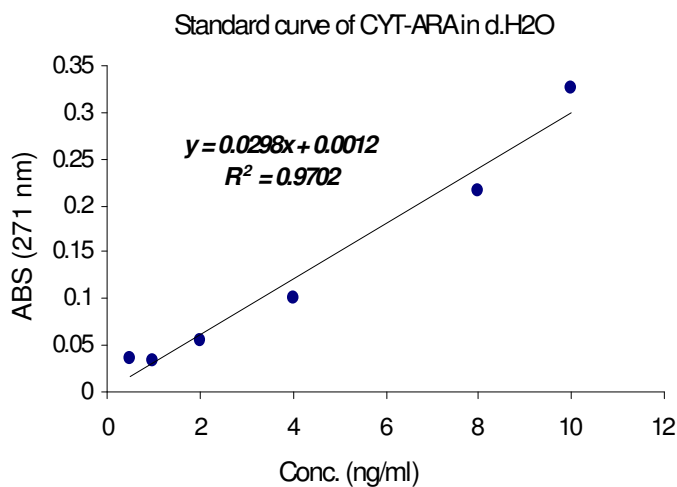
Fig. 3.11. Calibration curve for CYT-ARA in water

Sample (CYT-ARA)	ABS. (271nm)	Conc.(ng/ml) *10 (dilution factor)	µg/tot.fr.vol[†] (2.2ml)	Efficiency (%)	Avg. efficiency (SD)
Control-1	0.21	69.84	153.65	76.823	
Control-2	0.209	74.12	163.06	81.533	**76.1%**
Control-3	0.188	63.63	139.98	69.994	**(5.8)**

† total free volume

Table 3.4. Extraction efficiency for control samples of CYT-ARA

As it can be seen from Table 3.4 around 76% of the control amount was recovered. Average extraction efficiency was calculated and results obtained for drug loading were divided by 0.239 to calculate the drug loading of the samples.

3.4.3.4. Effect of chain length of Pendant acyl groups on loading

In order to observe to influence of acyl chain length on drug incorporation, a model drug DXMP was incorporated within completely acylated polymer backbone with varying acyl group chain lengths ranging from 2 to 10 carbon atoms.
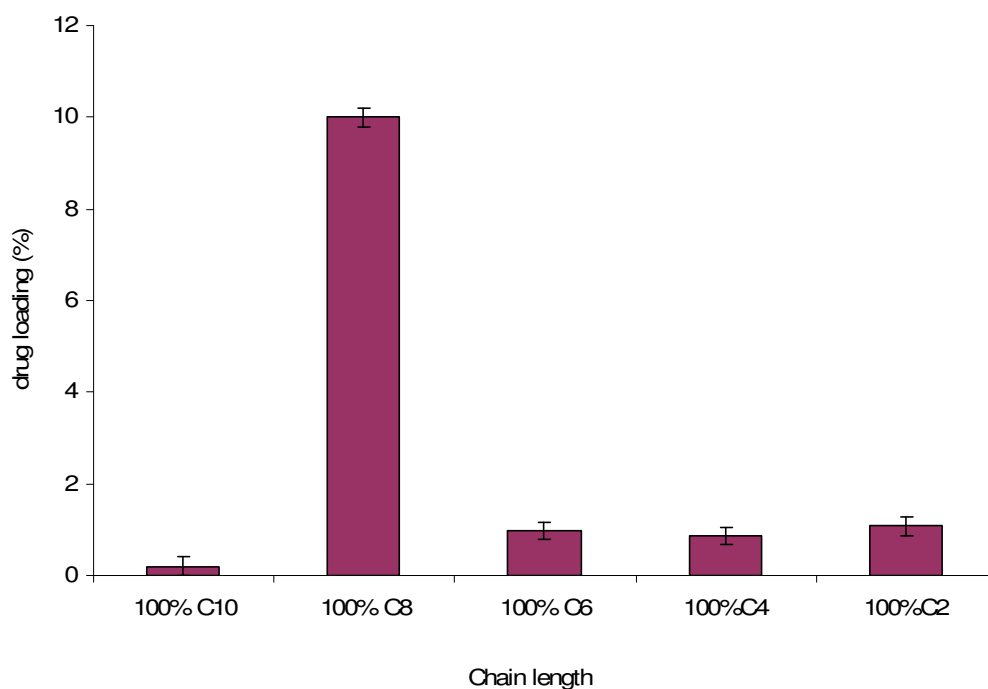
Fig. 3.12. Dexamethasone phosphate incorporation in nanoparticles made from 100% acylated polymers with varying acyl group chain lengths.

From Fig. 3.12, it can be clearly seen that acyl chain length of 8 carbon atoms led to maximum drug entrapment, 10% w/w drug loading being observed. Drug loading within the lower chain length polymers (C_2 to C_6) was minimal and not influenced by change in acyl group chain length. A substantial drop in drug loading was observed when the chain length was increased to 10 carbon atoms.

3.4.3.5. Effect of degree of acylation on drug loading

Next, the effect of change in degree of substitution on drug incorporation was investigated. C_8 chain length polymers were acylated to an extent of 20%, 40% and 100% and incorporation of DXMP and CYT-ARA within these polymers was studied.
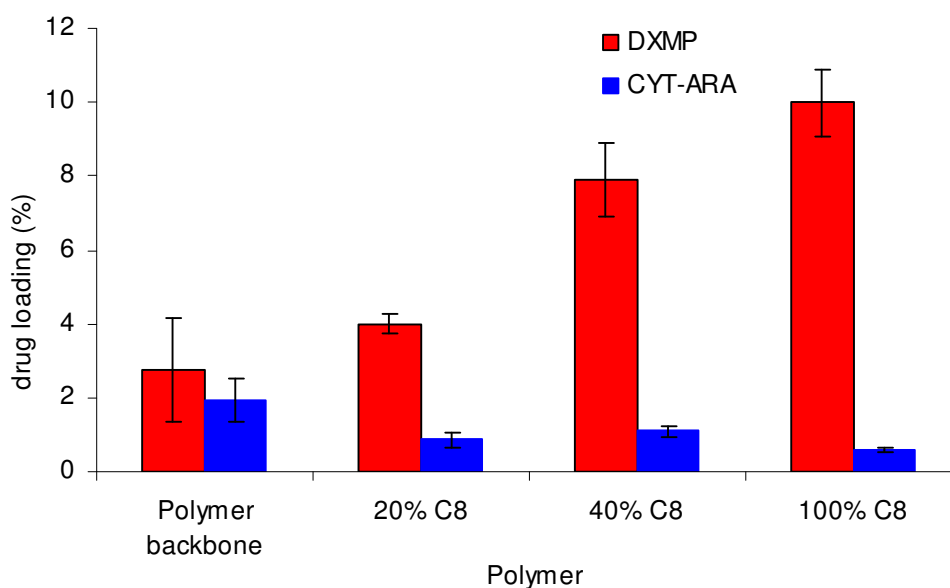
Fig. 3.13. Influence degree of polymer acylation on Dexamethasone phosphate and Cytosine Arabinoside loading in nanoparticles.

As can be seen in Fig 3.13, an increase in acylation led to increase in drug loading for DXMP. However, the exact opposite trend is observed for CYT-ARA. With increase in acylation CYT-ARA incorporation decreased with all the acylated series incorporating around 1% of drug. Incorporation of CYT- ARA was highest (2%) in the polymer backbone (Fig. 3.13) and it decreased as acylation increased. Incorporation of DXMP was highest in the 100% acylated polymer. 10.5% DXMP was encapsulated within this polymer. Comparing DXMP results with that obtained using the indirect estimation (Fig. 3.6), it can be seen that although the trend is similar for both methods the amount of drug loading estimated previously within the 100% acylated polymer using the indirect estimation was 30% which is 3 times greater than the direct estimation shown above.

3.4.3.6. Effect of Polymer backbone molecular weight

Polymer backbone was synthesised in various molecular weights and drug incorporation within them was studied.
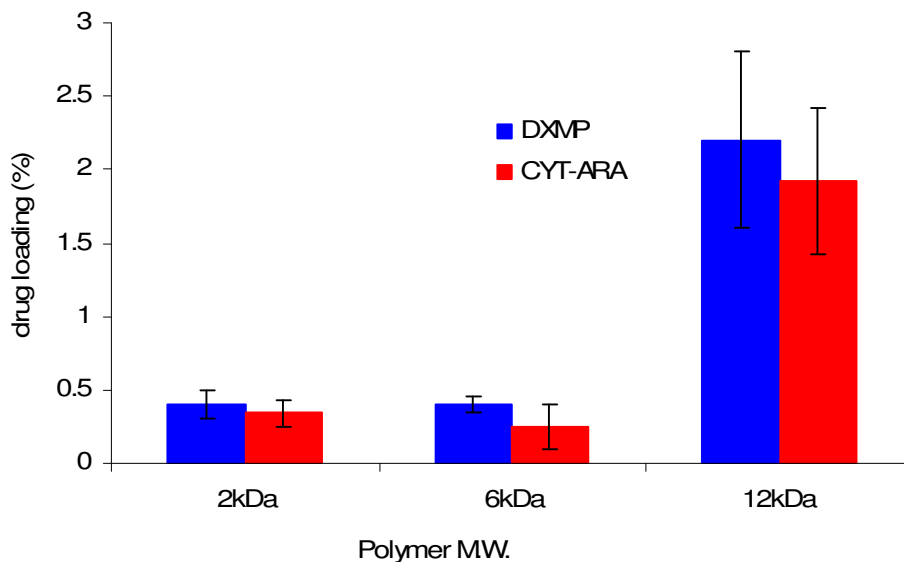
Fig. 3.14. Influence of backbone M.W on DXMP and CYT-ARA loading in nanoparticles

From Fig 3.14, for either drugs, backbone with highest molecular weight gave maximum incorporation. CYT-ARA was encapsulated to a significant extent within the 12 kDa polymer particles and minimum loading was observed in the 2 and 6 kDa polymers. Similarly, for DXMP, loading within the 2 and 6 kDa polymers was to a similar extent and considerably lower than for the 12 kDa polymer. Both DXMP and CYT-ARA were incorporated to a similar extent in the polymer backbone of different molecular weights.

3.4.3.7. Effect of nanoparticle production method

DXMP particles were prepared using two different methods, the interfacial deposition method (IPD) and emulsification method.
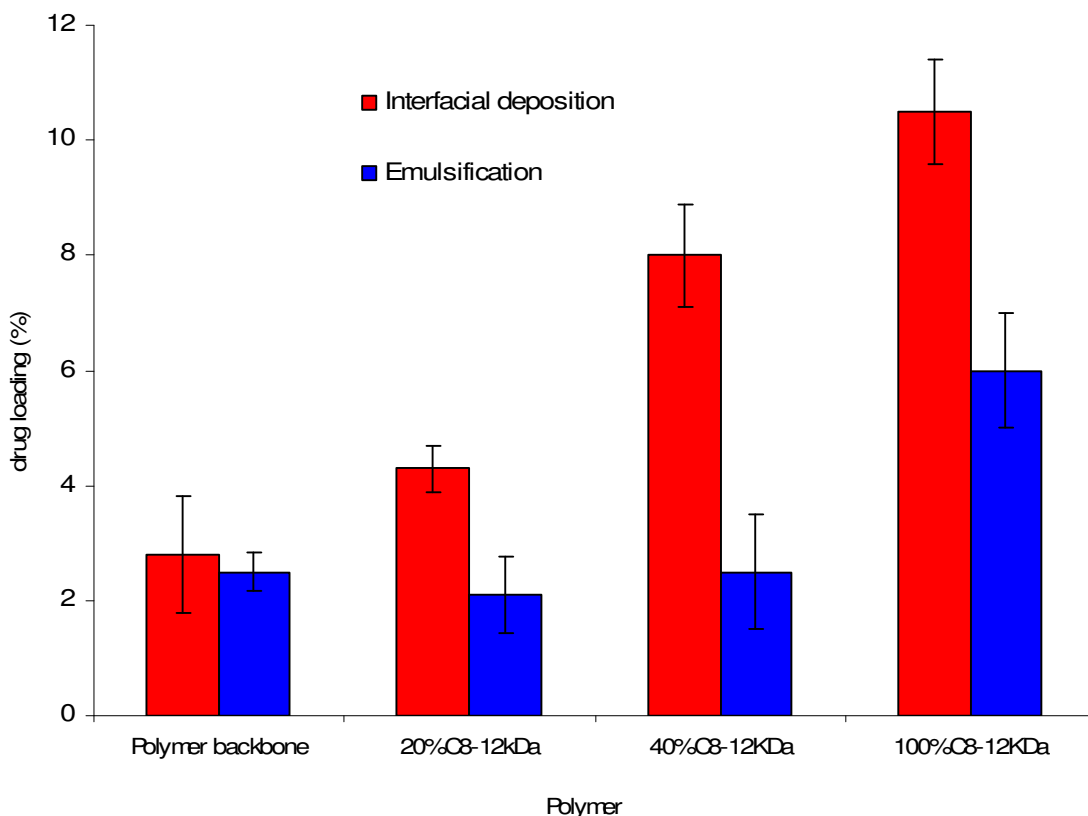
Fig. 3.15. Influence of method of preparation and degree of polymer acylation on Dexamethasone phosphate loading in nanoparticles.

The particles showed better incorporation in the particles prepared using the IPD method. (Fig. 3.15). Particles prepared using either the emulsification or ID method showed maximum incorporation in the 100% acylated polymer.

With the emulsification method 5.8% DXMP was incorporated within 100% acylated polymer while with the ID method 10.5% loading was observed. There was no significant difference in incorporation within the polymer backbone, 20% or 40% acylated polymers using the emulsification method. It was also

interesting to observe that the polymer backbone particles prepared using the two different methods had comparable incorporation of DXMP.

3.4.4. Drug Release

Drug release from nanoparticles is usually a biphasic phenomenon although on some occasions a triphasic profile is also seen. Firstly there is an initial rapid removal of the drug from nanoparticles possibly related to loss of drug associated loosely on the surface of the nanoparticle. This initial release is rapid and uncontrolled and is termed the burst release [155]. Most particles reported in the literature prepared using either ID or emulsification methods show this initial release. The drug loosely associated with the surface may occur due to the escape of drug during the organic solvent evaporation phase towards the external medium [11], and once the organic solvent evaporates there is re-adsorption of the drug on the nanoparticle surface. After the surface component release is complete, there is a slower much more controlled release of drug through the nanoparticle matrix. This latter release has been characterised by zero order release kinetics for biodegradable polymers like PLGA.

Change in morphology of polymer surface from being most porous to non porous has also been suggested as an important factor contributing to burst release [156]. The rapid initial drug release is also reported to be affected by hydrophobicity of polymer [157].

3.4.4.1. Effect of polymer acylation

Particles loaded with either DXMP or CYT-ARA in various polymers were studied for their drug release profiles in water. Effect of nature of drug and degree of polymer acylation on its release was determined.
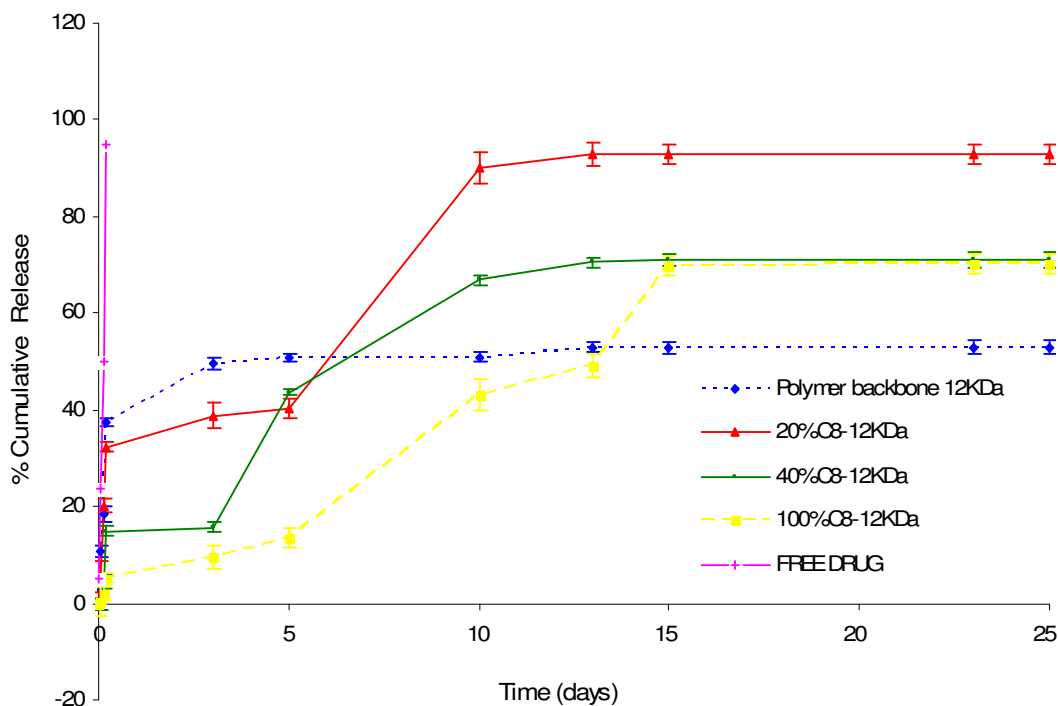
Fig. 3.16. Influence of degree of polymer acylation on Dexamethasone phosphate release from nanoparticles. Drug release studies were carried out in water at 37 °C for 25 days.
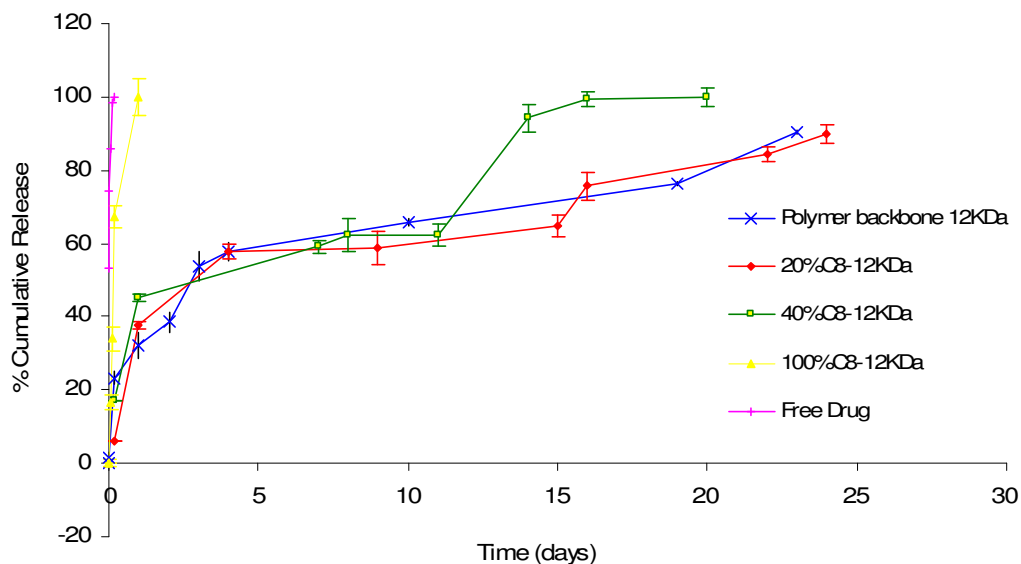
Fig. 3.17. Influence of degree of polymer acylation on Cytosine Arabinoside release from nanoparticles. Drug release studies were carried out in water at 37 °C up to 25 days.

From Fig. 3.16, it can be seen that for the steroid ring containing drug DXMP, polymer with 100% acylation showed controlled drug release without burst effect with 70% of initial drug released at the end of 25 days. The 40% acylated polymers also showed around 71% release at the end of 25 days however, initial release was faster with 40% drug released at the end of 5 days while only 11% drug was released from the 100% acylated polymer at the end of 5 days. The polymer backbone had the greatest burst followed by the 20% acylated polymer. However, total drug released at the end of 25 days was 85% with the 20% acylated polymer and only 40% from the polymer backbone.

For CYT-ARA which is also a hydrophilic drug but without steroid ring, release from the acylated polymers was rapid. The drug release from these polymers can be seen in Fig. 3.17. The fully acylated polymer showed a rapid and complete release. All the other polymers had a slower and comparable rate of release. The only difference between the other formulations was the increased release rate seen in the 40% C_8 polymer after 12 days resulting in a complete release by 20 days. Around 80% drug was released from the backbone and the 20% C_8 acylated polymers at the end of 25 days.

3.4.4.2.Effect of polymer backbone molecular weight

Rate of DXMP release was similar for both 6 and 12 kDa molecular weight polymers (Fig. 3.18). Fast initial release of 40% drug occurred with both polymers followed by a sustained release

81
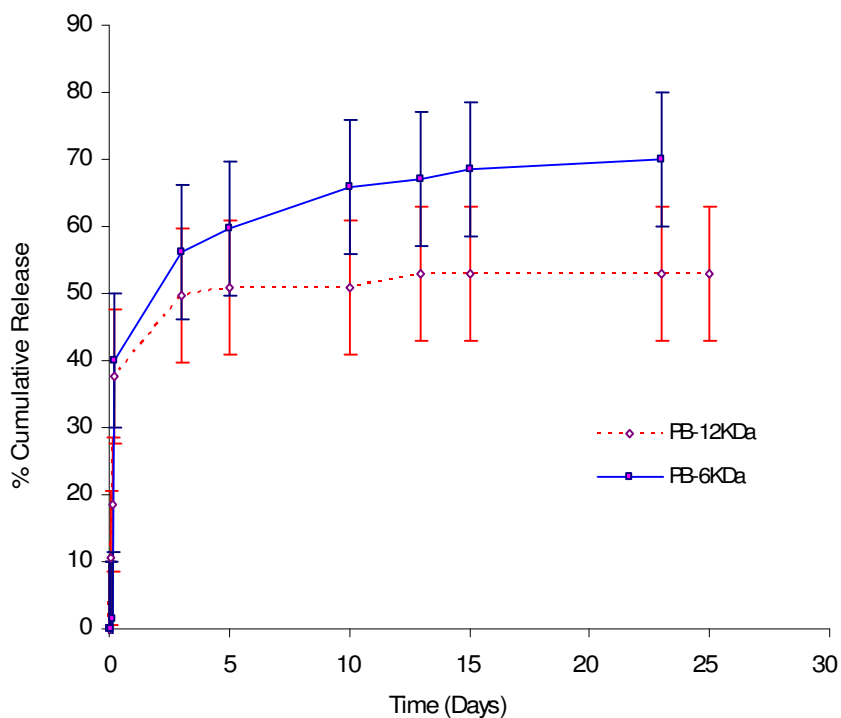
Fig. 3.18. Influence of Polymer backbone MW on DXMP release from nanoparticles. Drug release studies were carried out in water at 37 °C for 25 days.
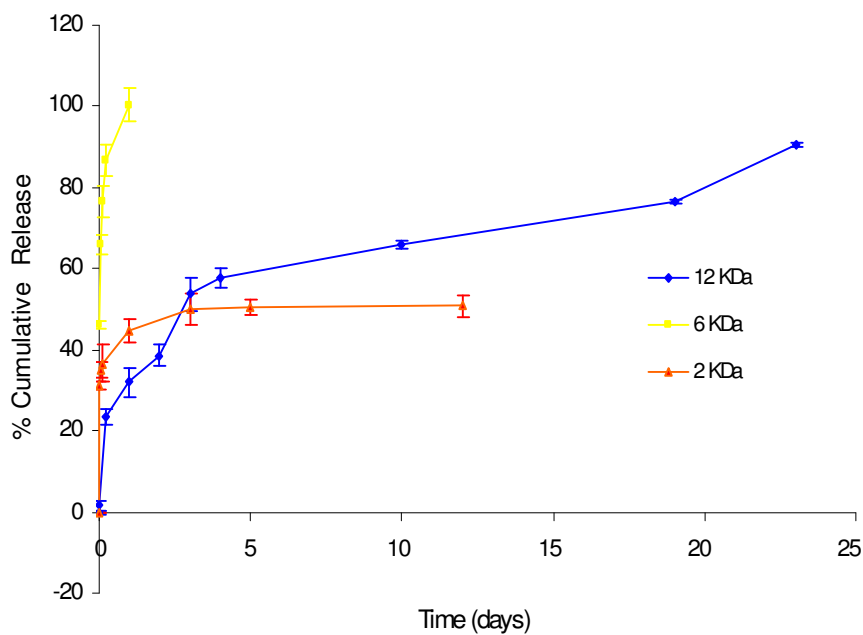
Fig. 3.19. Influence of Polymer backbone M.W on Cytosine Arabinoside release from nanoparticles. Drug release studies were carried out in water at 37 °C for 25 days.

The polymer backbone of 12 kDa molecular weight released 61% drug while the 2 kDa backbone released 44% drug after 12 days.

Rate of CYT-ARA release was rapid and complete from the 6 kDa molecular weight polymer (Fig. 3.19). Release from the 12 kDa and 2 kDa polymers were slower but similar. Between 40 to 50% drug was released rapidly followed by a slow sustained release from either polymer. However, the retention of drug was greater from the 12 kDa polymers compared to the lower molecular weight (2 kDa) polymer.

3.4.4.3. Effect of nanoparticle preparation method

Fig. 3.20 shows the influence of method of preparation on DXMP release profile. Particles prepared by the emulsification method showed a higher rate of drug release compared to the particles prepared using the IDP method after 5 days.
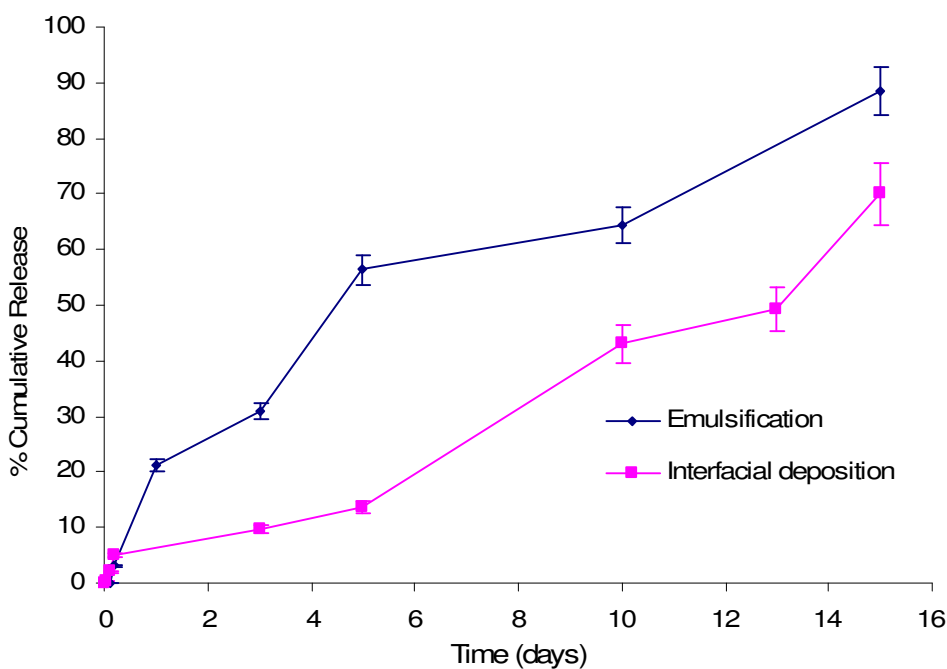
Fig. 3.20. DXMP release from 100% C_8 particles prepared using different techniques.

Both particles showed no burst release. However, release from the particles prepared from the IDP method was slower and more controlled. After 15 days, particles prepared using the emulsification method released 85% drug while particles prepared using the IDP method released around 65% drug.

3.4.5. Analysis of drug release kinetics

Several theories/kinetic models describe drug dissolution from immediate and modified release dosage forms. There are several models to represent the drug dissolution profiles where f_t is a function of t (time) related to the amount of drug dissolved from the pharmaceutical dosage system. The quantitative interpretation of the values obtained in the dissolution assay is facilitated by the usage of a generic equation that mathematically translates the dissolution curve into a function of some parameters related to the pharmaceutical dosage forms.

3.4.5.1. Higuchi Model

Higuchi [158] developed several theoretical models to study the release of water soluble and low solubility drugs incorporated in semi-solid and/or solid matrixes. Mathematical expressions were obtained for drug particles dispersed in a uniform matrix behaving as the diffusion media. To study the dissolution from a planar system having a homogeneous matrix, the relation obtained was the following:

$$ft = Q = \sqrt{D(2C - C_s)C_s t}$$

where Q is the amount of drug released in time t per unit area, C is the drug initial concentration, C_S is the drug solubility in the matrix media and D is the diffusivity of the drug molecules (diffusion constant) in the matrix substance.

This relation was first proposed by Higuchi to describe the dissolution of drugs in suspension from ointment bases, but is clearly also related to dissolution from other pharmaceutical dosage forms. For these dosage forms a concentration profile, which may exist after application of the pharmaceutical system, can be represented. In a general way it is possible to reduce the Higuchi model to the following expression, generally known as the simplified Higuchi model:

$$ft = K_H \sqrt{t}$$

where K_H is the Higuchi dissolution constant treated sometimes in a different manner by different authors and theories. Higuchi describes drug release as a diffusion process based on Fick's law, which is square root of time dependent. This relation can be used to describe the drug dissolution from several types of modified release pharmaceutical dosage forms, as in the case of some transdermal systems and matrix tablets with water soluble drugs [159].
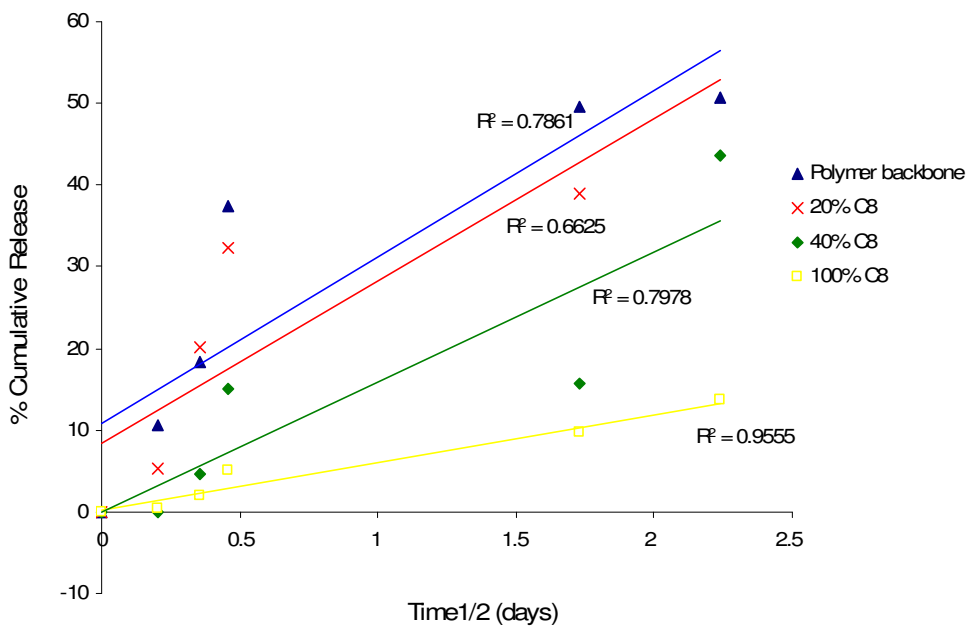
Fig. 3.21. Higuchi plots for DXMP particles
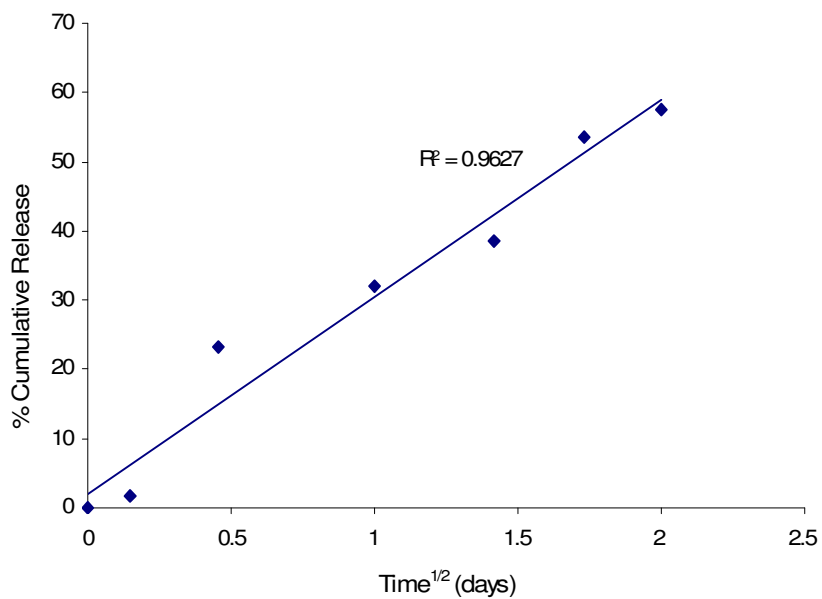
Fig. 3.22 . Higuchi plot for CYT-ARA in PB-12kDa

In Figs. 3.21 and 3.22 the cumulative release of drug (%) against square root of time for DXMP and CYT-ARA respectively has been plotted. Only the plot for DXMP particles in the 100% acylated polymer was linear indicating a diffusion

controlled mechanism. The release profile from the 100% C8 polymer had a correlation coefficient of 0.9555). For the remaining series the correlation coefficient was poor although it is interesting to see that the plot shows two separate linear portions but overall do not obey ficks law of diffusion. Usually, the Higuchi plotting applies to the situation when the amount of drug release does not exceed 60%. Thus the plot for DXMP was calculated for just 4 days. For CYT-ARA, all particles except polymer backbone showed a burst of more than 50% in 24 hours. Hence, these plots have not been calculated. The plot for polymer backbone is linear with a correlation coefficient of 0.969.

3.5. DISCUSSION

3.5.1. Particle size and zeta potential

The size of the empty particles was found to be larger than the drug loaded particles for the backbone as well as the acylated polymers. There could be two main possible explanations for these changes in particle size in the presence of drugs: change in the aggregation number of polymer molecules or change in the particle density due to increased interactions between drug and polymer. In this case, it is more likely to be due to the interactions between drug and polymer. Some interaction between the polymer and the drugs may cause them to form more compact and condensed particles. Also, since the drugs are water soluble they may also play a role at the interface; there could be steep concentration gradient at the interface or transfer of solute from higher viscosity phase, both leading to a decrease in interfacial tension and turbulence leading to rapid diffusion of acetone from organic phase and more condensed particles. Thus, presence of water soluble drugs may play a role in particle formation.

All the empty particles formed with the acylated polymers were larger in size than the 12 kDa polymer backbone. This could be the effect of the presence of acyl groups on the polymer as particle size also depends upon the packing which is influenced by the nature of chemical groups present on the polymer and drug (Fig. 3.1, 3.2). A larger substituent requires more space, but this may be offset by a greater packing efficiency. The increase in size of particles with increase in acylation and increase in molecular weight could also be attributed to increased lipophilicity i.e. increase in hydrophobic interactions within the particles. This would have the opposite effect. The increased lipophilicity may cause a subsequent increase in the aggregation number of polymer molecules leading to a rapid precipitation of the polymer thus increasing the size of the particles rather than the number of particles formed.

Comparing the two drugs, DXMP formed particles of smaller size compared to CYT-ARA for all polymers. Larger sizes of the CYT-ARA particles indicate possibly a more loosely packed arrangement compared to DXMP. This again could be attributed to the nature of interaction between the drug and polymer. We expect a better interaction between the steroid ring of DXMP and the acyl groups on the polymer that may have led to a more densely packed arrangement of the molecules (Fig. 3.1, Fig. 3.2.) In a majority of studies on nanoparticle formulations, particle sizes have been correlated to either the polymer or the drug physicochemical characteristics but not their combined effect.

Piskin *et al* reported that assembly of particles is largely dependant on hydrophobicity of polymer and the nature of the drug used. An increase in the number of hydrophobic domains was found to be associated with larger nanoparticles [160]. Some studies showed a decrease in chain length of the

polymer causes increase in hydrophilicity resulting in loosely packed nanoparticles [161]. Lin *et al* observed an increase in the size of indomethacin loaded PEG polylactone micelles with an increase in chain length of the lactones (L-lactide, δ-valerolactone and δ-caprolactone) [162].

For particles prepared by Emulsification in presence of surfactant Giannone *et al* suggested that size can be varied by modifying molecular weight and monomer stereochemistry [163]. Yoo *et al* studied DNA incorporation within hydrophobic glycol chitosan. Chitosan and its derivatives were complexed with DNA by ionic interactions between anionic phosphate backbones of DNA and primary amine groups of chitosan. The sizes of these particles were mainly dependent on the number of polymer nitrogen per DNA phosphate (N/P). They reported that upon increasing the hydrophobic glycol chitosan/glycol chitosan ratio, the encapsulation efficiency of DNA slowly increased with a decrease in a particle size and this was attributed to a hydrophobic interaction between 5β-cholanic acids of hydrophobic glycol chitosan and DNA complexes [164]. Govender *et al* studied the effect of procaine hydrochloride loading on the particle size of nanoparticles made from PLA–PEG diblock copolymers with a fixed PEG block (5 kDa) and a varying PLA segment (3–110 kDa). The sizes of drug free nanoparticles increased from 27.6 to 152.4 nm with an increase in the molecular weight of the PLA block of the polymer from 3 to 110 kDa. The PLA–PEG nanoparticle size remained unchanged with incorporation of drug into the 3:5; 15:5 and 30:5 series, while a slight increase was observed for the 75:5 and 110:5 series [165]. This has been explained on the basis of the polymer micelle assembly theory where PLA blocks associate as linear chains within the particle core. In the lower pegylated series PEG blocks would exert a weaker influence

during particle formation. As the molecular weight of the PLA block was increased the PLA–PEG 75:5 and 110:5 copolymer behaved more like PLA homopolymer itself   where the PLA blocks agglomerated as entangled chains following precipitation into the aqueous phase. There is more free space amongst the linear core-forming PLA chains of the micellar type PLA–PEG 3:5, 15:5 and 30:5 nanoparticles than in the 75:5 and 110:5 series and this would thus be responsible for accommodating the drug without increasing particle size in the 3:5, 15:5 and 30:5 series [166]. There are some studies where increased size with addition of drug was assigned to be due to the expansion of the polymer matrix by the drug [166]. However, this seems highly unlikely to be an important factor influencing increase in particle size as the amount of drug loaded within the particles and its subsequent volume within the matrix is negligible compared to the polymer mass. There are some studies reporting no difference between the sizes of the empty and the drug loaded particles thus indicating a lack of significant influence of drug-polymer interactions in particle formation. In a study by Gomez-Gaete on DXM incorporation within PLGA polymers of various LA/GA ratios, it was found that NP size and zeta potential were not modified in the presence of drug and both empty and drug loaded particles had a similar size of around 230 nm [154]. Similarly, Zhang *et al* studied incorporation of DXM in poly (trimethylene carbonate) polymers. Particles were between 70 to 200 nm in size and there was no difference between the drug loaded and empty nanoparticles [167]. From these previous studies where interaction between drug and polymer was not expected, little difference in particle size has been seen on drug incorporation. However, from our results, the most important factor influencing particle size appears to be the nature of interactions between drug

and polymer. With our polymers an increase in molecular weight of the backbone and substitution with acyl groups led to an increase in size of the drug free particles thus suggesting that the assembly of polymer chains in the aqueous phase changes with polymer substitution and the acyl groups could cause an increase in free volume between the polymer chains, however in presence of drug this assembly is altered and the interactions between polymer and drug predominate over the effects caused by the substituents alone suggesting that the result was either a compact and closely packed particle or more loosely packed arrangement.

Zeta potential of the empty particles was most likely to be due to the presence of terminal ionised carboxyl groups of the polymer present on the nanoparticle surface. Increase in polymer molecular weight is associated with an increase in the relative amount of pendant hydroxyl groups in the polymer and a decrease in carboxyl groups present on the surface [161]. In the case of our polymer, acylation led to a decrease in the amount of pendant hydroxyl groups. Both of these groups are hydrophilic so will either try to arrange themselves on the surface or alternatively will provide hydrophilic spaces/channels in the particle matrix. The zeta potential of empty particles did not vary much on acylation which could be an indication of the nature of assembly of particles. As there was no significant deviation in the zeta potential it could probably mean that the side chain groups orient facing the core of the particles and not on the surface.

In the presence of drugs, Zeta potential of CYT-ARA particles did not differ much from that of the empty particles. The reduction in negative charge for DXMP formulations as acylation increased could be the effect of DXMP interaction with the polymers thus influencing the assembly of polymer

molecules and appearance of carboxyl and hydroxyl groups present on surface. The only exception was the 20% C_8 polymer incorporating DXMP where a slight increase in the negative values of zeta potential was observed. Here, there could be a possibility of surface localisation of drug [168], and presence of ionised phosphate groups of DXMP in addition to the ionised carboxyl groups.

3.5.2. Drug incorporation

Drug loading estimated using the indirect method was significantly higher than the direct extraction method. Although the exact reason for this false high loading is not exactly clear it seems that there may be some loss of drug by its adsorbtion on the column during separation which could lead to a lower concentration of the anaylsed free drug fraction. Drug loading within polymers substituted with acyl groups of varying chain lengths from C_2 to C_{10} was investigated (Fig. 3.12). From C_2 to C_6, increase in chain length was not accompanied with any increase in drug incorporation. This indicates that loading of DXMP within the polymers was not influenced by hydrophobic interactions alone. On the contrary, increase in chain length of acyl groups from C_8 to C_{10} was accompanied by substantial drop in drug loading. Interaction between the steroid nucleus and the acyl groups seemed to be very specific for the number of carbon atoms and C_8 polymers could be most favourable for enhancing drug incorporation by promoting interaction with the drug and decreasing diffusion from the organic to aqueous phase during particle formation. Poor incorporation within the C_{10} polymers could be accounted by considering the marked increase in hydrophobicity of the polymer core which probably did not allow for sufficient encapsulation of the water soluble drug in the aqueous phase. However; this seems unlikely to be a complete explanation as previous studies

by the group on C_{18} substituted polymers did show good incorporation. Also, it is worth noting that batches of C_{10} showed heavy aggregation after complete evaporation of organic phase. The nanoparticle suspension had to be filtered before analysis. This could have led to substantial loss of drug entrapped in the precipitated polymer causing substantial decrease in amount of drug incorporated into the nanoparticles. Hence among the acylated polymers, C_8 acylated polymers were chosen for further studies.

DXMP is a hydrophilic drug containing a steroidal ring (Fig. 3.2). We expect the acyl groups on the acylated polymers to interact with the steroidal nucleus of the drug thus retaining it within the particle core [151]. The polymer drug interaction could be envisioned as the steroid nucleus occupying the space between the acyl chains of the polymer similar to the orientation of steroids within the phospholipid bilayer. The results from particle size support this theory, as more compact and condensed particles were formed with DXMP than the empty particles (Table 3.1). The higher the number of acyl groups, the greater the expected interactions between drug and polymer. Hence the polymer with 100% acylation showed maximum incorporation compared to the lower acyl substituted polymers (Fig. 3.13).

 Panyam *et al*. have reported greater Dexamethasone loading in PLGA/PLA polymers with high lactide content (100%) compared to that with polymer containing a fraction of glycolide and for lower molecular weight PLGA (12,000 Da) than higher molecular weight PLGA [169]. The incorporation and release of the water insoluble dexamethasone (DXM) from nanoparticles of poly (lactic-co-glycolic acid) (PLGA) embedded in alginate hydrogel (HG) matrices was investigated by Kim *et al* [170]. DEX-loaded PLGA nanoparticles were prepared

using a solvent evaporation technique. The amount of DXM loaded in the nanoparticles was approximately 13 wt. %. In a study on incorporation of water soluble corticosteroid Beclomethasone phosphate within PLGA polymers, Horisawa *et al* found that drug content in the particles depends upon polymer molecular weight and LA/GA ratio [171]. The highest incorporation of 5.8% was reported within PLGA containing LA/GA 75/25 and MW 19,500. In order to enhance encapsulation of the water soluble steroids beclomethasone phosphate and hydrocortisone succinate into PLGA nanoparticles, Ishihara *et al.* used metal ions like zinc in order to precipitate the water soluble steroids into their hydrophobic forms by forming water insoluble metal steroid complexes with the phosphate or succinate groups on the steroid rings. Incorporation of Beclomethasone phosphate and hydrocortisone succinate in the presence of zinc ions was only 5% and 1% respectively [172].

The acylated polymers did not seem to have a significant influence on CYT-ARA incorporation (Fig. 3.13). The unsubstituted hydrophilic backbone was more suitable for a highly polar drug like CYT-ARA thus further strengthening the hypothesis of increased interaction between steroid nucleus (DXMP) and acyl groups on the backbone. CYT-ARA binding is enhanced in presence of more hydroxyl groups (lower acyl substitution, higher MW) on the polymer indicating a possibility of hydrogen bonding as the main mechanism of interaction (Fig. 3.2) This hydrogen bonding could also involve the terminal carboxyl groups. At pH 7, Cytarabine is present in the 100% ionised state. The positively charged cytarabine molecules may however interact better with the negatively charged carboxyl groups of the polymer via electrostatic attraction [173]. Although there is little information on CYT-ARA nanoparticles within

polymers with fatty acyl groups, results obtained from a study of CYT-ARA encapsulation in dipalmitoylphosphatidylcholine: cholesterol: dicetylphosphate (DMPC) liposomes coated with O-palmitoylpullulan (OPP) can be compared with our results using acylated polymers. It was found that coating with OPP increases the stability of the liposomes as a drug delivery system in harsh environments such as encountered after oral administration. However, the reported encapsulation efficiency of CYT-ARA decreased from 27% in the uncoated liposomes to 15% after coating with fatty acyl groups [174]. Thus, presence of acyl groups could be responsible for either decreased interaction with the polymers or interference in affinity of the drug into the polymer core. However, this seems to be in contrast to the study by Stamp on factors affecting Cytarabine encapsulation within liposomes where it was reported that Cytosine arabinoside seems to interact with liposomal membranes at physiological pH and ionic conditions with high efficiency [175]. In a study by Gomez *et al.*, Cytarabine-loaded albumin microspheres were synthesized and were then included in poly (lactide-co-glycolide) to obtain a comatrix that showed a good drug loading [176]. The amount of cytarabine included in albumin microspheres was between 46-50 μg of drug/mg of microspheres depending on the composition of the disperse phase (i.e. 4.6 to 5.0% loading). The high solubility of cytarabine in aqueous medium (148 mg/ml) was reasoned to be responsible for some of the drug to be eliminated in the washing process after synthesis.

Influence of polymer molecular weight on drug loading showed that an increase in MW led to increase in drug loading (Fig. 3.14) for both drugs. This is in accordance with reported data showing that generally with increase in molecular weight there is an increase in drug incorporation [130, 132].

Labhasetwar *et al.* reported increased DNA loading within higher molecular weight PLGA polymer [177]. However, these results seem to be in contrast to the results of Panyam *et al.*, who reported a higher DXM loading in PLGA with 12,000 Da molecular weight compared to PLGA of higher molecular weight (143,000 Da) [169]. They concluded that drug is present in crystalline state within the lower molecular weight polymer and that must have led to increased solid state solubility of the drug in the polymer matrix. Studies with Poly lactide-co-glycolide polymers and their derivatives show decreased entrapment of Huperzine A with higher molecular weight polymers [178]. This has been attributed to the decreased hydrophilicity of high MW polymers as they contain fewer carboxylic acid terminal groups [178, 179]. However with our polymers the presence of pendant hydroxyl groups in addition to the terminal hydroxyl / carboxyl groups determines their hydrophilicity and hence the 12 kDa polymer backbone contains more OH groups per polymer chain that enhances counter ion interactions with DXMP and CYT-ARA leading to better incorporation of these drugs as compared to the 2 kDa and 6 kDa backbone units.

On comparing the drug loading in particles prepared by the IDP and emulsification methods, higher loading was seen in particles prepared using the IDP method (Fig. 3.15). The nanoprecipitation (IDP) method is more flexible and can be modified to achieve incorporation of drugs of varying physicochemical properties [180]. Emulsified particles were prepared in the presence of Tween 80. When the surfactant is present at a concentration exceeding its Critical Micelle Concentration, there is a formation of micelles of surfactant in the external phase. The Critical Micelle Concentration of Tween 80 solution is 13 mg/ml or 0.35% [181], while we have used a 1% solution in this

study. This may be responsible for solubilisation of drug into the external phase as the organic solvent used to prepare the polymer solution diffuses towards the external phase taking the drug along with it [182].

3.5.3. Drug release

DXMP particles prepared from the 100% acylated polymers showed a controlled release profile without burst release. Decrease in acylation resulted in a more rapid release along with a significant burst effect (Fig. 3.16). Similarly, the polymer backbone with a higher MW had a lower burst and greater retention of DXMP compared to the 6 kDa polymer (Fig. 3.18). These results may be due to strong hydrophobic interactions between hydrophobic domain of polymer and drug. The steroid - acyl interaction discussed in section 3.5.2 could also be responsible for the better retention of drug within acylated polymers. Thus, enhanced interaction between drug and polymer contributed to both sustained drug release and increased drug loading (Fig. 3.13). Also, the more hydrophobic domain of polymer should lead to a stronger hydrophobic interaction. Surface localisation of DXMP may have occurred with the lower percentage acylated polymers (Table 3.1) that led to rapid release of bound drug. Release from the 100% acylated polymer was probably due to diffusion of entrapped drug through polymer matrix and surface erosion of polymer [183]. The Higuchi analysis of DXMP release from the 100% acylated polymer (Fig. 3.21) suggests diffusion was a significant mechanism of drug release.

It has been reported that the lower molecular weight polymer fractions easily escape from the nanoparticles during the release conditions especially in the initial phase from PLA particles [86]. Low molecular weight PLGA particles in

the absence of a surfactant showed a great burst release of drug [176]. This was due to the presence of shorter hydrophobic blocks that are more water soluble and degrade faster.

Soo *et al.* studied the effect of PCL block length on the release of estradiol from polycaprolactone-*block*-poly (ethylene oxide) (PCL-*b*-PEO) micelles [184]. The drug was released more slowly from PCL_{151}-*b*-PEO_{44} than PCL_{23}-*b*-PEO_{44} because presumably it had a larger core due to the longer hydrophobic block (151 units of PCL), compared to the shorter hydrophobic block (23 units of PCL). The drug had a longer diffusion distance when in a core with a longer hydrophobic block. Jeong et al. showed that for poly (γ-benzyl L-glutamate)-*b*-poly (ethylene oxide) (PBLG-*b*-PEO) micelles with different PBLG contents, but similar loadings of adriamycin, the release was slower from the copolymer with higher poly (γ-benzyl L-glutamate) content [185]. The increased hydrophobic interactions between the drug and the micelles with higher PBLG content were responsible for the slower release. However, all micelle samples were associated with an initial burst of around 20 to 30% in the first hour. Similarly, Nah *et al.* incorporated norfloxacin and clonazepam into poly (γ-benzyl L-glutamate)-*b*-poly (ethylene oxide) micelles and observed that the drug release was slower from the longer PLBG chains [186]. Gorshokova *et al.* found that over a 15 day period, the release rate of daunomycin was reduced from 16% to 4% due to the introduction of hydrophobic blocks (decylamine) [187]. In an attempt to decrease the rate of release of DXM from NPs of PLGA, Kim *et al.* entrapped the PLGA NPs into alginate hydrogels at 1% and 3% concentrations [170]. Free NPs in PBS solution showed an initial burst of 60% during the first two days followed by gradual reduction of release. NPs entrapped in alginate hydrogels at both

concentrations showed a marked decrease in the burst with 20% drug being released after 24 hours. Song *et al.* reported a 25% release of DXM from PLGA particles in the initial 24 hours [88].

For CYT-ARA, as evident by the drug loading results, drug loading in the acylated polymers is low (Fig. 3.13). The polymer backbone had minimum initial release (20%) after 24 hours and there was no significant difference in the initial release rates from the 20% and 40% acylated polymers (Fig. 3.17). Also, there was no significant difference in the release from the 2 kDa and 12 kDa polymer backbones except that for the latter greater retention was observed and 90% of the drug was released by 24 days. The 6 kDa polymer released the drug rapidly (Fig. 3.19). The fully acylated polymer had a rapid and uncontrolled release. Incorporation of CYT-ARA was highest in the 12 kDa polymer backbone with no acylated groups (Fig. 3.14). This indicates that for CYT-ARA, the hydroxyl and carboxyl functions were important not only for enhancing the drug loading but also for retaining the drug within the core for a longer period. With an increase in polymer MW an increased loading was observed. Surprisingly, loading within the 2 and 6 kDa polymers was similar, yet retention and release was better with the lower MW polymer. Thus, it is evident that the water solubility of the lower MW fractions did not seem to be important for amount of drug loaded. Surface localisation of the drug could have occurred with the 6 kDa polymer resulting in its rapid release (Fig. 3.14). With an increase in acylation of the polymer the number of hydroxyl groups available was lower compared to the backbone and this could be responsible for the slight increase in the initial release rate. However, all three polymers (backbone 12 kDa, 20% and 40% acylated) retained the drug for a longer period of time compared to the 100%

acylated polymer. Solubility of DXMP in water is 500 mg/ml while that of CYT-ARA is 300 mg/ml. Both are highly water soluble drugs yet DXMP was retained best by the most hydrophobic polymer. CYT-ARA release was uncontrolled from the same polymer thus strongly suggesting an altered ability of the polymer to retain the drug depending upon the structure of drug and its interaction with the polymer.

When the drug-loaded hydrophilic polymeric carrier contacts water, swelling of the polymer might occur as a result of diffusion of water molecules into the polymer network and relaxation of macromolecular chains. Both of these processes result in a release of the entrapped drug. It is known that drug release may be diffusion controlled or dissolution controlled, depending on the parameters such as permeability of the polymer to water, the solubility of the drug in the polymer and in water, and size of the drug [173]. In the present case, release by dissolution is not applicable as both DXMP and cytarabine are water soluble. Thus, the mechanism of drug release is most likely to be diffusion or Fickian controlled.

Most studies have reported a higher initial rate of release and lower retention of water soluble drugs from hydrophilic polymers. Other factors contributing to high initial burst release are large surface area, high diffusion coefficient and low viscosity of matrix [188].

In a study of CYT-ARA release from gelatine nanoparticles it was found that drug release rate was more controlled with increasing percent of drug loading. This was attributed to decrease in the pore size of nanoparticles due to accumulation of drug molecules within the nanoparticles. The diffusion of water molecules into the loaded nanoparticles would hence be restrained resulting in a

lower release of cytarabine [173]. Ameri *et al.* reported sustained release of Ara-C from matrices prepared from triblock copolymers $C_{17}E_mC_{17}$ (where C denotes methylene or methyl, E denotes oxyethylene, and *m* is either 227 or 454) [189]. The particular copolymers were chosen as representatives of the class of copolymers which form elastic, cross-linked gels through association (micellisation) of their alkyl end blocks. The release of cytarabine from the copolymer matrices was predominantly by a Fickian diffusion mechanism and attributed to increase in matrix gel layer thickness as water diffused into the matrices. The release rate was dependent on drug loading and independent of co polymer molar mass. In our studies, for either drug, polymers with the highest drug loading had slowest release.

The release kinetics of Ara-C from Albumin-PLGA co matrix microspheres took place via swelling and showed a hyperbolic profile [176]. The maximum drug release from Ara C – PEG conjugates took place in the first 7 h, and a burst effect was observed in the first hour, where 29 to 37% of the drug was released. These conjugates of Ara-C with PEG release drug by a different mechanism compared to PGA or PLGA particles however, it is worth noting that even conjugated drug showed 60 to 80% release within 8 to 10 days at pH 7.4 [173].

Studies incorporating flurouracil in PLA-PEG-PLA triblock polymers showed that the rate of drug release was high (60%) in the initial period. Most drug was released within 2 to 3 days by diffusion and burst release. This was correlated with the hydrophilic nature of the drug which does not permit encapsulation in the micelle core [190]. In a study performed by McCarron *et al.* on release of 5-FU from PLGA particles, an initial burst effect of 50% drug was seen in the first hour followed by a slower release of 66% drug released over 24 hours [183]. As

evident from our results, for our polymers, drug release is not influenced by hydrophobic characteristics of the polymer or properties of the drug in isolation. Rather, it is a combined effect of both drug and polymer properties that influence their interactions and hence retention within the polymer core.

Most commonly it is reported that particles with a higher drug loading have a fast release rate mainly attributed to surface localisation [191]. The amounts of lidocaine released in PBS from PLA nanoparticles in the initial phase were related to the nanosphere size [29]. Their DSC and infrared studies showed that no strong chemical interaction between drug and polymer occurred. Release kinetics of praziquantel from PLGA particles was governed not only by actual drug loading but also by the particle size. The higher the drug content and the smaller the particle size, faster was the drug release [192].

Nah *et al*. correlated clonazepam release from block copolymers consisting of poly (γ-benzyl L-glutamate) (PBLG) as the hydrophobic part and poly (ethylene oxide) (PEO) as the hydrophilic part to drug loading contents [186]. They found that the polymer with a longer PBLG length had a greater drug loading and slower rate of release. In a study of Fluorescein isothiocyanate-dextran encapsulation within cross linked polyvinyl pyrolidone NPs, a 3.2% w/w loading of Fluorescein isothiocyanate–dextran in polyvinyl pyrolidone polymer released nearly 95% of drug in 10–12 days while about 60% release occurred from the nanoparticles during the same period when the dye loading was 6.4% w/w in the same polymeric material [193]. It was hypothesised that a larger population of dye (6.4%) within the same volume of nanoparticles may lead, at least partly, to the association of dye molecules as dimers, trimers, etc. or even to the formation of solid clusters inside the matrices of the nanoparticles [194]. When the

concentration of dye inside the core of the particle is very high, a part of it is associated or clustered, which has to be dissolved and released more slowly out of the nanoparticles. At low loadings of the compound, it may remain in the form of a molecular dispersion inside the polyvinyl pyrolidone nanoparticles.

For a number of polymer systems studied it has been reported that particles with the largest size have more controlled release compared to the particles with smaller sizes [89, 194, 195] and factors like increase in particle size, increase in polymer MW inhibit drug diffusion. This has been explained based on the fact that small sized nanoparticles have increased total nanoparticle surface area resulting in larger drug fraction exposed to leaching medium molecules. Thus, decrease in particle size may lead to increased diffusion from organic to aqueous phase during solvent evaporation causing low drug loading and fast release. Smaller nanoparticle size also leads to a shorter average diffusion path of entrapped drug. From our studies, we observed that difference in particle sizes cannot be considered as a predominant factor influencing drug release. Although, for DXMP particles it was found that the 100% acylated polymer forming particles with largest size had slowest release compared to polymer backbone that formed particles with smallest size. In presence of CYT-ARA, the 20 and 40% acylated polymers formed particles that were similar in size to the 100% acylated polymers; however, only the release rate from the 100% acylated polymers differed significantly from the others and was rapid.

The difference in release profile of DXMP prepared using the emulsification method may be due to the presence of Tween 80 as explained by Niwa *et al.* [86]. An increase in the concentration of Tween 80 led to enhanced release (Fig. 3.20). When the surfactant is initially present in the aqueous phase there is the

possibility of anchoring of the surfactant molecules to the polymer matrix. This surface bound fraction of the surfactant may contribute to the solubilisation of the drug molecules reaching the nanoparticle surfaces and facilitating their dissociation to the leaching medium. This may then be responsible for enhanced drug release and lower drug encapsulation [86, 190].

Surfactants also contribute to the burst release by promoting a more porous structure [190]. Arica *et al.* prepared betamethasone particles using surfactants PVA (8 -18%) or sodium cholate (25-35%). They observed an initial burst release followed by sustained release delivering 15 to 40% entrapped drug within 48 hrs [196]. Various other studies have also shown that increase in surfactant concentration leads to an increase in drug release [90, 194, 196].

3.6. CONCLUSIONS

PGA polymer backbone and its substituted acylated series can form stable nanoparticles in the presence and absence of drugs and in the absence of surfactants.

DXM-P loaded particles are smaller in size than CYT-ARA particles suggesting a possible role of drug polymer interactions in particle formation. Drug loading increases with acylation and molecular weight of polymer for DXMP, while CYT –ARA shows maximum incorporation within polymer which is non acylated and of maximum molecular weight. The degree of polymer acylation has less effect on drug loading of CYT-A than that of DXM-P. Burst release for DXMP decreased as acylation increased. Thus, increase in polymer acylation contributes to an increase in drug loading and decrease in rate of cumulative drug

released. Increase in Polymer acylation increased drug release for CYT-ARA with the most controlled release occurring from the polymer backbone particles.

CHAPTER 4. SYNTHESIS AND CHARACTERISATION OF AMINO ACID SUBSTITUTED POLYMERS

4.1. Introduction

The polymer backbone substituted with acyl groups has been investigated extensively for drug incorporation and release in the previous chapter. The backbone was further substituted with amino acids viz. N- acetyl tryptophan and N- acetyl tyrosine in order to study the influence of aromatic rings and ring stacking as a non covalent bond on the polymer characteristics, incorporation and release characteristics of hydrophilic and hydrophobic drugs. The polymer was substituted to a similar extent as the acylated polymer series (Chapter 3). The degree of substitution ranged from 1% to 60% substitution. In addition to the above, a combination polymer containing 40% acyl and 5% tryptophan side chains together was synthesised and investigated. The drugs included in the study were anti cancer drugs containing aromatic heterocycles (Etoposide, Paclitaxel) with an aim to study the effect of aromatic ring stacking between the polymer and the drugs and their influence on drug loading and release.

Aims of the chapter:

- Synthesis of amino acid and combined acyl-amino acid substituted polymers.
- Characterisation of the substituted polymers.

- Optimise degree of substitution for assembly into stable nanoparticles.

4.2. MATERIALS AND METHODS

4.2.1. MATERALS

Polymer backbone and the C_8 acylated polymers were obtained as described in Chapter 2. The amino acids N-Acetyl-tryptophan, N- acetyl tyrosine, Deuterated acetone, Methanol, EDAC, DMAP were purchased from Sigma. All solvents used were of HPLC grade.

4.2.2. METHODS

Tryptophan, tyrosine and the combination polymer were synthesised using the EDC mediated conjugation as described in sections 2.3.1, 2.3.2 and 2.3.3.

The reaction mechanism is illustrated in Fig. 4.1. Molecules with reactive amino or carboxyl groups can be coupled to polymers with reactive sites under gentle conditions using water soluble carbodiimides; example 1-ethyl-3-(3-dilethylaminopropyl) carbodiimide hydrochloride (EDAC) to form covalent conjugates via amide/ester bonds. The reaction involves the intermediary formation of the activated o-acylurea derivative of the carbodiimide. A subsequent nucleoplilic attack by the activated hydroxyl group on the polymer in the presence of dimethylaminopyridine as a catalyst brings about the formation of the ester linkage with the release of the soluble substituted urea [197]. The reaction was simple and straightforward and went smoothly without any difficulties.
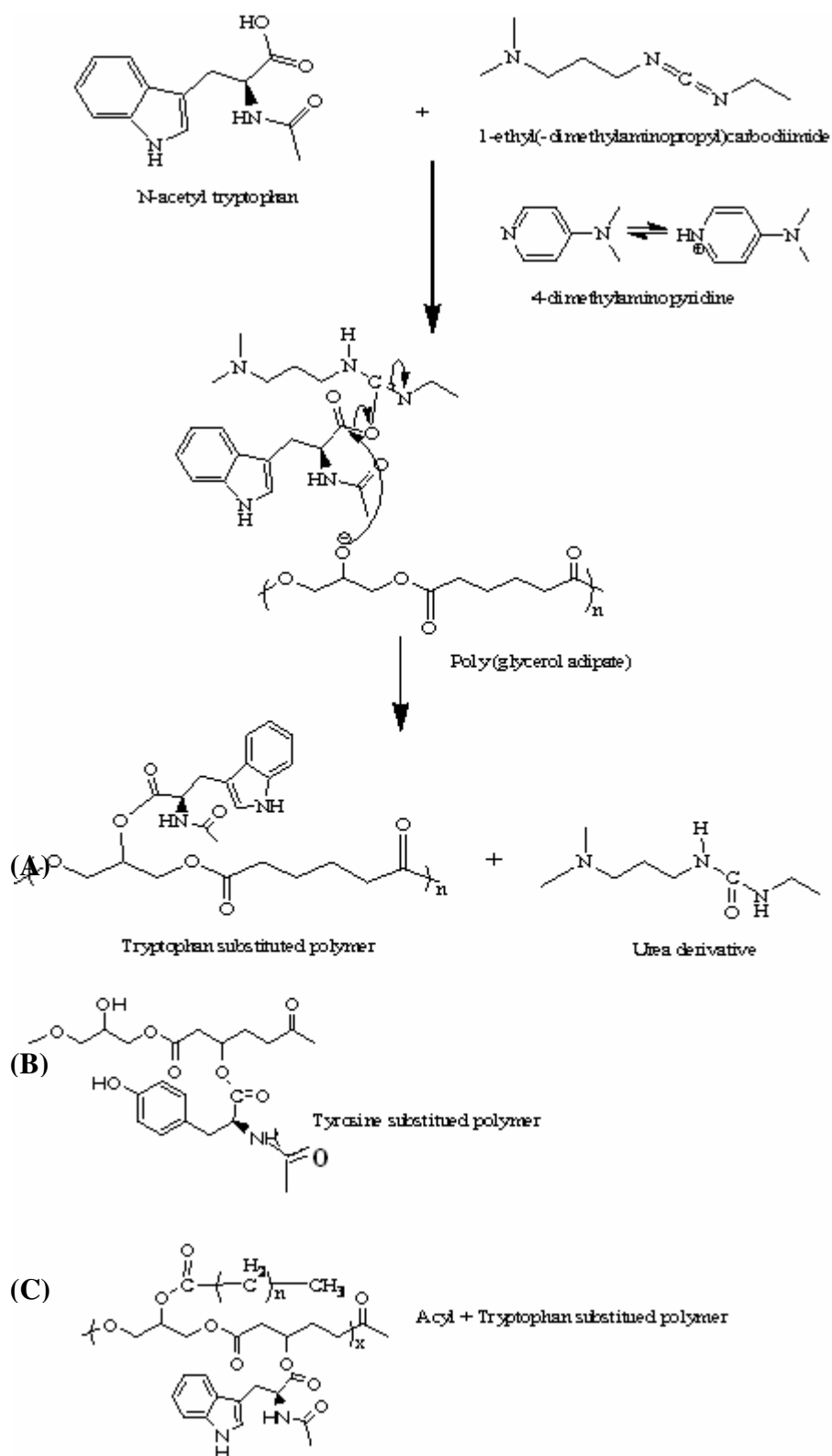
Fig. 4.1. Reaction mechanism of EDAC mediated (A) Tryptophan (B) Tyrosine
(C) Acyl-tryptophan conjugation to backbone/acylated poly (glycerol adipate).

4.3. RESULTS

The synthesised polymers were then characterised by NMR. Following are the
NMR scans of the polymer backbone, 40% tryptophan substituted polymer, 5%
tyrosine and 40% C_8 + 5% tryptophan substituted polymers.
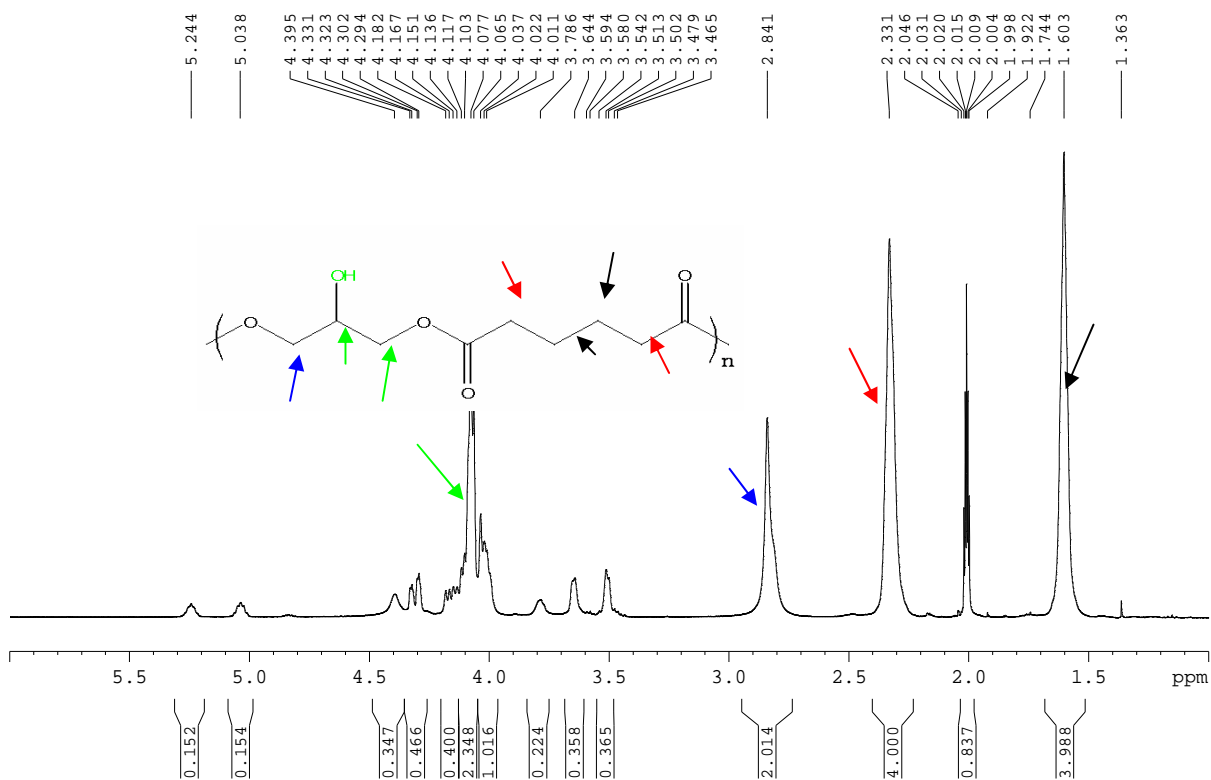
Fig. 4.2. NMR spectrum for poly (glycerol adipate) backbone
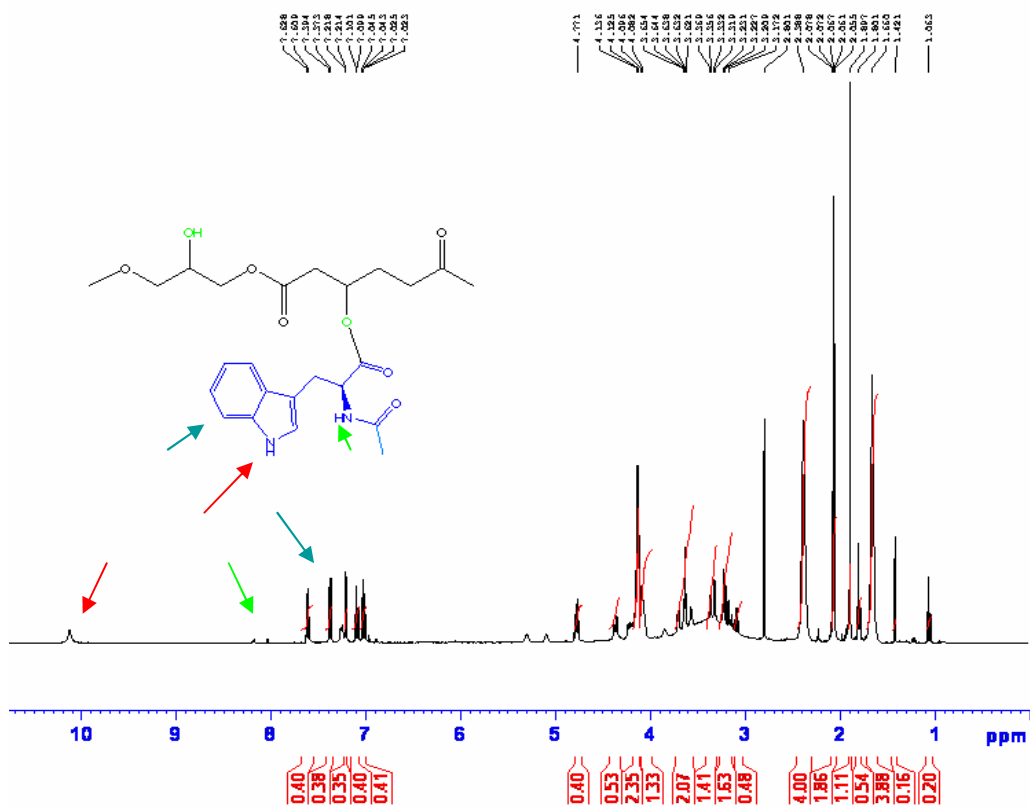
Fig. 4.3. NMR spectrum for poly (glycerol adipate) backbone substituted with tryptophan (40%)
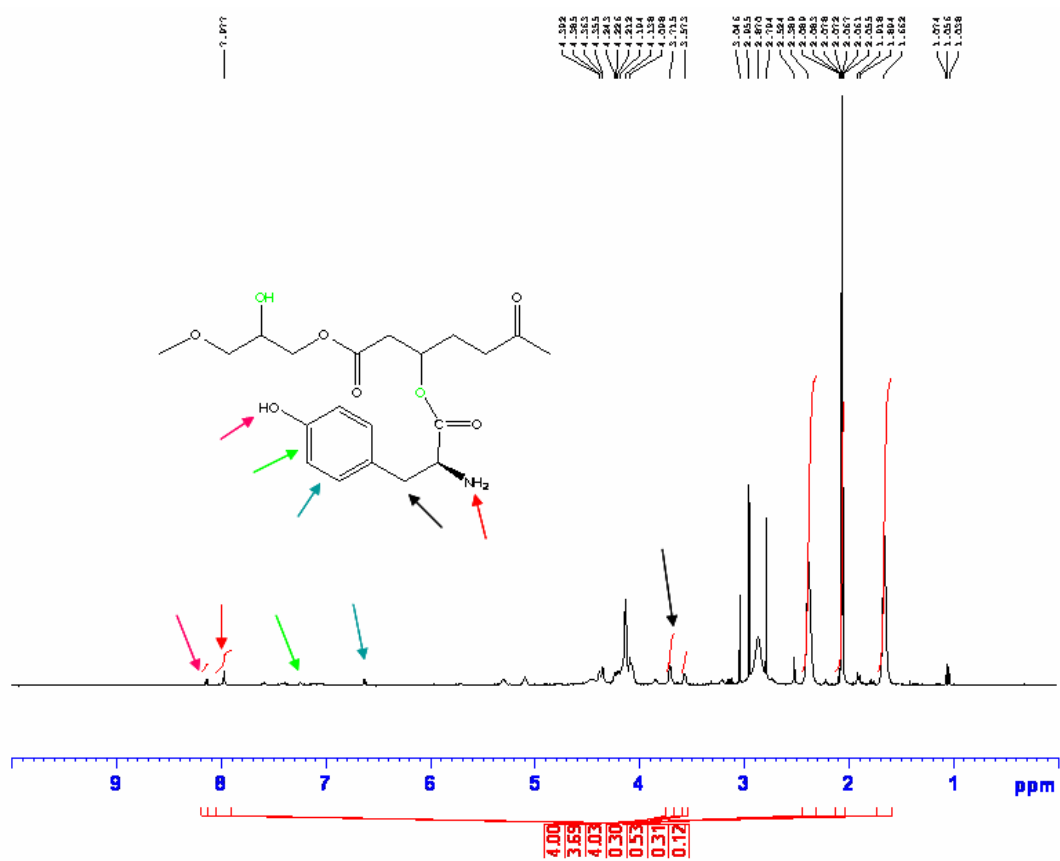
Fig. 4.4. NMR spectrum for poly (glycerol adipate) backbone substituted with tyrosine   (5%).
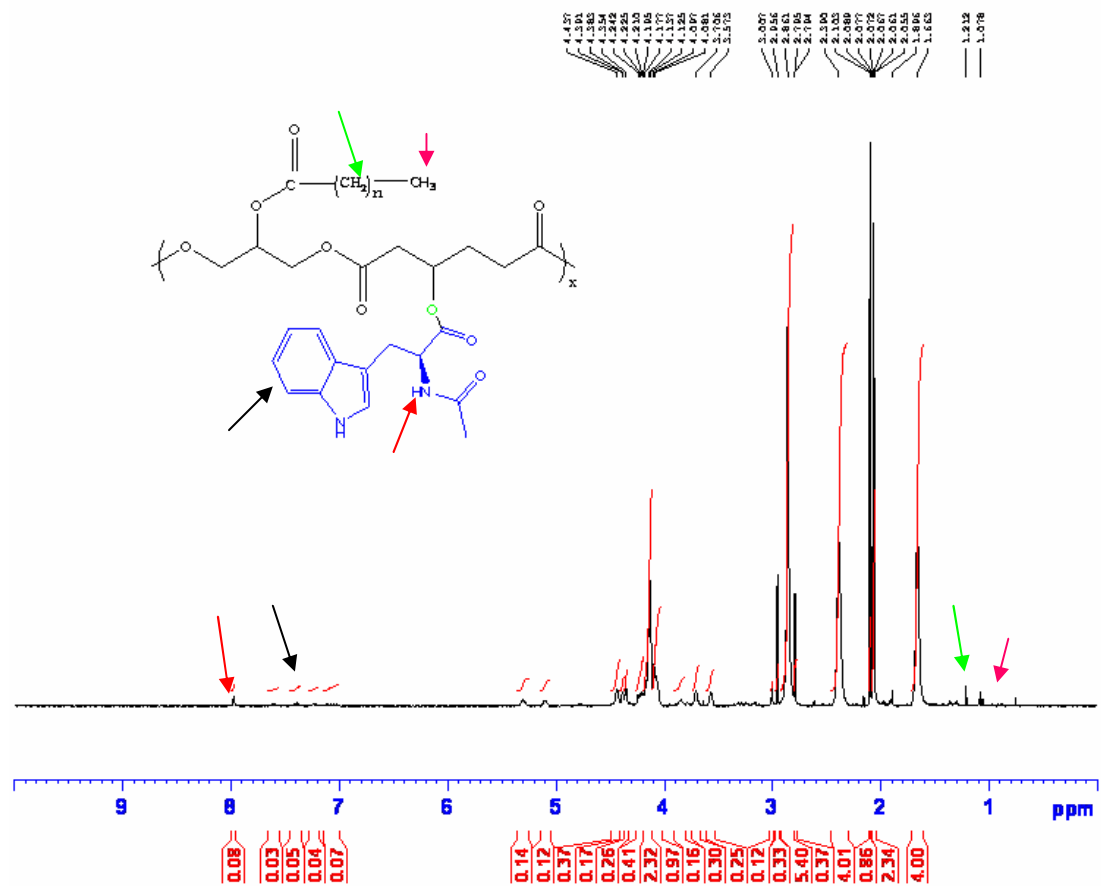
Fig. 4.5. NMR spectrum for 40% C_8 acylated polymer substituted with tryptophan (5%)
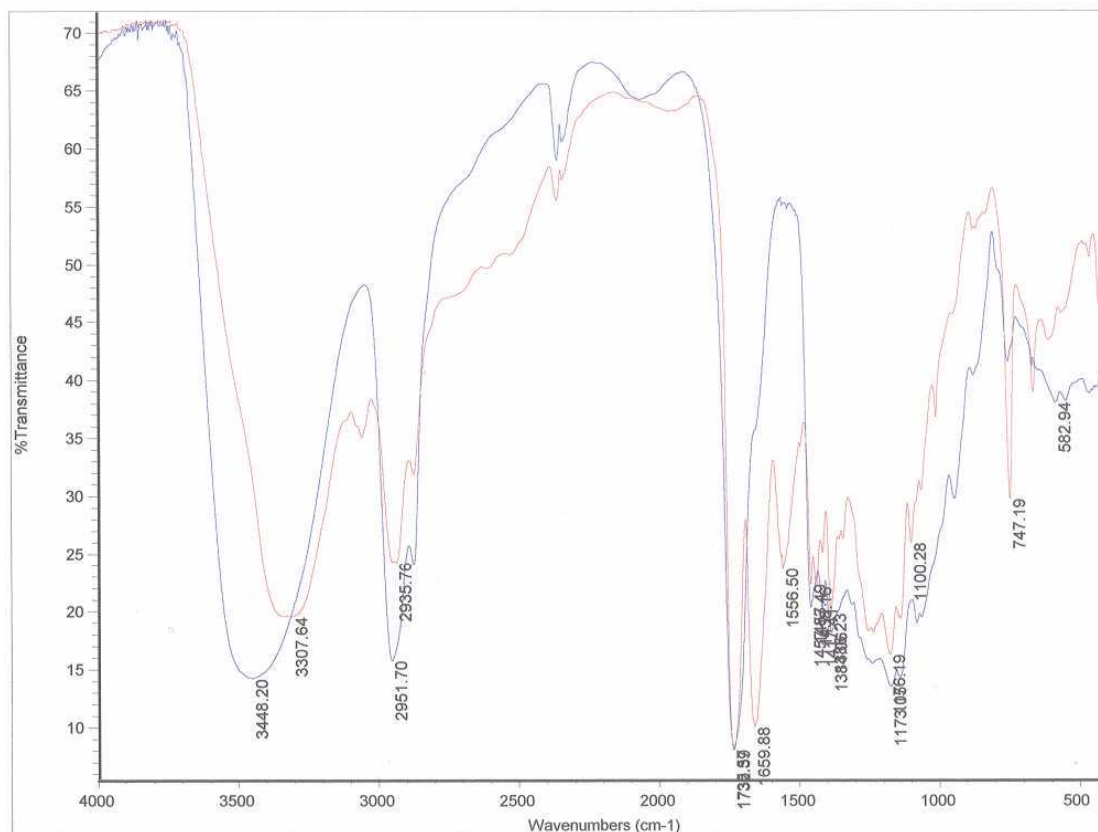
Fig. 4.6. FTIR of poly (glycerol adipate) substituted with tryptophan (40%).
(Polymer backbone ---, Polymer + Tryptophan ---).

4.4. DISCUSSION

The NMR for the polymer backbone is presented in Fig. 4.2.

Due to the random polymeric nature of these systems the NMR interpretation becomes somewhat complicated. The area between δ (4.5-3.5) appears cluttered. It could possibly indicate that the hydroxyl proton must be involved in hydrogen bonding which would account for the large number of peaks in this area due to the varying conformations viz intra and inter- molecular hydrogen bonding. The peaks for the 4 methylene protons –CH_2-O-CO- appear at δ(3.9-4.1) and the –CH_2-CO- are detected at 1.63 ppm while –CH_2-CO-O- at 2.09 ppm. The pendant hydroxyl group appears at 5 ppm.

However, for the tryptophan substituted polymer peaks at δ (7-7.5), characteristic to the benzene ring of tryptophan/ tyrosine and the peak at 10 ppm corresponding to the indole proton confirm the presence of amino acid attachment to the polymer. The spectrum in Fig. 4.3 is of a 40% substituted polymer in order to demonstrate the benzene protons with clarity. The degree of substitution was calculated by calibrating the 4 methylene protons of the protons. The integral of the protons of the benzene group correspond to the degree of substitution. Around 2 to 3 % substitution occurred for the tryptophan substituted polymers. (For NMR of pure tryptophan and tyrosine refer Appendix 16 and Appendix 17 respectively).

Similarly, with the addition of tyrosine (Fig. 4.4) the benzene ring protons are visible although they appear slightly downfield compared to tryptophan. The phenolic proton was detected at 8.2 ppm. The methylene protons from tyrosine were also visible between 3.5 and 4 ppm although the signal was very weak as it is a 5% substituted polymer. Also, since no protecting group was used for the hydroxyl groups on tyrosine before its conjugation with the polymer there might be some intramolecular hydrogen bonding and cross linked product although it cannot be distinguished distinctly in the NMR. However from the integral values of the benzene protons resulting in around 1 % substitution it could indicate cross linking in the product.

From Fig. 4.5, for the polymer substituted with both acyl and tryptophan groups the presence of methylene protons in the alkyl groups and the methyl proton in addition to the tryptophan protons were detected upfield at 1.02 and 0.9 ppm.

The FT-IR of the polymer substituted with 40% tryptophan further confirmed the presence of ester bonds at 1659 and 1556.50 cm^{-1}, which was absent in the scan

of the unmodified polymer. The peaks for the hydroxyl groups shifted from 3448.2 in the polymer backbone to 3307.64 cm^{-1} probably due to involvement of some protons in esterification reaction (Fig. 4.6).

4.5. CONCLUSIONS

Polymers were successfully substituted with tryptophan and tyrosine in varying degrees.

CHAPTER 5. INCORPORATION AND RELEASE OF ETOPOSIDE AND ETOPOSIDE PHOSPHATE FROM FUNCTIONALISED POLY (GLYCEROL ADIPATE) NANOPARTICLES

5.1. Introduction

Podophyllotoxin is an antimitotic natural product. Its inhibitory activity on cell growth led to the development of the clinically valuable anticancer agents, etoposide, teniposide and the water-soluble prodrug, etoposide phosphate. The cytotoxic mechanism of these drugs is the inhibition of topoisomerase II [198]. Etoposide is a highly hydrophobic molecule with lipophilic properties, and the formulation of etoposide is quite challenging. The major limiting step in the formulation of etoposide is its lipophilicity, and vehicles Cremophor® EL, (CrmEL) or polysorbate 80 (Tween® 80) used as solubilizers are associated with adverse side effects such as hypotension, anaphylaxis, bronchospasm, nephrotoxicity and cardiotoxicity, some of which can even be life threatening [199-201]. Commercial Etoposide formulations are eliminated rapidly from the blood circulation upon intravenous administration and produce myelosuppression. Etoposide Phosphate on the other hand, is water soluble and is converted to etoposide in vivo. No reported literature exists to date on Etoposide phosphate formulation into colloidal drug delivery systems. The nanoparticles containing ETO and ETO-P in functionalised poly glycerol adipate

nanoparticles were characterized by Photon correlation spectroscopy (PCS) for size and size distribution, Transmission electron microscopy (TEM) for morphological properties and zeta-potential for surface charge. We aim to investigate the influence of chemistry of drug and polymer on their interaction and retention within nanoparticles.

Aims of chapter:

- To assess the ability of poly glycerol adipate and its modifications to encapsulate ETO and ETO-P into stable nanoparticles.

- To study the influence of polymer functionalisation and nature of side chain functional groups on drug incorporation and release of ETO and ETO-P.

- To compare encapsulation and release of a hydrophobic drug (ETO) and its hydrophilic prodrug (ETO-P) with similar chemical structure, from various polymers with different properties.

5.2. MATERIALS AND METHODS

5.2.1. MATERIALS

Etoposide and Etoposide phosphate were obtained from Sigma UK. Polymer backbone, acyl substituted and amino acid substituted polymers were synthesised as described in Chapter 3. All organic solvents were of HPLC grade.
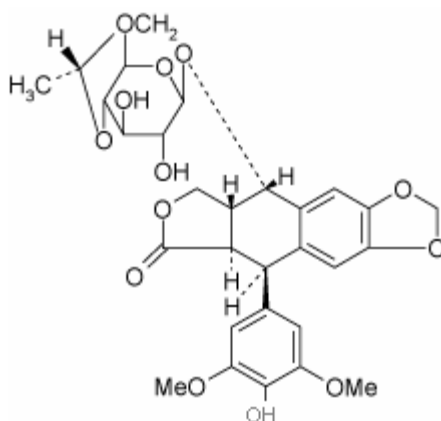
4'-demethyl-epipodophyllotoxin   9-[4,   6-O-(*R*)-ethylidene-beta-D-

glucopyranoside]

Formula: $C_{29}H_{32}O_{13}$

Mol. Weight: 588.557g/mol

Fig. 5.1. Molecular structure and identity of Etoposide (ETO).
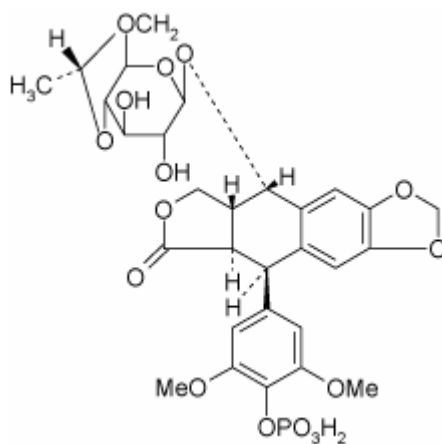
4'-Demethyl-epipodophyllotoxin   9-[4,   6-O-(R)-ethylidene-ß-D-

glucopyranoside], 4'-(dihydrogen phosphate).

Formula: $C_{29}H_{33}O_{16}P$

Mol. Weight: 650.557g/mol

Fig. 5.2. Molecular structure and identity of Etoposide phosphate (ETO-P).

5.2.2. METHODS

5.2.3. Preparation of Etoposide nanoparticles

Etoposide loaded nanoparticles using polymer backbone, acylated and amino acid substituted polymers were prepared using both the interfacial deposition method and the interfacial deposition method with preformed matrix as described in section 2.4.3, Chapter 2.

5.2.4. Preparation of etoposide phosphate nanoparticles

Etoposide phosphate nanoparticles were prepared using the interfacial deposition method described in section 2.4.3, Chapter 2.

5.2.5. Separation of free drug from nanoparticles

Nanoparticles were separated from unincorporated drug using methods 2.3 A and B described in Chapter 2.

5.2.6. Physicochemical Characterisation

Size, surface charge and external morphology of the nanoparticles were determined using methods detailed in Chapter 2.

5.2.7. Determination of drug loading

Drug loading was determined by extraction of drug from the nanoparticles followed by quantitation of drug extract.

Etoposide: The freeze dried nanoparticle powder was weighed and dissolved in a mixture of acetone/ MeOH (1:2), followed by centrifugation at 13500 rpm for 3 mins. Acetone was then allowed to evaporate and methanolic solution was analysed by HPLC. Samples were passed through a Lichrosphere 100 RP-18

(5μ) endcapped column Mobile phase MeOH: Water: Acetic acid 54:45:1, flow rate was 1 ml/min and the operating pressure was 2800 psi.

Etoposide phosphate: The freeze dried nanoparticle powder was weighed and dissolved in a mixture of acetone/ PBS (1:2), followed by centrifugation at a speed of 13500 rpm for 3 mins. The supernatant was then analysed using UV spectroscopy at 281 nm.

5.2.8. Drug Release

Drug release studies were performed with distilled water as the external media for Etoposide phosphate and with 0.1% Tween in HEPES for Etoposide at 37°C for 25 days.

5.3. RESULTS

5.3.1. Particle size and zeta potential

The effect of polymer substituents and properties of drug on particle size and surface charge were examined.

Table 5.1 compares the size and zeta potential of particles loaded with either Etoposide or its phosphate prodrug within various substituted polymers.

With the amino acid substitution, particle size decreased compared to size of particles produced with backbone and with the acylated polymers. The polymer substituted with both acyl and tryptophan groups produced particles which were larger than the tryptophan or tyrosine substituted polymer and smaller than the 40% acylated polymer. Comparing the size of drug loaded particles with empty particles; it was observed that the acylated polymers in the presence of either drug produced slightly smaller particles compared to the amino acid substituted polymers.

POLYMER TYPE	EMPTY PARTICLES		(+) ETO		(+) ETO-P	
	SIZE nm (SD) [polydispersity]	ξ-POTENTIAL mV (SD)	SIZE nm (SD) [polydispersity]	ξ-POTENTIAL mV (SD)	SIZE nm (SD)[polydispersity]	ξ-POTENTIAL mV (SD)
Polymer backbone	169.6(2.2)[0.57]	-35.3 (0.9)	130.2 (0.56) [0.2]	-25.3 (0.9)	125.1 (1.5) [0.4]	-31.3 (0.32)
40%C8-12	267.5 (3.09) [0.33]	-31.3 (0.3)	141.2 (1.4)[0.013]	-31.3 (0.3)	139 (2.1) [0.11]	-33.9 (2)
100%C8-12	201.3 (0.57) [0.23]	-39.3(0.8)	126.1 (0.2) [0.03]	-31.3(0.8)	141.8(1.1)[0.048]	-34.3 (0.5)
5 % Tryptophan	132.3 (0.3) [0.05]	-40.1 (2.9)	165.45 (0.16)[0.04]	-43.8 (2.5)	159.3 (0.53) [0.23]	-39.4 (1.2)
5 % Tyrosine	145.2 (2.9) [0.15]	-34.2 (1.87)	177.12 (0.67)[0.06]	-39.6 (0.5)	168.2 (0.5)[0.01]	-31.4 (3.5)
40%C8 + 5 % Tryptophan	190.7 (1.9) [0.35]	-35.9 (0.9)	184.1 (1.0) [0.08]	-29.9 (2.1)	149.3 (0.61) [0.09]	-34.5 (0.7)

Table 5.1 Particle size and Zeta potential of ETO and ETO-P loaded nanoparticles using various polymers by the Interfacial deposition method. Polymer type is designated by nature and degree of substitution, MW. Results are mean of 3 readings, SD standard deviation.

The 40% C_8 + 5% tryptophan substituted polymer produced particles smaller in size than in the absence of drug. For ETO these particles were larger than either the tryptophan or 40% C_8 drug loaded particles, but for ETO-P were of intermediate size.

Between the two different drug formulations it can be seen that the nature of the drug appears to influence particle size. Increase in acylation increased the size of ETO-P particles while particles produced using the acylated polymers were smaller in size than the amino acid substituted polymers. For ETO-P, the largest particles were produced using the polymer substituted with tyrosine moieties while for ETO the combination polymer produced particles larger is size compared to the other substitutents. The size of ETO-P particles with the amino acid substituted polymers was smaller than the empty particles with the same polymers. ETO, on the other hand did not follow a definite trend for acylated polymers although the smallest particles with ETO were produced with 100% acylated polymers. However, for amino acid substituted polymers, particle size was larger than the acylated polymers and the empty particles and was the largest with polymer containing both acyl and tryptophan substitutions.

Zeta potential of ETO-P loaded polymers was in the range of -31 to -35 mV with the exception of the 5% tryptophan polymers which was around -40 mV. For ETO the zeta potential was higher, in the range of -25 to -31 mV with the exception of the amino acid substituted polymers with values around -40 mV. Zeta potential of tyrosine substitution was more negative for ETO than ETO-P. In presence of either drug, zeta potential of the combination polymer became less negative than the tryptophan polymers alone.

5.3.2. TEM Images
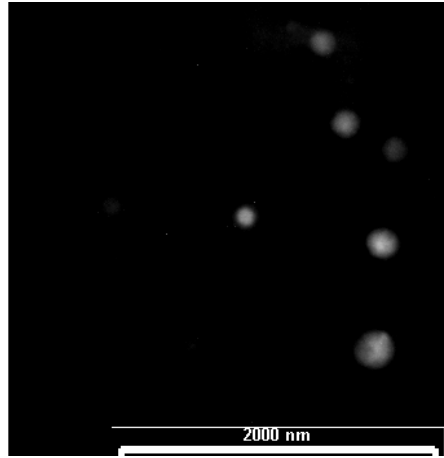
Fig. 5.3.TEM Image of ETO-P nanoparticle in 5% tryptophan substituted polymer, MW 12kDa
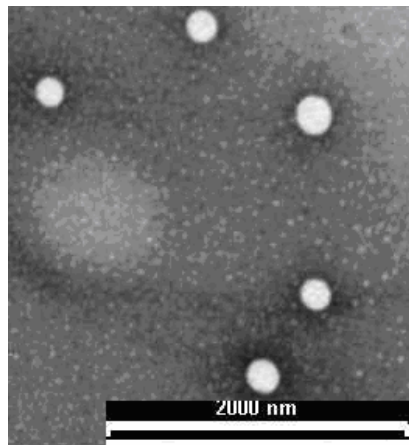
Fig. 5.4. TEM Image of ETO nanoparticle in 5% tryptophan substituted polymer, MW 12kDa
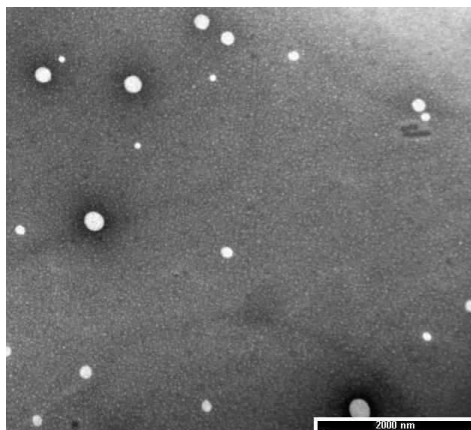
Fig. 5.5. TEM Image of ETO nanoparticle in 100% C_8 polymer, MW 12kDa

Particles prepared using the acylated polymers were spherical and homogenously dispersed for both drugs as can be seen with the TEM images in Figures 5.3. However, within the 5% tryptophan substituted polymers, particles prepared using ETO were larger than ETO-P particles. Polydispersity was higher for ETO-P loaded particles (Figs. 5.4, 5.5).

5.3.3.Determination of Drug Loading

5.3.3.1.Method validation for ETO (HPLC Assay)

Standard solutions of ETO in MeOH were analysed on the HPLC using the method described in section 5.2.7 and a calibration curve was prepared (Fig. 5.6).
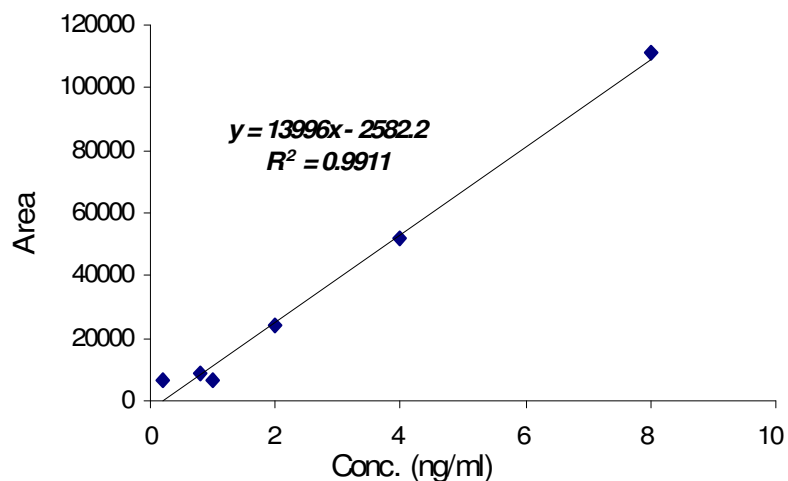
Fig. 5.6. Calibration curve for Etoposide standard solutions in MeOH using HPLC.
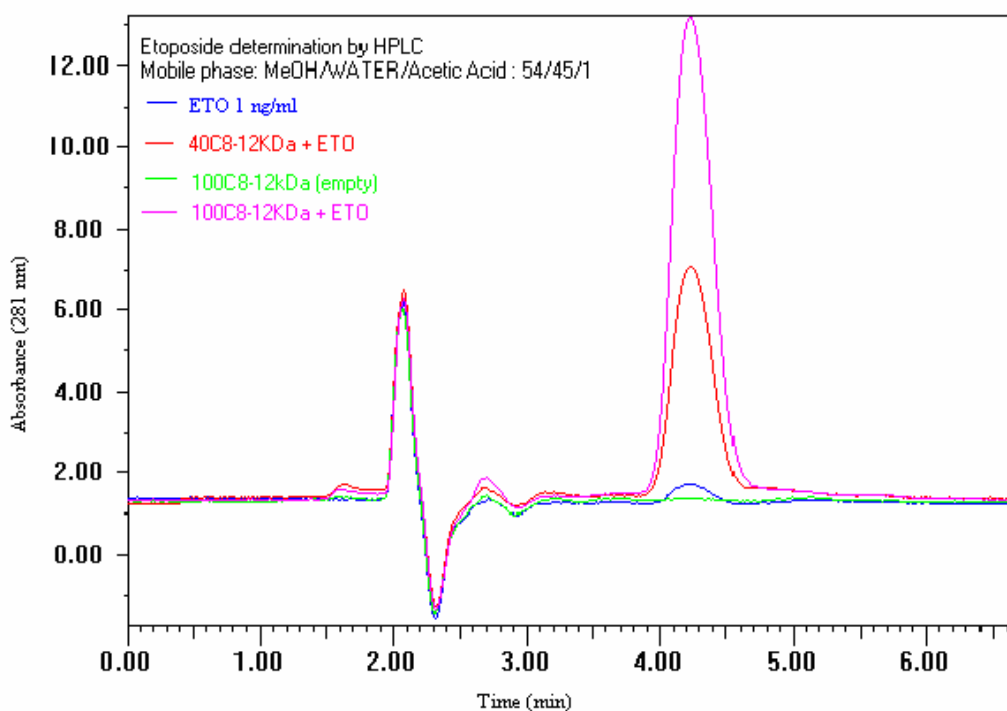
Fig. 5.7. HPLC chromatogram for ETO determination. Standard solutions of ETO in MeOH were analysed to determine retention time on the column.

Retention time of ETO under operating conditions described earlier was 4.23 minutes'. Empty particles do not show any peak at elution time of drug (Fig. 5.7). As a control, 200 μg of pure drug was added to a suspension of empty nanoparticles and their recovery was analysed in order to estimate the efficiency of the procedure (Table 5.2).

Sample	Area	Conc.(ng/ml) (* 100)	μg/tot.fr.vol.† (4ml)	Efficiency (%)	Avg. Efficiency (SD)
Control-1	5899	47.32	169.25	84.63	
Control-2	4788	34.45	137.62	68.79	**77.3%**
Control-3	5456	39.2	157.58	78.28	**(7.97)**

† total free volume

Table 5.2. Extraction efficiency of known amount of control ETO.

As it can be seen from Table 5.2, ETO from controls was recovered in a range from 78 to 84% efficiency. Average drug loading was calculated and results were divided by 0.773 to give the final amount of drug in the samples.

5.3.3.2. Method Validation for ETO-P

ETO-P was analysed spectroscopically. Standard solutions of known concentrations of ETO-P in water were analysed at 281 nm on a UV-Vis spectrophotometer and a calibration curve was prepared (Fig. 5.8). Samples were extracted using the method described in Chapter 3. Control samples containing known amount of ETO-P (200 μg) was added to the empty nanoparticles and analysed to determine efficiency of the method.
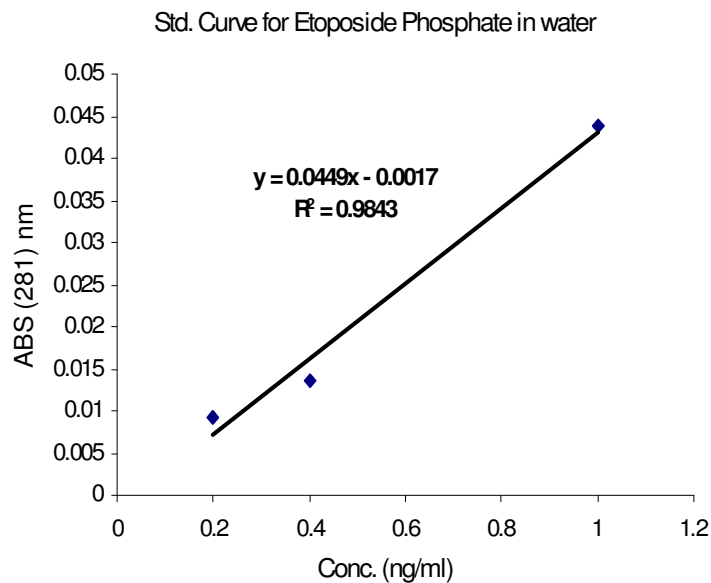
Fig. 5.8. Calibration curve for Etoposide phosphate standard solutions in water using UV spectroscopy.

Sample	Abs. (281nm)	Conc.(ng/ml) *100	μg/tot.fr.vol.† (4ml)	Efficiency (%)	Avg. Efficiency (SD)
Control-1	0.0153	33.93	135.68	67.84	
Control-2	0.0175	39.12	156.06	78.03	**67.9%**
Control-3	0.0157	34.77	139.15	69.57	**(5.45)**

† total free volume

Table 5.3. Extraction efficiency of control ETO-P

As it can be seen from Table 5.3, around 68% of the control was recovered. Average extraction efficiency was calculated and the average drug loading result was divided by 0.68 to calculate the final drug loading of the samples.

5.3.3.3. *Effect of method of preparation on ETO loading*

Fig. 5.9 shows the incorporation of ETO achieved using the original IDP method compared with a modified method. Using the standard method resulted in a small increase in ETO incorporation with increasing acylation and maximum drug (0.74%) incorporated by the 100% acylated polymer (Fig. 5.9).
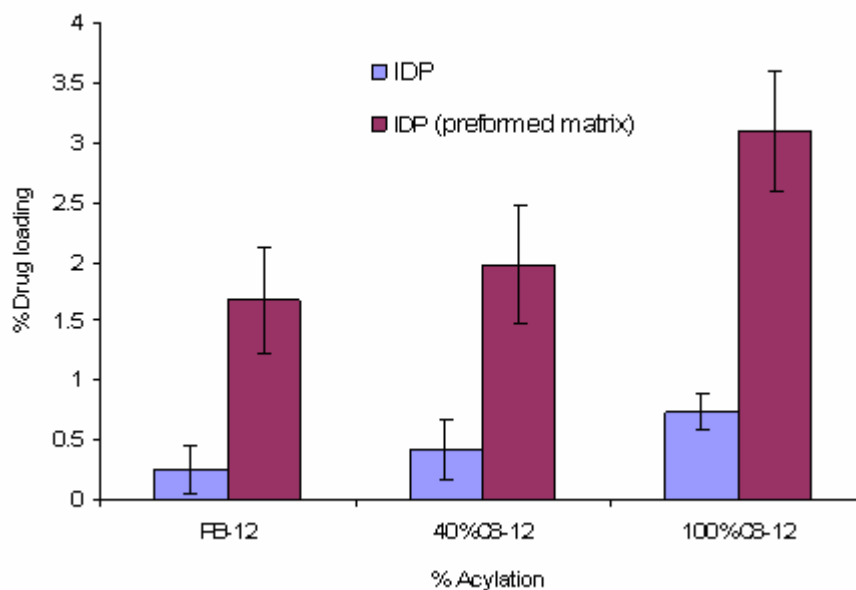
Fig. 5.9. Comparison of ETO loading using IDP and Modified IDP methods. Modified IDP increased the loading within the polymers.

There was a very low drug incorporation using the original ID method as compared to results obtained previously using water soluble drugs (DXMP, CYT-ARA(500 μg/ml)>ETO(150 μg/ml). Hence, a modified ID method was investigated. Here a matrix of the polymer was first prepared with the drug in a common solvent followed by its addition into the aqueous phase as opposed to adding the drug and polymer directly into the aqueous phase. Drug loading increased substantially and followed a similar trend with increase in acylation.

5.3.3.4. Effect of polymer substitution

Fig 5.10 compares incorporation of Etoposide in various substituted polymers using the modified ID with Etoposide phosphate; a water soluble prodrug incorporated by the standard IDP method. Among the acylated polymers increase in acylation led to increase in incorporation of both Etoposide and Etoposide phosphate (3% and 1.7% respectively in the 100% C_8 polymers).
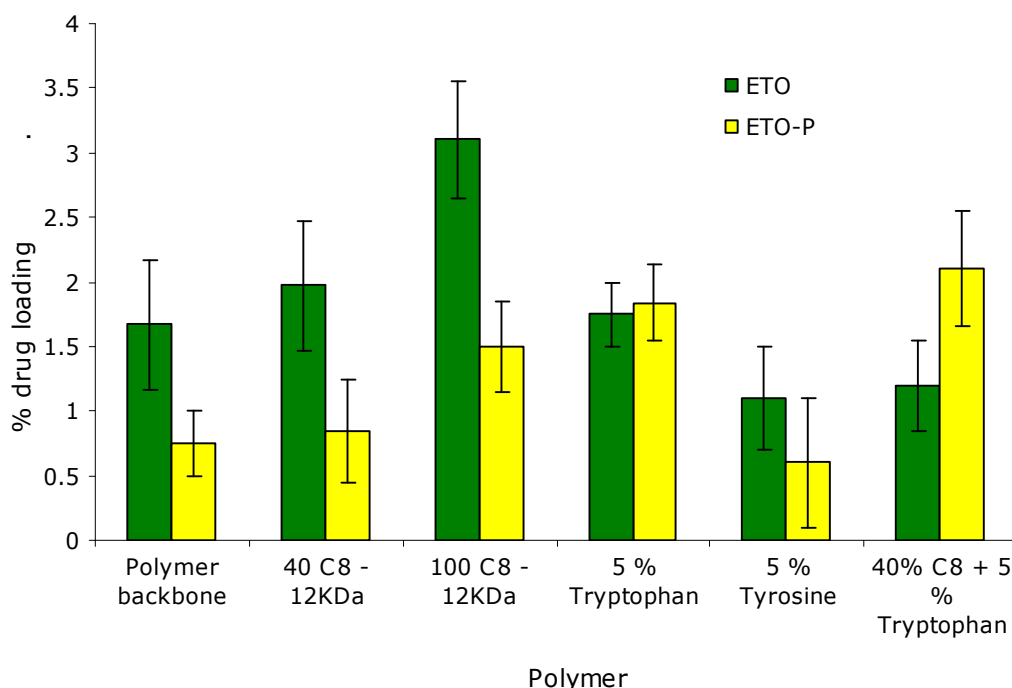
Fig. 5.10. Influence of Polymer substitution on ETO and ETO-P incorporation
Polymer backbone substituted with acyl, amino acid or combination of acyl and
tryptophan were analysed for drug loading.

ETO incorporation in the amino acid substituted polymers was reduced substantially compared to the 100% acylated polymer. Among these amino acid substituted polymers, maximum incorporation was 1.8% in the tryptophan substituted polymer. A combination of tryptophan and acyl groups gave a lower ETO loading than either substituent alone (1.1%) and was comparable to the loading in tyrosine substituted polymer.

Incorporation of ETO-P was similar to ETO incorporation in the tryptophan substituted polymer. Maximum ETO-P incorporation was found in the polymer containing both C_8 and tryptophan substitutions while ETO loading was maximum in the 100% acylated polymer and minimum in the combination polymer. Also, ETO loading in this combination polymer was comparable to that in the tyrosine substituted polymer. Surprisingly, encapsulation of both drugs was reduced markedly with the tyrosine substituted polymer to that seen in the backbone polymer alone.

5.3.4. Determination of Drug Release

Effect of nature of polymer substitution on the drug release profile was investigated. Etoposide release from the polymer backbone and substituted polymers is compared in Fig. 5.11.
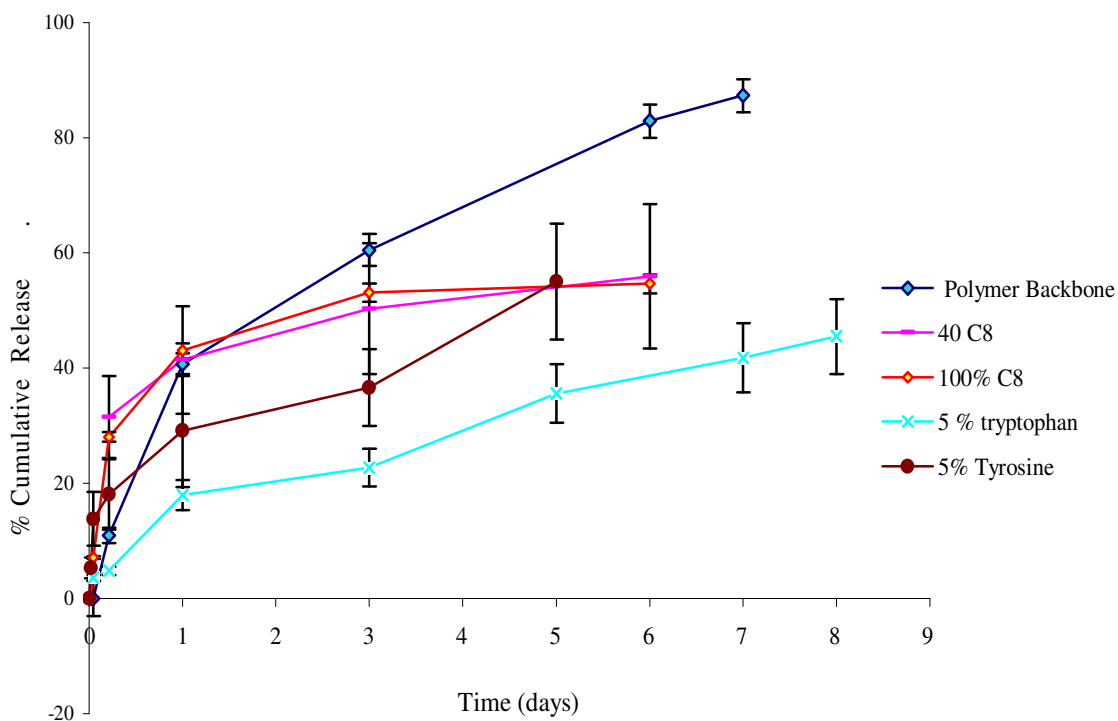
Fig. 5.11. Influence of polymer substitution on ETO release from various polymers. Drug release studies performed in 0.1% tween in HEPES (pH 7) for 10 days
.

ETO release from the acylated polymers seemed to occur faster than from the tryptophan substituted polymers (Fig. 5.11). Release from the tyrosine substituted polymer was similar to the acylated polymer in the first 5 hours following which a much slower release rate was observed. There was a very small burst release for all the formulations. After the initial rapid release, the acylated polymers had a slower rate of drug release than the backbone. The slowest release was observed from the 5% tryptophan substituted polymer followed by the 5% tyrosine substituted polymer. Drug release was slower in the presence of all the substituted polymers compared to the polymer backbone.
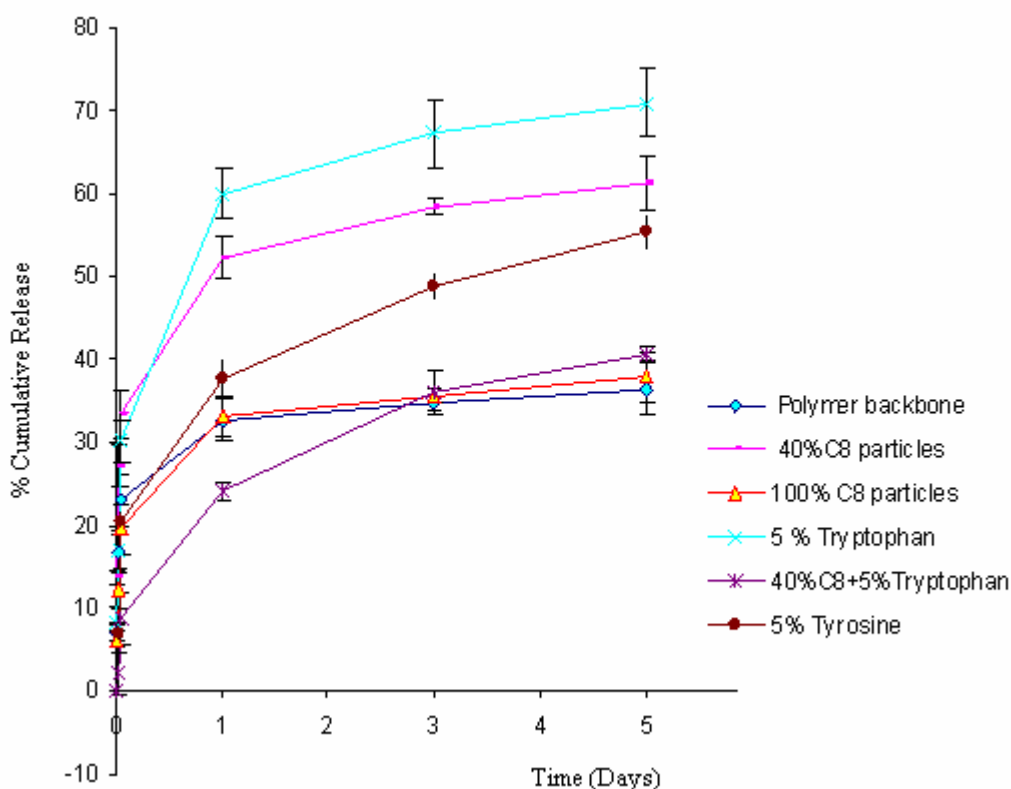
Fig. 5.12. Influence of polymer substitution on ETO-P release from various polymers Drug release studies performed in 0.1% tween in HEPES (pH 7) (5 days).
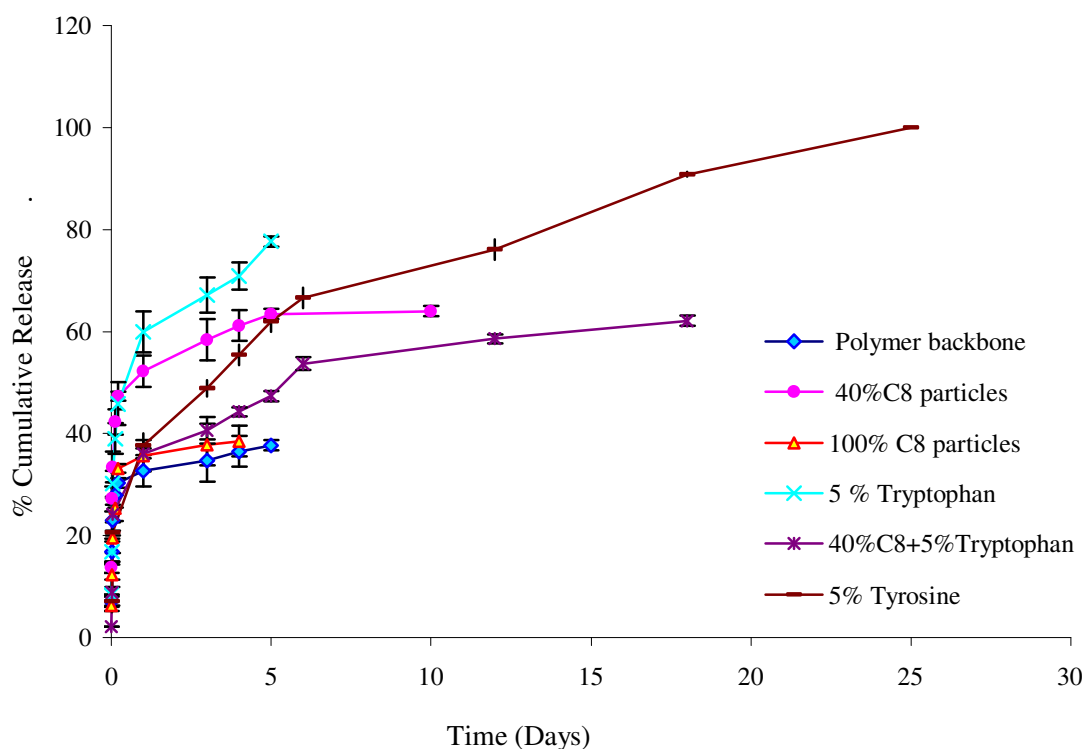
Fig. 5.13. Influence of polymer substitution on ETO-P release from various
polymers (25 days).

Drug release profile of hydrophilic ETO-P is described in Figs 5.12 and 5.13. In Fig. 5.12 drug release for only the initial 5 days has been presented. All the formulations except the combination polymer showed fast initial release which varied in extent with the formulation. The polymer substituted with acyl and tryptophan groups together did not show a burst release and only 10% drug was released after 5 hours. Both polymer backbone and 100% acylated polymer had a similar slow rate of release which was incomplete. Only 30% drug was released at the end of 5 days (Fig.5.12). Compared to the results obtained from acylated polymers, the rate of ETO-P release from the tyrosine and tryptophan substituted polymers was high. The fastest release was observed from the tryptophan substituted polymer contrary to ETO release profile where tryptophan substituted

polymer had the slowest release. Polymer with 40% acylation had faster rate of release compared to backbone and other acylated series and was similar to release from the tryptophan substituted polymer. The polymer substituted with tyrosine showed greater retention after the initial burst and complete release was seen at the end of 25 days followed by the combined acyl-tryptophan substituted polymer that released 60% drug by the end of 20 days.

5.3.5. Analysis of drug release kinetics

In Fig. 5.14 (A) and (B) we plotted the cumulative release of drug (%) against square root of time.

For ETO, only the Higuchi plots from the 5% tyrosine and 40% C_8 polymers had correlation values greater than or equal to 0.95 (Fig. 5.14 A) and these plots were visibly linear curves. Hence, only these polymers follow Fick's law of diffusion for ETO release. All the plots were linear for ETO-P (Fig. 5.14 B) indicating a diffusion controlled mechanism. Usually, the Higuchi plot applies to the situation when the amount of drug release does not exceed 60%. Thus the plot was only performed for data over 24 hours for the ETO-P particles.

A

B
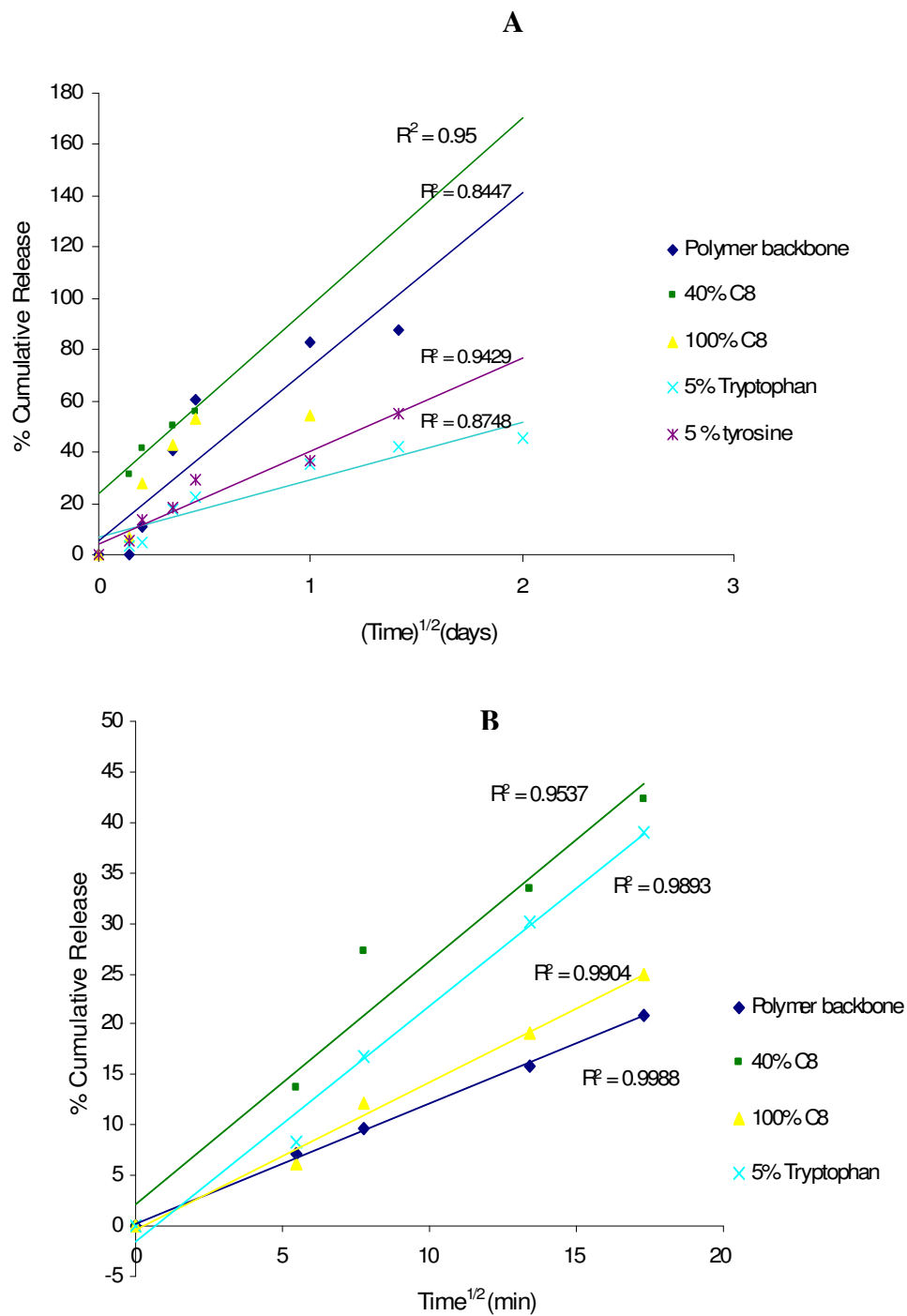
Fig. 5.14. Higuchi plots for (A) ETO and (B) ETO-P in various polymers.

5.4. DISCUSSION

5.4.1. Particle size and zeta potential

Etoposide being a hydrophobic drug would be expected to interact strongly with the more hydrophobic polymers. The 100% acylated polymer produced particles of smallest size amongst the acylated series of polymer (Table 5.1). This observation was similar to the DXMP incorporation by the 100% acylated polymer (Chap 3, Table 3.1). Particles from the 100% acylated polymers were either more condensed or had a lower aggregation number compared to the less substituted polymers. Here we expect this to be due to a more compact arrangement of molecules forming a particle due to drug polymer interactions as discussed in section 3.5.1. The influence of method of preparation where size is largely controlled by interfacial tension between the aqueous and organic layers cannot be applied here as the drug is water insoluble.

Polymers with tryptophan and tyrosine substitution on the other hand were larger in size compared to the acyl substituted polymers which could be attributed to less efficient packing of the polymer's bulky substituents and the etoposide molecules. Alternatively, there could be a further increase in the number of molecules associating to form a particle leading to greater increase in size compared to the acylated polymers. Also, the method of preparation of these particles differed from the method of preparation for previously investigated drugs and ETO-P particles. Polymer and drug were allowed to interact before adding into the aqueous phase thus allowing for greater chances of drug polymer interactions.

Etoposide phosphate is highly water soluble and could best be solubilised in the more hydrophilic polymers. Increase in acylation led to an increase in the size of

particles. Although ETO-P is water soluble it did not follow the trend for DXMP (Table 3.1) thus further strengthening the influence of drug and polymer functional chemical characteristics on their interaction and hence particle size. With the amino acid substituted polymers, particle size increased further compared to acylated polymers. The only exception was the polymer containing 40% acyl and 5% tryptophan substitutions together, where particle size decreased compared to the individually substituted polymers. In general, particles produced with ETO-P were smaller than those produced by ETO. This could indicate influence of the density of the side groups that influences size and packing arrangement of molecules and was more compact in the presence of water soluble drug compared to the hydrophobic drugs.

Zeta potential did not vary significantly between different polymer substitutions and drugs although there was a tendency to form particles with a less negative zeta potential values with ETO than with ETO-P. This indicates that surface charges on the particles are not influenced by substituents present on the polymer but there may have been some ETO on the surface. Probably, when molecules assemble to form particles, the side groups and drug orient towards the core and not on the surface. The charge is mainly due to presence of ionised carboxyl group of the polymer matrix. With a charge of -30 mV all particles were inherently stable to aggregation or precipitation in absence of the surfactant [202].

5.4.2. Drug incorporation

The nanoparticles prepared with the ID method showed very little drug incorporation (Fig. 5.9). This could be due to insufficient opportunity for interaction between the polymer chains and the drug when added to the aqueous

phase. Hence, in order to promote interaction between the drug and polymer, we first prepared a mixture of both drug and polymer followed by its addition into the aqueous phase. Also, this may be due to stronger interaction between the drug and polymer matrix than the solvent drug interaction when allowed to interact before adding to the aqueous phase. This simple modification led to a marked increase in drug incorporation in all the polymer series for the hydrophobic drug. A similar extraction method for comparing the loading was designed in a study by Wang *et al.* wherein, Etoposide incorporation was carried out by two different methods and compared. In the solid extraction method a measured volume of a methanol solution of etoposide was added to a vial, and the solvent was removed under vacuum, leaving a solid film of Etoposide. A polymer micelle solution was agitated with etoposide for 24 hours. After filtration, the total etoposide concentration in the micelle solution was determined by UV spectroscopy. While in the solution extraction method, a stock solution of etoposide (19.2 mg/mL) in 1:1 (vol) acetonitrile/methanol was added slowly with agitation to the polymer solutions of various concentrations. They reported 6% and 22% drug loading using the solution and solid extraction methods respectively [202].

Aromatic interaction (or π-π interaction) is a noncovalent interaction between organic compounds containing aromatic moieties. π-π interactions are caused by intermolecular overlapping of p-orbitals in π-conjugated systems, so they become stronger as the number of π-electrons increases. Other noncovalent interactions that could be acting are hydrogen bonds, van der Waals forces, charge-transfer interactions, and dipole-dipole interactions. π-π interactions act strongly on flat polycyclic aromatic hydrocarbons such as anthracene,

triphenylene, and coronene because of the many delocalized π-electrons [203]. This interaction, which is slightly stronger than other noncovalent interactions, may be responsible for increased association of ETO-P within the tryptophan substituted polymer (Fig. 5.10). Although we would expect a similar interaction to take place between Etoposide and tryptophan we found that the incorporation of etoposide is higher with the acylated polymer which indicates that incorporation of drug is also influenced by a number of other factors such as, its structure, hydrophobicity, stereochemistry and more importantly solubility in the solvent (water). These are responsible collectively for influencing precipitation of the drug and its association with polymer chains and hence its retention within the particles. Tyrosine however did not incorporate either of the drugs to a significant extent and was lowest of all other polymers. This could probably be due to the presence of the phenolic group of tyrosine that may have interfered in the rate of precipitation of the polymer during particle formation compared to the polymer backbone. Tyrosine lacks the indole group of tryptophan that could be responsible for greater interaction with the drugs.

In order to study the combined effect of both these substituents simultaneously, we substituted the 40% acylated polymer with 5% tryptophan and studied drug loading of ETO-P and ETO in it. This new polymer slightly increased encapsulation of ETO-P while it decreased ETO encapsulation to an extent lower than the individually substituted polymers. Contrary to most studies where it has been reported that water soluble drugs are difficult to incorporate in hydrophobic polymers; ETO-P was best incorporated in the acyl-tryptophan combination polymer which was the most hydrophobic compared to the other polymers. Also, its loading within the most hydrophilic polymer backbone was lower than that of

ETO (water insoluble). There may be a steric influence of both acyl and tryptophan groups when present in combination that did not allow for sufficient accommodation of hydrophobic ETO into the polymer. Better ETO-P loading by the combination polymer suggests the influence of water solubility of the drug due to the presence of ionised phosphate groups that led to an electrostatic interaction in addition to the ring stacking interaction with the polymer and hence its better incorporation. There could also be some influence of the method of preparation as in case of ETO-P, drug was present in the aqueous phase and had a better opportunity to accommodate into the polymeric matrix as opposed to ETO which was present in the organic phase.

ETO-P loading within the acyl-tryptophan combination polymer was comparable to that of the tryptophan substituted polymer which probably means that the ring stacking is more predominant than other non covalent interactions between drug and polymer and degree of acylation does not influence this interaction to a great extent. However for ETO where we would expect both these substitutions to enhance drug incorporation, it was found to be lowered significantly. ETO consists of a bulky, extended fused ring with several hydrophobic substituents and hence proved highly hydrophobic when present with acylated and tryptophan substituted polymer. The increased hydrophobicity could lead to precipitation of the drug before the polymer and hence its low entrapment. Both acyl and tryptophan chains when present together may have interfered in their association with the drug causing a marked decrease in drug encapsulation. It appears that the presence of acyl groups favoured ETO incorporation better than ETO-P. The polymer backbone and 40% acylated polymers did not show any difference in drug loading while the 100% acylated polymer showed a marked increase in

ETO loading. This also indicates that the acyl groups are significant only when the polymer is fully acylated or in other words does not contain any hydroxyl groups. Probably interference from the residual hydroxyl groups could have led to the displacement of the drug towards the external aqueous phase. For ETO-P, the combination of acyl and tryptophan may have rendered sufficient solubility characteristics to both the drug and the polymer leading to their co precipitation when added to the solvent and enhanced loading within this polymer.

Wang and co workers synthesised an amphiphilic block copolymer of PCL and PEG [196]. The feasibility of using star-PCL-PEG copolymer as a delivery carrier for lipophilic drugs was evaluated using indomethacin, doxorubicin and etoposide as the drug candidates. They found that there is little dependence of etoposide solubility on the polymer concentration in the range studied, when the solution extraction method was used. This was explained on basis of studies carried out on solubilization of aromatic compounds within polymers [204]. The solute partition coefficient in the polymer was shown to have a strong dependence on the solute concentration for all polymers. The amount solubilized was at its highest for the high mol. weight, hydrophobic polymers. For the less hydrophobic or lower molecular weight polymers, it was determined that solubilization capacity was a function of the polymer concentration.

In a study on ETO loading in Glycerol Monostearate, Distearate, Tripalmitin and HSPC (Human serum) in presence of sodium tauroglycholate, maximum incorporation was found in tripalmitin [205]. Around 4% incorporation within particles of around 390 nm size and zeta potential -46 mV was reported. Particles were prepared by melt homogenisation and in the presence of surfactant. Etoposide loading was related to solubilisation capacity of the drug into the lipid

portion thus correlating hydrophobicity with encapsulation. However, from our studies we showed that incorporation of etoposide does not depend only on polymer hydrophobicity. Increased drug loading was observed with the 100% acylated polymer; however substitution of amino acids like tryptophan and tyrosine made the polymer more hydrophobic but did not lead to a corresponding increase in drug loading. This could suggest that binding of etoposide is more specific with the acyl groups and higher than amino acids.

Lo Prete *et al*. reported association of etoposide to cholesterol rich nanoemulsion (LDE) and evaluated its antitumoral action and toxicity [206]. ETO-LDE demonstrated reduced drug toxicity; however it does exhibit stability problems which are very important in colloidal drug delivery systems. Studies on interaction of Etoposide with Dipalmitoylphosphatidyl choline liposomes have proved Etoposide localization at C_1-C_9 methylene region of the bilayer [152]. This could be responsible for the enhanced incorporation of ETO in the 100% acylated polymer. Valduja *et al.* reported synthesis of ETO-LDE complex with improved stability when ETO is attached to oleoyl groups [207]. Patlolla *et al.* synthesised ETO in lipid emulsions. These were stable at 4 °C for 25 days and are being developed to obtain ETO therapeutic levels in brain and thus targeting brain tumour [208].

No existing literature is available on ETO-P encapsulation within polymeric nanoparticles. From our studies it is evident that the presence of phosphate group on ETO nucleus changes its affinity towards polymers to a great extent. Amongst the acylated polymers, it shows greater incorporation with the 100% acylated polymer similar to ETO; however the loading is half of that obtained with ETO. The presence of tryptophan enhances encapsulation to some extent. Both acyl

and tryptophan moieties act in conjunction to retain highly water soluble drug within its core and this enhanced interaction works better to retain a hydrophilic drug than a hydrophobic drug.

5.4.3. Drug Release

Although incorporation of Etoposide is highest in 100% acylated polymer (Fig 5.10) release from this polymer occurs faster compared to the amino acid substituted polymers. Interestingly, it was observed that both 40% and 100% acylated polymers had similar rate of release. From the tyrosine substituted polymer, 50% of drug was released at the end of 9 days. However this polymer had minimum drug incorporation. Between the acyl and amino acid substitutions, the amino acid substituted polymers had a better ability to retain the drug within the core and provide more controlled and slower release. Faster rate of release with the acylated polymers could be due to the location of drug. It could be possible that ETO localisation occurred at / near the surface of the particles, which could be attributed to the nature of association of the polymer and drug molecules. Although the tyrosine substituted polymer had the least drug loading it had a better retention capacity compared to the acylated polymers. This highlights the influence of aromatic substituents on drug release. Probably tryptophan and tyrosine groups held the drug towards the core of the polymeric matrix and decreased its movement towards the external phase thus providing controlled release.

From Table 5.1, Zeta potential of the ETO particles with the tryptophan substituted polymers was more negative than with the 100% acylated polymers. Also, increased size of the particles could indicate that the tryptophan and etoposide molecules are present at the surface rather than towards the core thus

enhancing its diffusion outwards. However, slow drug release from this combination could suggest possible role of drug polymer interactions that delay rapid drug removal from the surface.

In a study on ETO incorporation by Glycerol Monostearate, Distearate, Tripalmitin and human serum all formulations showed an initial burst release of approximately 20% within the first five hours [205]. Tripalmitin showed more prolonged release of ETO compared to other formulations and this could be due to a greater retention of drug within the more hydrophobic polymer. In case of our polymers, the amino acid substituted polymers provided a better retention than the acylated polymers. There could be also be a possibility that in the presence of amino acids on the polymer the ability of the dissolution medium to penetrate the polymer matrix is less than the acylated polymers. A number of studies have reported a direct correlation between drug loading and release. Higher drug loading would increase the concentration gradient of the drug at the interface thus enhance its diffusion towards the external phase [154]. This is possible only for the water soluble drugs. Most formulations with faster rate of release also had a higher incorporation. In our study, although the acylated polymers could incorporate more drug, release from these polymers was faster.

Drug loading of ETO-P in 100% acylated polymer was similar to that in the 5% tryptophan polymer (Fig. 5.10) but release from the 100% acylated polymer was slower. Although the drug loading trend is similar to ETO, the release profile is exactly opposite as the 100% acylated polymer provided slowest ETO-P release but fastest ETO release (Fig. 5.13). Similarly, ETO-P release from tryptophan polymers was fastest while ETO release was slowest. Thus, the presence of a phosphate group on ETO-P is responsible for its better interaction with the acyl

groups on polymer and hence better retention compared to ETO, whereas the lack of phosphate group makes it difficult for such an interaction and retention (Fig. 5.1, 5.2). The polymer substituted with both acyl and tryptophan groups further enhanced ETO-P incorporation and retention within the core providing a slow and more complete release. It does not follow the general correlation of higher loading and fast release. It is interesting to observe that the polymer backbone and the 100% acylated polymer had a comparable rate of release. There could be localisation of the drug towards the surface. An increase in acylation led to an increase in loading however for drug retention and release rate the acyl groups were not very significant in comparison to the hydroxyl groups of the unsubstituted polymer. ETO-P particles in the acylated polymers were smaller than the amino acid substituted polymers. The correlation between small size and faster release is hence not applicable for these particles. Thus, the difference in chemistry of drug influences its affinity and interaction with the polymer along with its retention within the core matrix. ETO release only from the 5% tyrosine and 40% acylated polymers obeyed Fick's law of diffusion while all the plots for ETO-P were linear as seen in the Higuchi plots in Figs. 5.14 (A) and (B). It is highly unlikely that PGA dissolves under existing experimental condition and hence drug release is not due to the erosion of the matrix. TEM images of particles observed after 25 days of studies showed no disintegration or loss of shape of the particles (Appendix 18) and hence probably its biodegradation starts at a time longer than that taken into consideration. Dunne *et al* observed the SEM of the PLGA particles after 28 days of drug release studies and reported a gradual loss of shape of the microparticles. At 22 days some pitting of the surface of the larger particles was observed while after 28 days

these larger microspheres developed a porous outer surface. The smaller particles only showed a fusion at the earlier time points [209]. It was concluded that particle size could influence their degradation behaviour

5.5. CONCLUSIONS

Particles were formed using both ETO (water insoluble) and ETO-P (water soluble) and were stable in the absence of surfactants. A preformed matrix of drug and polymer enhanced drug loading to a significant extent. Drug loading varied according to the polymer type and the nature of drug. Etoposide was best incorporated in the 100% acylated polymer, and its incorporation decreased in the lower acylated polymers. Amino acid substitution increased hydrophobicity of polymer compared to the backbone and acylated polymers but decreased drug loading. Thus, Etoposide interaction was greater with the acyl groups compared to the amino acid side chains indicating loading did not depend upon hydrophobicity of polymer alone.

ETO-P, with similar chemical structure but water soluble, showed decreased incorporation in acylated polymers. However, it followed a similar trend compared to ETO, with increase in acylation increasing loading. Maximum drug loading was found with the polymer having a combination of acyl and tryptophan substitution. Drug release from this polymer was the slowest and most complete compared to all other polymer substitutions. Thus, for a water soluble drug like ETO-P better drug loading and slow release rate could be a contribution of enhanced interaction with tryptophan by formation of ionic bonds, aromatic groups may on the other hand be responsible for better retention of water insoluble aromatic ring containg drugs within particle matrix by aromatic ring stacking.

CHAPTER 6. INCORPORATION AND RELEASE OF PACLITAXEL FROM FUNCTIONALISED POLY (GLYCEROL ADIPATE) NANOPARTICLES

6.1. Introduction

Taxol is a novel antitumor alkaloid that has shown clinical activity against several tumours especially prostate, ovarian and breast cancers. However, due to its low aqueous solubility, Cremophor EL (polyoxyethylated castor oil) and ethanol are used as excipients in the pharmaceutical drug formulations. These agents are implicated in hypersensitivity reactions as described in section 5.1, Chapter 5. In addition to the hypersensitivity reactions to Cremophor® EL, the multiple dosing of the drug, required to maintain the therapeutic drug concentration in the tumour, causes nonspecific toxicity [210]. To increase the therapeutic efficacy of anticancer agents, polymeric-, micellar- and liposome-based delivery systems conjugated to tumour-specific ligands have been investigated.

Paclitaxel nanoparticles produced using a range of functionalised polymers were characterized by Photon correlation spectroscopy (PCS) for size and size distribution, Transmission electron microscopy (TEM) for morphological properties and zeta-potential for surface charge. The aim is to achieve a better understanding of various aspects of drug polymer interactions and based on this

identify formulations that could provide high encapsulation and controlled release.

Aims of chapter:

- To assess ability of poly glycerol adipate and its modifications to encapsulate PTx into stable nanoparticles.

- To study the influence of polymer functionalisation, nature of side chain functional groups and formulation parameters on drug incorporation and release of PTx.

6.2. MATERIALS AND METHODS

6.2.1. MATERIALS

Paclitaxel was obtained from Sigma, UK. All other chemicals were of analytical grade and organic solvents of HPLC grade.
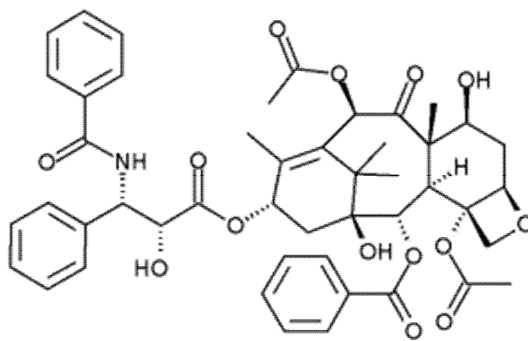
Chemical name: β-(benzoylamino)-α-hydroxy-,6,12b-bis(acetyloxy)-12 (benzoyloxy)-2a,3,4,4a,5,6,9,10,11,12,12a,12b-dodecahydro-4,11-dihydroxy-4a,8,13,13-tetramethyl-5-oxo-7,11-methano-1H-cyclodeca(3,4)benz(1,2-b)oxet-9-ylester,(2aR-(2a-α,4-β,4a-β,6-β,9-α(α-R*,β-S*),11-α,12-α,12a-α,2b-α))-benzenepropanoicacid.

Formula: $C_{47}H_{51}NO_{14}$

Mol.Weight: 853.906 g/mol

Fig. 6.1. Molecular structure and identity of Paclitaxel

6.2.2. METHODS

6.2.3. Preparation of Paclitaxel nanoparticles

Paclitaxel nanoparticles were prepared using the modified IPD method described in Chapter 2.

6.2.4. Separation of free drug from nanoparticles

Nanoparticles were separated from unincorporated drug using methods 2.5 A and B described in Chapter 2.

6.2.5. Physicochemical Characterisation

Size, surface charge and external morphology of the nanoparticles were determined using methods detailed in Chapter 2.

6.2.6. Method validation and Drug loading

The freeze dried nanoparticle powder was weighed and dissolved in a mixture of acetone/ ACN (1:2), followed by centrifugation. The ACN solution was analysed by HPLC. Samples were passed through a Lichrosphere 100 RP-18 (5μ) endcapped column Mobile phase 0.01% Acetic acid: ACN 35:65, flow rate was 1 ml/min and operating pressure 1280 psi.

6.2.7. Drug Release

Drug release studies were performed as described for Etoposide in Chapter 5, section 5.2.8.

6.3. RESULTS

6.3.1. Particle size and zeta potential

Table 6.1 shows the influence of polymer substitution on size and zeta potential of PTx nanoparticles. In the presence of PTx, increase in acylation led to an increase in size of the particles. Tyrosine substituted particles were smaller than the tryptophan substituted polymers. However, a combination of acyl and tryptophan groups on the polymer reduced the size significantly compared to presence of 5% tryptophan on the polymer alone. In the presence of PTx, most loaded particles were larger than the empty particles with the exception being 40% C_8 acylated particles. Overall, the particles were in the size range of 190 to 240 nm with most particles around 200 to 220 nm in size.

Zeta potential varied between -27 to -37 mV for drug loaded particles and did not change much with polymer substitution. Values for the 40% acylated and tryptophan polymers were slightly less negative compared to the other polymers.

POLYMER TYPE	EMPTY PARTICLES		(+) PTx	
	SIZE nm (SD) [polydispersity]	ξ-POTENTIAL mV (SD)	SIZE nm (SD) [polydispersity]	ξ-POTENTIAL mV (SD)
Polymer backbone	169.6(2.2)[0.57]	-20.2(0.4)	188.2 (2) [0.45]	-32.9 (1)
40%C8-12	267.5 (3.09) [0.33]	-31.3 (0.3)	195.65(2.6)[0.03]	-26.9(1.8)
100%C8-12	201.3 (0.57) [0.23]	-29.3(0.8)	216.0(1)[0.04]	-37.2 (0.55)
5 % Tryptophan	132.3 (0.3) [0.05]	-43.8 (2.5)	240.3 (2.5) [0.37]	-28.9 (0.02)
5 % Tyrosine	145.2 (2.9) [0.15]	-34.2 (1.87)	205.7(0.9)[0.58]	-32.5 (1.5)
40%C8 + 5 % Tryptophan	190.7 (1.9) [0.35]	-35.9 (0.9)	202.7 (0.56)[0.6]	-30.1 (0.4)

Table 6.1 Particle size and Zeta potential of empty and PTx loaded nanoparticles using various polymers by the Interfacial deposition method. Polymer type is designated by nature and degree of substitution, MW. Results are mean of 3 readings, SD standard deviation

6.3.2. TEM images

(A)

(B)

(C)
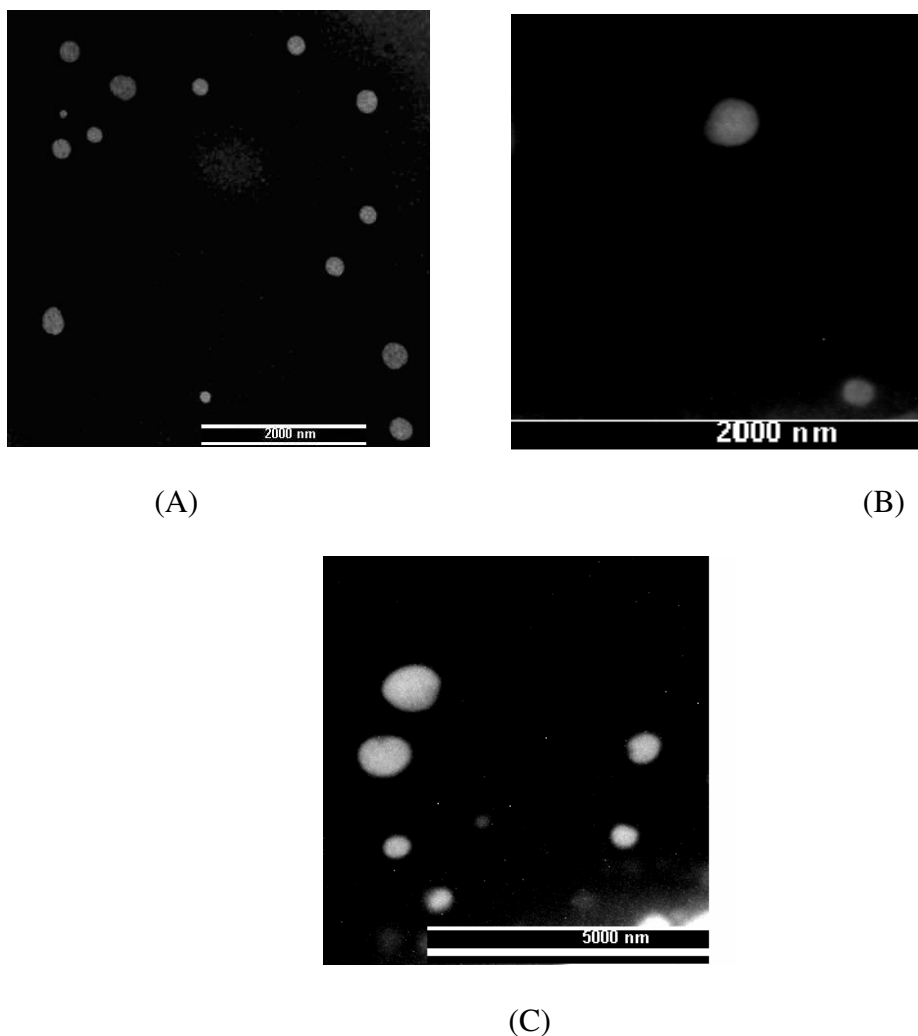
Fig. 6.2. TEM Images of PTx nanoparticles in (A) 100% C_8 (B) 5% tryptophan and (C) 40% C_8 + 5% tryptophan polymers.

Particles were spherical in shape with well rounded surfaces. The 100% acylated polymers produced particles smaller in size than the tryptophan substituted polymer (Table 6.1, Fig. 6.2A) and with low polydispersity. Particles in the tryptophan and combined acyl-tryptophan substituted polymers appear larger in size and aggregated.

6.3.3. Method validation (HPLC analysis for PTx)

The determination of the calibration curve for PTx was performed in ACN (Fig. 6.4), as PTx undergoes rapid trans esterification in methanolic solutions.

The retention time for PTx under the operating conditions and mobile phase as described in 6.2.6 was 4.5 minutes (Fig. 6.3). Control drug (100 µg) was added to empty particles and 92% extraction efficiency was obtained. The average drug loading was divided by 0.92 to obtain to final amount of drug in the samples (Table 6.2).

A
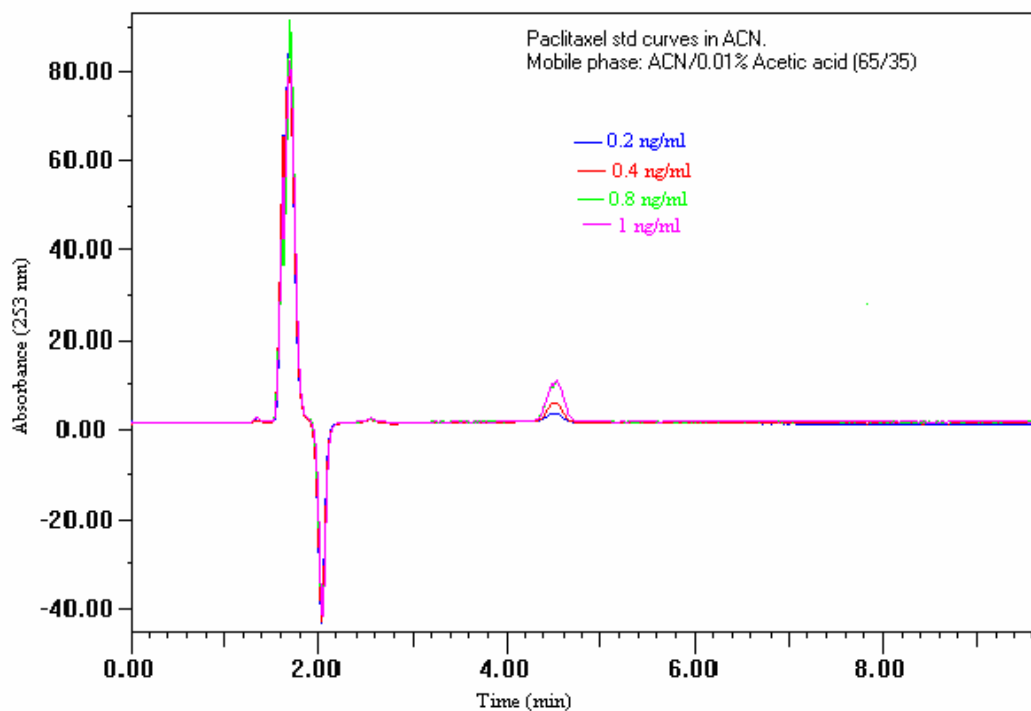
B
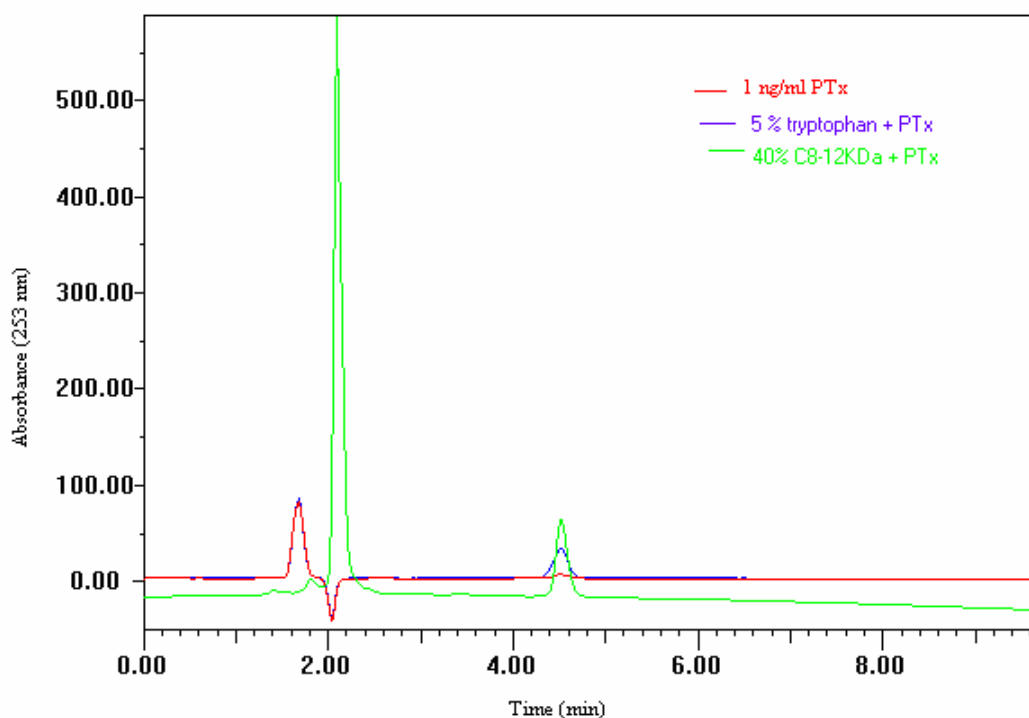
Fig. 6.3. (A) Chromatogram for std. solutions of PTx in ACN, (B) PTx particles
in ACN
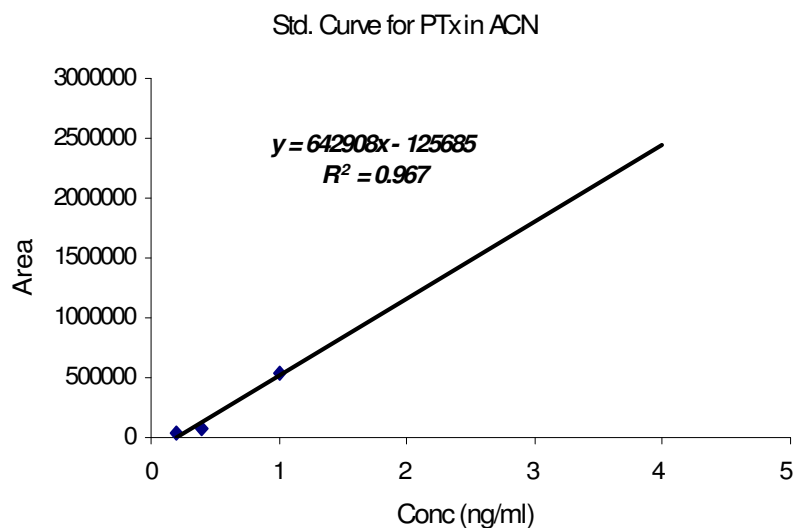
Fig. 6.4. Calibration curve for PTx in ACN

Sample	Area	Conc.(ng/ml) (*10)	µg/tot.fr.vol.[†] (4ml)	Efficiency (%)	Avg. efficiency (SD)
Control-1	1387820	21.78	87.13	87.13	
Control-2	1554879	24.38	97.52	97.52	**92.6%**
Control-3	1485125	23.29	93.18	93.18	**(5.22)**

† total free volume

Table 6.2. Extraction efficiency for control PTx samples using HPLC

154

6.4. Drug Loading

6.4.1. Effect or organic/aqueous phase ratio

Effect of organic/aqueous phase ratio on loading of PTx within various polymers is described in Fig. 6.5.

From previous studies on our polymers, we optimised the ratio of organic to aqueous phase at 2:5 to produce particles within the desired size range and zeta potential that were stable and prepared in the absence of surfactant. However with PTx as the drug, the 100% acylated polymer and the amino acid substituted polymers did not form particles. After evaporation of organic solvent, polymer aggregated and formed a separate layer.
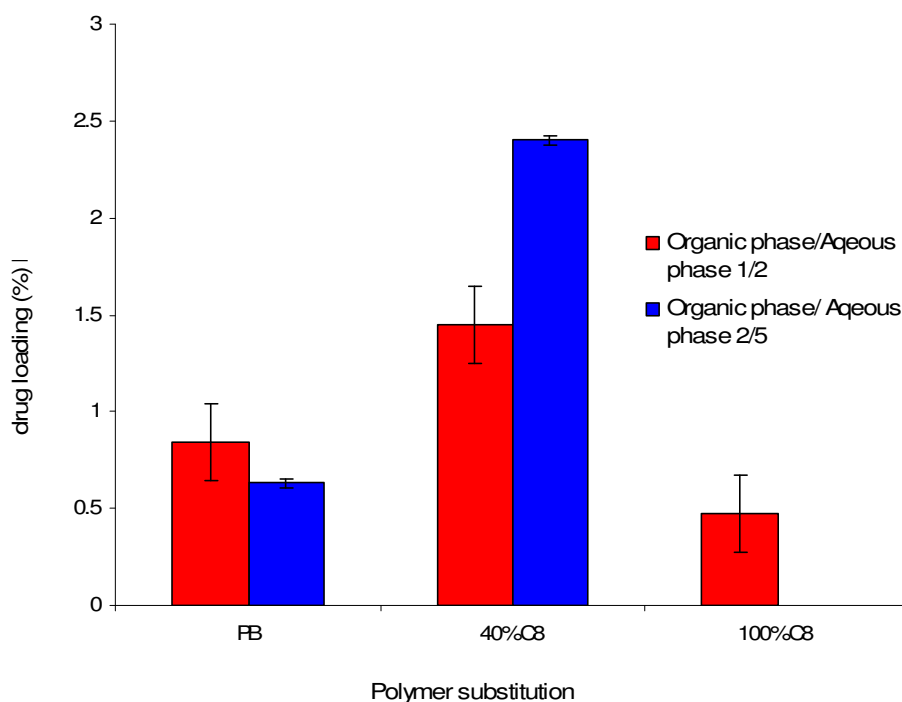
Fig. 6.5. PTx loading within various polymers under different conditions.

When this ratio was increased to 1:2, all polymers formed stable particles. It is however, interesting to observe a significant drop in drug loading within the 40% acylated polymer under these conditions (Fig 6.5). Loading decreased from 2.5%

to 1.5% when the Organic/Aqueous (O/A) phase ratio was changed from 2/5 to 1/2.

6.4.2. Effect of polymer substitution

Fig. 6.6 shows loading of PTx within various polymers formulated using O/A 1/2. 1.5% incorporation was seen in the 40% acylated polymer, and higher incorporation (2.5%) was observed with change in O/A ratio from 1/2 to 2/5 (Fig. 6.5).
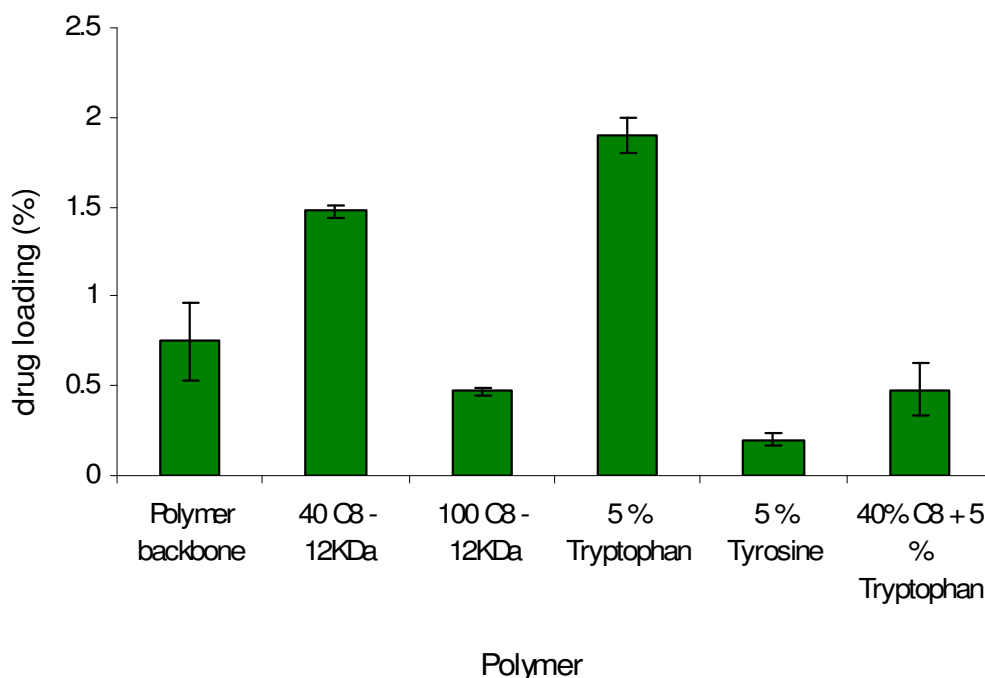
Fig. 6.6. PTx incorporation within various substituted polymers, organic/aqueous phase 1:2

Further increase in acylation decreased incorporation. For tryptophan substituted polymer, incorporation of Paclitaxel was higher than that obtained using acylated polymer (2%). Tyrosine and a combination of acyl and tryptophan substitutions led to a significant drop in drug loading.

6.5. Drug Release

The Paclitaxel release profile from various polymers is shown in Fig. 6.7. The slowest release occurred from the 5% tryptophan polymer and the 40% acylated polymer followed by polymer backbone, while further increase in acylation led to a larger burst release and comparatively faster rate of release.
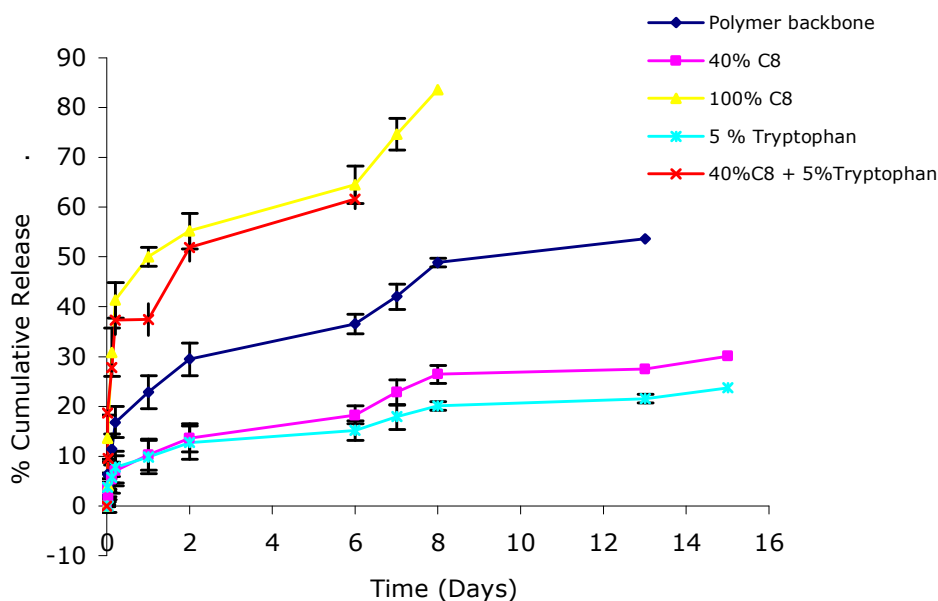
Fig. 6.7. PTx release from various polymers

The tryptophan substituted polymer had the slowest rate of release followed by the 40% acylated polymer. Approximately 30% drug was released after 15 days. Drug incorporation within the tyrosine polymer was negligible and hence drug release was not carried out from this polymer. Drug release from the polymer with combined acyl and tryptophan groups was similar to the 100% acylated polymer. PTx release from backbone, 40% acylated polymer and tryptophan substituted polymers did not show the typical burst release profile.

6.6. Analysis of drug release kinetics

 A plot of Cumulative drug release Vs √T gave an almost linear plot for most particles indicating that the drug release followed Fick's law of diffusion (Fig. 6.8). Higuchi plot for particles prepared from the 5% tryptophan polymers gave a correlation coefficient less than 0.95 and hence may not be following Fick's law of diffusion for drug release. Usually, the Higuchi plotting applies to the situation when the amount of drug release does not exceed 60%. Thus the plot was performed for 24 hours. The plot for 40% C_8 + 5% tryptophan was omitted since the initial burst reached about 55%.
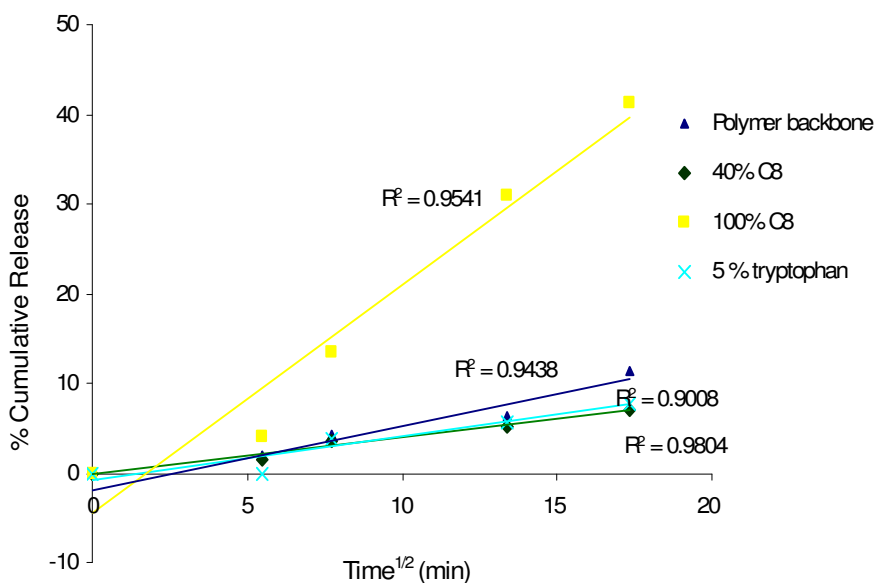
Fig. 6.8. Higuchi plot for PTx in various polymeric NPs

6.7. DISCUSSION

6.7.1. Particle size and zeta potential

PTx particles prepared using the acylated polymers produced smaller particles than the amino acid substituted polymers. On comparing the sizes of empty and drug loaded particles only the 40% C_8 polymer showed a reduction in particle size on drug loading while those of the backbone and 100% C_8 particles were only slightly larger in size. However, the tryptophan and tyrosine substituted polymers produced particles of larger size. The presence of drug and aromatic rings probably led to a loosely packed structure suggesting a difference in the mechanism of interaction of PTx with various polymers. This largely depends upon the properties of the different functional groups attached to the polymers discussed in Chapter 3, section 3.5.1. It is also worth noting that the formulation conditions had to be changed for the amino acid substituted polymers in order to form stable particles after complete evaporation of the organic phase. The organic/aqueous phase ratio had to be reduced to 1:2 from 2:5. The exact reason for the failure of 100% C_8, tryptophan and tyrosine substituted polymers to form nanoparticles when the phases are in a ratio of 2:5 is not completely understood. It might be due to the influence of the aqueous phase on particle formation. Since the hydrophobicity of the drug was the highest (aqueous solubility only 3 μg/ml at 37°C) among the drugs investigated previously in this project. It could be possible that in the presence of more hydrophobic polymers excess water interferes with the process of drug – polymer co-precipitation. Hence, particles do form initially but on evaporation of the organic phase the polymer aggregates. With the acylated polymers, PTx probably encouraged a closely packed arrangement of the molecules and hence formation of more condensed particles

with a very narrow polydispersity. With the amino acid substituted polymers the combination of the aromatic rings in both the drug and the polymer could have led to a less efficient packing of molecules associating to form a particle with more free volume between the polymer chains and hence a larger size. Hydrophobicity of the polymer alone is not a criterion influencing particle size, as can be seen from our results with the tryptophan substituted polymers. Particles were larger in size than those produced by the more hydrophobic polymer viz. 40% acyl + 5% tryptophan substituted polymer.

Some authors have reported drug loaded particles to be larger in size than empty particles due to the presence of drug in polymeric matrix based on the assumption that presence of drug in the matrix is responsible for expansion of matrix volume and hence size [166]. However, comparing the % drug loading in the particles with the % increase in size this seems highly unlikely. There is no indication towards the influence of drug and polymer structures which are the main factors influencing association of polymer molecules into particles. As can be seen from Table 6.1, drug loaded particles using polymer backbone and 40% acylated polymers produced smaller particles while amino acid substituted polymers produced larger particles for the same drug. Thus polymer–drug chemistry seems to be an important parameter in governing particle size by influencing the packing arrangement, density and interactions of molecules.

Zeta potential values changed only very slightly between formulations and overall indicated good stability of the nanoparticle dispersion.

Venkartaraman *et al.* studied incorporation of PTx in PLA (x)-PEG91- PLA x of different molecular weights. They reported an increase in particle size with increase in length of PLA segments. A longer PLA chain length was associated

with larger hydrophobic cores and hence a larger size. However, in presence of PEG 45, there was no significant effect of PLA chain length on particle size [195].

6.7.2. Drug incorporation

The ratio of Organic/Aqueous phases seems to be important for PTx loading using the modified IDP method (Fig. 6.5). Stable drug loaded particles by the 100% C_8 acylated, tryptophan, tyrosine and the combined substituted polymers could only be formed when this ratio was increased to 1:2. This could be an influence of the amount of aqueous phase on particle formation or due to the difference in the interaction of the various side groups with the drug as discussed in section 6.7.1. With the 40% acylated polymer this interaction was best when the aqueous phase is double the organic phase. When the more hydrophobic polymers were used, PTx being a bulky hydrophobic molecule probably did not encapsulate well within the polymeric particles when the O/A phase ratio was 2/5. When added to the aqueous phase, polymer precipitation did not favour drug entrapment leading to aggregation. Failure of the nanoprecipitation method (IDP) has been reported to occur when the viscosity of the polymeric solution is enhanced significantly. Addition of bulky drug PTx to the polymeric phase thus, may hamper diffusion of solvent towards non solvent. It was found that the interaction with the acyl groups was more specific with the 40% acylated polymer under the conditions employed. It is worth noting that despite the hydrophobicity of the complex and bulky drug, there are a number of hydroxyl groups and a secondary amine function as well. It is possible that these groups may either undergo hydrogen bonding with the free hydroxyl groups on the polymer, or that these polymer hydroxyl groups allow some incorporation of

water molecules favouring hydrogen bonding. A similar finding of the advantage of 40% C_{18} polymer for incorporation of DXMP has previously been noted [72]. Comparable loading was obtained with the 5% tryptophan substitution; however, the decrease in ratio of o/w from 1/2 to 2/5 did not allow particle formation and led to complete precipitation of polymer (Fig. 6.6). Complete acylation of polymer led to decrease in drug loading. Also, binding to the tryptophan substituted polymer (2.1%) was favored compared to the tyrosine substituted polymer (0.5%) (Fig. 6.6).

Fonseca *et al.* investigated the influence of various formulation parameters on PTx incorporation efficiency within PLGA nanoparticles using the IDP method. They observed that doubling the volume of the external aqueous phase while maintaining constant the volume for the organic phase resulted in reduction of the incorporation efficiency of the drug for all the copolymers tested by around 15 to 20% compared to the formulations obtained with organic/aqueous phase ratio 1:1 [211].

Ruan *et al*. encapsulated PTx in PLA-PEG-PLA triblock polymers and studied the effect of varying the length of the PLA segments [89]. The PLA chain length had no significant effect on the drug loading. Rodrigues *et al.* reported greater tolerance, therapeutic potential and reduced toxicity when PTx- oleate (chemical conjugation) was complexed with LDE (cholesterol rich nanoemulsion) rather than PTX alone. This finding provides some indication that attachment of the oleate group to PTx increased affinity of PTx to interact with fatty acyl groups of cholesterol [212]. Liang *et al*. prepared PTx particles with block co polymers: poly (γ- glutamic acid) and poly (lactic acid). Particles had a 5% drug loading. An increase in the ratio of PTx / polymer increased loading but decreased

encapsulation efficiency. The optimum ratio between the drug and polymer concentrations was found to be 1/10 [213]. Mu *et al*. studied incorporation of PTx in PLGA using vitamin E TPGS (Alpha-tocopheryl polyethylene glycol succinate) as an emulsifier due to its amphipathic nature or blended it with PLGA in order to formulate a system that overcomes side effects of Cremophor EL [214]. Varying the concentration of TPGS, a number of NPs were fabricated. The mixture of PLGA and TPGS had a self emulsifying effect which resulted in the formation of NPs without use of an additional stabiliser. Vitamin E TPGS in a concentration of 0.03% produced particles with good yield and loading. The high solubility of TPGS in water may be responsible for decreased yield when the concentration of TPGS was increased above this level. A 2.4% loading was reported with PLGA 50:50, 75:25 and 85:15. Dong *et al.* have reported a decrease in the encapsulation efficiency of PTx with increase in initial drug loading in the methoxy poly (ethylene glycol)-poly (lactide) nanoparticles. They reported 21% encapsulation efficiency of 3mg PTx in 40 mg polymer equivalent to 1.58% drug loading [94], while in our study we obtained 1.75% w/w PTx loading using 2 mg drug and 10mg polymer. Cavallaro *et al*. conjugated poly (N-2-hydroxy ethyl)-DL- aspartamide [PHEA], a freely water soluble plasma substitute with PTx [215]. Lu *et al.* incorporated PTx in gelatine for intravesicular bladder cancer. They reported a 0.7% drug loading within this polymer [216].

Lundberg *et al.* synthesised a lipophilic derivative of PTx in a lipid o/w emulsion covered with a hydrophilic polymer. They reported improved pharmacokinetics of PTx in this system [217]. Many studies have reported a need for the presence of hydrophobic surfactants in the formulation system for successful incorporation

for paclitaxel [218]. Mu and Feng [141] reported enhanced drug loading (1.46%) within PLGA microspheres with addition of surfactants like lecithin, DPPC or cholesterol compared to microspheres without additives (1.3%).

However, Mitra *et al.* reported a lower encapsulation in the presence of cholesterol and / or lecithin as surfactants [219]. They attributed this to the fact that an increase in surfactant concentration results in a decrease in the particle size and an increase in surface area per unit volume, which consequently increases the possibility of drug loss by diffusion into the medium during the fabrication process.

From our studies we have shown that paclitaxel forms stable particles with appreciable drug loading in the absence of surfactants. A simple manipulation in the formulation method allowed stable particle formation by all the polymers investigated. The presence of fatty acyl groups on the polymer enhanced paclitaxel incorporation. However, it is worth mentioning that unlike previous studies where fatty acyl groups were added to enhance solubility of drug in the aqueous phase here these groups did not act as surfactants. They probably helped enhance drug interaction with the polymer by formation of hydrogen bonds between the N and OH groups in the drug and the polymer (

Fig. **6.1**).

Various literature studies have reported PTx binding to microtubuler proteins as their main mode of antitumoral action. More specifically, the N terminus of β tubulin is the site of binding for most vinca alkaloids and taxol. This area was sequenced by Rao *et al.* and found to be composed of 31 amino acid residues that included tryptophan [220]. This was an important finding in the study of

paclitaxel incorporation by the tryptophan substituted polymers. We could expect a similar binding between paclitaxel and tryptophan and probably a substantial drug loading. Panda *et al.* studied binding of Estramustine (EM), which is an anticancer alkaloid with similar mode of action as taxol and other alkaloids, to tubulin [221]. The extent of binding was studied by measuring the change in the fluorescence intensity of a tryptophan solution equivalent to the tubulin concentration in the presence of EM. They found that EM quenched the intrinsic fluorescence of tubulin due to tryptophan residues in a concentration-dependent manner.

Sackett *et al.* have also demonstrated quenching of tubulin tryptophan fluorescence in presence of vinca alkaloids binding to tubulin. The quenching of fluorescence is due to the fact that the vinca-site occupancy results in the conformational changes on the tubulin structure [222]. Also, the interaction of taxol with human serum albumin (containing tryptophan residues) has major biochemical importance and has been used as a model for elucidation of the taxol–protein complexation [223].

6.7.3. Drug Release

PTx release was controlled and was slowest from the 5% tryptophan and the 40% acylated polymer (Fig. 6.7). Even for the other polymers 30 to 40% drug release is observed in the initial phase which is lower than the burst effect shown by various other researchers [94]. Although the polymer backbone is more hydrophilic than the substituted polymers it retained the drug for a longer time. Hydrophilic polymers have been associated with a significant burst and fast rate of release. A number of reports on particles prepared using surfactants have attributed burst release to the enhanced erosion of the polymer matrix due to

surfactants as they may promote water penetration or reduce hydrophobic interactions between polymer and drug [93]. The polymer substituted with tryptophan had the slowest release while the 100% acylated polymer was associated with a significant burst and the fastest rate of release. The rate of release from the tryptophan and 40% acylated polymer were similar to each other. Drug loading was also highest in the 5% tryptophan substituted polymer (Fig. 6.6). From results with ETO we found that the tryptophan substituted polymers also have a better retention of aromatic ring containing groups and provide a slower and sustained release compared to the other polymers. The 40% acylated polymer had the highest drug incorporation within the acylated series thus indicating the possible influence of acyl and hydroxyl groups on the polymer solubility profile and on the location of the drug either at / near the surface or within the core. In a 40% acylated polymer the drug could have interacted better with the acyl and the residual hydroxyl groups or could be present in the interior of the particles thus showing a controlled release from the matrix. However, when all the hydroxyl groups were acylated, this arrangement was altered and made the drug easily accessible to the external media thus explaining the significant burst with the 100% acylated polymer.

For the combination polymer the mechanism of interaction between drug and polymer is different from the acylated polymers and probably the strength of this interaction is weaker than with the tryptophan or the 40% acylated polymer. This is reflected in the drug release profile as the drug release is fastest compared to all other polymers. Another explanation could be the effect of the hydroxyl groups on the polymer which seemed to be important for both loading and retention within the interior or surface localisation of drug. With the combined

acyl and tryptophan groups the polymer still had around 55% hydroxyl groups however, the steric configuration and hence orientation of the drug was altered in this polymer compared to the unsubstituted polymer such that the drug was easily diffused towards the external medium. The particle sizes with the combined amino acid - acyl substituted polymers were larger than the acylated polymers (Table 6.1) and hence do not follow the trend of large size, slow release rate. An interesting observation was the sudden increase in the amount of drug released at the end of 6 days from all polymers. Studies on PTx nanoparticles made from gelatin showed a rapid release of drug in PBS. Approximately 90% release was observed after 2 hours. Release was rapid and completed within 3 hours of the study [216].

Another problem associated with paclitaxel is extremely slow rate of drug release, especially from more hydrophobic polymers. The conjugation of PTx to PHEA showed no PTx release for up to 30 hours at pH 7.4 in the presence of plasmin. This system is being developed for long term treatment with PTx. [215]. Less than 5% PTx was released from PLGA/MPEG films after 16 days [214]. From their previous studies, Ruan *et al*. reported only 50% PTx release from PLGA particles at the end of 3 months. Hence, in an attempt to obtain faster and more complete release they studied PTx release from PLA-PEG- PLA triblock polymers. The paclitaxel-loaded PLA–PEG–PLA microspheres resulted in significantly faster release of the drug from the microspheres compared with that from PLGA samples [89]. Liggins *et al.* observed incomplete release and slowing of release rate of paclitaxel after 12 days which led to the development of the two compartment model for describing the release kinetics of paclitaxel. It was assumed that release from the two compartments was independent.

Compartment 1 was diffusion controlled while compartment 2 did not allow paclitaxel diffusion at a measurable rate. It was also assumed that the first compartment was depleted over the course of the 14 day release study and that in the second compartment paclitaxel was essentially immobilised by the crystalline domains in the matrix such that diffusion is almost negligible over the course of time of these studies [224]. The release from the 5% tryptophan substituted polymers also seems to have slowed down greatly after 8 days and this could be attributed to the same reasons hypothesised by Liggins *et al*. in their study. This drug polymer combination did not fit into the Higuchi model (Fig. 6.8) However, the two compartment model could be reduced to the Higuchi model if a pore density existed within a polymeric matrix sufficient to affect the polymer domains of compartment 2 [224].

Various researchers have also correlated size of the particles to release rates. The smaller the size of the particles greater is the surface area and hence the faster the release [94, 225]. Some studies have also correlated the rate of drug release with drug loading [30, 89]. PTx release from PLA-PEG-PLA triblock polymers showed a decrease in the rate of release with an increase in drug loading. Venkatraman, Liggins reported an exact opposite trend. They attributed the faster rate of release to enormously decreased size of the particles i.e. 300 nm as opposed to 20 microns in their previous work [195, 224]. However, with our polymers the backbone and 40% acylated polymers also provided controlled release and these were smaller in size than other PTx loaded polymers used in this study (Table 6.1).

6.8. CONCLUSIONS

Paclitaxel could be successfully incorporated within polymer backbone and functionalised polymers using the modified Interfacial deposition method in the absence of surfactant. Particle sizes were between 200 to 240 nm and surface charge around -30 to -32 mV. Drug loading was influenced by the ratio of organic to aqueous phase and type of polymer. The tryptophan substituted polymer had highest drug loading (2.1%) at an organic / aqueous phase ratio 1:2. The maximum loading of 2.5% was observed with the 40% acylated polymer when the organic to aqueous phase ratio was 2:5. Drug release from various formulations varied depending upon the type of polymer used. Slowest, controlled drug release was observed from the tryptophan and the 40% acylated polymer followed by polymer backbone, while the combined acyl tryptophan substituted polymer demonstrated the highest burst release followed by the 100% acylated polymer. Thus, paclitaxel interaction was greatest for tryptophan substituted polymer and 40% C_8 polymer under different formulation conditions, indicating that the drug loading was influenced significantly by both of these factors. The drug release profile indicates the influence of chemistries of different functional groups on the ability of the polymer matrix to retain drug and release it in a controlled manner. Again, this ability seemed to be best with the 5% tryptophan polymer which is less hydrophobic than the 40% acylated polymer, of intermediate hydrophobicity, and is slower than the most hydrophilic polymer i.e. the polymer backbone. Increase in hydrophobicity (combination polymer) led to an increase in the burst release. Drug release thus, does not depend upon hydrophilic – hydrophobic properties of polymer alone and it can be concluded that particle properties are specific for drug and side group

interactions. In this case, polymers with either acyl or tryptophan substitution provided good drug incorporation and a controlled release profile and were specific depending upon the degree of acylation and the formulation parameters.

CHAPTER 7. PHYSICOCHEMICAL CHARACTERISATION OF DRUG POLYMER INTERACTIONS IN NANOPARTICLES

7.1. Introduction

In order to assess whether or not interactions between various substituted polymers and drugs did occur and to confirm the presence of drug in the NPs either in its crystalline or amorphous form, FT-IR and DSC studies were performed. Results from various drug polymer combinations were compared with those obtained for NPs prepared using the polymer alone. Thus, to some extent, the effect of the nature of drug and polymer functional groups on polymer drug interactions could be investigated. These results could then be correlated to drug loading and release characteristics from various drug-polymer formulations.

DIFFERENTIAL SCANNING COLORIMETRY (DSC)

Differential scanning calorimetry can be used to measure a number of characteristic properties of a sample. Using this technique it is possible to observe fusion and crystallization events as well as glass transition temperatures (T_g). The change from a glassy to a viscous rubbery state defines the (Tg) of a polymer and is a function of chain motility (Fig. 7.1). Glass transitions may occur as the temperature of an amorphous solid is increased. These transitions

appear as a step in the baseline of the recorded DSC signal and are due to the sample undergoing a change in heat capacity; no formal phase change occurs.

As the temperature increases, an amorphous solid will become less viscous. At some point the molecules may obtain enough freedom of motion to spontaneously arrange themselves into a crystalline form. This is known as the crystallization temperature (T_c). This transition from amorphous solid to crystalline solid is an exothermic process, and results in a peak in the DSC signal. As the temperature increases the sample eventually reaches its melting temperature (T_m). The melting process results in an endothermic peak in the DSC curve (Fig. 7.2)

The DSC also provides insight into morphology of drug loaded particles and how this morphology changes under a range of conditions.
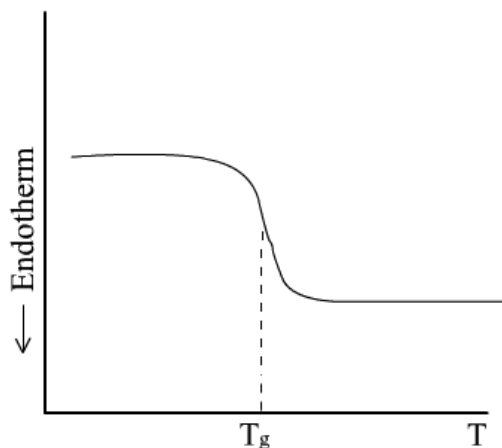
Fig. 7.1. DSC scan indicating Tg of a polymer
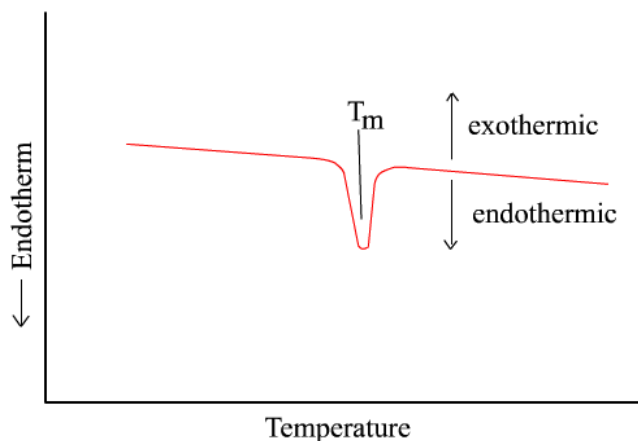
Fig. 7.2. DSC scan indicating Tm for a polymer
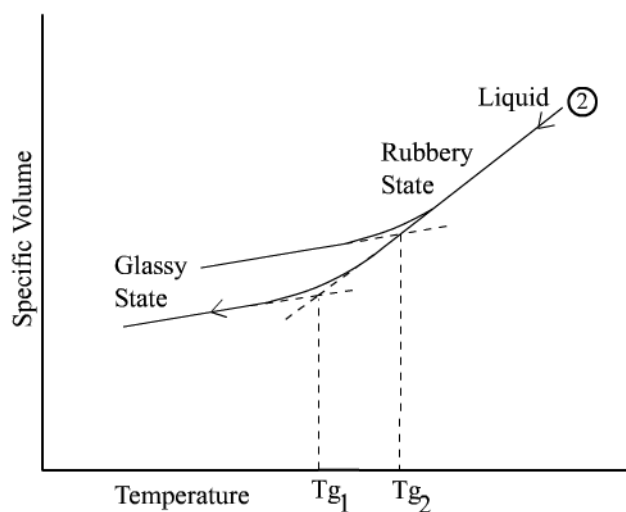
Fig. 7.3. DSC scan indicating change in polymer state from glassy to rubbery

The glass transition is a second order phase transition in which a supercooled melt yield, on cooling, a glassy structure and properties similar to those of crystalline materials e.g. of an isotropic solid material. Phase transitions are associated with the symmetry breaking. The translation-rotation symmetry in the distribution of atoms and molecules is unchanged at the liquid-glass transition, which retains the topological disorder of fluids. From Fig. 7.3, above the T_g, the secondary, non-covalent bonds between the polymer chains become weak in comparison to thermal motion, and the polymer becomes rubbery and capable of

elastic or plastic deformation without fracture [226]. Polydisperse polymers of the same mean molecular weight may differ in their tensile strength if their low molecular weight fractions are substantially different. Plasticisers enhance chain mobility and lower the Tg value. They are added to restore or maintain mobility by interposing themselves between the chains like solvent molecules. A small amount of entrapped or residual solvent could also have a pronounced effect on the Tg of a polymer.

The assembly of nanoparticles and the way an active agent is dispersed in a microparticle may affect the drug loading. This in turn is determined by the interactions an active agent experiences with the solvent and polymer used to form microparticles.

Crystalline solid particles that are insoluble in the casting solvent and suspending medium often are unchanged by incorporation in a microparticle. An active agent that is a crystalline solid which is completely soluble in the casting solvent and insoluble in the continuous phase may do several things: It may crystallise as removal of the volatile solvent progresses. Crystallisation could occur inside the polymer nanoparticles, on the surface or in the continuous phase or combinations of the above. Alternatively, it could be molecularly dispersed in a nanoparticle, by forming a true solution with the carrier or as a metastable dispersion because it is trapped in the carrier [119].

FOURIER TRANSFORMATION SPECTROSCOPY (FT-IR)

FT-IR spectroscopy is a very powerful method for the identification of functional groups. The most important regions of the IR spectrum are >1650 cm^{-1}, whereas the fingerprint region (600-1500 cm^{-1}) of the spectrum cannot

easily be used for identification of unknown compounds. Many references exist which tabulate the IR frequencies for various functional groups and organic compounds. In a molecule, the atoms are not held rigidly apart. Instead they can move, as if they are attached by a spring of equilibrium separation R_e. This bond can either bend or stretch. If the bond is subjected to infrared radiation of a specific frequency (between 300 and 4000 cm^{-1}), it will absorb the energy, and the bond will move from the lowest vibrational state, to the next highest.

In a simple diatomic molecule, there is only one direction of vibration; stretching. This means there is only one band of infra red absorption. Weaker bonds require less energy, as if the bonds are springs of different strengths. If there are more atoms, there will be more bonds, and therefore more modes of vibrations. This will produce a more complicated spectrum. For a linear molecule with "n" atoms, there are 3n-5 vibrational modes, if it is nonlinear, it will have 3n-6 modes.

The graph obtained from an FT-IR analysis shows percentage transmission against wave number. If no radiation is absorbed at a particular frequency, then the line on the graph will be at 100% at the corresponding wave number. Different types of bonds have characteristic regions of the spectrum where they absorb (Fig. 7.4).
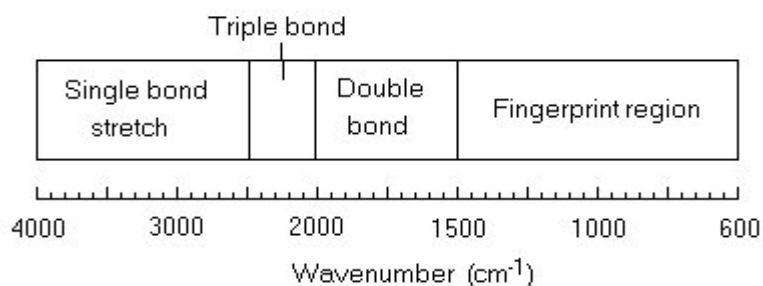
Fig. 7.4. Typical Interferogram with FT-IR spectroscopy

7.2. RESULTS

7.2.1. Effect of substitution on thermal behaviour of drug free polymers

The DSC thermogram of the empty unsubstituted polymer backbone is compared

with the thermograms of the various substituted polymer particles in Fig. 7.5 in

order to study the influence of nature of substituted functional group on the DSC

profiles of the polymers.
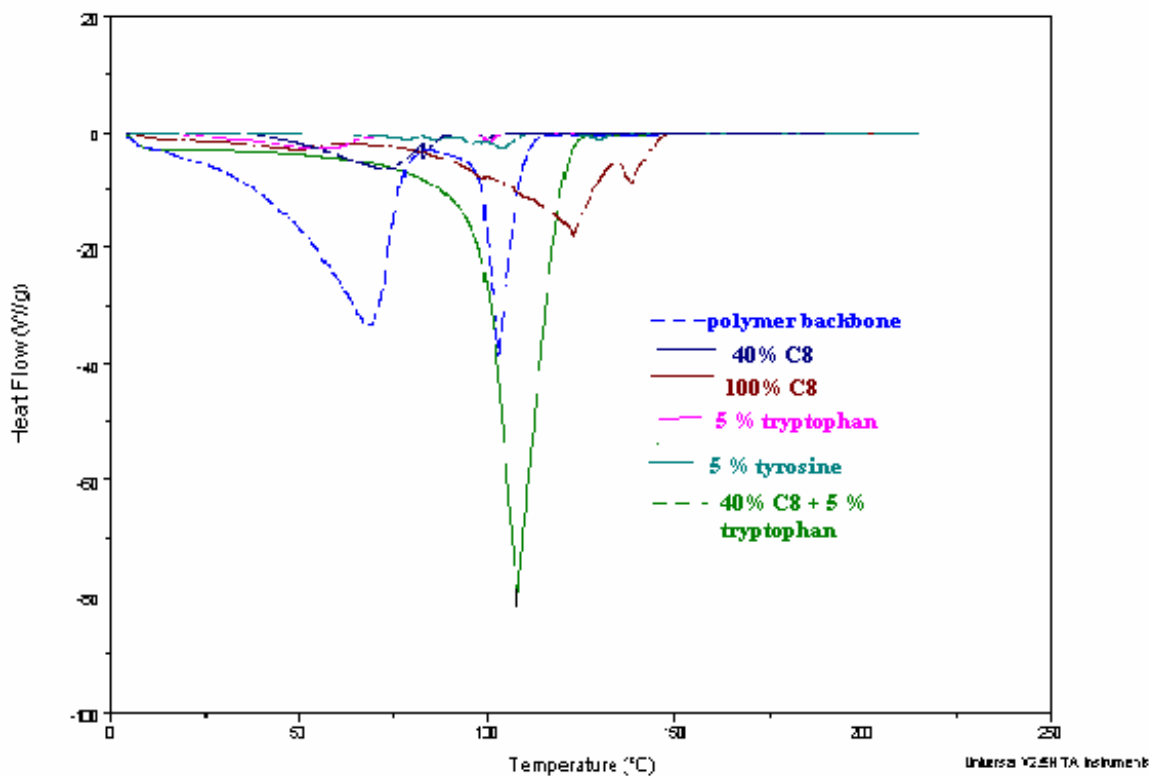
Fig. 7.5. DSC thermograms of polymer backbone and various substituted polymers

POLYMER	Tg °C	Tm (1) °C -heat flow (W/g)	Tm (2) °C -heat flow (W/g)
Polymer Backbone	ND	70 (-27.5)	101 (-35)
40% C8	35	45 (-4)	102 (-0.9)
100% C8	55	-	110 (-16.2)
5% Tryptophan	30	55 (-3)	100
5% Tyrosine	ND	115 (-2.5)	135
40% C8 + 5% Tryptophan	ND	-	103 (-75)

Table 7.1. DSC thermograms of drug free polymer backbone and substituted polymers. Tm 1 and 2 refer to the melting endotherms, ND= not detected.

From Table 7.1, the polymer backbone without any substitution shows two melting curves Tm1 and Tm2 at 70°C and 101°C respectively. On substituting the polymer with acyl groups the Tg of the polymer was detected at 35°C and 55°C in the 40% and 100% acylated polymers respectively. There was an increase in the Tg with increase in degree of acylation. The temperature and peak height of Tm1 of the polymer backbone decreased in the 40% acylated polymer while it completely disappeared in the 100% acylated polymer. There was no significant difference in the Tm2 of the acylated polymers. Addition of tryptophan to the polymer backbone lowered the Tg of the polymer compared to the acylated polymers. Tm1 and Tm2 appeared at similar temperatures as the acylated polymers; however the peak heights were reduced significantly. With the attachment of tyrosine the Tg of the polymer was not clearly detected. Both Tm1 and Tm2 increased and were higher than all the other polymers. For the combination polymer, again the Tg could not be clearly distinguished. Tm1 was absent while Tm2 appeared at the same temperature as in the polymer backbone, acylated and tryptophan substituted polymers.

7.2.2. DSC thermograms of DXMP and CYT-ARA particles

In order to obtain a better understanding of possible effects of drug and polymer interactions and correlate it with drug incorporation and release data, the thermal behaviour of the particles was analyzed with DSC.
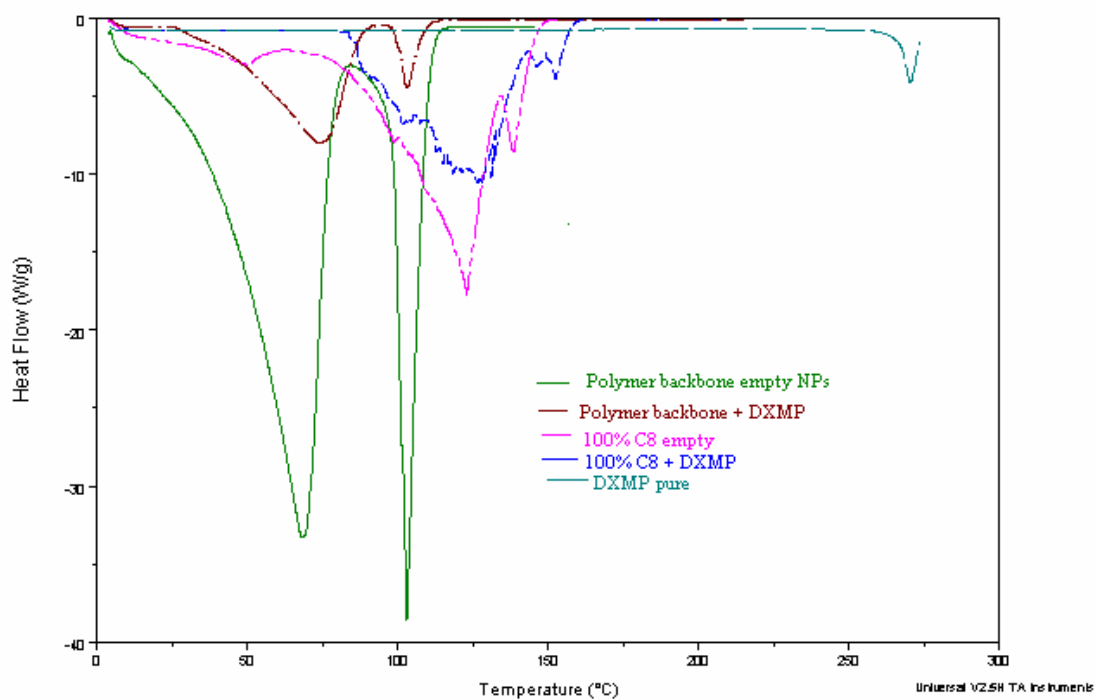
Fig. 7.6. DSC thermograms of DXMP particles in various polymers. Tm 1 and 2 refer to the melting endotherms, ND= not detected.
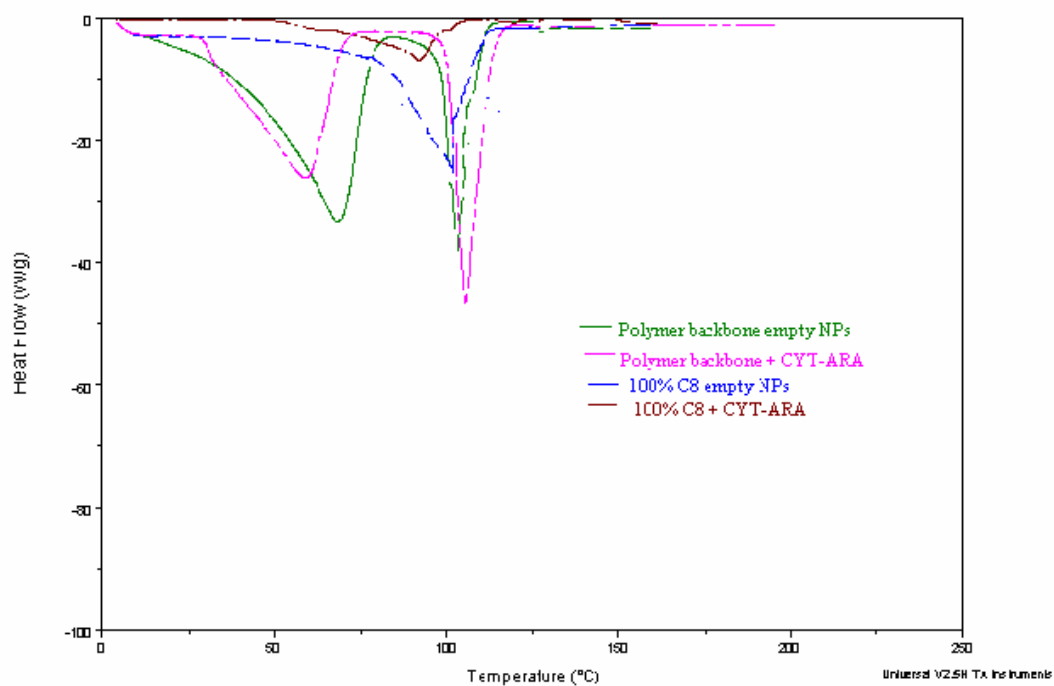
Fig. 7.7. DSC thermograms of CYT-ARA particles in various polymers. Tm 1 and 2 refer to the melting endotherms, ND= not detected.

POLYMER	Tg °C	Tm (1) °C -heat flow (W/g)	Tm (2) °C -heat flow (W/g)
Backbone empty	ND	70 (-28)	101 (-35)
Backbone + DXMP	ND	74 (-8)	100 (-3.5)
Backbone+CYT-ARA	38	55 (-28)	101 (-47.2)
100% C8 empty	55	-	110 (-17)
100% C8+ DXMP	ND	-	115 (-9)
100% C8 + CYT-ARA	ND	-	95 (-8)

Table 7.2. Peak temperature and heat flow for various nanoparticle formulations. Tm 1 and 2 refer to the melting endotherms, ND= not detected.

From Figs. 7.6 and 7.7, for nanoparticles prepared using polymeric backbone without functional side chains and in absence of drug, a broad endothermic peak (Tm1) at 70° C and a sharp peak at 101°C (Tm2) were observed (Table 7.2). Polymer backbone particles with DXMP significantly differed in peak heights compared to the empty particles. The peak at 70° C (Tm1) of the empty polymer became broader and shifted to 74°C (Tm1) while Tm2 appeared at the same temperature, it was significantly smaller.

The thermograms of acylated polymers differed from that of the polymer backbone.

The 100% acylated polymer particles in the absence of drug showed a main endothermic peak at 110°C while in the presence of DXMP; this peak broadened and appeared at a slightly higher temperature (115 °C).

From Fig. 7.7, in the presence of CYT-ARA for the 100% acylated polymer this peak decreased from 110°C to 95°C. The thermograms for the polymer backbone

empty particles and particles containing CYT-ARA were similar in shape and the Tm1 and Tm2 were recorded at 55°C and 101°C respectively. The peak heights also decreased to a great extent compared to the empty particles for both the backbone and the 100% acylated polymers (Table 7.2). The Tg of the polymer backbone though not very distinct in the other formulations could be detected for the CYT-ARA particles in the polymer backbone at around 38°C.

DSC of the pure drugs showed the melting peaks of DXMP at 260°C (Fig. 7.6) or CYT-ARA at 212°C (not shown). However all the nanoparticle formulations containing either drug did not show these peaks.

7.2.3. DSC Thermograms for ETO and ETO-P particles in various polymers

Fig. 7.8 shows the physical state of ETO within nanoparticles made from the 5% tryptophan substituted polymer. Etoposide free drug showed two endothermic peaks at 190°C and 295°C respectively along with a small crystallisation peak at around 220° C. However, these did not appear in the curves for the drug loaded particles in any of the polymers investigated (Figs. 7.8, 7.9, 7.10).
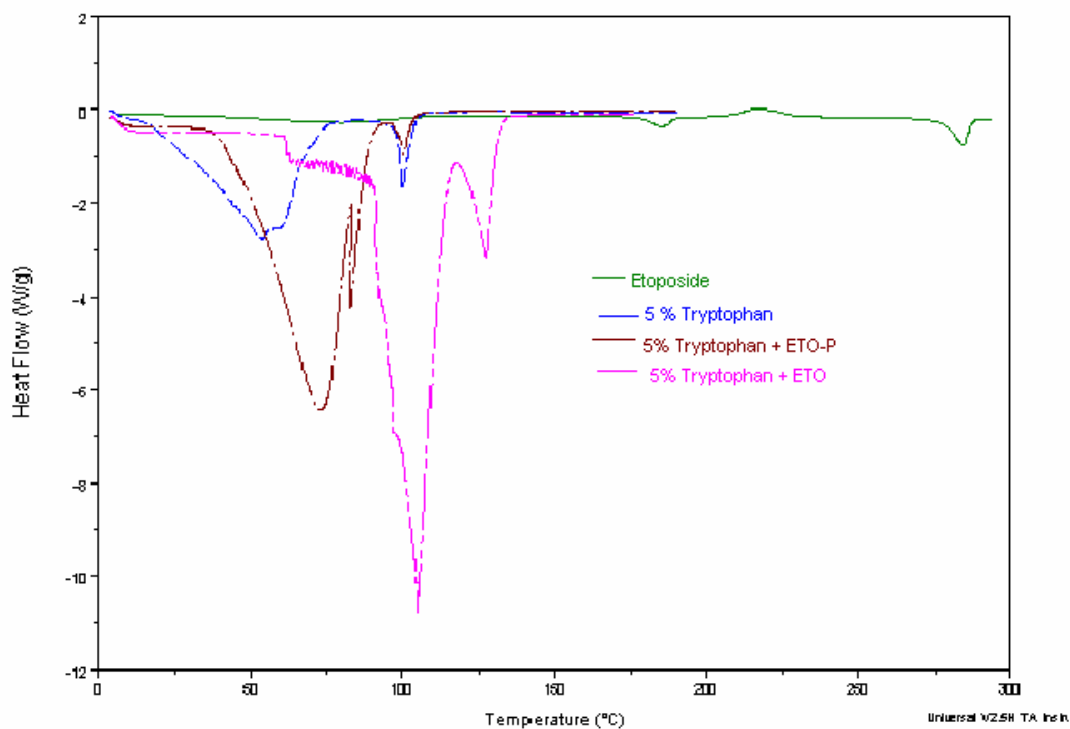
Fig. 7.8. DSC thermograms of ETO and ETO-P in tryptophan substituted polymers. Tm 1 and 2 refer to the melting endotherms, ND= not detected.
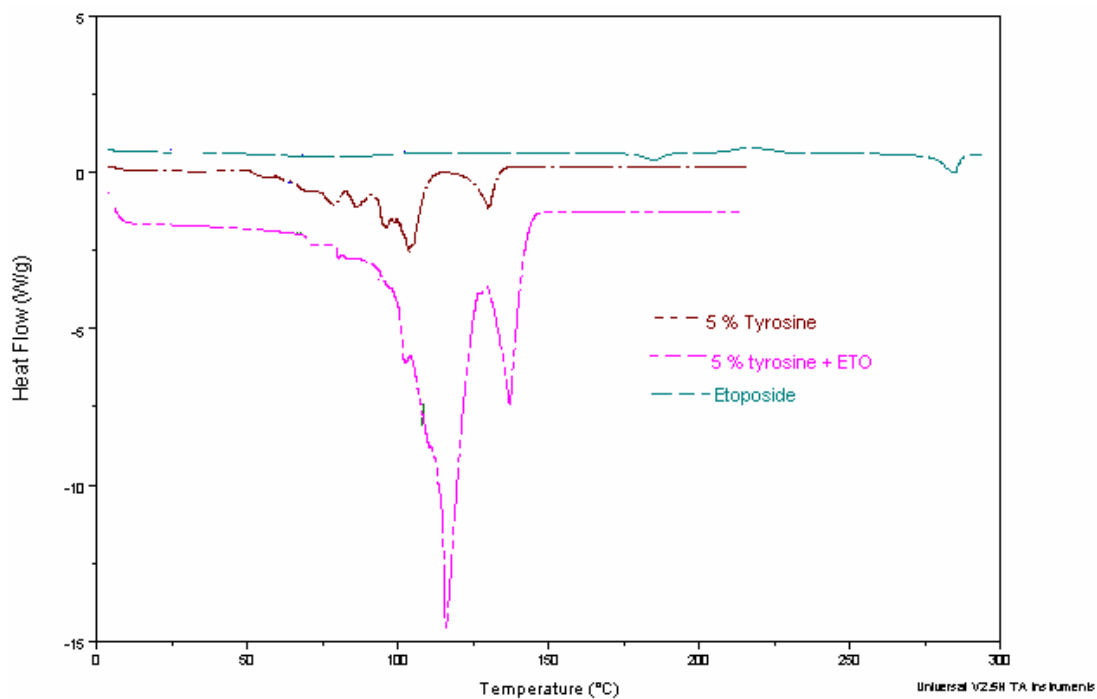
Fig. 7.9. DSC thermograms of ETO in Tyrosine substituted polymers. Tm 1 and 2 refer to the melting endotherms, ND= not detected.

182
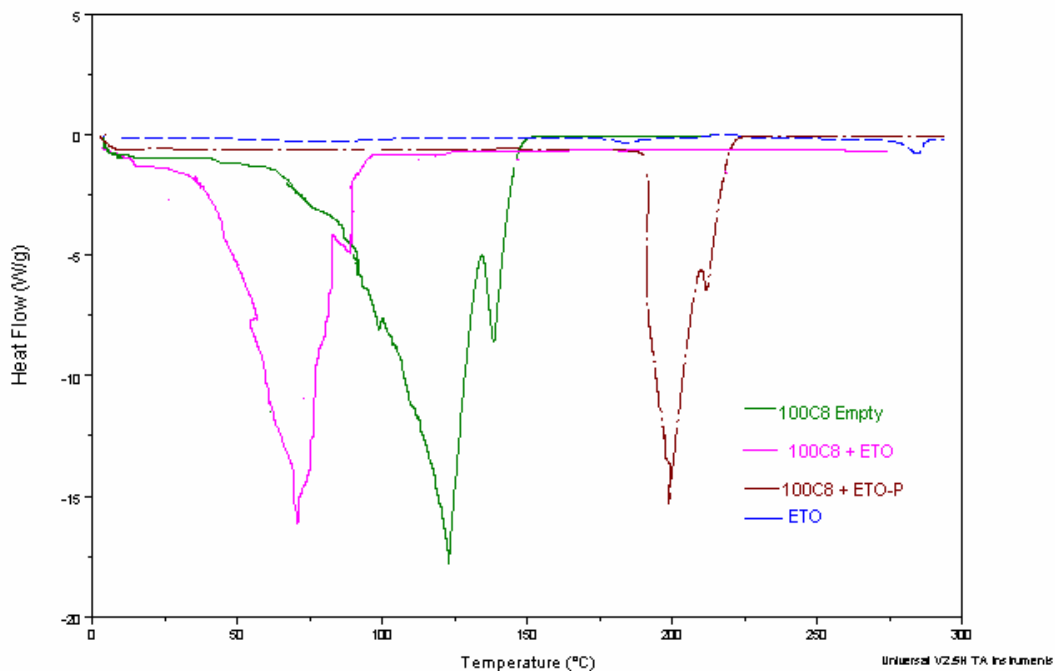
Fig. 7.10. DSC thermograms of ETO and ETO-P in 100% C_8 substituted polymers. Tm 1 and 2 refer to the melting endotherms, ND= not detected.

POLYMER	Tg °C	Tm (1) °C - heat flow (W/g)	Tm (2) °C -heat flow (W/g)
5% Tryptophan empty	30°C	55°C (-3)	100 (-1.8)
5% Tryptophan + ETO	80°C	101°C (-10)	126°C
5% Tryptophan + ETO-P	50°C	75°C (-6.8)	100°C
5% Tyrosine empty	ND	115°C (-2.6)	135°C (-1)
5% Tyrosine + ETO	ND	124°C (-13.5)	147°C (-3.6)
100% C8 empty	58°C	-	125°C (-16.2)
100% C8 + ETO	35°C	-	68 (-16.2)
100% C8 + ETO-P	ND	-	200°C (-15)

Table 7.3. Peak Temperatures and heat flow for ETO and ETO-P in various polymers. Tm 1 and 2 refer to the melting endotherms, ND= not detected.

In the DSC curves for the empty nanoparticles formed using the 5% tryptophan polymer alone, two endothermic peaks appeared at 55°C and 100°C respectively (Table 7.3). The Tg of the polymer was around 30°C.

In the presence of ETO, the Tg increased to 80°C. Tg for the ETO-P particles was around 50°C. For the ETO particles, endothermic peaks Tm1 and Tm2 increased to 101°C and 126°C respectively (Fig. 7.8). While for ETO-P loaded particles in the same polymer, these peaks were recorded at 75°C and 100°C. The Tm2 for ETO-P particles appeared at the same temperature as Tm2 for the empty polymer particles. However the shape of Tm2 for ETO-P appeared broader while Tm2 of the ETO loaded curve was steeper. Both drugs increased the Tg and Tm of the polymer. Increase was greater for the ETO particles than ETO-P.

The thermogram for ETO particles in the tyrosine substituted polymers is illustrated in Fig. 7.9. Two melting endotherms were recorded at 115°C and 135°C for the empty particles. There was a slight increase in the Tm1 of the drug loaded particles compared to the empty polymer. Tm1 appeared at 125°C and Tm2 at 148°C (Table 7.3). The region between 60°C to 100°C was smoother in the drug loaded particles. There appear to be the same number of peaks but they are better resolved in the unloaded polymer because the peak heights are lower. Also the curve for the drug loaded polymer was steeper.

For the 100% acylated polymer (Fig. 7.10), both Tm and Tg of empty polymer particles decreased in the presence of ETO (Table 7.3). While Tm increased in the presence of ETO-P, Tg was not very distinct.

7.2.4. DSC Thermograms of PTx loaded nanoparticles in various polymers.
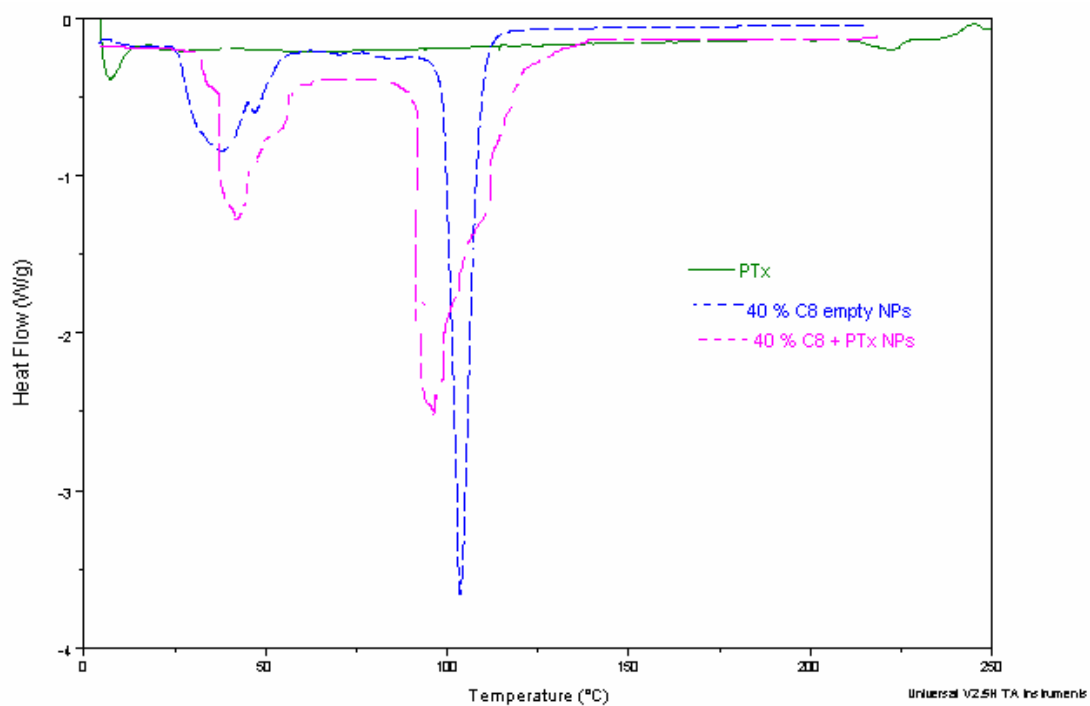
Fig. 7.11. DSC thermograms for PTx powder, PTx particles in 40% C_8 polymers, empty 40% C_8 polymers. Tm 1 and 2 refer to the melting endotherms, ND= not detected.
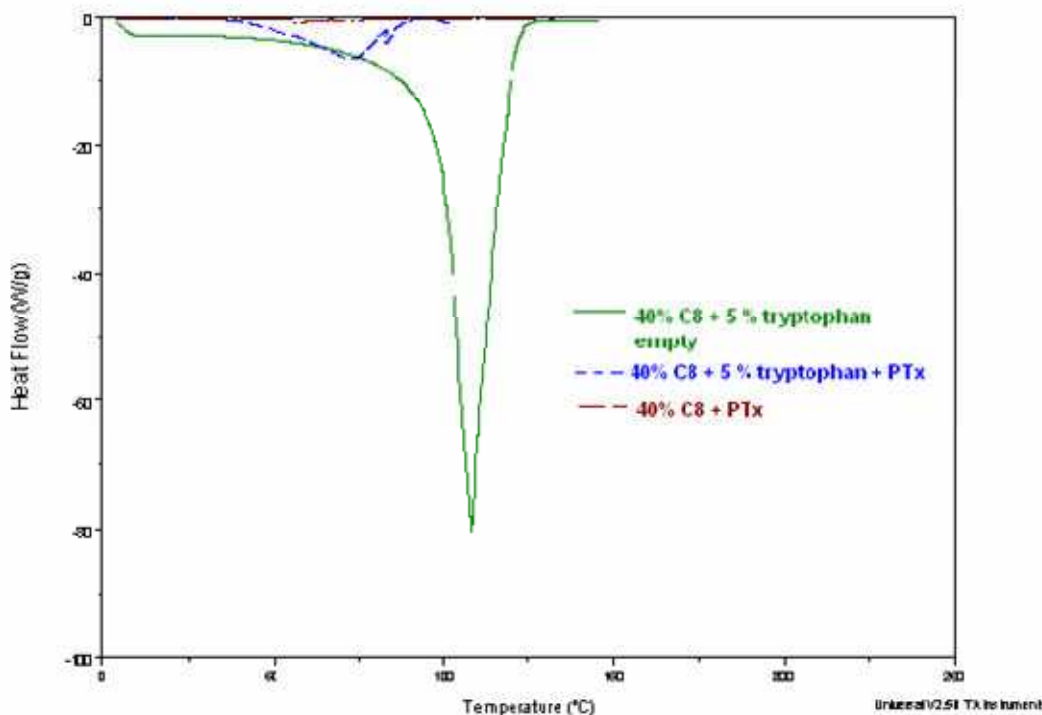
Fig. 7.12. DSC thermograms for PTx particles in 40% C_8, 40% C_8 + 5% Tryptophan. Tm 1 and 2 refer to the melting endotherms, ND= not detected.

POLYMER	Tg °C	Tm (1) °C -heat flow (W/g)	Tm (2) ° C -heat flow (W/g)
40% C8 empty	32°C	45°C (-0.8)	102°C (-3.5)
40% C8 + PTx	35°C	48°C (-1.5)	98°C (-2.4)
40% C8 + 5% Tryptophan empty	ND	-	103 °C (-75)
40% C8 + 5% Tryptophan + PTx	ND	-	73°C (-9.7)

Table 7.4. Peak Temperatures and heat flow for PTx in various polymers. ND (not detected).

Fig. 7.11 compares the thermograms of PTx powder along with PTx loaded in 40% C_8 polymer nanoparticles. PTx alone shows a small endothermic peak at 223°C (Tm) and a small exotherm around 247°C (Tc). The empty 40% C_8

polymer particles showed two sharp endothermic peaks at 45°C (Tm1) and 102°C, while Tg of the polymer was around 32°C.

In the presence of PTx, the Tg increased slightly to 35°C and the melting endotherms Tm1 and Tm2 appeared at 48°C and 98°C respectively. The shape of the Tm2 for the PTx loaded melting curve was steeper than for the empty polymer although there was no significant difference in the temperature of appearance of the peaks.

Fig. 7.12 compares the profile of PTx within the 40% acylated + 5% tryptophan polymers with the drug free polymer. A single endothermic peak for the empty combination polymer particles was recorded at 103°C (Tm2) while in the drug loaded particles the (Tm2) was recorded at a lower temperature (73°C). Crystallisation peak for pure drug was absent for all drug loaded polymers. There was a significant difference in the peak heights of drug loaded particles within the 40% acylated polymer and in the polymer substituted with both acyl and tryptophan groups. The latent heat of melting for the PTx particles with the 40% C_8 polymers seems negligible compared to that of the PTx loaded combination polymer particles (Table 7.4).

7.3.(B) FTIR of particles

FTIR studies were performed on the drug loaded particles in order to obtain some information regarding surface chemistry of the particles. Empty polymer particles were chosen as a reference and compared to drug loaded particles.

7.3.1. FT-IR for DXMP and CYT-ARA particles

Polymer	Position	Intensity
PB empty	3444.49	77.87
	2950.99	78.12
	1739.29	56.93
	1455.93	81.42
	1385.46	80.39
	1174.43	67.26

Table 7.5. FTIR peaks for empty polymer backbone particles

Polymer	Position	Intensity
PB+ CYT-ARA	3358	31.54
	2950.22	26.74
	1735.45	5.984
	1530.53	70.21
	1489.53	80.39
	1177.52	26.74
	1650.44	30.952
	1140.25	71.72
	1062.69	41.39

Table 7.6. FTIR peaks for CYT-ARA loaded particles

7.3.2. ETO and ETO-P

FTIR peaks for ETO particles in the tryptophan substituted polymers are presented in Tables 7.8 and 7.10. Interferograms for the pure drugs ETO and ETO-P had a similar profile

Appendix 3, Appendix 4) and hence significant differences could not be detected in the IR scans of their nanoparticle formulations.

Polymer	Position	Intensity
5% tryptophan (empty NPs)	3318.48	34.97
	2947.56	53.413
	2844.07	57.397
	2553.33	56.656
	1737.25	50.085
	1568.15	52.641
	1215.84	21.977
	765.90	56.311
	588.89	46.236
	543.72	49.508

Table 7.7. FTIR peaks for 5% tryptophan empty nanoparticles.

Polymer	Position	Intensity
5% tryptophan + ETO	3444.16	87.289
	2951.66	89.985
	1737.65	63.848
	1171.61	77.822
	1140.94	80.175
	1078.63	87.447
	472.09	95.439
	446.39	95.639
	423.76	95.624

Table 7.8. FTIR peaks for 5% tryptophan + ETO nanoparticles

Polymer	Position	Intensity
100% empty NPs	2923.98	85.149
	1736.90	84.933
	1104.71	74.368

Table 7.9. FTIR peaks for 100% C_8 empty nanoparticles.

Polymer	Position	Intensity
100% C$_8$ + ETO NPs	2929.06	67.793
	1740.41	40.234
	1484.60	77.146
	1229.51	61.733
	1115.60	57.852
	1036.90	72.211

Table 7.10. FTIR peaks for 100% C$_8$ + ETO nanoparticles.

7.4. (A) DISCUSSION

7.4.1. DSC thermograms for polymer backbone and substituted polymers

The polymer backbone is predominately rich in hydroxyl groups. The polymer seems to be crystalline in nature with two melting curves Tm1 and Tm2 at 70°C and 101°C respectively. Melting is a transition which occurs in crystalline polymers. Melting happens when the polymer chains fall out of their crystal structures, and become a disordered liquid. The glass transition is a transition which happens to amorphous polymers. But even crystalline polymers may have some amorphous portion. This portion usually makes up 40-70% of the polymer sample. This is why the same sample of a polymer can have both a glass transition temperature and a melting temperature. But the amorphous portion undergoes the glass transition only, and the crystalline portion undergoes melting only. The differences in the latent heat of melting and peak heights are indicative of low and high energy melting components within the polymeric backbone. The hydroxyl and carboxyl groups could most likely be the low melting components while the adipate groups could be the higher melting components. There also

exist intermolecular forces within the polymer molecules that could either melt at low energy or high energy input depending upon the nature of interactions (hydrogen bonding, or hydrophobic interactions) and the degree of disorder.

On substituting the polymer with acyl groups, the crystalline nature of the polymer seems to have a less stable conformation and the appearance of the Tg suggests the presence of both amorphous and crystalline regions within the polymer. Thus acylation increases the disorder of the polymer and hence its stability in terms of its conformation. The Tg increases with acylation thus indicating the effect of the pendant groups on chain mobility. Increase in the number of acyl groups serve to act as an anchor to the molecules in its vicinity thereby restricting their flexibility and movement. The Tm1 of the polymer backbone decreases with increase in acylation and completely disappears in the 100% acylated polymer which does not contain hydroxyl groups. The increase in the Tm2 suggests that increase in hydrophobicity has affected the melting of this hydrophobic domain.

Amongst the amino acid substituted polymers, tryptophan substitution showed a Tg at 30 °C which was lower than the acyl substituted polymers. The Tm1 was lower than the backbone but higher than the acylated polymers which would be expected as the polymer still has 95% hydroxyl groups. However, the addition of tyrosine showed a completely different profile. The Tg of the polymer could not be detected. Both Tm1 and Tm2 were increased significantly compared to the backbone and was higher than all other polymers. This could be attributed to the phenolic group of tyrosine that contains an additional hydroxyl group. The combination polymer again did not have a distinct Tg, Tm1 completely disappeared from this polymer while Tm2 did not deviate from that of the

polymer backbone, 40% acylated and tryptophan substituted polymer but had a greater heat flow. Again this could be attributed to the combined effect of the tryptophan and acyl groups that could have affected the appearance of the low melting domains. The massive Tm2 of the combination polymer compared to the 40% C_8 or the tryptophan substituted polymers suggests a great increase in the hydrophobicity of the polymer. Also the Tm1 for the 40% acylated polymer decreased greatly compared to the backbone and completely disappeared when tryptophan was attached to it thus further strengthening the hypothesis of predominating hydrophobic interactions.

7.4.2. DSC of Drug components

Crystallinity of any of the pure drugs could not be detected by DSC in any of the polymers irrespective of the type of drug. This could be due to the small amount of drug or the influence of method of preparation. It indicated the presence of drug either in the form of a molecular dispersion or in an amorphous state. The particles when observed under the TEM did not show the presence of grain boundaries, instead, the particles were smooth with a uniform exterior (Figs. 5.3, 5.4, 5.5) indicating the amorphous structure of nanoparticles obtained. Nanoparticles formed are amorphous due to rapid evaporation of organic solvent [163]. In the amorphous structure, drug is solubilised by the polymer and the two components form an amorphous solution [155].

7.4.3. DSC thermograms of DXMP and CYT-ARA particles

The DSC scans of the empty polymer backbone particles show two melting endotherms. The Tg of the polymer is distinctly observed only with the 100% C_8 polymer and when the backbone is loaded with CYT-ARA (Table 7.1)

From the DSC scans of our polymers, it seems that some of the polymer drug combinations show both amorphous and crystalline regions while some are predominantly crystalline. Double or multiple melting endotherms are often found in semi crystalline polymers crystallized isothermally from the melt at selective crystallization temperature [126, 153]. The possible origin of the double or multiple melting endotherms may be listed as follows: (1) melting, recrystallization and remelting during the DSC heating process, (2) the presence of more than one crystal modifications (polymorphism), (3) variation in morphology (such as lamellar thickness, distribution, perfection or stability), (4) physical aging or/and relaxation of the rigid amorphous fraction, (5) different molecular weight species and so on. On the other hand, double or multiple melting endotherms are also occasionally found in the polymers crystallized nonisothermally from the melt at various constant cooling rates [227].

It is possible that the Tm1 for our polymers occurs as a result of the low melting components such as the hydroxyl groups while Tm2 is a result of the divinyl adipate and fatty acyl groups. DXMP particles produced by the backbone and the 100% acylated polymer led to a slight increase in the Tm while it decreased in the presence of CYT-ARA. Peak heights for either drug loaded particles were significantly smaller than the empty particles with the polymer backbone (Tm1 and Tm2, Table 7.1).

With the 100% acylated polymers there was a marked difference in the scans of the empty polymers compared to the polymer backbone and in presence of the two drugs; DXMP and CYT-ARA (Fig. 7.6 and 7.7). The empty 100% acylated polymer showed only one main melting endotherm. This further strengthens the

possibility that Tm2 could be due to the high melting components such as the adipate or the fatty acyl groups. It was similar to the Tm2 of the unsubstituted polymer backbone and the absence of Tm1 could correspond to the absence of free hydroxyl groups. In the DSC analysis of palm stearin by Busfield *et al.*, the high melting component consisted mainly of triglycerides and higher fatty groups [228]. In the presence of CYT-ARA, Tm1 of the empty particles at 110°C decreased to 95°C and decreased in height significantly. In the presence of DXMP this peak broadened and Tm increased to 115°C. This could suggest the influence of acyl groups on interaction with the drug. As DXMP loading was highest in the 100% C8 polymer, this could reduce the ability of the polymer chains to reorganise and recrystallise during evaporation phase by interrupting molecular interactions of polymer. This could be responsible for the increase in Tm of DXMP nanoparticles. Also, the 100% acylated polymer and DXMP combination did not show any burst release (Fig 3.15). The polymer might be present in a glassy state that retards drug release [229]. Thus it could be reinforced that the steroid nucleus of DXMP interacts best with the acyl groups on the polymer forming smaller particles (Table 3.1), with a better drug incorporation (Fig. 3.13) and a controlled drug release profile (Fig. 3.15).

Another possibility is that the crystallinity of the acylated polymer decreased in the presence of CYT-ARA causing a decrease in Tm of the polymer. There could also be an influence of the method of preparation [230]. Fast evaporation of the organic solvent dissolving the polymer inhibits crystallisation of polymer; giving it less time to organise into crystals [163]. The absence of DXMP and CYT-ARA pure drug peaks in the particles indicates the drug might have been transformed into an amorphous state either due to the method or the miscibility of the drug in

polymer or the low amount of drug (4 mg) compared to polymer (20 mg). It was

interesting to observe that for the polymer backbone particles prepared using

either drug; there was no appreciable difference in the drug loading (Fig.3.13).

The DSC scans also seem to support this as the Tm1 values along with peak

heights for DXMP and CYT-ARA particles were similar (Fig. 7.5, 7.6)

Another important observation is the increase in the Tg of the polymer with

addition of pendant acyl groups on the backbone. Pendant groups have a big

effect on chain mobility. Even a small pendant group can act as a fish hook that

will catch on any nearby molecule when the polymer chain tries to move. But

bulky pendant groups can lower the *T*g too as will be discussed in section 7.4.4.

Yoon *et al.* reported an absence of Tc for DXMP at 269°C in DXM scaffolds

with PLGA prepared by the salt leeching method [231]. Softening and thermal

degradation of polymer above 200 °C may also be a possible reason. In a study

on estradiol incorporation in PCL polymers of various block lengths, it was

reported that longer PCL blocks had a higher Tg and higher crystallinty that

retards estradiol release compared to shorter hydrophobic block lengths [184].

Liggins and Burt reported for PTx incorporation in microspheres of PLA, drug

miscibility in particles led to decrease in Tm of polymeric blend [224].

Eerikainen *et al.* observed an absence of signal attributable to a melting peak of

free ketoprofen in the Eudragit L nanoparticles when the drug amount was equal

to or less than 33% w/w and concluded that drug was incorporated in these

nanoparticles in the amorphous form [232]. Cavalier *et al.* reported for PLA

microparticles loaded with 12.6% hydrocortisone had an endothermic event at

208°C. This was attributed to the melting of HC crystal domains which is below

the reported Tm for HC (228°C). This may reflect the formation of imperfect HC crystal domains in the polymer matrix during particle formation [233].

Several studies have reported use of low molecular weight PLA (2000 Da) as an additive to enhance release rates of several drugs from microparticles formed from a high molecular weight sample [234].

7.4.4. ETO and ETO-P

An increase in Tm occurred in the 5% tryptophan and tyrosine substituted polymers in the presence of ETO and in the 5% tryptophan polymer with ETO-P (Table 7.2 and Table 7.3) compared to the Tm of the empty polymer. A greater increase in Tm occurred in the presence of ETO compared to ETO-P in these polymers.

Similarly an increase in Tg and Tm was recorded in the DSC scan of ETO-P in the 100% acylated polymers. However, the exact opposite was observed when the 100% acylated polymers were loaded with ETO. A decrease in Tg and Tm was recorded compared to the empty polymers. ETO release from the 5% tryptophan and tyrosine substituted polymers was slower than the acylated polymers (Fig. 5.10), while ETO-P release was slowest from the acylated polymer and rapid from the tryptophan substituted polymers (Fig. 5.12).

A number of authors have tried to correlate polymer crystallinity and its effect on drug release. In the case of crystallinity, there are conflicting reports about its effect: some report an increase in rate [235] while others report a rate reduction [236]. From a study conducted by Ge *et al*. it was reported that, the higher the crystallinity of the polymer matrix the faster was the nimodipine release from the nanoparticles [237]. The high crystallinity could lead to formation of a

microchannel structure and large surface area in the polymer matrix, making the drug escape easily from the nanoparticles [238]. From these results, we could also consider that the crystallinity of the polymer played an important role in the drug release of the nanoparticles as the decrease in Tg and Tm of ETO in the 100% acylated polymer and ETO-P in the 5% tryptophan polymer correlated with a fast release. The fastest release rate might be attributed to the lower crystallinity of fully acylated matrix in presence of ETO.

Interactions between the drug and polymer molecules determine solubility of these molecules in each other. When the drug polymer interactions are weaker compared to drug – drug or polymer – polymer interactions, the drug and the polymer have a preference to interact with similar molecules, leading to potential drug or polymer crystallisation. A small amount of drug below its solubility limit in the polymer can be solubilised in the matrix [239]. Crystallisation of drug requires the diffusion of drug molecules and their arrangement into a crystal lattice. Diffusion of drug in the polymer matrix is shown to be governed by drug polymer interactions and size of the molecules. The stronger the interaction, the slower the drug diffusion [240]. Izumikawa *et al.* have reported that the crystallinity of the polymer matrices greatly affect the drug release rate [238].

When a high molecular weight polymer is exposed to a smaller molecule such as a drug, the extent to which a Tg will change depends on the balance between the loss of elastic energy and the gain in free energy due to solubilization [241]. It would be expected that the incorporation of such molecules will generally lower Tg because the small molecules allow the polymer chain segments to have greater freedom. This phenomenon is known as plasticization and the diluent is called as a plasticizer. A similar observation was reported by Benoit and Thies.

They hypothesised a solid solution of the drug i.e. the drug molecules are embedded between the macromolecular chains of the polymer in a solid solution. By separating the polymer chains, it would tend to reduce the secondary polymer-polymer bonds. The free volume available for each chain and hence its degree of freedom, would accordingly increase. Therefore, the drug would act as a sort of plasticizer for the polymer and apart from the absence of crystalline regions in the polymer mass, Tg of the latter would be lowered [242].

However, there are some exceptions to this phenomenon. Due to strong intermolecular interactions between the drug and the polymer, the Tg of the mixture can be higher than either of the pure components. These intermolecular interactions between drug and polymer decrease the free volume of the polymer and increase the Tg which is commonly known as an antiplasticization effect [243]. This decrease has been attributed generally to the size of particles or the presence of surfactant. This seems to be in accordance with our results for drug release studies. The ETO particles produced with the 5% tryptophan polymers had an increased Tg and Tm and also showed slower release compared to the 100% acylated polymers where a lowered Tg was recorded. Similarly ETO-P particles in the 100% acylated polymers showed an increased Tm compared to the empty polymers and was associated with a slower rate of release from these particles. Moreover, between the ETO and ETO-P formulations in the tryptophan polymers, rate of ETO-P release was faster than ETO release. Incorporation of either drug led to an increase in Tg and Tm. However, this increase was greater in the ETO formulations than in ETO-P. Thus, ETO acts as a plasticizer in the 100% acylated polymer and may have maximum solubility within this polymeric matrix compared to the other drug polymer combinations which also explains its

highest drug loading in this polymer. In the 5% tryptophan particles ETO acts as an antiplasticizer as described above.

Reddy *et al*. observed a decrease in the melting temperature of spray dried etoposide nanoparticles prepared from various glycerol derivatives compared to the endotherm of the bulk lipids alone [205].

7.4.5. Paclitaxel

Only a few studies have been reported on DSC characterisation of PTx NPs. The DSC pattern varies for different polymer- drug particles based on the type of polymer, physical state, presence of additives and method of preparation. For example PLGA polymers are amorphous in nature; PLA is crystalline and PCL is semi crystalline. The nanoprecipitation method lowers the crystallinity of polymers [244]. The presence of drug may either promote an amorphous or a crystalline state of the polymer. For the 40% C_8 polymers, the Tm of the polymer increased slightly in the presence of PTx, while it decreased in the 40% C_8 + 5% tryptophan polymer. This may indicate a difference in interaction between PTx and polymer causing fast melting of the low melting component of the polymer. Polymer does not show any crystallisation exotherm indicating it may be crystalline. However, the absence of a drug crystallisation peak indicates that drug may be present in an amorphous form or molecularly dispersed state in a crystalline polymer.

The increase in the Tg of the acylated polymer on incorporation of PTx could be due to the antiplasticization effect of drug on polymer. The pendant groups and the bulkiness of the drug may limit how closely the polymer chains can pack together and thus increase the free volume of this polymer drug combination.

Hyoven *et al*. studied Beclomethasone diphosphate incorporation within nanoparticles prepared from PLA polymers [230]. They observed an increase in Tg of polymer in the presence of amorphous drug indicating that drug promotes the amorphous form of polymer. A similar observation holds true for PTx in the 40% acylated polymer where a slight increase in polymer Tg was observed. For the combination polymer drug acts as an impurity and decreases Tm of polymer and hence decreases its crystallinity. Increase in Tg of polymer in the presence of drug is also an indication of polymer drug interaction. Drug polymer interactions may interrupt intermolecular interactions of the polymer during the evaporation of the solvent [245]. When the DSC thermograms of PLA powder and empty PLA nanoparticles were compared, a cold-crystallization exotherm at about 100 °C appeared in the thermogram of nanoparticles. The exotherm indicated that nanoprecipitation lowered the degree of crystallinity of PLA.

The disappearance of the drug-melting peak is explained by the miscibility of the drug in the polymer rather than by, for example; transformation to an amorphous state due to the preparation technique [246].

Liggins and Burt reported that PTx was miscible within PLA microparticles as shown by increasing Tg, Tc and decreasing Tm of microparticles with various MWs PLA blends with PTx [224]. Polymer Tg values can also provide some indication as to drug release characteristics. Below the Tg, polymer is in a glassy state where mobility of polymer is low and free volume available for diffusion decreases. On the other hand, in the rubbery state polymer is more mobile, the nanoparticle surface is easier to erode and drug release is accelerated. Although the Tg of the combination polymer was not clearly distinguishable the Tm2 was lowered significantly (Fig. 7.12). In accordance with results from Liggins and

Burt, an increased Tg was associated with slower and controlled release from our polymers as discussed in sections 7.2.2 and 7.2.3.

7.5. (B) FT-IR

7.5.1. DXMP and CYT-ARA

The FT-IR spectrum of the empty nanoparticles prepared using the polymer backbone clearly indicates the hydroxyl group at 3444 cm^{-1}. There is little else in these spectra except the peaks for the various C-H and C-O stretches and deformations (2950 cm^{-1}, 1455 cm^{-1}, 1385 cm^{-1}, 1174 cm^{-1}) and the large carbonyl peak around 1735 cm^{-1} (Table 7.5).

In addition to the peaks seen in the empty particles there was a new peak with the CYT-ARA particles at 1650 cm^{-1} which corresponds to the NH$_2$ group of the drug and the peak at 1734 cm^{-1} corresponding to the ketonic group of the drug, thus confirming the presence of CYT-ARA (Table 7.6). The peaks for the CH3, CH2 and O=C-O-C=O stretching appeared at a similar position as in the empty polymer backbone particles but with lower intensities. This could probably indicate the effect of polymer drug interactions leading to change in vibration energies of free groups. Also, an additional peak appeared at 1062 cm^{-1} in the drug loaded particles corresponding to O=C-O-C groups that were not prominent in the empty particles.

The decrease in intensity of the carbonyl group peak could also indicate its deviation from the free state.

With the 40% acylated polymer particles, there was a decrease in intensity of the hydroxyl peaks while these peaks disappeared completely in the 100% acylated

polymers as expected (Appendix 1, Appendix 11). There was also a consistent increase in peak for the carbonyl group with increase in amount of acylation.

Addition of CYT-ARA to 40% C_8 polymers did not change the spectrum significantly. The peak for NH_2 and the one at 1062 cm^{-1} was absent. It could be related to amount of drug incorporation as well as interaction. The addition of DXMP to 100% acylated polymers showed a new peak at 1161 cm^{-1} which was absent in empty particles and corresponds to a C-F (aromatic interaction) in DXMP (Appendix 2). There was an increase in the peak heights at 1743, 2985 and 2926 cm^{-1}.

Bajpai *et al*. studied the FTIR spectra of Cytarabine in gelatine nanoparticles [173]. The presence of —CH_2 group at 2920 cm^{-1} due to C—H stretching vibration of furane ring and ketonic group at 1637 cm^{-1} due to C═O stretching vibration confirmed the presence of drug molecule in the nanoparticles. Similarly, the peaks observed at 1464 cm^{-1} due to C═N stretching vibration of pyrimidine and at 1031 cm^{-1} due to O—H stretching of primary and secondary alcoholic group also provide evidence for the presence of cytarabine.

7.5.2. ETO and ETO-P

On comparing the IR spectrum of tryptophan substituted empty particles (Table 7.7) with ETO loaded particles, a significant difference was observed in the regions between 2900 cm^{-1} to 2400 cm^{-1} and from 1500 cm^{-1} to 500 cm^{-1} (Table 7.8). Peaks at 1568 cm^{-1}corresponding to the NH_2 groups, peaks at 1274 cm^{-1}, 1215 cm^{-1}, 1234 cm^{-1} corresponding to the C-O-C= O and C-OH stretching seen in the empty polymer completely disappeared. The region between 1000 cm^{-1} to 500 cm^{-1} especially showed particularly high interference. The spectrum showed

additional peaks at 1381 cm^{-1} which was also seen in the spectra of the ETO particles in the 100% C8 polymers corresponding to free OH groups.

The FT-IR peaks of 100% C$_8$ acylated empty nanoparticles are presented in Table 7.9. The spectrum showed a broad peak region at 3400 to 2400 cm^{-1} due to the hydroxylic group while a sharp peak at 1737 cm^{-1} is characteristic of the carbonyl group. However, in the presence of ETO (Table 7.10) a significant reduction in the signal intensities in the region from 1500 cm^{-1} to 1000 cm^{-1} was observed.

Additional peaks at 1613 cm^{-1} and 1484 cm^{-1} characteristic of a secondary amine salt and at 1115 cm^{-1} and 1036 cm^{-1} corresponding to the C-O-C= O and O=C-O-C=O respectively appeared (Appendix 5). On comparing this scan to the FT-IR of pure Etoposide it could be confirmed that these additional peaks are a contribution of the drug.

Ge *et al*. studied the FTIR spectra of nimodipine in PCL nanoparticles and observed the peaks for both the drug and the pure polymer with little or no significant changes and concluded that drug is only physically entrapped within the particles without any interactions with the polymer [237].

7.5.3. Paclitaxel

The FT IR scan for PTx within the 40% acylated polymers did not show any significant difference compared to the empty polymers (

Appendix 14).

7.6. CONCLUSIONS

(A) For all drug-polymer formulations, drug was present either in the amorphous state or as a molecular dispersion. DXMP incorporation by the polymer backbone 100% acylated polymers increased the Tm of the polymer, while CYT-ARA decreased it. However, ETO incorporation led to a decrease in the Tm of the 100% acylated polymer whereas ETO-P produced an opposite effect.

For both the amino acid substituted polymers ETO and ETO-P increased the Tm of the polymers. In the presence of PTx an increase in Tg of the polymer was recorded.

Polymer drug formulations with a slow and controlled release profile showed increased Tm and Tg of the polymers while the exact opposite trend was observed for the rapid release formulation (ETO in 100% C_8). Hence, these could be correlated indicating enhanced polymer crystallinity in presence of drugs and strong intermolecular interactions between drug and polymer led to increased Tg and Tm of the formulations.

(B) Since for most drug loaded particles there were no additional functional groups that were significantly different from the ones already existing on the empty polymers, it was difficult to make a distinct identification of either presence of drug in the polymers or the extent of drug polymer interactions on the basis of their IR scans.

However in some cases, for example, the ETO particles with the tryptophan or acyl substituted polymers, appearance of peaks specific to certain regions of the pure drug were observed which could confirm presence of drug.

The influence of drug polymer interactions could also be clearly seen in the spectra of ETO loaded within the tryptophan and 100% acyl substituted polymer and the spectra for ETO-P in the acyl – tryptophan combination polymer. As an

influence of drug polymer interactions, significant changes could occur in the vibrational energy of certain groups of atoms resulting in a significant difference in positions and intensities of certain peaks or regions or complete disappearance of peaks specific for the pure compounds when compared to that of the empty particles lacking the drug.

The FTIR scans provided evidence of presence of drug while the DSC was more useful in terms of understanding the effect of polymer substitutions and drugs on the particles which could then be correlated with the nature of interactions existing within the drug loaded particles. For example the tryptophan substituted polymers in the presence of ETO, showed the highest increase in the Tg of the polymer compared to all other formulations while the FTIR scans of these particles also showed significant high interference regions compared to the particles prepared using only the polymer. This particular formulation had the slowest release of ETO and satisfactory drug loading.

These studies are still in the initial stage and would require a more extensive analysis in order to characterise the nature of drug polymer interactions. Nevertheless, it helps to provide valuable information regarding confirmation of presence of drug within the particles and to some extent its influence on interaction with the polymer molecules.

CHAPTER 8. SUMMARY AND CONCLUSIONS

8.1. SUMMARY

8.1.1. Objectives and background of study

This study was devised mainly with two objectives; firstly, to obtain a tool for understanding in depth the influence of physicochemical properties of different drugs and their interaction with polymers of various properties. Secondly, to identify polymer drug formulations with good drug loading and slow release for use in anticancer therapy. Through this study we are also trying to understand the effect of these drug polymer interactions on the drug entrapment and release profile from the polymeric matrix. Polymers such as PLA, PGA and their co polymers (PLGA) have been extensively studied for nanoparticle formulations however due to limited chemical functionality in their backbone, the physicochemical properties of these polymers is nearly constant.

The block copolymers developed so far either contain no functional groups at all in the hydrophobic block such as PCL, PLA or contain a functional group in every monomer unit as in poly (aspartic acid) [247]. When functional groups are not contained in the hydrophobic block of the polymer, no other interactions such as hydrogen bonding, ionic interactions can be expected between the copolymer and the drug. Consequently for many studies reported in the literature, drug is not very well loaded into the particle or micelle and these polymers have a relatively low drug loading efficiency. In the case of fully functionalised polymers the polymers may be water-soluble and unable to form a micelle or a particle in an

aqueous medium. Thus, the amphiphilicity of the polymer results in a problem—that is, the chemical conjugation of a hydrophobic drug is needed with the functional group of the core block. Hence, functionalisation of polymer blocks has been attempted. For example PEO–PLA block copolymers containing a small quantity of carboxylic acid in the PLA block were successfully synthesized [248]. The nanoparticles prepared from the functionalized block copolymer had a very low CMC value, which suggests good stability of the nanoparticles. The drug loading efficiency of nanoparticles was dramatically increased with the content of carboxylic acid in the block copolymers. This result may be attributed to the hydrogen bonding between copolymer and drug. The release rate of drug was much slower from nanoparticles containing higher amounts of carboxylic acid in the copolymer, which might be associated with the enhanced interaction between the carboxylic group of copolymers and the drug [248]. The nature of drug polymer interactions may therefore significantly influence the drug loading and release pattern.

The aims of this study were:

- To assess the potential of a novel Poly (glycerol Adipate) backbone and various substituted variants of this polymer to assemble into nanoparticles using a simple method and in the absence of a surfactant.

- To provide nanoparticle formulations for both, hydrophobic and hydrophilic drugs with good drug loading and sustained drug release profile compared to existing polymeric nanoparticles.

- To modify the properties of the polymer by attaching different functional groups and to study their influence on drug loading and release for a wide range of drugs with differing structures and chemistries.

- Overall, to provide a better understanding of effect of drug polymer chemistries on their interactions in nanoparticles.

The study began with the detailed investigation of DXMP, a water soluble steroid which was chosen as the model drug, for drug incorporation and release from backbone and various acyl substituted polymers. Influence of chain length of acyl group substituent along with degree of substitution on drug incorporation and release was studied. Further into the study, drugs such as CYT-ARA, ETO, ETO-P and PTx were included. Along with the acylated polymers, amino acid substituted polymers were also investigated. Drug release studies provided significant insight into the influence of drug polymer interactions on the release pattern as release from a dispersion of drugs in the presence of polymer matrices was much faster than its release pattern from nanoparticles. DSC and FTIR were also employed to obtain a better insight into the influence of drug polymer interactions in NPs.

8.2. OVERALL DISCUSSION

The effect of polymer side chain functional groups and properties of the drug on nanoparticle physicochemical properties such as size, shape and zeta potential and their drug loading and release profile have been summarised in Tables 8.1 and 8.2.

Drug	Polymer	Size (empty) nm	Size (with drug) nm	Drug loading % w/w	Drug Release	
					% at 24 hours	**% at 10 days**
DXMP	PB-12kDa	169.6	115.6	2.35	38	50
	20% C_8	217.1	124.3	4	36	87
	40% C_8	267.5	147.3	8	17	60
	100% C8	201.3	152.5	10.5	6.1	38.2
CYT- ARA	PB-12kDa	169.6	159.2	1.9	20	60
	20% C_8	217.1	211.5	0.33	37.3	58
	40% C_8	267.5	200.8	0.3	26	60
	100% C_8	201.3	196.35	0.23	26	99

Table 8.1. Summary of particle size, drug loading and release of water soluble drugs

Drug	Polymer	Size (empty) nm	Size (with drug) nm	Drug loading % w/w	Drug Release	
					% at 24 hours	% at 10 days
ETO	PB-12kDa	169.6	130.2	1.7	40	85
	40% C_8	267.5	141.2	1.95	41	87
	100% C_8	201.3	126.1	3.1	43	55
	5% Tryptophan	132.3	165. 5	1.73	17	45
	5% Tyrosine	145.2	177.1	1.1	29	55
	40% C_8 + 5% Tryptophan	190.7	184.1	1.2	50	94
ETO-P	PB-12kDa	169.6	125.1	0.7	23	31
	40% C_8	267.5	139	1.48	47	63
	100% C_8	201.3	141.8	1.75	39	77
	5% Tryptophan	132.3	159.3	1.8	45	80
	5% Tyrosine	145.2	168.2	0.55	37	80
	40% C_8 + 5% Tryptophan	190.7	149.3	2	32	62
PTx	PB-12kDa	169.6	188.2	0.77	16	50
	40% C_8	267.5	195.6	1.43	10	25
	100% C_8	201.3	216	0.44	40	85
	5% Tryptophan	132.3	240.3	1.8	11	23
	5% Tyrosine	145.2	205.7	0.3	55	95
	40% C_8 + 5% Tryptophan	190.7	202.7	0.48	37	80

Table 8.2. Summary of particle size, drug loading and release of water insoluble drugs

8.2.1. Particle size

Physicochemical characterisation of the various particles formed using different drug polymer combinations revealed certain important changes that occurred in the particles when drug was present within the polymers.
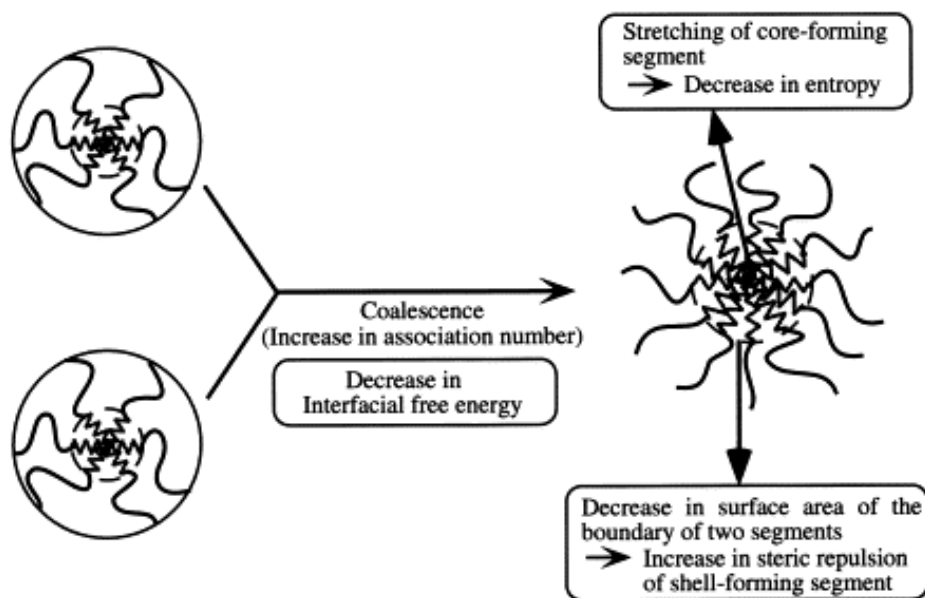
Fig. 8.1. Factors affecting particle formation and size.

According to existing literature reports, once the organic droplets contact water, the diffusion of acetone from the organic to aqueous phase produces very small droplets and makes the polymer molecules aggregate and precipitate instantaneously. Furthermore, these small droplets will break up into smaller and smaller ones until the polymer precipitates completely, which leads to the formation of nanoparticles. As illustrated in Fig. 8.1, aggregation of the polymer molecules is the main factor responsible for assembly into particles. Factors leading to an increase in association number of the particles could form loosely packed particles or a decrease in the interfacial free energy could lead to compact or dense particles. While most studies have reported polymer or drug

hydrophobicity influences the aggregation number of particles, this parameter was not measured in our studies.

DXMP, CYT-ARA and ETO-P, all water soluble drugs prepared using the Fessi method showed different trends for influence of particle size depending upon the type of polymer used. Increase in acylation was accompanied by increase in particle size for DXMP, ETO-P and ETO. CYT-ARA on the other hand showed no specific trend with degree of acylation.

Compared to the empty particles, DXMP, ETO and ETO-P in the acylated polymers were smaller in size indicating these drugs played some role in particle formation; probably at the interface or by reacting with the polymer to form dense and compact particles. CYT-ARA particles on the other hand were of similar size to the empty particles. Also, ETO-P particles followed trends similar to ETO but their sizes were smaller in all polymers compared to the ETO particles suggesting influence of the phosphate group and water solubility on aggregation and association of polymer molecules.

ETO and PTx when formulated using the amino acid substituted polymers produced particles of larger size than the acylated polymers. PTx particles with the amino acid polymers were around 240 nm in size and were the largest compared to the all other drug polymer combinations. Thus particle size depends upon the nature of arrangement of the polymer molecules and it is influenced by the nature of interactions between the drug and the polymer. In this study, the decrease of the mean particle size of copolymers might be attributed to polymer drug interactions that may reduce the crystallinity of the polymer and modify the solubility of the polymer in acetone. This might make the acetone droplets break up into finer nanodroplets before the polymer precipitation.

More hydrophobic drugs with most hydrophobic polymers have produced particles of the smallest size thus indicating that the presence of drug and its interaction with the polymer molecules is important in determining the arrangement and packing efficiency of polymers to produce either dense or loosely packed particles. More bulky drugs like ETO and PTx formed particles of the largest size with amino acid substituted polymers. This could be explained on basis of bulkiness and density of polymer molecules along with drugs associated with it.

8.2.2. Drug loading

Poly (glycerol adipate) is a water insoluble polyester. The presence of hydrophilic groups confers some hydrophilic characteristics to the backbone. The addition of acyl groups led to an increase in polymer hydrophobicity by decreasing the number of free OH groups on the backbone. On substituting the pendant hydroxyl groups of the backbone with hydrophobic acyl groups (C_8) in varying proportions, marked differences were observed in the % loading of various drugs. Amongst the acyl groups of varying chain lengths from 2 to 10, highest drug loading was observed when the chain length of acyl group was 8 carbon atoms. Hence, all further studies were carried out with these specifications for direct comparison with other drugs.

The 100% acylated polymer was identified as most promising drug delivery system for DXMP with 10% drug loading and 43% drug release at the end of 15 days without any burst release, thus providing significant indication of drug polymer interactions and its effect on drug loading and release. A consideration of polymer drug interactions suggest that the largest amount of drug loaded per

particle will be reached when the core-forming block is most suitably matched with the drug to be loaded. Therefore, in order to enhance the encapsulation of the drug, the compatibility between polymer and drug should be increased [249].
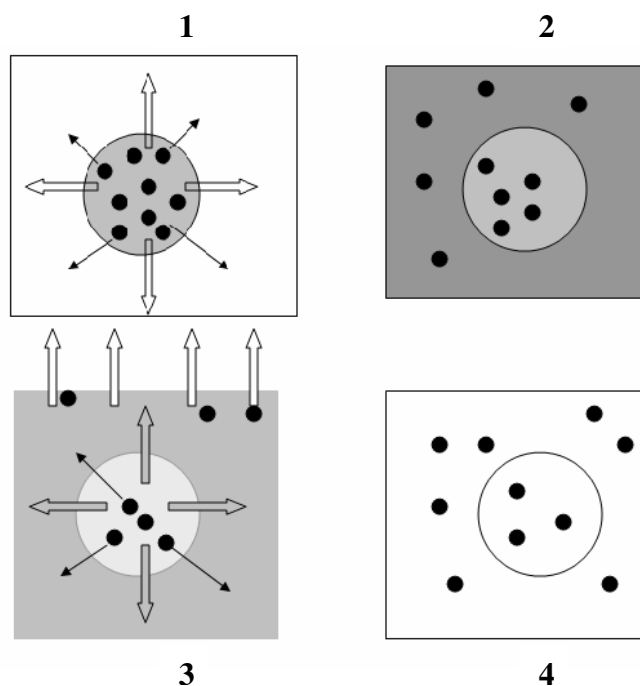
Fig. 8.2. Drug leakage during the manufacturing process. Diffusion of acetone towards the external medium along with the drug followed by evaporation of drug and its loss

Previous studies on poor drug incorporation have been explained only on the basis of either hydrophilicity of polymer or water solubility of drug. DXMP, ETO-P (both water soluble, DXMP>ETO-P) and ETO (water insoluble) showed a similar trend despite differences in chemical structures and solubility characteristics. They showed maximum incorporation with addition of acyl groups. Comparing results obtained with DXMP to those of CYT-ARA and ETO-P strengthened the hypothesis of acyl – steroid nucleus affinity. This interaction was attributed to be the major factor responsible for maximum incorporation of DXMP and governing its rate of release compared to CYT-ARA

(1%) and ETO-P (1.85%) loading within the 100% acylated polymer. Only for CYT-ARA was the best incorporation observed with the polymer backbone while an increase in acylation decreased the amount of drug loaded in the polymer. This has been attributed to the presence of both a sugar molecule and a free NH_2 group in its structure that could promote its interaction with the pendant hydroxyl groups to a significant extent. Since the drug is water soluble, polymer precipitation could also have occurred at a rate that enhanced drug loading in the polymer.

Thus the fully functionalised polymer provided optimum hydrophilic - hydrophobic characteristics that increased loading of DXMP and ETO compared to the polymer backbone. Individual differences in the amount of drug loaded within each of the acylated polymers varied depending on nature of drug and its interaction with the polymer side groups. A significant decrease in PTx loading with the 100% acylated polymer gave an indication of the specificity of degree of acylation and its subsequent influence on polymer hydrophobicity. The polymer with 40% acylation and 60% hydroxyl groups was apparently best suited to promote drug polymer interaction. Further increase in acylation probably decreased the affinity of the drug and failed to accommodate this extremely hydrophobic drug within its matrix to a significant extent. However, in the case of CYT-ARA, even a 40% acylation led to decrease in loading and for this drug the properties of polymer in its unsubstituted form were more favourable for better incorporation.

In order to introduce aromatic groups in the polymer, tryptophan and tyrosine residues were substituted on the backbone. The rationale was to study the possible effect of ring stacking as a mechanism of interaction between these

groups and drugs containing aromatic rings such as ETO and PTx. In addition to water soluble drugs, versatility of the polymer to accommodate hydrophobic drugs was also assessed. Since, some combinations contained polymers with hydrophobic substituents along with extremely hydrophobic drugs; aggregation of particles in absence of surfactant could be a possibility. However, all particles were stable under the given experimental conditions.

With tryptophan substitution there was no difference in the amount of ETO and ETO-P incorporation indicating that the phosphate group on the drug did not did not have a significant effect on loading within this polymer. From the DSC scans it was found that the Tg and Tm of the empty polymer increased in presence of either drug and this increase was greater in presence of ETO (Table 7.2). However, ETO-P incorporation was higher than ETO in the combination polymer. Thus, although it has a similar structure as ETO, interaction with the amino acid + acyl substituted polymer is influenced by presence of ionised phosphate as it allows for additional interaction with the unsubstituted hydroxyl groups on polymer.

 For PTx, the degree of acylation seemed to be more important for enhanced interaction and retention within the polymeric matrix. Also, formulation parameters like organic/aqueous phase ratio seemed to influence PTx incorporation more than that of ETO or ETO-P as it does not contain functional groups that can be ionized by pH alteration or allow salt formation [250]. The highest drug loading was achieved with the tryptophan substituted polymer (2.1%) and organic phase/aqueous phase 1/2. Thus there is an influence of the method of preparation and formulation parameters. A preformed matrix of drug dissolved in polymer solution added to the aqueous phase significantly increased

loading of water insoluble drugs using the interfacial deposition method. Drug incorporation also depended on the affinity of the drug in the polymer and hence the rate of precipitation of polymer and drug molecules. DXMP incorporation was better with the IDP method than the emulsification method.

According to the previous reports by Liu *et al*. on the solubilization of hydrophobic compounds in aqueous conventional surfactants and block copolymer micellar solutions, the number of molecules solubilized is closely correlated with molecular volume of solubilizates, and Van der Waals dispersion forces, hydrogen bonding and dipole–dipole interactions between micellar core and solubilizates. Calculation of the partial solubility parameters and mixing enthalpy enables prediction of polymer–drug compatibility [251].

In a recent study by Zhang *et al*., drug incorporation and release of 6 hydrophobic drugs, viz. medroxyprogesterone acetate, ibuprofen, ketoprofen, indomethacin, dexamethasone, and prednisone acetate were selected to elucidate the effect of drug type on its encapsulation into polymeric micelles based on amphiphilic polyphosphazenes bearing poly (*N*-isopropylacrylamide) and ethyl tryptophan as side groups [167]. Both the drug loading and entrapment efficiency for dexamethasone, medroxyprogesterone acetate and prednisone acetate was significantly lower independent of copolymer compositions (0.2%, 0.5% and 0.51% respectively). The corresponding values, however, were higher for ibuprofen, ketoprofen and indomethacin (3.6%, 0.9% and 7.1% respectively). In addition, for all these drugs, the actual drug loading and entrapment efficiency seemed to increase as the molar content of ethyl tryptophan group in the copolymer was increased. This lower loading level of dexamethasone,

medroxyprogesterone acetate and prednisone acetate drugs in polymeric micelles was explained on the basis of the large molecular volume of these drugs. While for drugs like ibuprofen, ketoprofen and indomethacin, in addition to their relatively small molecular volume they also have carboxylic group which could have allowed for hydrogen bonding interaction between amide groups in PNIPAAm chains and carboxyl groups.

A similar effect of adjusting the hydrophobicity of the polymer has been reported by Kwon *et al.* to enhance the encapsulation of aliphatic drugs such as amphoterecin B [252]. Micelle-forming Poly (ethylene oxide)-*b* poly (L-aspartic acid) (PEO-*b*-PLAA) block copolymers with stearic acid side chains on the PLAA block were synthesised and the effect of polymer structure on micellar properties and encapsulation of AmB was assessed. An increase in the level of stearic acid substitution on PEO-*b*- poly (N-hexylstearate-L-aspartamide) improved the encapsulation of AmB while reducing its haemolytic activity.

According to Avgoustakis *et al*. drug loading and encapsulation in PLGA-mPEG nanoparticles appeared to be governed by the partition coefficient of the drug between the organic phase and the external aqueous phase employed in nanoparticle preparation. Relatively low loading and encapsulation values were obtained, suggesting that the physical entrapment of drugs in PLGA-mPEG nanoparticles could only be an option in the development of formulations of potent drugs. Only the least water-soluble theobromine was efficiently sustained by its entrapment in the nanoparticles, indicating that the physical entrapment of drugs provides the means for the development of controlled-release PLGA-mPEG nanoparticulate formulations only in the case of drugs with low aqueous

solubility [26]. The physicochemical properties such as relative solubility of the drug + polymer may prevent appropriate drug incorporation.

8.2.3.Drug Release

The most hydrophilic polymer backbone showed a significant burst effect and the fastest rate of release for DXMP. However the same polymer gave a more controlled and sustained release for CYT-ARA. Increase in acylation decreased rate of release for DXMP while increased it for CYT-ARA and ETO-P. However, in case of ETO-P, the release from the backbone and the acylated polymers was incomplete. Amongst the acylated polymers and water insoluble drugs none of the acylated polymers showed a sustained release. ETO followed a similar profile to ETO-P. The order for rate of release was polymer backbone < 100% C_8 < 40% C_8 acylated polymers. For PTx, no specific trend could be observed. Release from the 40% acylated polymer was slower than the polymer backbone. Complete acylation showed a significant burst release.

Thus for the water soluble drugs, the acylated groups retained the steroid drugs (DXMP) to a greater extent than drug with heterocyclic rings (ETO-P). For ETO, both the parent compound and its water soluble counterpart showed slowest release with the polymer backbone indicating that the acyl groups and the phosphate groups on the drug are not predominantly involved in retaining the drug within the polymer.

The amino acid substituted polymers especially the tryptophan substituted polymer seemed to retain the water insoluble drugs better. The tryptophan substituted polymer had the slowest release for ETO followed by the tyrosine substituted polymer. For ETO-P, the combination polymer had a slower rate of

release than either the tryptophan or tyrosine substituted polymers. Release from the polymer backbone was slow but incomplete. ETO-P release from the amino acid substituted polymers was faster than that of ETO. However, for both drugs it was slower than the acylated polymer series. Thus the aromatic groups on the polymer and the ring stacking between the drug and polymer could be responsible for better retention of the drug within the polymer. For PTx, drug release was slowest from the tryptophan substituted polymer and rapid from the combined acyl-tryptophan substituted polymers compared to the 40% acylated or the 5% tryptophan substituted polymer.

 ETO and PTx incorporation and release from various polymers differed from each other and also from water soluble drugs thus indicating a difference in the mechanism of interaction of these drugs with the polymer molecules. ETO incorporation was highest in the 100% acylated polymer and it decreased in presence of aromatic rings on the polymer. Hence, an optimum level of hydrophobicity and side group chemistry was important following which any further modification of side chain groups was not as effective. However, release of ETO from this polymer was faster than from the tryptophan substituted polymer (2% loading). The particles that demonstrated controlled release for ETO were the largest compared to its other formulations

For PTx, maximum incorporation and most controlled release was seen from the tryptophan substituted polymer. For DXMP and PTx, particles providing the most controlled release also had highest drug loading. Also the slowest releasing formulations had varying sizes, 40% C_8 (195.65 nm) and 5% tryptophan (240.3 nm). Hence size alone is not a primary factor influencing rate of release and is

mainly an indication of effect of drug polymer interactions on assembly and packing of polymer molecules into particles.

Drug release from NPs appears to be mostly influenced by the strength of interactions between the drug and polymer which also strongly influences the amount of drug loaded within the particles. The nature of the drug and polymer and size of the particles are other factors that may also influence rate of drug release. This is in contrast to various published reports where higher drug loading and small particle size have been identified as the primary factor responsible for the burst effect or a rapid rate of release.

Thus, it is proposed that the affinity of polymer towards the drug to be encapsulated that actually determines drug loading efficiency and rate of release. These are dependant upon the properties of drug and chemistry of polymer which in turn are interrelated. Higher incorporation indicates high affinity possibly due to factors influencing particle formation / encapsulation; however this may not necessarily provide particles with a sustained release. Release of water soluble drug from polymer again depends upon side group chain and its ability to retain drug within its matrix rather than only water solubility of drug or molecular weight and hydrophilicity of polymer alone.

A number of literature reports have attributed poor drug incorporation and fast release of water soluble drugs using the interfacial deposition method to extreme water solubility of the drug and its rapid release into the external aqueous phase. Also, incorporation and release of water soluble drugs from hydrophobic polymers has always been poor and associated with a large burst effect. However, the % cumulative release from polymers at a fixed time point also depends on the drug solubility in water [154]. Hydrophilic drugs with high water

solubility may increase rate of water diffusion into matrix and accelerate bulk erosion while highly hydrophobic drugs may inhibit water diffusion thereby decreasing release rate and inducing surface erosion [253].

Some studies on nanoparticle formulations typically with PLGA and related polymers have hypothesised that as polymer degradation is achieved via hydrolysis, rate of degradation is controlled by chemistry of drug particularly presence of OH groups or pH of water dissolved products. Rate of release of the encapsulated agent has been correlated in some cases to the rate of degradation of PLGA. Release of said agent occurs through both diffusion and erosion as the polymer hydrolysis. It has also been reported that factors that may influence formation of or retention of acidic monomers could accelerate drug release. However, drug release rate from a degrading matrix is not necessarily correlated to the rate of polymer degradation. Drug may diffuse or leech out of a non degrading matrix. This is more likely to be applicable in the PGA polymer system as TEM images of our polymer particles after drug release revealed that most particles aggregated after the release studies, however they retained their shape and did not show signs of degradation or disintegration (Chapter 5).

Some studies have established a correlation between nanoparticle size and its influence on rate of drug release and drug loading to some extent. The smaller the size of the particles more rapid the rates of drug release. On the other hand, smaller sizes of particles have also been associated with lower drug loading and hence rapid release of all the contents. The amounts of lidocaine released in PBS from PLA nanoparticles in the initial phase were related to the nanosphere size [29]. DSC and infrared studies showed that no strong chemical interaction between drug and polymer occurred. Release kinetics of praziquantel from

PLGA particles was governed not only by actual drug loading but also by particle size. The higher the drug content and the smaller the particle size, the faster the drug release [192].

In the case of nanoparticles formulated with Poly (glycerol adipate) polymers no such direct correlation could be established. Particle size and zeta potential was more influenced by nature of substitution on polymers and type of drug used.

Release of antiestrogen RU from various polymers (PCL, PLA, PLGA) showed different release profiles with slowest release occurring from the most hydrophobic polymer; PLGA. High encapsulation within all the polymers was attributed only to properties of RU viz, poor water solubility and high hydrophobicity [253].

Barichello *et al.* reported that poor interaction between drug and polymer led to diffusion of the drug from the organic phase to the aqueous phase during spontaneous emulsification of the polymer. However lipophilic drugs did not suffer from leakage to the external medium and hence may be released slowly. In our studies we have observed extremely lipophilic drugs like PTx and ETO were released rapidly from the hydrophobic polymers. Thus, polymer/ drug hydrophobicity alone is not a criterion for drug loading and release but strongly suggestive that the combined chemistry of interaction between drug and polymer is more significant.

8.2.4. Physicochemical characterisation of drug polymer interactions

Analytical techniques such as the DSC and the FTIR provided basic evidence regarding drug polymer interactions. Drugs such as DXMP and ETO-P increased the Tm of the 100% acylated polymer while PTx increased the Tg of the 40%

acylated polymer thus leading to a slower rate of drug release. FTIR scans of ETO in the tryptophan substituted and the 100% acylated polymers showed appearance of peaks specific to the pure drug along with a marked change in the spectra of the pure polymer thus indicating some evidence of drug polymer interactions for the tryptophan substituted and 100% acylated polymers in the presence of ETO. Increased Tg of the PTx loaded 40% C_8 polymers indicated polymer was in the glassy state and the antiplasticization effect was predominant which hence showed the slowest rate of drug release.

8.3. CONCLUSIONS

A number of stable drug polymer nanoparticle formulations have been prepared using a simple method in the absence of surfactant and were assessed for drug loading and release.

From the various drug loading and release profiles it has been demonstrated that contrary to the reported literature, particle size is not the primary factor influencing drug release over the relatively small range of particle sizes seen in this study. Particle size is influenced by the substituents on the polymer and its interaction with the drug to form either dense or loosely packed particles. Similarly drug polymer interactions also influence drug loading and release and unlike commonly reported in literature hydrophilicity, molecular weight or concentration of polymer / drug are less likely to affect these parameters in isolation.

From our studies it has been demonstrated that particles smaller in size (DXMP in 100% C_8, ETO in 100% C_8) had highest drug loading and thus presence of more drug did not cause any expansion of the polymer matrix. Increase in

hydrophobicity of polymers (40% C$_8$ + 5% tryptophan) increased encapsulation of water soluble ETO-P while it decreased the encapsulation of water insoluble PTx. The hydrophilic polymer backbone showed highest loading for water soluble CYT-ARA. These results suggest that there is some binding between the drug and the polymer that depends upon the collective properties of the two and hence it is not necessarily true that a water soluble drug will always be washed off in the particle preparation method and be poorly incorporated.

In the same way drug release profile also varied depending upon the strength of the interactions and ability of the polymer to retain the drug. It was found that for hydrophobic drugs; tryptophan substituted polymers showed better retention and slowest release (PTx in 5% tryptophan, ETO in 5% tryptophan).

The following drug polymer combinations had both, a good drug loading and a sustained release profile and could be explored further as a promising nanoparticle delivery system for anti cancer or anti inflammatory agents:

1. DXMP in the 100% C$_8$ acylated polymers had the highest drug loading (10%) and slowest drug release profile (38%w/w after 10 days).

2. ETO-P in the 40% C$_8$ + 5% tryptophan substituted polymer with 2% w/w loading released approximately 60% drug after 10 days.

3. PTx in the 5% tryptophan substituted polymers had a drug loading of 1.8% and released around 25% drug after 10 days.

Most conclusions drawn from the study regarding drug polymer interactions on drug loading and release are based on circumstantial evidence. However, from the initial DSC and IR studies certain specific drug polymer interactions have been identified that correlate well with the results obtained for physicochemical properties of the particles and their drug loading and release profile. A more

detailed study involving drug chemistry, extent of loading and properties relating to polymer chemistry is needed to determine the relationship between drug – polymer interactions, drug incorporation and release rate.

8.4. FUTURE WORK

Having established the flexibility of the core polymer backbone to undergo substitutions with various functional groups, a lot needs to be explored in terms of nature and degree of substitution that could be achieved.

Modifications in terms of the monomers used in the formation of the polymer backbone and the nature of side groups that could be attached.

The basic monomeric units could be changed to included polyhydroxyl alcoholic groups or amino alcohol groups instead of glycerol. The successful conjugation of tryptophan and tyrosine could be extended to various other amino acid groups such as phenylalanine, histidine or sulphur containing cysteine. These substituents could also be investigated along with drugs belonging to different categories thus providing a library of polymer drug combinations that could be assessed for their ability to form nanoparticles with good loading and release characteristics.

The study has also helped in understanding and identifying various key factors that primarily contribute to successful incorporation of drugs within nanoparticles. It has also provided significant information on influence of drug polymer interactions on drug release profiles. However this information is still in its very basic stages. Use of in depth analytical techniques like the DSC, IR, XPS (X-ray photoelectron spectroscopy) needs to be explored further in order to

quantify the nature and extent of drug polymer interactions existing within nanoparticle formulations.

REFERENCES

1. Kreuter, J., *Nanoparticles*, in *Encyclopaedia of Pharmaceutical Technology*, Swarbrick J, Editor. 1994, Marcel Dekker Inc.: New York, USA. p. 165-90.

2. Barratt, G., M., *Therapeutic applications of colloidal drug carriers.* Pharm. Sci. Technol. To., 2000. **3**: p. 163-171.

3. Pitt, C., G., Chasalow, F.,I., Hibionada, Y.,M., Klimas, D.,M., Schindler, A., *Aliphatic polyesters 1. The degradation of poly-caprolactone in vivo.* J. Appl. Polym. Sci., 1983. **28**: p. 3779–87.

4. Couvreur, P., Dubernet, C., Puisieux, F., *Controlled drug delivery with nanoparticles: current possibilities and future trends.* Eur. J. Pharm. Biopharm., 1995. **41**: p. 2-13.

5. Vauthier-Holtzscherer, C., Benabbou, S., Spenlehauer, G., Veillard, M., Couvreur, P., *Methodology for the preparation of ultra-dispersed polymer systems.* STP Pharma Sciences 1991. **1**: p. 109-116.

6. Vanrell, R., H., Rincon, A.,C., Alonso, M., Reboto, V., Molina-Martnez, I.,T., Rodriguez-Cabello, J.,C., *Self- assembled particles of an elastin-like polymer as vehicles for controlled drug release.* J. Controlled Release, 2005. **102**: p. 113-122.

7. Vauthier, C., Dubernet, C., Chauvierre, C., Brigger, I., Couvreur, P., *Drug delivery to resistant tumors: the potential of poly(alkyl cyanoacrylate) nanoparticles.* J. Controlled Release, 2003. **93**(2): p. 151-60.

8. Panyam, J., Sahoo, S., K., Prabha, S., Bargar, T., Labhasetwar, V., *Fluroescence and electron microscopy probes for cellular and tissue uptake of poly (DL-co-glycolide) nanoparticles.* Int. J. Pharm., 2003. **262**: p. 1-11

9. Panyam, J., Labhasetwar, V., *Biodegradable nanoparticles for drug and gene delivery to cells and tissue.* Adv. Drug Delivery Rev., 2003. **55**(329-47).

10.   Moghimi, S., M., Hunter, A.,C., Murray, J.,C., *Long-circulating and target-specific nanoparticles: theory to practice.* Pharmacol. Rev., 2001. **53**(2): p. 283-318.

11.   Kreuter, J., *Nanoparticles*, in *Colloidal Drug Delivery Systems*, J.Kreuter, Editor. 1994, Marcel Dekker: New York. p. 219- 342.

12.   Haixiong, G., Yong, H., Jiang, X., Cheng, D., Yuan, Y., Bi,H., Yang, C., *Preparation, characterization, and drug release behaviors of drug nimodipine-loaded poly(ϵ-caprolactone)-poly(ethylene oxide)-poly(ϵ-caprolactone) amphiphilic triblock copolymer micelles.* J. Pharm. Sci., 2002. **91**(6): p. 1463-73.

13.   Desai, M., P., Labhasetwar, V., Walter, E., Levy, R., J., and Amidon, G.,L., *The mechanism of uptake of biodegradable microparticles in caco-2 cells is size dependant.* Pharm. Res., 1997. **14**: p. 1568-73.

14.   Linhardt, R., J., *Biodegradable polymers for controlled release of drugs*, in *Controlled Release of Drugs* M. Rosoff, Editor. 1989, VCH Publishers: New York p. 53–95.

15.   Redhead, H., M., Davis, S., S.,Illum, L., *Drug delivery in poly(lactide-co-glycolide) nanoparticles surface modified with poloxamer 407 and poloxamine 908: in vitro characterisation and in vivo evaluation.* J. Controlled Release, 2001. **70**(3): p. 353-63.

16.   Barrera, D., A., Zylstra, E., Lansbury, P., T., Langer, R., *Synthesis and RGD peptide modification of a new biodegradable co polymer; poly(lactic acid-co-lysine).* J Am Chem Soc, 1993. **115**: p. 11010-11.

17.   Davda, J., Labhasetwar, V., *Characterisation of nanoparticle uptake by endothelial cells.* Int J Pharm 2002. **223**: p. 51-59.

18.   Woodward, S., C., Brewer, P., S., Montarned, F., Schindler, A., Pitt, C., G, *The intracellular degradation of polycaprolactone.* J. Biomedical Mater. Res., 1985. **19**: p. 437– 44.

19.   Redhead, H., *Drug loading of biodegradable nanoparticles for site specific drug delivery.* 1997, University of Nottingham Nottingham.

20.   Lamprecht, A., Ubrich, N., Yamamoto, H., Schäfer, U., Takeuchi, H., Maincent, P., Kawashima, Y., Lehr, C.,M., *Biodegradable nanoparticles*

for targeted drug delivery in treatment of inflammatory bowel disease. J. Pharmacol. Exp. Ther., 2001. **299**: p. 775.

21. Maeda, H., *The enhanced permeability and retention (EPR) effect in tumour vasculature: the key role of tumour-selective macromolecular drug targeting.* Adv. Enzyme Regul., 2001. **41**: p. 189-207.

22. Sahoo, S., K., Sawa, T., Fang, J., Tanaka, S., Miyamoto,. Y., Akaike, T., Maeda, H., *Pegylated zinc protoporphyrin: a water soluble heme oxygenase inhibitor with tumour targeting capacity.* Bioconjugate Chem., 2002. **13**: p. 1031-38.

23. Guzman, L., A., Labhasetwar, V., Song, C., Jang, Y., Lincoff, A.,M., Levy, R., Topol, E.,J., *Local intraluminal infusion of biodegradable polymeric nanoparticles, A novel approach for prolonged drug delivery after balloon angioplasty.* Circulation, 1996. **94**: p. 1441-48.

24. Lockman, P., R., Mumper, R., J., Khan, M.,A.,and Allen, D.,D., *Nanoparticle technology for drug delivery across the blood brain barrier.* Drug Dev. Ind. Pharm., 2002: p. 1-13.

25. Fisher, R., S., Ho, J., *Potential new methods for antiepileptic drug delivery.* CNS drugs 2002. **16**(9): p. 579-593.

26. Avgoustakis, K., Beletsi, A., Panagi, Z., Klepetsanis, P., Karydas, A.,G., Ithakissios, D.,S., *PLGA-mPEG nanoparticles of cisplatin: in vitro nanoparticle degradation, in vitro drug release and in vivo drug residence in blood properties.* J. Controlled Release, 2002. **79**(1-3): p. 123-35.

27. Beletsi, A., Leontiadis, L., Klepetsanis, P., Ithakissios, D.,S., Avgoustakis, K., *Effect of preparative variables on the properties of poly(dl-lactide-co-glycolide)-methoxypoly(ethyleneglycol) copolymers related to their application in controlled drug delivery.* Int. J. Pharm., 1999. **182**: p. 187-197.

28. Schwendeman, S., Costantino, H., R., Gupta, R.,K., Langer, R., *Peptide, protein and vaccine delivery from implantable polymeric systems: Processes and challenges*, in *Controlled Drug Delivery: Challenges and Strategies* K. Park, Editor. 1997, American Chemical Society: Washington D.C. p. 229-267.

29. Witschi, C., Doelker, E., *Influence of the microencapsulation method and peptide loading on poly(lactic acid) and poly(lactic-co-glycolic acid) degradation during in vitro testing.* J. Controlled Release, 1998. **51**: p. 327–41.

30. Wang, J., Wang, B., M., Schwendeman, S.,P., *Characterization of the initial burst release of a model peptide from poly(D,L-lactide-co-glycolide) microspheres.* J. Controlled Release, 2002. **82**: p. 289–307.

31. Ratner, B., D., Hoffman, S., Schoen, F.,J., Lemons, J.,E, *Biomaterials Science: An Introduction to Materials in Medicine,* 1996, Academic Press: San Diego.

32. Pitt, C., G., *The controlled parenteral delivery of polypeptides and proteins.* Int. J. Pharm., 1990. **59**: p. 173–196.

33. Cohen, S., Yoshioka, T., Lucarelli, M., Hwang, L., H., Langer, R., *Controlled delivery systems for proteins based on poly(lactic/glycolic acid) microspheres.* Pharm. Res. , 1991. **8**: p. 713–20.

34. Ravivarapu, H., B., Lee, H., DeLuca, P., P., *Enhancing initial release of peptide from poly(D,L-lactide-co-glycolide) (PLGA) microspheres by addition of a porosigen and increasing drug load.* Pharm. Dev. Technol., 2000. **5**: p. 287–96.

35. Husmann, M., Schenderlein, S., Lück, M., Lindner, H., Kleinebudde, P., *Polymer erosion in PLGA microparticles produced by phase separation method.* Int. J. Pharm., 2002. **242**: p. 277–80.

36. Gref, R., Luck, M., Quellec, P., Marchand, M., Dellacherie, E., Harnisch, S., Blunk, T., Muller, R., H., *'Stealth' corona-core nanoparticles surface modified by polyethylene glycol (PEG): influences of the corona (PEG chain length and surface density) and of the core composition on phagocytic uptake and plasma protein adsorption.* Colloids Surf., B 2000. **18**: p. 301–13.

37. Tobio, M., Sanchez, A., Vila, A., Soriano, I., I., Evora, C., Vila-Jato, J.,L., Alonso, M.,J., *The role of PEG on the stability in digestive fluids and in vivo fate of PEG-PLA nanoparticles following oral administration.* Colloids Surf. B, 2000. **18**: p. 315–23.

38.   Vila, A., Sanchez, A., Tobio, M., Calvo, P., Alonso, M., J., *Design of biodegradable particles for protein delivery.* J. Controlled Release, 2002. **78**: p. 15–24.

39.   Kissel, T., Li, Y., Unger, F., *ABA-triblock copolymers from biodegradable polyester A-blocks and hydrophilic poly(ethylene oxide) B-blocks as a candidate for in situ forming hydrogel delivery systems for proteins.* Adv. Drug Delivery Rev., 2002. **54**: p. 99-134.

40.   Jeong, B., Bae, Y.,H., Kim, S.,W., *Drug release from biodegrdable injectable thermosensitive hydrogel of PEG-PLGA-PEG triblock copolymers.* J. Controlled Release, 2000. **63**: p. 155-163.

41.   Bae, Y., H., Huh, K., M., Kim, Y., Park, K.,H., *Biodegradable amphiphilic multiblock copolymers and their implications for biomedical applications.* J. Controlled Release, 2000. **64**: p. 3-13.

42.   Huh, K., M., Cho, Y., W., Kinam, P., *PLGA-PEG block copolymers for drug formulations.* Drug delivery technology, 2003. **3**(5).

43.   Neil, P., Desai, P., Shiong, S., Sandford, P., *Water-soluble polymeric carriers for drug delivery*, U.S. Patents, 5,648,506. (1997), Vivorax, Inc: United States of America.

44.   Cai, Q., Wan, Y., Bei, J., Wang, S., *Synthesis and characterization of biodegradable polylactide-grafted dextran and its application as compatilizer.* Biomaterials, 2003. **24**(20): p. 3555-62.

45.   Hagan, S., A., Coombes, A.,G.,Garnett, M.,C., Dunn, S.,E., Davies, M.,C., Illum, L., Davis,S.,S., *Polylactide–poly(ethylene glycol) copolymers as drug delivery systems. 1. Characterization of water dispersible micelle-forming systems.* Langmuir, 1996. **12**: p. 2153–61.

46.   Soo, P., L., Luo, L., Maysinger, D., Eisenberg, A., *Incorporation and release of hydrophobic probes in biocompatible polycaprolactone-block–poly(ethylene oxide) micelles: implications for drug delivery.* Langmuir, 2002. **18**: p. 9996–10004.

47.   La, S., B., Okano, T., Kataoka, K., *Preparation and characterization of micelle-forming polymeric drug indomethacin-incorporated poly(ethylene oxide)–poly(β-benzyl -aspartate) block copolymer micelles.* J. Pharm. Sci., 1996. **85** p. 85–90.

48.   Cho, C., S., Nah, J., W., Jeong, Y., I., Cheon, J., B., Asayama, S., Ise, H., Akaike, T., *Conformational transition of nanoparticles composed of poly(γ-benzyl -glutamate) as the core and poly(ethylene oxide) as the shell.* Polymer, 1999. **40**: p. 6769–75.

49.   Torchilin, P., *Structure and design of polymeric surfactant-based drug delivery systems.* J. Controlled Release, 2001. **73**: p. 137–172.

50.   Jones, M., C., Leroux, J.,., *Polymeric micelles—a new generation of colloidal drug carriers.* Eur. J. Pharm. Biopharm., 1999. **48**: p. 101–11.

51.   Gao, Z., Eisenberg, A., *A model of micellization for block copolymers in solutions.* Macromolecules, 1993. **26**: p. 7353–60.

52.   Pitt, C., G., *Poly-ε-caprolactone and its copolymers*, in *Biodegradable Polymers as Drug Delivery Systems*, M. Chasin, Langer, R., Editor. 1990, Marcel Dekker Inc: New York, NY. p. 71-119.

53.   Molpeceres, J., Chacón, M., Guzmán, M., Berges, L., Aberturas, M., R., *A polycaprolactone nanoparticle formulation of cyclosporin-A improves the prediction of area under the curve using a limited sampling strategy.* Int. J. Pharm., 1999. **187**(1): p. 101-113

54.   Lemarchand, C., Chattopadhyay, P., Besnard, M., Constantini, D., Gref, R., *Novel Polyester- Polysaccharide nanoparticles.* Pharm. Res., 2003. **20**(8).

55.   Iooss, P., Le Ray, A., M., Grimandi, G., Daculsi, G., Merle, C., *A new injectable bone substitute combining poly(ε-caprolactone) microparticles with biphasic calcium phosphate granules.* Biomaterials, 2001. **22**: p. 2785-94.

56.   Couvreur, P., Kante, B., Roland, M., Goit, P., Bauduin, P., Speiser, P., *Poly cyano acrylate nanocapsules as potential lysosmotropic carriers: reparation, morphology and sorptive properties.* J. Pharm. Pharmacol., 1979. **31**: p. 331–32.

57.   Oliver, J., C.,Fenart, L.,Chauvet, R., Pariat, C.,Cecchelli, R.,Couet, W., *Indirect evidence that drug brain targeting usinh polysorbate 80 coated polybutylcyanoacrylate nanoparticles is related to toxicity.* Pharm. Res., 1999. **16**: p. 1836-42.

58.   Layre, A., M., Couvreur, P., Chacun, H., Chodur C., A., *Busulphan loading into poly(alkyl cyanoacrylate) nanoparticles:physico-chemistry and molecular modelling.* J. Biomed. Mater. Res., Part B, 2006. **79**(2).

59.   Nemati, F., Dubernet, C., Fessi, H., Verdière, A., C., Poupon, M., F., Puisieux, F., Couvreur, P., *Reversion of multidrug resistance using nanoparticles in vitro: influence of the nature of the polymer.* Int. J. Pharm., 1996. **138**: p. 237–46.

60.   Verdière, A., C., Dubernet, C., Némati, F., Soma, E., Appel, M., Ferté, J., Bernard, S., Puisieux, F., Couvreur, P., *Reversion of multidrug resistance with polyalkylcyanoacrylate nanoparticles: towards a mechanism of action.* Br. J. Cancer, 1997. **76**: p. 198–205.

61.   Andrew, C., A., Wan, H., M., Wang, S., Su Hui Phua, Lee, G., P., Pan, J., Lu, S., Wang, J., Leong, K., W., *Poly(phosphoester) ionomers as tissue-engineering scaffolds.* J. Biomed. Mater. Res., Part B, 2004. **70B** (1): p. 91-102.

62.   Kumar, N., Langer, R., S., Domb, A., J., *Polyanhydrides: an overview* Adv. Drug Delivery Rev., 2002. **54**: p. 889-910.

63.   Ghosh, S., *Recent research and development in synthetic polymer based drug delivery systems.* J. Chem. Res., 2004. **4**: p. 241-246

64.   Dumitriu, S., *Polysaccharides as biomaterials*, in *Polymeric Biomaterials*, S. Dumitriu, Editor. 2001, Marcel Dekker: New York p. 1–61.

65.   General, S., Thunemann, A., F., *pH-sensitive nanoparticles of poly(amino acid) dodecanoate complexes.* Int. J. Pharm., 2001. **230**(1-2): p. 11-24.

66.   Nakanishi, T., Fukushima, S., Okamoto, K., Suzuki, M., Matsumura, Y., Yokoyama, M., Okano, T., Sakurai, Y., Kataoka, K., *Development of the polymer micelle carrier system for doxorubicin.* J. Controlled Release, 2001. **74**: p. 295–302.

67.   Li, M., X., Zhuo, R., X., Qu, F., Q., *Synthesis and Characterization of Novel Biodegradable Poly(ester amide) with Ether Linkage in the Backbone Chain.* J. Polym. Sci.: Part A: Polym. Chem., 2002. **40**: p. 4550-55.

68. In't Veld, P., J., A., Dijkstra, P., J., Feijen, J., *Copolymerization of ε-caprolactone and morpholine-2, 5-dione derivatives.* Makromol.Chem. and Phy., 1992. **193**(8): p. 1927-42.

69. Zhao, J., Quan, D., Liao, K., Wu, Q., *PLGA- (L-Asp-alt-diol)x-PLGAs with different contents of pendant amino groups: synthesis and characterisation.* Macromol. Biosci., 2005. **5**: p. 636-43.

70. Yao, F., Bai, Y., Zhou, Y., liu,C., Wang, H., Yao, K., *Synthesis and characterization of multiblock copolymers based on L-lactic acid, citric acid, and poly(ethylene glycol).* J. Polym. Sc.i A: Poly. Chem., 2003. **41**: p. 2073.

71. Ni, Q., Yu, L.,P., *Synthesis of Novel Poly(ε -caprolactone)s Functionalized with a thioester end-group via a living ring opening polymerization and their application in chemoselective ligation with compounds containing a Cysteine terminal.* J. Am. Chem. Soc., 1998. **120**(5): p. 1645-46.

72. Kallinteri, P., Higgins, S., Hutcheon, G., A., Pourcain, C., B., Garnett, M., C., *Novel functionalized biodegradable polymers for nanoparticle drug delivery systems.* Biomacromolecules, 2005. **6**(4): p. 1885 -94.

73. Tian, D., Dubois, P., Grandfils, C., Jerome, R., *Ring-opening polymerization of 1,4,8-Trioxaspiro[4.6]-9-undecanone: A new route to aliphatic polyesters bearing functional pendent groups.* Macromolecules, 1997. **30**(406): p. 2575.

74. Gimenez, S., Ponsart, S., Coudane, J., Vert, M., *Synthesis, properties and in vitro degradation of carboxyl-bearing PCL.* J. Bioact. Compt. Polym., 2001. **16**: p. 32.

75. Lim, Y., B., Choi, Y., H., Park, J., S., *A Self-Destroying Polycationic Polymer: Biodegradable Poly(4-hydroxy-L-proline ester).* J. Am. Chem. Soc., 1999. **121**: p. 5633.

76. Taniguchi, I., Mayes, A., M., Chan, E., W., Griffith, L., G., *A chemoselective approach to grafting biodegradable polyesters.* Macromolecules, 2005. **38**: p. 216.

77.   Jiang, H., L., Zhu, K., J., *Synthesis, characterisation and in vitro degradation of a new family of alternate poly (ester-anhydrides) based on aliphatic and aromatic diacids.* Biomaterials, 2001. **22**: p. 211-218.

78.   Prego, C., Fabre, M., Torres, D., Alonso, M., J., *Efficacy and mechanism of action of Chitosan Nanocapsules for oral peptide delivery.* Pharm. Res., 2006. **23**(3): p. 549-56.

79.   Zhang, X., Jackson, J., K., Burt, H., M., *Development of amphiphilic diblock copolymers as micellar carriers of paclitaxel.* Int. J. Pharm., 1996. **132**: p. 195-206.

80.   Kwon, G., Suwa, S., Yokoyama, M., Okano, T., Sakurai, Y., Kataoka, K., *Enhanced tumour accumulation and prolonged circulation times of micelle-forming poly(ethylene oxide-aspartate) block copolymer adriamycin conjugates.* J. Controlled Release, 1994. **29**: p. 17–23.

81.   Kataoka, G., S., Kwon, M., Yokoyama, Okano, T., Sakurai, Y., *Block copolymer micelles as vehicles for drug delivery.* J. Controlled Release, 1993. **24**: p. 119–132.

82.   Gref, R., Minamitake, Y, Peracchia, M.,T., Trubetskoy, V., Torchilin, V., Langer, R., *Biodegradable long-circulating polymeric nanospheres.* Science, 1994. **263**: p. 1600–03.

83.   Li, C., Newman, R., A., Wu, Q., P., Shi, K., Chen, W., Hutto, T., *Biodistribution of paclitaxel and poly(l-glutamic acid)-paclitaxel conjugate in mice with ovarian OCa-1 tumour.* Cancer Chemoth. Pharm., 2006. **46**(5): p. 416-22.

84.   Dosio, F., Brusa, P., Crosasso, P., Arpicco, S., Cattel, L., *Preparation and characterization and properties in vitro and in vivo of a paclitaxel-albumin conjugate.* J. Controlled Release, 1997. **47**: p. 293–304.

85.   Jung, T., Breitenbach, A., Kissel, T., *Sulfobutylated poly(vinylalcohol)-graft-poly (lactide-co-glycolide) facilitate the preparation of small negatively charged biodegradable nanospheres for protein delivery.* J. Controlled Release, 2000. **67**: p. 157–169.

86.   Niwa, T., Takeuchi, H., Hino, T., *Biodegradable submicron carriers for peptide drugs. Preparation of DL-lactide/glycolide copolymer(PLGA)*

nanospheres with narfelin acetate by novel emulsion-phase separation method in an oil system. Int. J. Pharm., 1995. **121**: p. 45-54.

87.   Barrera, D., A., Zylstra, E., Lansbury, P., T., Langer, R., *Synthesis and RGD peptide modification of a new biodegradable co polymer; poly(lactic acid-co-lysine).* J. Am. Chem. Soc., 1993. **115**: p. 11010-11.

88.   Song, C., X., Labhasetwar, V., Murphy, H., Qu, X., Humphrey, W., R., Shebuski, R., J., Levy, R., J., *Formulation and characterisation of biodegradable nanoparticles for intravascular local drug delivery.* J. Controlled Release, 1998. **43**: p. 197-212.

89.   Ruan, G., Feng, S., S., *preparation and characterisation of poly (lactic acid)-poly(ethylene glycol)-poly(lactic acid) microspheres for controlled release of paclitaxel.* Biomaterials, 2003. **24**: p. 5037-44.

90.   Scholes, P., D., Coombes, A.,G., Illum, L., Davis, S., S., Watts, J., F., Ustariz, C., Vert, M., Davies, M., C., *Detection and determination of surface levels of poloxamer and PVA surfactant on biodegradable nanospheres using SSIMS and XPS.* J. Controlled Release, 1999. **59**(3): p. 261-78.

91.   Fessi, H., Puisieux, F., Devissague, J., P., Ammoury, N., Benita, S., *Nanocapsule formation by interfacial polymer deposition following solvent displacement.* Int. J. Pharm., 1995. **113**: p. 57-63.

92.   Maillard, M., Motte, L., Ngo, A., T., Pileni, M., P., *Rings and hexagons made of nanocrystals: A Marangoni Effect.* J. Phys. Chem. B, 2000. **104**: p. 11871- 877.

93.   Carla, V., Mosquiera, F., Legrand, P., Alphandry, H., Puisieux, F., Barratt, G., *Poly (D,L- Lactide) nanocapsules prepared by a solvent displacement process: influence of the composition on physicochemical and structural properties.* J. Pharm. Sci., 2000. **89**(5): p. 614-26.

94.   Dong, Y., Feng, S., S., *Methoxy poly (ethylene glycol)-poly (lactide) (mEG-PLA) nanoparticles for controlled delivery of anticancer drugs.* Biomaterials, 2004. **25**: p. 2843-49.

95.   Bindschaedler, C., Gurny, R., Doelker, E., *Process for preparing a powder of water-insoluble polymer which can be redispersed in a liquid*

phase, the resulting powder and utilization thereof. Switzerland. 88/08011 (1988).

96. Allemann, E., Leroux, J.,C., Gurny, R., Doelker, E., *In vitro extended release properties of drug-loaded poly (DL-lactic acid) nanoparticles produced by a salting out procedure.* Pharm. Res., 1993. **10**: p. 1732–37.

97. Dominy, B., N., Perl, D., Schmid, F., X., Brooks, C., L., III., *The effects of ionic strength on protein stability: The cold shock protein family.* J. Mol. Biol., 2002. **319**: p. 541-54.

98. Chattopadhyay, P., Gupta, R., B., *Protein nanoparticles formation by supercritical antisolvent with enhanced mass transfer.* AIChE Journal,2002. **48**(2): p. 235-44.

99. Shekunov, Y., Chattopadhyay, P., Seitzinger, J., Huff, R., *Nanoparticles of Poorly Water-Soluble Drugs Prepared by Supercritical Fluid Extraction of Emulsions* Pharm. Res., 2006. **23**(1): p. 196-204.

100. Kaibara, K., Okazaki, T., Bohidar, H., B., Dubin, P., L., *pH-induced coacervation in complexes of bovine serum albumin and cationic polyelectrolytes.* Biomacromolecules, 2000. **1**: p. 100–107.

101. Sanchez, C., Renard, D., *Stability and structure of protein–polysaccharide coacervates in the presence of protein aggregates.* Int. J. Pharm., 2002. **242**: p. 319–24.

102. Li, X., T., Wang, and Zhang, X., B., *Studies on alginate–chitosan microcapsules and renal arterial embolization in rabbits.* J. Controlled Release, 2002. **84**(3): p. 87–98.

103. Jiang, B., Hu, L., Gao, C., Shen, J., *Ibuprofen-loaded nanoparticles prepared by a co-precipitation method and their release properties.* Int. J. Pharm., 2005. **304**(1-2): p. 220-30.

104. Reeve, M., S., McCarthy, S., P., Downey, M., J., Gross, R., A., *Polylactide stereochemistry: effect on enzymatic degradability.* Macromolecules, 1994. **27**: p. 825.

105. Li, S., Garreau, H., Vert, M., *Structure-property relationships in the case of the degradation of massive aliphatic poly-(α-hydroxy acids) in aqueous media.* J Mater Sci: Mater Med 1990. **1**(3): p. 123-30.

106. Fukuzaki, H., Yoshida, M., Asano, M., Kumakura, M., *Synthesis of copoly (D,L-lactic acid) with relatively low molecular weight and in vitro degradation.* Eur. Polym. J., 1989. **25** (10): p. 1019-26.

107. Zhu, K., J., Hendren, R., W., Jensen, K., Pitt, C., G., *Synthesis, properties, and biodegradation of Poly (1,3-trimethylene carbonate).* Macromolecules, 1991. **24**: p. 736.

108. Belbella, A., Vauthier, C., Fessi, H., Devissaguet, J., Puisieux, F., *In vitro degradation of nanospheres from poly lactides) of different molecular weights and polydispersities.* Int. J. Pharm., 1996. **129**: p. 95–102.

109. Kenley, R., A, Lee, M., O., Mahoney, T., Sanders, L., *Poly(glycolide-co-lactide) decomposition kinetics in-vivo and in-vitro.* Macromolecules, 1987. **20**: p. 2398–2403.

110. Katakai, R., Goodman, M., *Polydepsipeptides.9. Synthesis of sequential polymers containing some amino acids having polar side chains and (S)-lactic acid.* Macromolecules, 1982. **15**(1): p. 25.

111. Darby, R., T., Kaplan, A., M., *Fungal susceptibility of polyurethanes.* Appl. Microbiol., 1968. **16**: p. 900.

112. Couvreur, P., Kante, B., Roland, M., Speiser, P., *Adsorption of antineoplastic drugs to polyalkylcyanoacrylate nanoparticles and their release in calf serum.* J. Pharm. Sci., 1979. **68**: p. 1521-23.

113. Albertsson, A., C., Lundmark, S., *Melt Polymerization of Adipic Anhydride (Oxepan-2, 7-Dione).* J. Macromol. Sci., Part A: Pure Appl. Chem., 1990. **27**.

114. Hegyeli, A., F., *Use of organ cultures to evaluate biodegradation of polymer implant materials.* J. Biomed. Mater. Res., Part A, 1973. **7**. p. 205.

115. *An approach to classify degradable polymers*, ed. T. Neenan, Marcolongo, M., Valentini, R., F. 1999. 17-22.

116. Chiu, L., K., Chiu, W., J., Cheng, Y., L., *Effects of polymer degradation on drug release — a mechanistic study of morphology and transport properties in 50:50 poly (DL-lactide-co-glycolide).* Int. J. Pharm., 1995. **126**: p. 169–178.

117. Washington, C., *Drug release from microdisperse systems: a critical review.* Int. J. Pharm., 1990. **1990**(58): p. 1-12.

118. Anderson, J., M., Shive, M.,S., *Biodegradation and biocompatibility of PLA and PLGA microspheres.* Adv. Drug Delivery Rev., 1997. **28**: p. 5–24.

119. Hans, M., L., Lowman, A., M., *Biodegradable nanoparticles for drug delivery and targeting.* Curr. Opin. Solid St. M., 2002. **6**: p. 319-327.

120. Maulding, H., V., Tice, T., R., Cowsar, D., R., Fong, J., W., Pearson, J., E., Nazareno, J., P., *Biodegradable microcapsules: acceleration of polymeric excipient hydrolytic rate by incorporation of a basic medicament.* J. Controlled Release, 1986. **3**: p. 103-117.

121. Li, S., Girod-holland, S., Vert, M., *Hydrolytic degradation of poly (DL - lactic acid) in presence of caffeine base.* J. Controlled Release, 1996. **40**: p. 41-53.

122. Leroux, J., C., Allemann, E., De Jaeghere, F., Doelker, E., Gurny, R., *Biodegradable nanoparticles from sustained release formulations to improve site specific drug delivery.* J. Controlled Release, 1996. **39**: p. 339-50.

123. Sant, S., Nadeau, V., Hildgen, P., *Effect of porosity on the release kinetics of propafenone-loaded PEG-g-PLA nanoparticles.* J. Controlled Release, 2005. **107**(2): p. 203-14.

124. Okada, H., Doken, Y., Ogawa, Y., Toguchi, H. , *Preparation of three-month depot injectable microspheres of leuprorelin acetate using biodegradable polymers.* Pharm. Res., 1994. **11**: p. 1143–47.

125. Fresta, M., Puglisi, G., Giammona, G., Cavallaro, G., Micali, N., Furneri, P., M., *Pefloxacin mesilate- and ofloxacin- loaded polyethylcyanoacrylate nanoparticles; characterization of the colloidal drug carrier formulation.* J. Pharm. Sci., 1995. **84**(7): p. 895–901.

126. Yoo, H., S., Oh, J., E., Lee, K., H., Park, T., G., *Biodegradable nanoparticles containing doxorubicin–PLGA conjugate for sustained release.* Pharm. Res., 1999. **16**: p. 1114–18.

127. Duan, Y., Sun, X., Gong, T., Wang, Q., Zhang, Z., *Preparation of DHAQ-loaded mPEG-PLGA-mPEG nanoparticles and evaluation of*

drug release behaviors in vitro/in vivo. J. Mater. Sci. Mater. Med., 2006. **17**(6): p. 509-16.

128. Watanabe, J., Iwamoto, S., Ichikawa, S., *Entrapment of some compounds into biocompatible nano-sized particles and their releasing properties.* Colloids Surf., B 2005. **42**: p. 141-6.

129. Hata, Y., Taira, H., Sato, J., Iinuma, S., *Sustained release preparation for bioactive substance having an acidic group.* 1997.

130. Oh, J., E., Nam, S., Lee, K., H., Park, T., G., *Conjugation of drug to poly(lactide-co-glycolic acid) for controlled release from biodegradable microspheres.* J. Controlled Release, 1999. **57**: p. 269-80.

131. Shenderova, B., T., G., Schwendeman, S., P., *The acidic microclimate in poly(DL-lactide-co-glycolide) microspheres stabilizes camptothecins.* Pharm. Res., 1999. **16**: p. 241–48.

132. Gref, R., Minamitake, Y., Peracchia, M., T., Trubetskoy, V., Torchilin, V., Langer, R., *Biodegradable long circulating polymeric nanospheres.* Science 1994. **263**: p. 1600-03.

133. Hsieh, D., S., Rhine, W., D., Langer, R., *Zero-order controlled-disease polymer matrices for micro- and macromolecules.* J. Pharm. Sci., 1983. **72**: p. 17-22.

134. Lemaire, V., Belair, J., Hildgen, P., *Structural modeling of drug release from biodegradable porous matrices based on a combined diffusion/erosion process.* Int. J. Pharm., 2003. **258**: p. 95–107.

135. Rafler, G., Jobmann, M., *Controlled release systems of biodegradable polymers – 5th communication: microparticle preparation by a salting-out process.* Pharm. Ind., 1997. **59**: p. 620-624.

136. Zweers, M., Engbers, G., Grijpma, D., Feijen, J., *Release of anti restenosis drugs from poly (ethylene oxide)-poly (DL-lactide-co-glyclic acid) nanoparticles.* J. Controlled Release, 2006. **114**(3): p. 317-24.

137. Moes, S.P., *In vitro evaluation of the hydrolytic degradation of dispersed and aggregated poly(-lactide-co-glycolide) microspheres.* J. Controlled Release, 1997. **43**: p. 47–58.

138. Spenlehauer, G., Vert, M., Benoit, J., Boddaert, A., *In vitro and in vivo degradation of poly(DL -lactide/glycolide) type microspheres made by solvent evaporation method.* Biomaterials, 1989. **10**: p. 557–63.

139. Park, T., G., *Degradation of poly(lactic-co-glycolic acid) microspheres: effect of copolymer composition.* Biomaterials 1995. **16**: p. 1123–30.

140. Thomasin, C., Trân, H., N., Merkle, H., P., Gander, B., *Drug microencapsulation by PLA/PLGA coacervation in the light of thermodynamics. 1. Overview and theoretical considerations.* J. Pharm. Sci., 2000. **87**(3): p. 259-68.

141. Mu, L., Feng, S., S., *Fabrication, characterization and in vitro release of paclitaxel (Taxol®) loaded poly (lactic-co-glycolic acid) microspheres prepared by spray drying technique with lipid/cholesterol emulsifiers.* J. Controlled Release, 2001. **76**(3): p. 239-54.

142. Hombreiro- Perez, M., Siepmann, J., Zinutti, C., Lamprecht, A., Ubrich, N., Hoffman, M., Bodmeir, R., Maincent, P., *Non-degradable microparticles containing a hydrophilic and/or lipophilic drug: preparation, characterisation and drug release modelling.* J. Controlled Release, 2003. **88**: p. 413-428.

143. Jeong, Y., Shim, Y., Choi, C., Jang, M., Shin, G., Nah, J., *Surfactant free nanoparticles of poly (DL-lactide-co-glycolide) prepared with poly (lactide)/poly(ethylene glycol).* J. Appl. Polym. Sci., 2003. **89**: p. 1116-23.

144. Radwan, M., A., *In vitro evaluation of poly isobutylcyanoacrylate nanoparticles as a controlled drug carrier for theophylline.* Drug Dev. Ind. Pharm., 1995. **21**: p. 2371–75.

145. Nagarajan, R., Barry, M., Ruckenstein, E., *Unusual selectivity in solubilization by block copolymer micelles.* Langmuir 1986. **2**: p. 210–15.

146. Gabor, F., Ertyl, B., Wirth, M., Mallinger, R., *Ketoprofen-poly (D,L-lactic-co-glycolic acid) microspheres: influence of manufacturing parameters and type of polymer on the release characteristics.* J. Microencapsulation, 1999. **16**(1): p. 1-12.

147. Birnbaum, D., T., Kosmala, J., Henthorn, D., Brannon-peppas, L., *Controlled release of beta-estradiol from PLGA microparticles: the effect*

of organic phase solvent on encapsulation and release. J. Controlled Release, 2000. **65**(3): p. 375-87.

148. Kwon, H., Y., Lee, J., Y., Choi, S., W., Jang, Y., Kim, J., H., *Preparation of PLGA nanoparticles containing estrogen by emulsification-diffusion method.* Colloids Surf., 2001. **182**: p. 123-130.

149. Heiss, J., D., Papavassiliou, E., Merrill, M., J., Nieman, L., Knightly, J., J., Walbridge, S., Edwards, N., A., Oldfield, E., H., *Mechanism of dexamethasone suppression of brain tumour-associated vascular permeability in rats. Involvement of the glucocorticoid receptor and vascular permeability factor.* J. Clin. Invest., 1996. **98**(6): p. 1400-08.

150. Ishihara, T., Mizushima, Y., *Intravenous nanoparticles for targeting drug delivery and sustained drug release*, U.S. Patent, 20060233883. (2006) USA.

151. Ramstedt, B., Slotte, J., P., *Interaction of Cholesterol with Sphingomyelins and Acyl-Chain-Matched Phosphatidylcholines: A Comparative Study of the Effect of the Chain Length.* Biophysics. J., 1999. **76**: p. 908-915.

152. Liu, F., Liao, S., *Study of the effect of etoposide on the fluidity of dipalmitoylphosphatidylcholine liposome by differential scanning calorimetry and Raman spectroscopy.* Acta Pharmaceutica Sinica, 1989. **24**(5): p. 372-75.

153. Qiu, Z., B., Ikehara, T., Nishi, T., *Miscibility and crystallization in crystalline/crystalline blends of poly(butylene succinate)/poly(ethylene oxide)* Polymer, 2003. **44**: p. 2799.

154. Gomez-Gaete, C., Tsapis, N., Besnard, M., Bochot, A., Fattal, E., *Encapsulation of dexamethasone into biodegradable polymeric nanoparticles.* Int. J. Pharm., 2007. **331**(2): p. 153-9.

155. Tse, G., Blankschtein, D., Shefer, A., Shefer, S., *Thermodynamic prediction of active ingredient loading in polymeric microparticles.* J. Controlled Release, 1999. **60**: p. 77-100.

156. Matsumoto, J., Nakada, Y., Sakurai, K., *Preparation of nanoparticles consisted of poly(l-lactide)-poly(ethylene glycol)- poly(L- lactide) and their evaluation in vitro.* Int. J. Pharm., 1999. **185**(1): p. 93-101.

157. Juan, W., Wang, B., M., Schwendeman, S., P., *Characterisation of the initial burst release of a model peptide from poly(D,L-lactide-co-glycolide) microspheres.* J. Controlled Release, 2002. **82**: p. 289-307.

158. Higuchi, T., *Mechanism of sustained-action medication. Theoretical analysis of rate of release of solid drugs dispersed in solid matrices.* J. Pharm. Sci., 1963. **52**: p. 1145–49.

159. Costa, P., Lobo, J., M., *Modeling and comparison of dissolution profiles.* Eur. J. Pharm. Sci., 2001. **13**(2): p. 123-133.

160. Piskin, E., Kaitian, X., *Novel PDLLA/PEG copolymer micelles as drug carriers.* J. Biomater. Sci., Polym., 1995. **7**(4): p. 359-73.

161. Ryu, J., Young, J., Kim, I., *Clonazepam release from core-shell type nanoparticles of poly (ε-caprolactone) triblock copolymers.* Int. J. Pharm., 2000. **200**: p. 231-242.

162. Lin, W., Juang, L., Lin, C., *Stability and Release Performance of a Series of Pegylated Copolymeric Micelles.* Pharm. Res., 2003. **20**(4): p. 668-73.

163. Musumeci, T., Ventura, C., A., Giannone, I., Ruozi, B., Montenegro, L., Pignatello, R., Puglisi, G., *PLA/PLGA nanoparticles for sustained release of docetaxel.* Int. J. Pharm., 2006. **325**(1-2): p. 172-9.

164. Yoo, H., S., Lee, J., E., Chung, H., Kwon, I., C., Jeong, S., Y., *Self-assembled nanoparticles containing hydrophobically modified glycol chitosan for gene delivery.* J. Controlled Release, 2005. **103**(1): p. 235-43.

165. Govender, T., Riley, T., Ehtezazi, T., Garnett, M., C., Stolnik, S., S., *Defining the drug incorporation properties of PLA-PEG nanoparticles.* Int. J. Pharm., 2000. **199**: p. 95-110.

166. Stolnik, S., S., Garnett, M., C., Davies, M., C., Illum, L., Bousta, M., Davis, S., S., *The colloidal properties of surfactant-free biodegradable nanospheres from poly (β-malic acid-co-benzyl malate)s and poly(lactic acid-co-glycolide).* Colloids Surf., 1995. **97**: p. 235–245.

167. Zhang, Z., Grijpma, D., W., Feijen, J., *Poly(trimethylene carbonate) and monomethoxy poly(ethylene glycol)-block-poly(trimethylene carbonate) nanoparticles for the controlled release of dexamethasone.* J. Controlled Release, 2006. **111**(3): p. 263-70.

168. Alejandro, S., Belen, V., Guo, Y., *Formulation strategies for the stabilization of tetanus toxoid in poly(lactide-co-glycolide) microspheres.* Int. J. Pharm., 1999. **185**: p. 255-266.

169. Panyam, J., Labhasetwar, V., *Solid-State Solubility Influences Encapsulation and Release of Hydrophobic Drugs from PLGA/PLA Nanoparticles.* J. Pharm. Sci., 2005. **93** (7): p. 1804-14.

170. Kim, D., H., Martin, D., C., *Sustained release of dexamethasone from hydrophilic matrices using PLGA nanoparticles for neural drug delivery.* Biomaterials, 2006. **27**(15): p. 3031-37.

171. Horisawa, E., Hirota, T., Kawazoe, S., Yamada, J., Yamamoto, H., Takeuchi, H., *Prolonged anti-inflammatory action of DL-lactide/glycolide copolymer nanospheres containing betamethasone sodium phosphate for an intra-articular delivery system in antigen-induced arthritic rabbit.* Pharm. Res., 2002. **19**: p. 403–10.

172. Ishihara, T., Izumo, N., Higaki, M., Hagi, T., *Role of zinc in formulation of PLGA/PLA nanoparticles encapsulating betamethasone phosphate and its release profile.* J. Controlled Release, 2005. **105**: p. 1-2.

173. Bajpai, A., K., Choubey, J., *In vitro release dynamics of an anticancer drug from swellable gelatin nanoparticles.* J. Appl. Polym. Sci., 2006. **101**(4): p. 2320-32.

174. Sehgal, S., Rogers, J., A., *Polymer-coated liposomes: improved liposome stability and release of cytosine arabinoside (Ara-C).* J. Microencapsulation, 1995. **12**(1): p. 37-47.

175. Stamp, D., Julliano, R., *Factors affecting encapsulation of drugs within liposomes.* Can. J. Physiol. Pharmacol., 1979. **57**(5): p. 535-9.

176. Gomez, C., Blanco, M., D., Bernardo, M., V., Olmo, R., Muniz, E., Teijon, J., M., *Cytarabine release from comatrices of albumin microspheres in a poly(lactide-co-glycolide) film: in vitro and in vivo studies.* Eur. J. Pharm. Biopharm., 2004. **57**(2): p. 225-33.

177. Prabha, S., Labhasetwar, V., *Crtical Determinants in PLGA/PLA Nano mediated gene expression.* Pharm. Res., 2004. **21**(2): p. 354.

178. Liu, W., H., Song, J., L., Liu, K., Chu, D., F., Li, Y., X., *Preparation and in vitro and in vivo release studies of Huperzine A loaded microspheres*

for the treatment of Alzheimer's disease. J. Controlled Release, 2005. **107**: p. 417-27.

179.	Graves, R., A., Pamujula, S., Moiseyev, R., Freeman, T., Bostanian, L., A., Mandal, T., K., *Effect of different ratios of high and low molecular weight PLGA blend on the characteristics of pentamidine microcapsules.* Int. J. Pharm., 2004. **270**: p. 251-64.

180.	Alonso, M., J., *Nanoparticulate Drug Carrier Technology*, in *Pharmaceutical Dosage Forms: Disperse Systems* H. Lieberman, A., Rieger, M., M., Banker, G., S., Editor. 1996, Marcel Dekker: New York. p. 203-242.

181.	Blanco, M., D., Gomez, C., Olmo, R., *Chitosan microspheres in PLG films as devices for cytarabine release.* Int. J. Pharm., 2000. **202**: p. 29-39.

182.	Bilati, U., Allemann, E., Doelker, E., *Development of a nanoprecipitation method intended for the entrapment of hydrophilic drugs into nanoparticles.* Eur. J. Pharm. Sci., 2005. **24**(1): p. 67-75.

183.	McCarron, P., A., Woolfson, A., D., *Sustained release of 5-Flurouracil from nanoparticles.* J. Pharm. Pharmacol., 2000. **52**: p. 1451-1459.

184.	Soo, L., Lovric, J., Davidson, P., Maysinger, D., Eisenberg, A., *Polycaprolactone-block-poly(ethylene oxide) Micelles: A Nanodelivery System for 17β-Estradiol.* Mol. Pharm., 2005. **2**(6): p. 519 – 527.

185.	Jeong, Y., I., Nah, J., W., Lee, H., C., Kim, S., H., Cho, C., S., *Adriamycin release from flower-type polymeric micelle based on star-block copolymer composed of poly(g-benzyl L-glutamate) as the hydrophobic part and poly(ethylene oxide) as the hydrophilic part* Int. J. Pharm., 1999. **188**: p. 49-58.

186.	Nah, J., W., Jeong, Y., I., Cho, C., S., Kim, S., I., *Drug-delivery system based on core-shell-type nanoparticles composed of poly (g-benzyl L-glutamate) and poly(ethylene oxide)* J. Appl. Polym. Sci., 2000. **75**: p. 1115-26.

187.	Gorshkova, M., Y., Stotskaya, L., L., *Micelle-like macromolecular systems for controlled release of daunomycin.* Polym. Adv. Technol., 1998. **9**: p. 362-67.

188. Akinobu, H., Kawaguchi, T., *Clinical Pharmacokinetics of Cytarabine formulations.* Drug Disposition, 2002. **41**(10): p. 705-18.

189. Ameri, M., Collett, J., H., Attwood, D., Booth, C., *In vitro release of cytarabine from swellable matrices of $C_nE_mC_n$ triblock copolymers.* J. Controlled Release, 1998. **56**(1-3): p. 1-6.

190. Feng, J., Zeng, Y., Ma, C., Cai, X., Zhang, Q., Tong, M., Yu, B., Xu, P., *The surfactant tween 80 enhances biodesulfurization.* Appl. Environ. Microbiol., 2006. **72**(11): p. 7390-3.

191. Peng, T., Cheng, S., Zhuo, R., *Synthesis and characterization of poly-,-[N-(2-hydroxyethyl)-L-aspartamide]-g-poly(L-lactide) biodegradable copolymers as drug carriers* J. Biomed. Mater. Res., Part A 2006. **76**(1): p. 163 – 173.

192. Mainaredes, R., M., Evangelista, R., C., *Praziquantel-loaded PLGA nanoparticles: preparation and characterization.* J. Microencapsulation, 2005. **22**(1): p. 13-24.

193. Bharali, D., J., Sahoo, S., K., Mozumdar, S., Maitra, A., *Cross-linked polyvinylpyrrolidone nanoparticles: a potential carrier for hydrophilic drugs.* J. Colloid Interface Sci., 2003. **258**(2): p. 415-23.

194. Peracchia, M., T., Gref, R., Langer, R., *PEG coated nanospheres from amphiphilic di and multiblock copolymers.* J. Controlled Release, 1997. **46**: p. 223-31.

195. Venkatraman, S., Pan, J., Feng, M., *Micelle like nanoparticles of PLA-PEG-PLA triblock copolymer as chemotherapeutic carrier.* Int. J. Pharm., 2005. **298**: p. 219-32.

196. Arica, B., Lamprecht, A., *In vitro evaluation of Betamethasone loaded nanoparticles.* Drug Dev. Ind. Pharm., 2005. **31**(1): p. 9-24.

197. Sehgal, D., Vijay, I., K., *A method for the high efficiency of water soluble carbodiimide mediated amidation.* Analytical Biochem., 1994. **218**: p. 87-91.

198. You, Y., *Podophyllotoxin derivatives: current synthetic approaches for new anticancer agents.* Curr. Pharm. Des. Review, 2005. **11**(13): p. 1695-1717.

199. O'Dwyer, P., J., Weiss, R., B., *Hypersensitivity reactions induced by etoposide.* Cancer Treat. Rep., 1984. **68**: p. 959-61.

200. Hande, K., R., *Etoposide pharmacology.* Semin. Oncol., 1992. **19**(13): p. 3-9.

201. Sharma, D., Chelvi, T., P., Kaur, J., Chakravorty, K., De, T., K., Maitra, A., Ralhan, R., *Novel Taxol formulation: polyvinylpyrrolidone nanoparticle-encapsulated Taxol for drug delivery in cancer therapy.* Oncol. Res., 1996. **8**(7-8): p. 281-6.

202. Wang, F., Bronich, T., K., Kabanov, A.,V., Rauh, R., D., Roovers, J., *Synthesis and evaluation of a star amphiphilic block copolymer from poly(epsilon-caprolactone) and poly(ethylene glycol) as a potential drug delivery carrier.* Bioconjug. Chem., 2005. **6**(2): p. 397-405.

203. Newcomb, L., Gellman, S., *Aromatic Stacking Interactions in Aqueous Solution: Evidence that neither Classical Hydrophobic Effects nor Dispersion Forces are important.* J. Am. Chem. Soc., 1994. **116**: p. 4993-94.

204. Gadelle, F., Koros, W., J, Schechter, R., S., *Solubilization of aromatic solutes in block copolymers.* Macromolecules, 1995. **28**: p. 4883.

205. Reddy, L., H., Sharma, R., K., Chuttani, K., Mishra, A.,K., *Etoposide-incorporated Tripalmitin Nanoparticles with different surface charge: Formulation, Characterization, Radiolabeling, and Biodistribution Studies.* AAPS J 2004. **6**.

206. Lo Prete, A., C., Maria, D., A., Rodrigues, D., G., Valduga, C., J., Ibanez, O., C., Maranhao, R., C., *Evaluation in melanoma-bearing mice of an etoposide derivative associated to a cholesterol-rich nano-emulsion.* J. Pharm. Pharmacol., 2006. **58**(6): p. 801-8.

207. Valduga, C., J., Fernandes, D., C., Lo Prete, A., C., Azevedo, C., H., M., Rodrigues, D., G., Maranha, R., C,. *Use of a cholesterol rich microemulsion that binds to low-density lipoprotein receptors as vehicle for etoposide.* J. Pharm. Pharmacol., 2003. **55**: p. 1615–22.

208. Patlolla, R., R., Vobalaboina, V., *Pharmacokinetics and tissue distribution of etoposide delivered in parenteral emulsion.* J. Pharm. Sci., 2005. **94**(2): p. 437-45.

209. Dunne, M., Corrigan, O., I., Ramtoola, Z., *Influence of particle size and dissolution conditions on the degradation properties of polylactide-co-glycolide particles.* Biomaterials, 2000. **21**: p. 1659-68.

210. Gelderblom, H., Verweij, J., Van Zomeren, D., M,. Buijs, D., Ouwens, L., Nooter, K., Stoter, G., Sparreboom, A., *Influence of Cremophor El on the bioavailability of intraperitoneal paclitaxel.* Clin. Cancer Res., 2002. **8**: p. 1237-41.

211. Fonseca, C., Simoes, S., Gaspar, R., *Paclitaxel loaded PLGA nanoparticles: preparation, physicochemical characterization and in vitro anti tumoral activity.* J. Controlled Release, 2002. **83**: p. 273-286.

212. Rodrigues, D., G., Maria, D., A., Fernandes, D.,C., Valduga, C., J . *Improvement of paclitaxel therapeutic index by derivatization and association to a cholesterol-rich microemulsion: in vitro and in vivo studies.* Cancer Chemother. Pharmacol., 2005. **55**(6): p. 565-76.

213. Liang, H., Chen, C., Chen, S., Kulkarni, A., *Paclitaxel- loaded poly (γ-glutamic acid)-poly(lactide) nanoparticles as a targeted drug delivery system for the treatment of liver cancer.* Biomaterials, 2006. **27**: p. 2051-59.

214. Mu, L., Feng, S., S., *A novel controlled release formulation for the anticancer drug paclitaxel (Taxol): PLGA nanoparticles containing vitamin E TPGS.* J. Controlled Release, 2003. **86**: p. 33-48.

215. Cavallaro, G., Licciardi, M., Caliceti, P., Salmaso, S., Giammona, G., *Synthesis, physico-chemical and biological characterization of a paclitaxel macromolecular prodrug.* Eur. J. Pharm. Biopharm., 2004. **58**: p. 151-9.

216. Lu, Z., Yeh, T., K., Tsai, M., Au, J., S., Wientjes, M., G., *Paclitaxel loaded gelatine nanoparticles for intravesical bladder cancer therapy.* Clin. Cancer Res., 2004. **10**: p. 7677-84.

217. Lundberg, B., B., Risovic, V., Ramaswamy, M., Wasan, K., M., *A lipophilic paclitaxel derivative incorporated in a lipid emulsion for parenteral administration.* J. Controlled Release, 2003. **86**: p. 93–100.

218. Görner, T., Gref, R., Michenot, D., Sommer, F., Tran, M., N., Dellacherie, E., *Lidocaine-loaded biodegradable nanospheres. I.*

Optimization Of the drug incorporation into the polymer matrix. J. Controlled Release, 1999. **57**: p. 259–68.

219. Mitra, A., Lin, S., *Effect of surfactant on fabrication and characterization of paclitaxel-loaded polybutylcyanoacrylate nanoparticulate delivery systems.* J. Pharm. Pharmacol., 2003. **55**(7): p. 895-902.

220. Rao, S., Krauss, N., E., Heerding, J., M., Swindell, C., S., Ringel, I., Orr, G., A., Horwitz, S., B., *3'-(p-azidobenzamido)taxol photolabels the N-terminal 31 amino acids of beta-tubulin.* J. Biol. Chem., 1994. **269**(5): p. 3132-4.

221. Panda, D., Miller, H., P., Islam, K., Wilson, L., *Stabilization of microtubule dynamics by estramustine by binding to a novel site in tubulin: A possible mechanistic basis for its antitumor action.* Proc. Natl. Acad. Sci. USA., 1997. **94**: p. 10560-64.

222. Sackett, D., L., *Vinca site agents induce structural changes in tubulin different from and antagonistic to changes induced by colchicine site agents.* Biochemistry, 1995. **34**: p. 7010–19.

223. Purcell, M., Neault, J., F., Tajmir-Riahi, H., A., *Interaction of Taxol with human serum albumin.* Biochem. Biophys. Acta., 2000. **1478**: p. 61-68.

224. Liggins, R., T., Burt, H., M., *Paclitaxel loaded poly(L-lactic acid) microspheres: properties of microspheres made with low molecular weight polymers.* Int. J. Pharm., 2001. **222**: p. 19-33.

225. Feng, S., S., Mu, L., Win, K., Y., Huang, G., *Nanoparticles of biodegradable polymers for clinical administration of Paclitaxel.* Curr. Med. Chem., 2004. **11**: p. 413-24.

226. Vitkup, D., Ringe, D., Petsko, G., A., Karplus, M., *Solvent mobility and the protein 'glass' transition".* Nat. Struct. Mol. Biol., 2001. **7**: p. 34–38.

227. Liu, T., Petermann, J., *Multiple melting behavior in isothermally cold-crystallized isotactic polystyrene* Polymer, 2001. **42**: p. 6453.

228. Busfield, W., K., Proschogo, P., *Thermal analysis of palm stearin by DSC.* J. Am. Oil Chem. Soc, 1990. **67**(3): p. 171-175.

229. Yin, J., Noda, Y., Yotsuyanagi, T., *Properties of poly (lactic-co-glycolic acid) nanospheres containing protease inhibitors: Camostat mesilate and nafamostat mesilate.* Int. J. Pharm., 2006. **314**: p. 46-55.

230.   Hyvonen, S., Peltonen, L., Karjalainen, M., Hirvonen, J., *Effect of nanoprecipitation on the physicochemical properties of low molecular weight poly (L-lactic acid) nanoparticles loaded with salbutamol sulphate and beclomethasone dipropionate.* Int. J. Pharm., 2005. **295**: p. 269-81.

231.   Yoon, J., J., Kin, J., H., Park, T., G., *Dexamethasone-releasing biodegradable polymer scaffolds fabricated by a gas-foaming/salt-leaching method.* Biomaterials 2003. **24**(13): p. 2323-9.

232.   Eerikainen, H., Peltonem, L., Raula, J., Hirvonen, J., Kauppinen, E., I., *Nanoparticles containing ketoprofen and acrylic polymers prepared by an aerosol flow reactor method.* AAPS Pharm. Sci. Tech., 2004. **5**(4): p. 68.

233.   Cavalier, M., Benoit, J., P., Thies, C, *The formation and characterization of hydrocortisone loaded poly(d,l-lactide) microspheres.* J. Pharm. Pharmacol., 1986. **38**: p. 249-53.

234.   Bodmeier, R., Oh, H., Chen, H., *The effect of the addition of low molecular weight poly(D,L-lactide) on drug release from biodegradable poly(D,L-lactide) drug delivery systems.* Int. J. Pharm., 1989. **51**: p. 1–8.

235.   Hurrel, S., Cameron, R., E., *The effect of initial polymer morphology on the degradation and drug release from polyglycolide.* Biomaterials, 2002. **23**(2401–2409).

236.   Li, S., M., Garreau, H., Vert, M., *Structure–property relationships in the case of the degradation of massive poly (a-hydroxy acids) in aqueous media, part 3.* J. Mater. Sci.: Mater. Med., 1990. **1**: p. 198–206.

237.   Ge, H., Hu, Y., Yang, S., Jiang, X., Yang, C., *Preparation, characterization, and drug release behaviors of drug-loaded poly -caprolactone/L-lactide copolymer nanoparticles.* J. Appl. Polym. Sci., 2000. **75**(7): p. 874 – 82.

238.   Izumikawa, S., Yoshioka, S., Aso, Y., Takeda, Y., *Preparation of poly (L-lactide) microspheres of different crystalline morphology and effect of crystalline morphology on drug release rate.* J. Controlled Release, 1991. **15**: p. 133.

239. Pignatello, R., Ferro, M., Puglisi, G., *Preparation of solid dispersions of nonsteroidal anti inflammatory drugs with acrylic polymers and studies on mechanisms of drug-polymer interactions.* AAPS Pharm. Sci. Tech., 2002. **3**: p. E10.

240. Wunderlich, B., *Thermal Analysis*. 1990, San Diego, CA: Academic Press, Inc.

241. Chokshi, R., J., Sandhu, H., K., Iyer, R., M., Shah, N., H., Malick, A., W., Zia, H., *Characterization of physico-mechanical properties of indomethacin and polymers to assess their suitability for hot-melt extrusion processs as a means to manufacture solid dispersion/solution.* J. Pharm. Sci., 2005. **94**(11): p. 2463- 74.

242. Benoit, J., P., Thies, C., *Benita, S.*, in *Microencapsulation. Methods and industrial applications*. 1996, Marcel Dekker: New York p. 133.

243. Painter, P., C., Coleman, M., M., *Fundamentals of polymer science, an introductory text*. 2 ed. 1997, New York: CRC press

244. Dubernet, C., *Thermoanalysis of microspheres.* Thermochem. Acta 1995. **248**: p. 259–69.

245. Cha, Y., Pitt, C., G., *The acceleration of degradation-controlled drug delivery from polyester microspheres.* J. Controlled Release, 1989. **8**: p. 259–65.

246. Jenquin, M., R., McGinity, J., *Characterization of acrylic resin matrix films and mechanisms of drug–polymer interaction.* Int. J. Pharm., 1994. **101**: p. 23–34.

247. Yokoyama, M., Okano, T., Sakurai, Y., Kataoka, K., *Improved synthesis of adriamycin-conjugated poly(ethylene oxide)– poly(aspartic acid) block copolymer and formation of unimodal micellar structure with controlled amount of physically entrapped adriamycin.* J. Controlled Release, 1994. **32**: p. 269–77.

248. Lee, J., Cho, E., C., Cho, K., K., *Incorporation and release behavior of hydrophobic drug in functionalized poly (DL-lactide)-block– poly(ethylene oxide) micelles.* J. Controlled Release, 2004. **94**(2-3): p. 323-35.

249. Allen, C., Maysinger, D., Eisenberg, A., *Nano-engineering block copolymer aggregates for drug delivery.* Colloids Surf., B 1999. **16**: p. 3–27.

250. Nuijen, B., Bouma, M., Schellens, J., H., M., Beijnen, J., H., *Progress in the development of alternative pharmaceutical formulations of taxanes.* Invest. New Drug, 2001. **19**: p. 143-53.

251. Liu, J., B., Xiao, Y., H., Allen, C., *Polymer–drug compatibility: a guide to the development of delivery systems for the anticancer agent, ellipticine.* J. Pharm. Sci., 2004. **93**: p. 132–43.

252. Kwon, L., *The effect of fatty acid substitution on the in vitro release of amphotericin B from micelles composed of poly(ethylene oxide)-block-poly(N-hexyl stearate-L-aspartamide).* J. Controlled Release, 2002. **79**(1-3): p. 165-72.

253. Ameller, T., Marsaud, V., Legrand, P., Gref, R., Barratt, G., Renoir, J., M., *Polyester-poly (ethylene glycol) nanoparticles loaded with the pure antiestrogen RU 58668: physicochemical and opsonization properties.* Pharm. Res., 2003. **20**(7): p. 1063-70.

APPENDICES
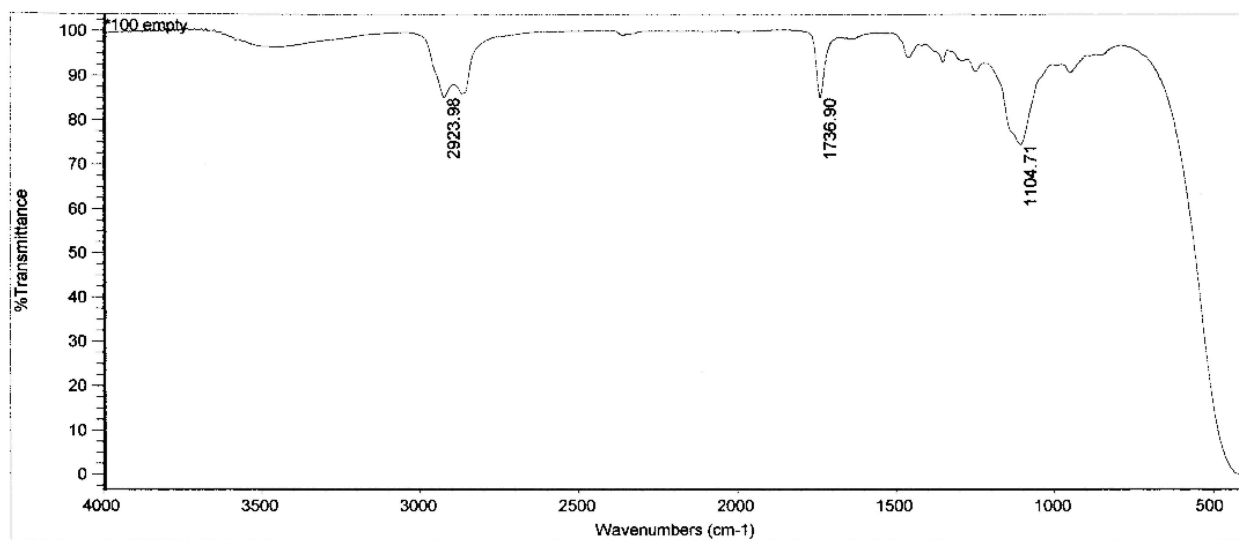
Tue Dec 16 00:29:12 1997
FIND PEAKS:
    Spectrum: *100 empty
    Region: 4000.00   400.00
    Absolute threshold: 96.107
    Sensitivity: 50
    Peak list:
               Position: 1104.71   Intensity: 74.368
               Position: 1736.90   Intensity: 84.933
               Position: 2923.98   Intensity: 85.149

Appendix 1. FTIR scan for 100% C_8 empty particles

Tue Dec 16 00:16:20 1997
FIND PEAKS:
    Spectrum: *100c8 +dxmp
    Region: 4000.00   400.00
    Absolute threshold: 94.677
    Sensitivity: 50
    Peak list:
                        Position: 1739.42   Intensity: 36.794
                        Position: 1169.67   Intensity: 58.213
                        Position: 2962.03   Intensity: 85.674
                        Position: 1381.49   Intensity: 86.210
                        Position: 1458.80   Intensity: 88.133

Appendix 2. FTIR scan for 100% C_8 + DXMP particles
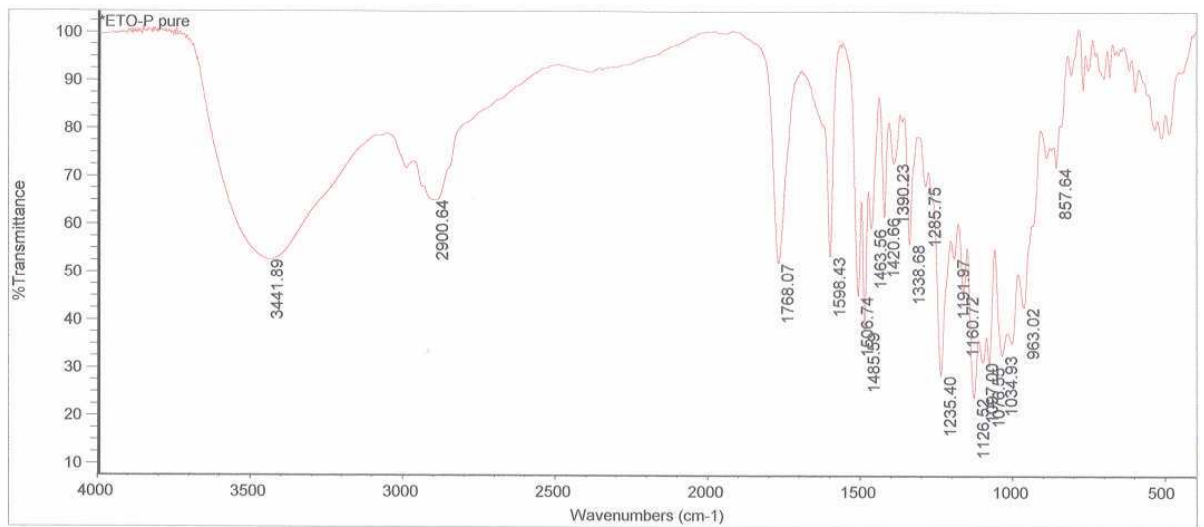
Tue Dec 16 01:52:21 1997
FIND PEAKS:
    Spectrum: *ETO-P pure
    Region: 4000.00   400.00
    Absolute threshold: 75.121
    Sensitivity: 50
    Peak list:
                        Position: 1126.52   Intensity: 23.842
                        Position: 1235.40   Intensity: 28.424
                        Position: 1076.55   Intensity: 30.312
                        Position: 1097.00   Intensity: 31.215
                        Position: 1034.93   Intensity: 32.722
                        Position: 1485.59   Intensity: 37.550
                        Position: 963.02   Intensity: 42.699

Appendix 3. FTIR scan for ETO-P pure drug

Tue Dec 16 02:14:01 1997
FIND PEAKS:
    Spectrum: ETO pure
    Region: 4000.00   400.00
    Absolute threshold: 49.147
    Sensitivity: 50
    Peak list:
                         Position: 1116.18   Intensity: 14.843
                         Position: 1075.04   Intensity: 16.706
                         Position: 1232.03   Intensity: 22.960
                         Position: 1033.60   Intensity: 24.462
                         Position: 1485.79   Intensity: 24.889
                         Position: 996.77   Intensity: 25.126
                         Position: 1161.54   Intensity: 28.007

Appendix 4. FTIR scan for Etoposide (pure drug).
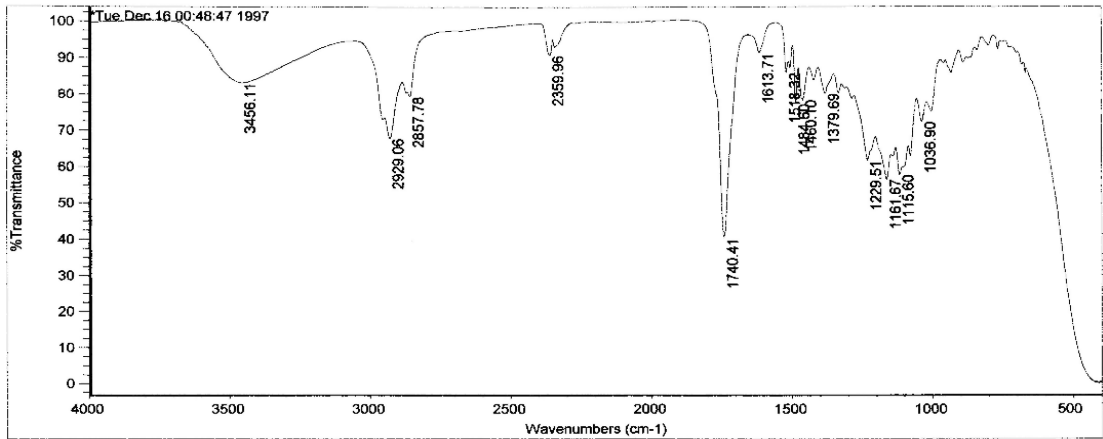
Tue Dec 16 00:50:47 1997
FIND PEAKS:
    Spectrum: *Tue Dec 16 00:48:47 1997
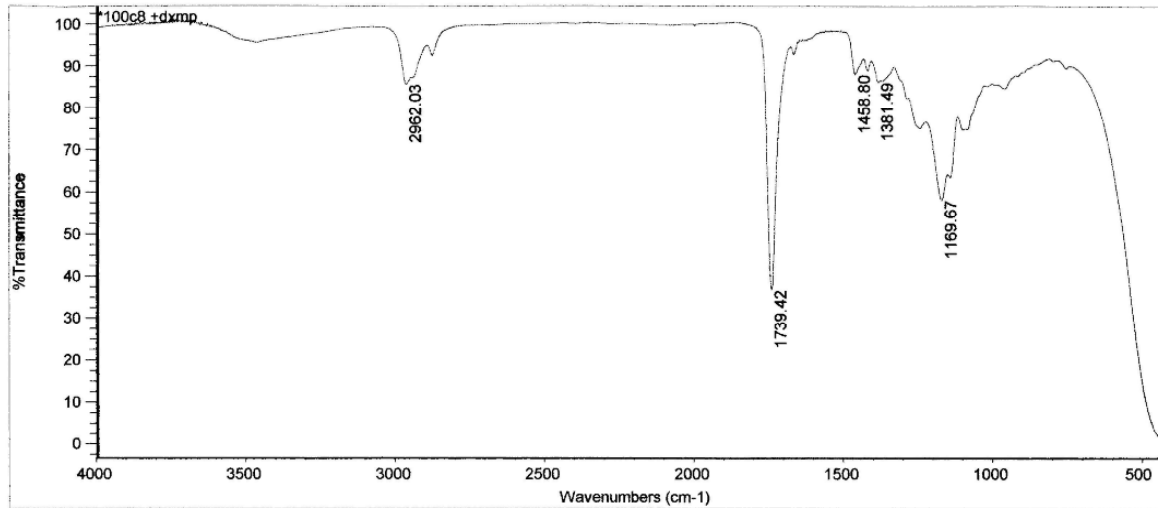   Region: 4000.00   400.00
    Absolute threshold: 92.690
    Sensitivity: 50
    Peak list:
                         Position: 1740.41   Intensity: 40.234
                         Position: 1161.67   Intensity: 56.668
                         Position: 1115.60   Intensity: 57.852
                         Position: 1229.51   Intensity: 61.733
                         Position: 2929.06   Intensity: 67.793
                         Position: 1036.90   Intensity: 72.211
                         Position: 1484.60   Intensity: 77.146
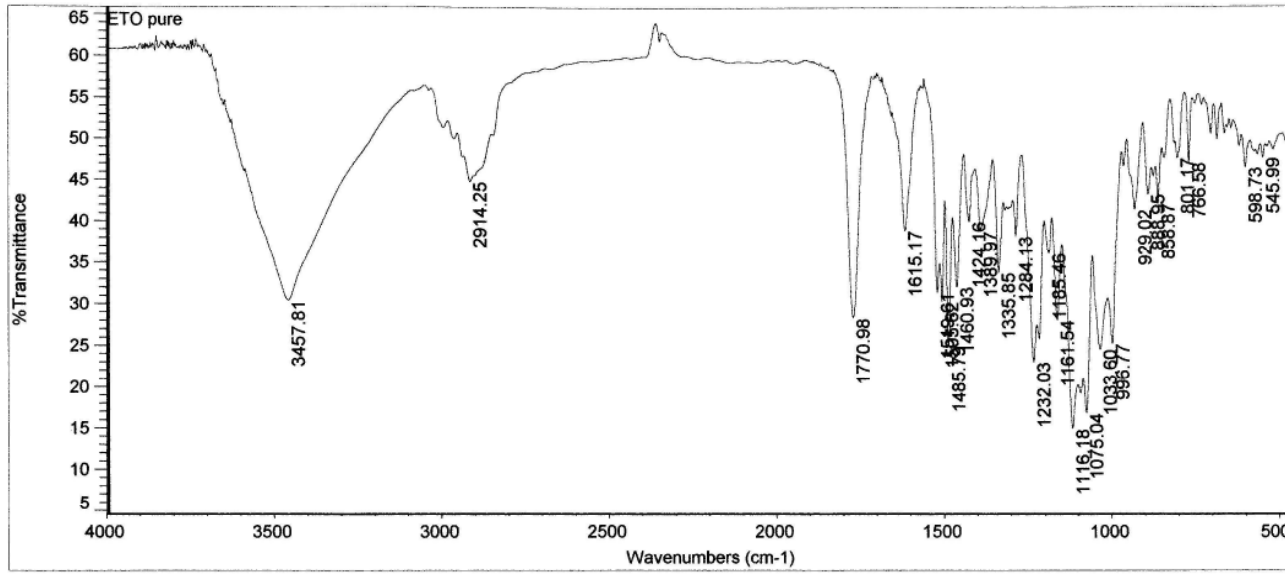
Appendix 5. FTIR scan for 100% C8+ ETO particles
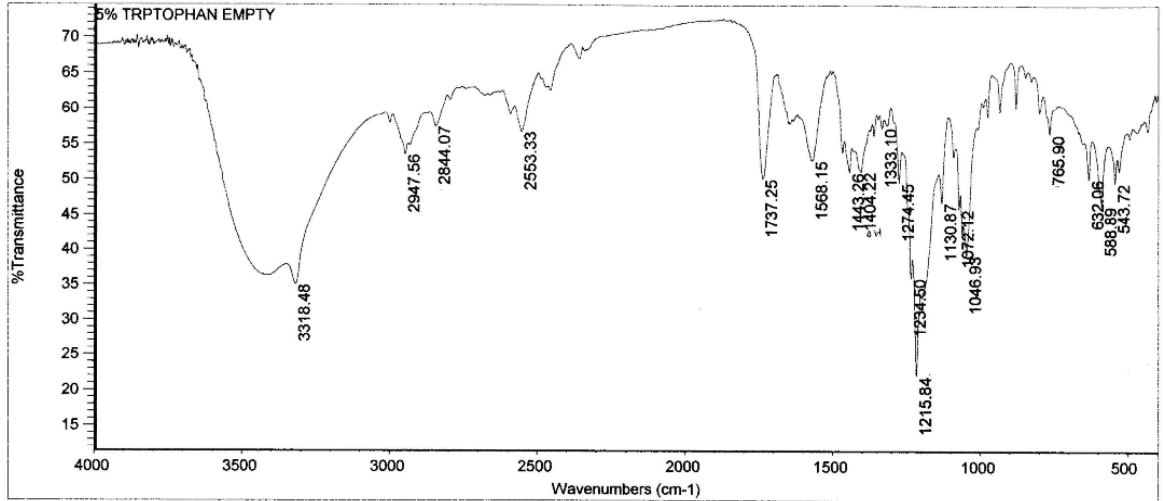
Tue Dec 16 00:26:53 1997
FIND PEAKS:
Spectrum: 5% TRPTOPHAN EMPTY
Region: 4000.00   400.00
Absolute threshold: 57.497
Sensitivity: 50
Peak list:
                   Position: 1215.84   Intensity: 21.977
                   Position: 3318.48   Intensity: 34.970
                   Position: 1234.50   Intensity: 35.963
                   Position: 1046.93   Intensity: 39.180
                   Position: 1072.12~ Intensity: 45.778
                   Position: 588.89   Intensity: 46.236
                   Position: 1130.87   Intensity: 46.709

Appendix 6. FTIR scan for 5% tryptophan empty particles.

Tue Dec 16 00:40:09 1997
FIND PEAKS:
Spectrum: *5% Tryptpphan + Eto
Region: 4000.00   400.00
Absolute threshold: 95.797
Sensitivity: 50
Peak list:
                   Position: 1737.65   Intensity: 63.848
                   Position: 1171.61   Intensity: 77.822
                   Position: 1140.94   Intensity: 80.175
                   Position: 3444.16   Intensity: 87.289
                   Position: 1078.63   Intensity: 87.447
                   Position: 1381.24   Intensity: 89.287
                   Position: 1455.60   Intensity: 89.751

Appendix 7 FT-IR scan for 5% tryptophan + ETO particles

257

Tue Dec 16 00:20:58 1997
FIND PEAKS:
    Spectrum: *pb empty
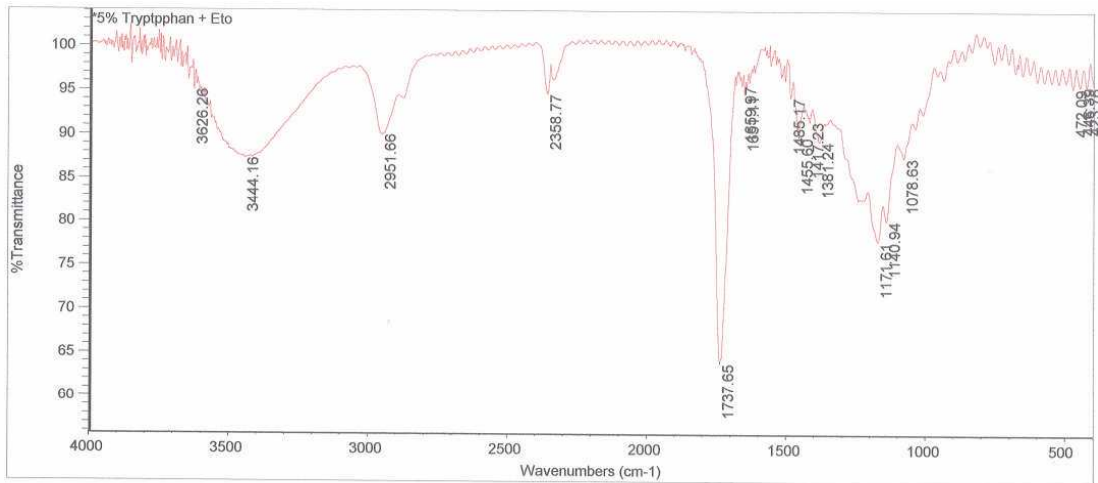   Region: 4000.00   400.00
    Absolute threshold: 83.949
    Sensitivity: 50
    Peak list:
                       Position: 1732.29   Intensity: 56.939
                       Position: 1174.43   Intensity: 67.259
                       Position: 3444.49   Intensity: 77.887
                       Position: 2950.99   Intensity: 78.122
                       Position: 1385.46   Intensity: 80.391
                       Position: 1455.93   Intensity: 81.420

Appendix 8 FT-IR scan for empty polymer backbone particles

Tue Dec 16 00:33:38 1997
FIND PEAKS:
    Spectrum: *pb+eto
    Region: 4000.00   400.00
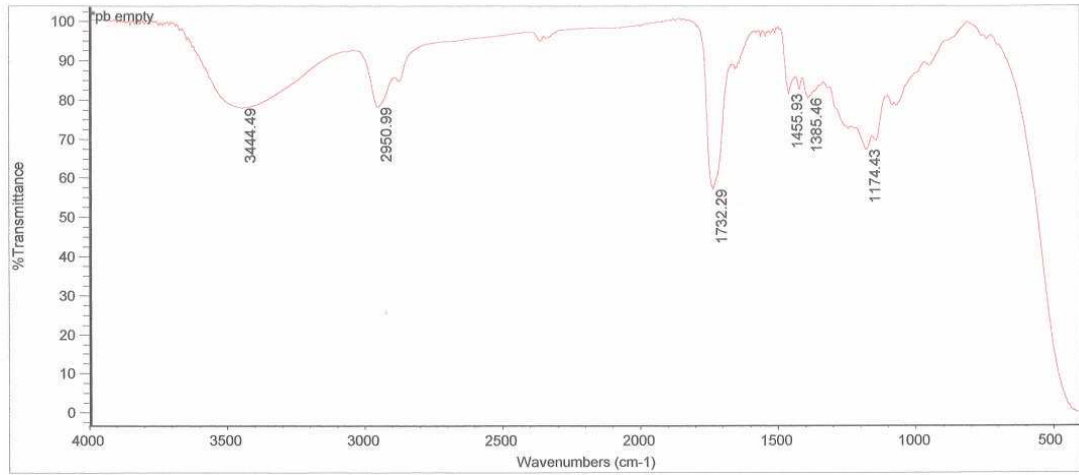   Absolute threshold: 97.712
    Sensitivity: 50
    Peak list:
                       Position: 1733.93   Intensity: 75.637
                       Position: 1171.44   Intensity: 84.657
                       Position: 2359.60   Intensity: 95.259
                       Position: 2950.50   Intensity: 95.827
                       Position: 3445.82   Intensity: 96.063

Appendix 9. FT-IR scan for Polymer backbone+ ETO particles

258

Tue Dec 16 00:28:22 1997
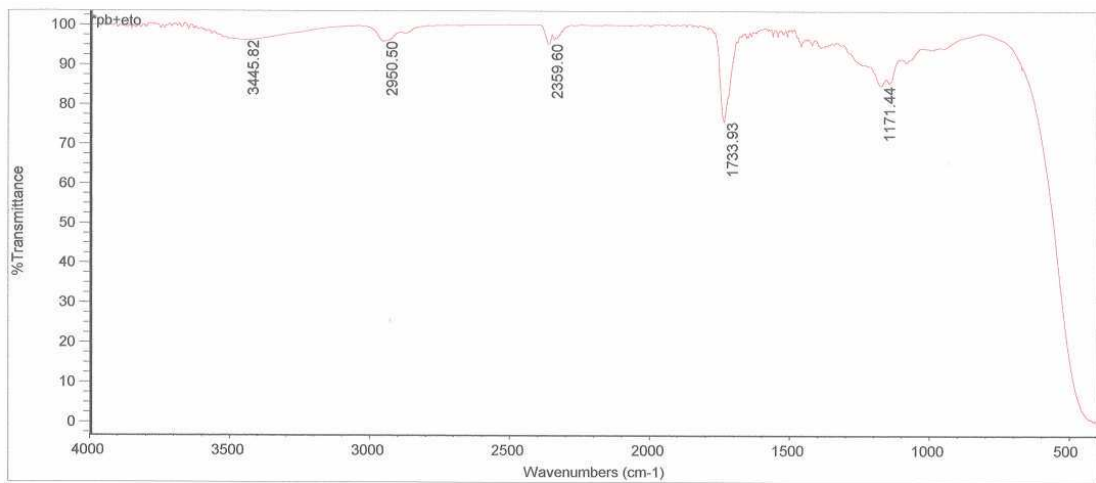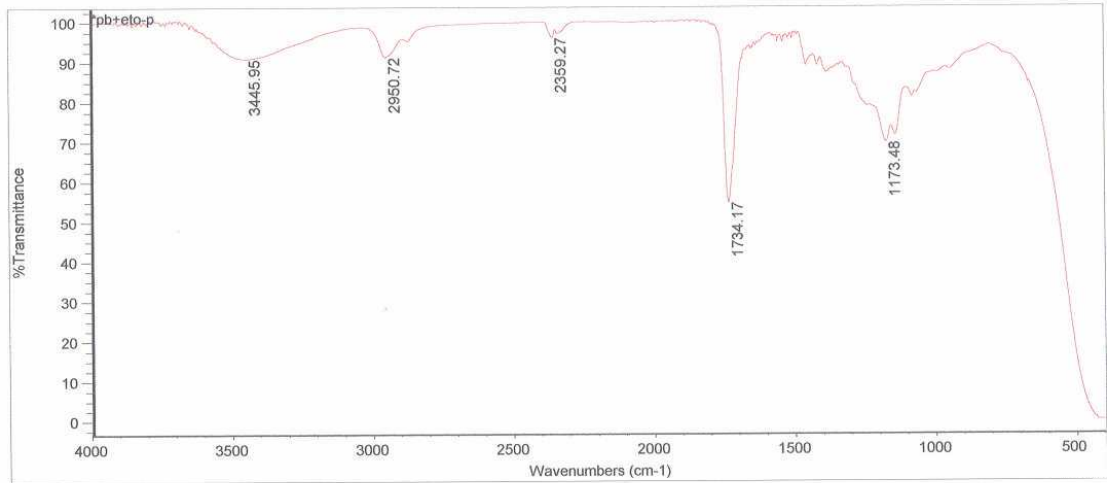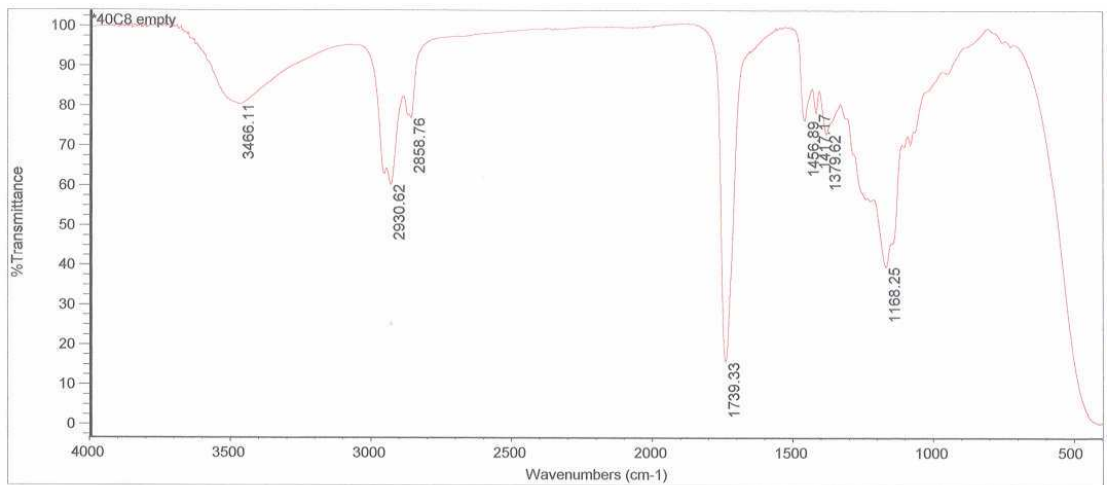FIND PEAKS:
    Spectrum: *pb+eto-p
    Region: 4000.00   400.00
    Absolute threshold: 96.033
    Sensitivity: 50
    Peak list:
                    Position: 1734.17   Intensity: 54.616
                    Position: 1173.48   Intensity: 69.764
                    Position: 3445.95   Intensity: 90.683
                    Position: 2950.72   Intensity: 91.133
                    Position: 2359.27   Intensity: 96.002

Appendix 10. FT-IR scan for Polymer backbone+ ETO-P particles

Tue Dec 16 00:05:35 1997
FIND PEAKS:
    Spectrum: *40C8 empty
    Region: 4000.00   400.00
    Absolute threshold: 85.287
    Sensitivity: 50
    Peak list:
                    Position: 1739.33   Intensity: 15.605
                    Position: 1168.25   Intensity: 39.573
                    Position: 2930.62   Intensity: 60.232
                    Position: 1379.62   Intensity: 72.848
                    Position: 1456.89   Intensity: 76.333
                    Position: 2858.76   Intensity: 76.974
                    Position: 1417.17   Intensity: 78.179

Appendix 11 FT-IR scan for 40% C8 empty particles

Tue Dec 16 00:39:08 1997
FIND PEAKS:
    Spectrum: *40 C8+CYT-ARA
    Region: 4000.00   400.00
    Absolute threshold: 65.336
    Sensitivity: 50
    Peak list:
                       Position: 1738.97   Intensity: 9.527
                       Position: 1169.98   Intensity: 19.859
                       Position: 2932.56   Intensity: 38.052
                       Position: 1380.49   Intensity: 46.034
                       Position: 1456.49   Intensity: 51.689
                       Position: 1417.19   Intensity: 52.633
                       Position: 3466.38   Intensity: 52.842

Appendix 12. FT-IR scan for 40% C8+ CYT-ARA particles.

Tue Dec 16 00:54:33 1997
FIND PEAKS:
    Spectrum: *POlymer backbone+Cyt-Ara
    Region: 4000.00   400.00
    Absolute threshold: 72.870
    Sensitivity: 50
    Peak list:
                       Position: 1735.45   Intensity: 5.984
                       Position: 1177.52   Intensity: 26.744
                       Position: 1650.44   Intensity: 30.952
                       Position: 3358.00   Intensity: 31.544
                       Position: 1140.25   Intensity: 31.721
                       Position: 1062.69   Intensity: 41.390
                       Position: 2950.22   Intensity: 47.514

Appendix 13. FT-IR scan for Polymer backbone + CYT-ARA particles.

260

Tue Dec 16 00:12:26 1997
FIND PEAKS:
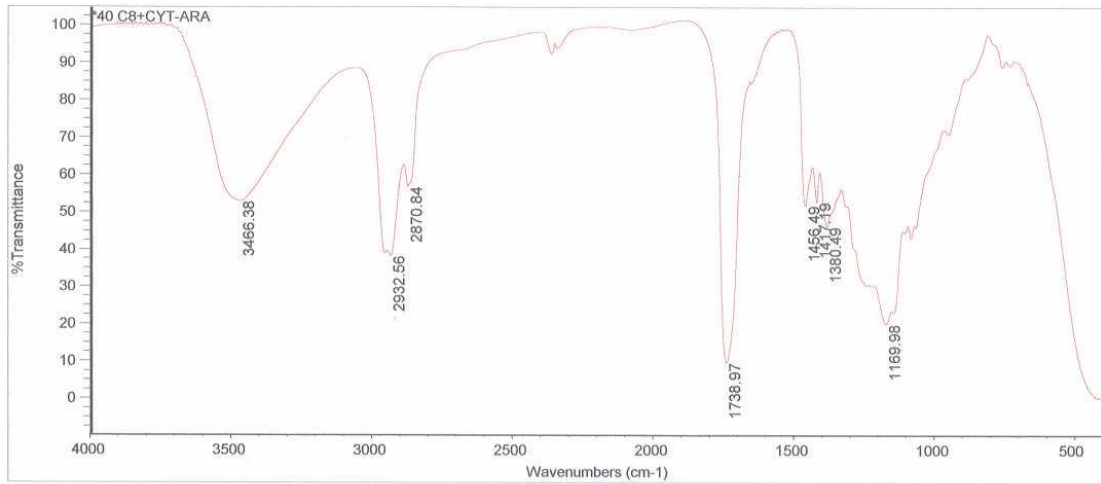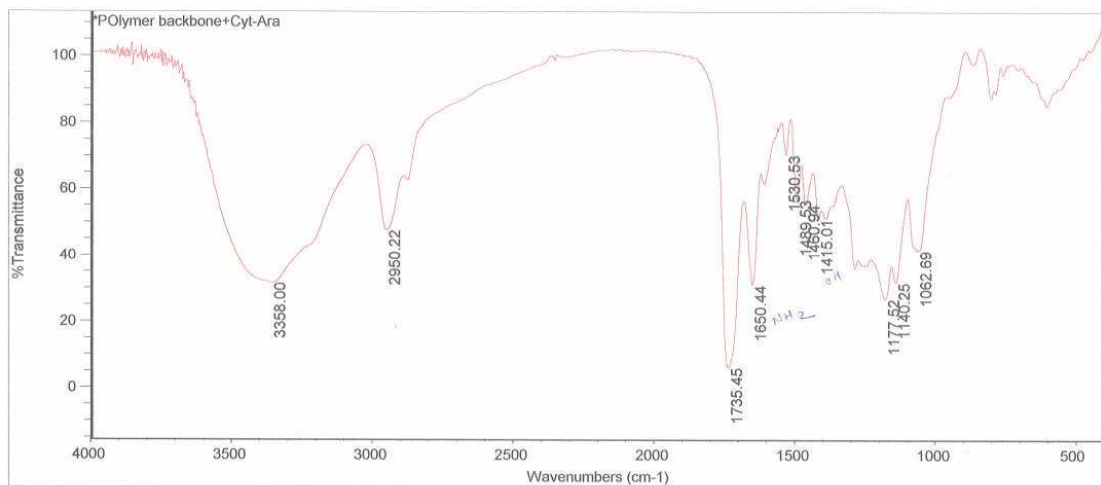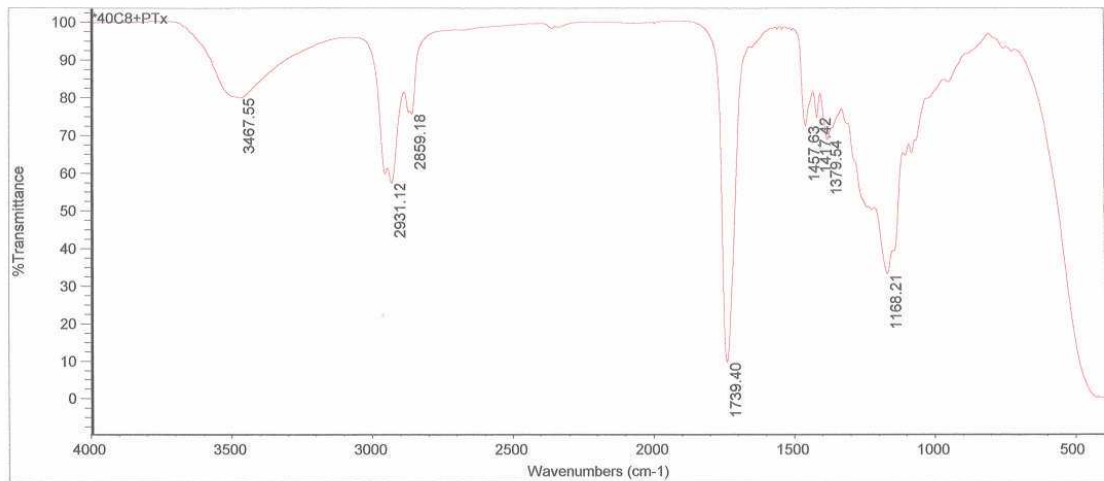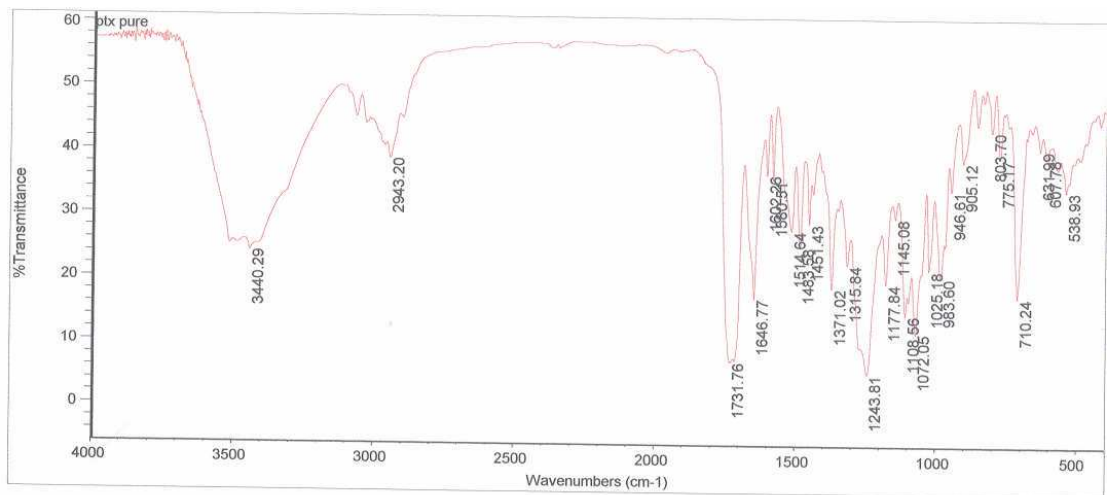   Spectrum: *40C8+PTx
    Region: 4000.00   400.00
    Absolute threshold: 91.528
    Sensitivity: 50
    Peak list:
                    Position: 1739.40   Intensity: 9.583
                    Position: 1168.21   Intensity: 33.114
                    Position: 2931.12   Intensity: 57.425
                    Position: 1379.54   Intensity: 68.809
                    Position: 1457.63   Intensity: 72.522
                    Position: 1417.42   Intensity: 74.695
                    Position: 2859.18   Intensity: 75.662

Appendix 14. FT-IR scan for 40% C8 + PTx particles.

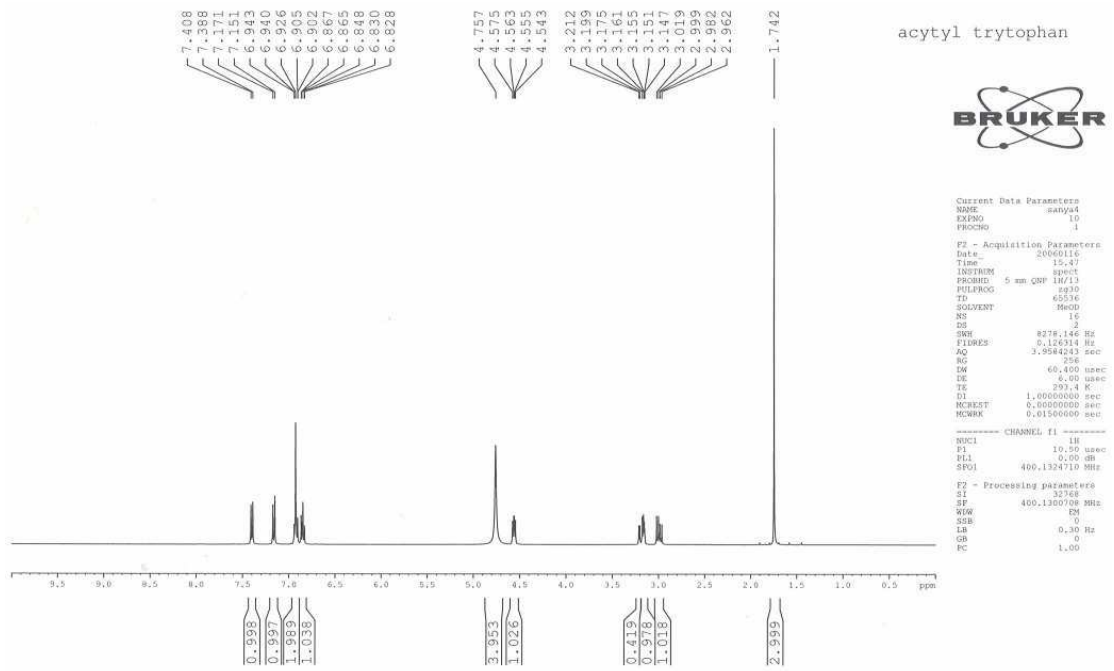Tue Dec 16 02:46:46 1997
FIND PEAKS:
   Spectrum: ptx pure
    Region: 4000.00   400.00
    Absolute threshold: 44.297
    Sensitivity: 50
    Peak list:
                    Position: 1243.81   Intensity: 5.249
                    Position: 1731.76   Intensity: 6.997
                    Position: 1072.05   Intensity: 11.644
                    Position: 1108.56   Intensity: 14.542
                    Position: 1646.77   Intensity: 16.990
                    Position: 710.24   Intensity: 17.362
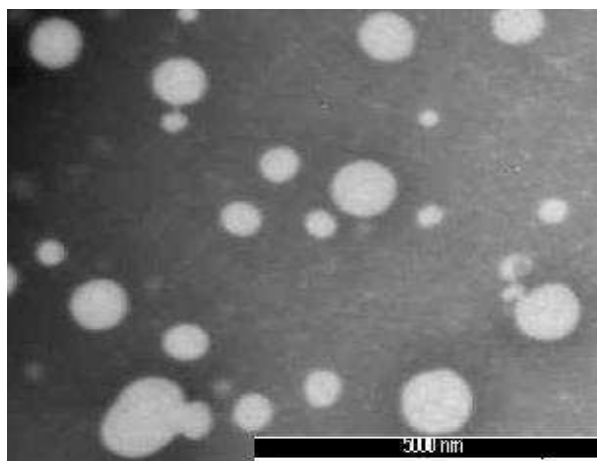   Position: 1371.02   Intensity: 18.703

Appendix 15. FT-IR scan for PTx pure drug

261

Appendix 16. NMR scan for N-Acetyl tryptophan in MeOD
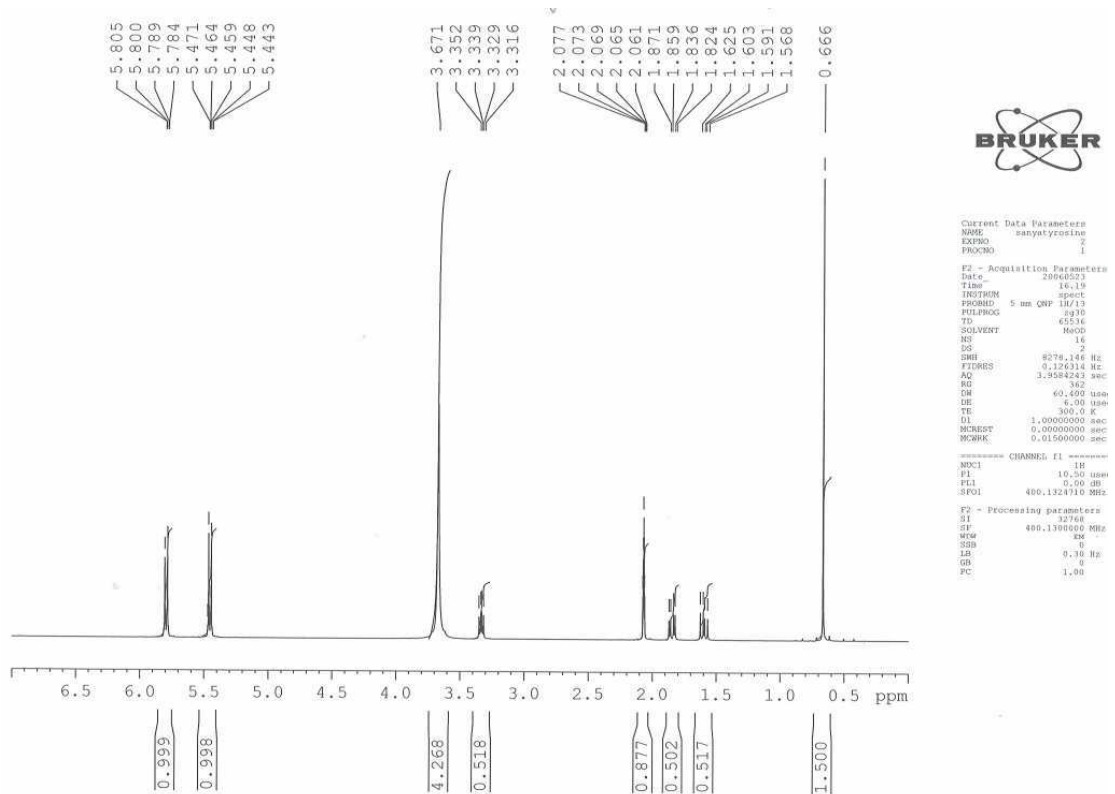
Appendix 17 NMR scan for N- acetyl tyrosine in MEOD

Appendix 18. TEM Image of ETO in 5 % tryptophan substituted polymer after 25 days of drug release studies in HEPES+ tween at 37°C.